

NSB 2023 - Book of Technical Papers - 13th Nordic Symposium on Building Physics

Johra, Hicham

DOI (link to publication from Publisher):
[10.54337/aau549347670](https://doi.org/10.54337/aau549347670)

Creative Commons License
CC BY 4.0

Publication date:
2023

Document Version
Publisher's PDF, also known as Version of record

[Link to publication from Aalborg University](#)

Citation for published version (APA):
Johra, H. (Ed.) (2023). *NSB 2023 - Book of Technical Papers - 13th Nordic Symposium on Building Physics*. Department of the Built Environment, Aalborg University. <https://doi.org/10.54337/aau549347670>

General rights

Copyright and moral rights for the publications made accessible in the public portal are retained by the authors and/or other copyright owners and it is a condition of accessing publications that users recognise and abide by the legal requirements associated with these rights.

- Users may download and print one copy of any publication from the public portal for the purpose of private study or research.
- You may not further distribute the material or use it for any profit-making activity or commercial gain
- You may freely distribute the URL identifying the publication in the public portal -

Take down policy

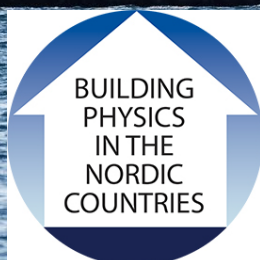
If you believe that this document breaches copyright please contact us at vbn@aub.aau.dk providing details, and we will remove access to the work immediately and investigate your claim.

NSB 2023 BOOK OF TECHNICAL PAPERS



13th Nordic Symposium on Building Physics

Editor-in-Chief: Hicham Johra



NSB 2023

BOOK OF

TECHNICAL

PAPERS

NSB 2023

Book of Technical Papers: 13th Nordic Symposium on Building Physics

TITLE	NSB 2023 - Book of Technical Papers: 13th Nordic Symposium on Building Physics
FORMAT	PDF
ISSUE	1
PUBLICATION DATE	September 2023
AUTHORS	Hicham Johra (Editor-in-Chief) & all the authors of the NSB 2023 Technical Papers
LANGUAGE	English
PAGE COUNT	289
KEYWORDS	Building physics, heat-air-moisture transport, building envelope, moisture safety and durability, integrated and applied aspects of building physics
DOI	https://doi.org/10.54337/aau549347670
ISBN	87-91606-37-3
FRONT COVER PICTURE	Rasmus Hjortshøj
PUBLISHER	Department of the Built Environment, Aalborg University Thomas Manns Vej 23, 9220 Aalborg Øst E-mail build@build.aau.dk www.build.aau.dk This publication is covered by the Danish Copyright Act.

Table of Contents

Preface	7
Conference Organising Committee	9
Scientific Committee	10
List of Sponsors	14
List of all Technical Papers	14
Compilation of all Technical Papers	18

Preface

The 13th Nordic Symposium on Building Physics (NSB 2023) took place at Aalborg University in the city of Aalborg, Denmark, from the 12th to the 14th of June, 2023. This conference was organised by the Department of the Built Environment of Aalborg University, with the help of fellow researchers from Aarhus University, the University of Southern Denmark and the Technical University of Denmark.

NSB is a renowned international conference series in Building Physics, held every three years since 1987. Although organised in Nordic countries, the conference is in English and is not limited to cold climates. It has grown to attract participants worldwide, to the point that more than half of the participants have been from other countries.

This symposium is intended to be a forum for scientists, practitioners, PhD students and other building professionals to share new research results, demonstrate innovative and sustainable building technologies, and discuss current and future challenges and solutions within building physics, heat, air and moisture transfer in buildings, and on aspects of moisture problems in the built environment, energy performance and indoor environmental quality.

The NSB 2023 central theme is “Building physics as a key player for the sustainable built environment”. The conference focus is primarily on the following aspects that all require a throughout understanding of building physics:

- Heat, air and moisture transport
- Measurement and modelling techniques
- Material properties
- Contaminant transfer (gas phase, airborne pollutants)
- Outdoor and indoor climate for building physics analysis
- Hygrothermal performance of building envelope
- Advanced building envelope systems
- Air-tightness, air movement inside and around the buildings
- Building materials and components
- Facades
- Climate change and climate adaptation of buildings
- Moisture and mould problems
- Investigation methods of moisture and microbial damages
- Moisture safety in design, construction, and maintenance
- Durability of materials and structures
- Repair methods
- Architectural design integration
- Interaction with HVAC systems and solar shading
- Indoor environmental quality: air quality, daylight, thermal comfort and acoustics
- Passive, active and low-energy buildings, zero-emission buildings
- Retrofitting and conservation of buildings, including historical buildings
- Building sustainability and circularity
- Integrated BIM solutions for building physics, energy performance and indoor environmental quality
- Education about building physics: innovative tools and methods

The 250 participants of NSB 2023 attended a total of 3 keynotes, 186 paper presentations (149 Scientific Papers and 37 Technical Papers) and one workshop over 3 days and 34 sessions. The Scientific Papers (6-8 pages) are published in the conference proceedings: IOP Journal of Physics – Conference Series. The Technical Papers (1-6 pages) are published by Aalborg University and compiled in the present book of technical papers.

All papers presented at NSB 2023 and published in the proceedings or book of technical papers went through a 3-stage double-blind peer-review process: review and acceptance of the abstract, first round of review for the full paper, second round of review of the revised paper, final decision on the paper. All reviews were conducted by the 124 members of the scientific community.

More information about NSB 2023 can be found on the dedicated website: <https://www.en.build.aau.dk/web/nsb2023> and <https://vbn.aau.dk/en/activities/nsb-2023-13th-nordic-symposium-on-building-physics>.

Dr. Hicham Johra
Scientific Committee Chair
Associate Professor
Department of the Built Environment
Aalborg University
Denmark

Conference Organising Committee

Ruut Hannele Peuhkuri, Conference Chair
Research Director, Aalborg University

Per Heiselberg, Deputy Conference Chair
Professor, Aalborg University

Hicham Johra, Scientific Committee Chair
Associate Professor, Aalborg University

Helen Halkjær Andersen
Division Secretary, Aalborg University

Vivi Søndergaard
Academic Officer, Aalborg University

Kim B. Wittchen
Senior Researcher, Aalborg University

Carsten Rode
Professor, Technical University of Denmark

Steffen Petersen
Professor, Aarhus University

Torben Valdbjørn Rasmussen
Senior Researcher, Aalborg University

Nebojsa Jakica
Associate Professor, University of Southern Denmark

Scientific Committee

Hicham Johra, Scientific Committee Chair, Associate Professor, Aalborg University

Thomas Lewis, University Assistant, Vienna University of Technology, Austria

Evy Vereecken, Researcher, Buildwise, Belgium

Dirk Saelens, Professor, KU Leuven, Belgium

Hans Janssen, Professor, KU Leuven, Belgium

Staf Roels, Professor, KU Leuven, Belgium

Bert Blocken, Professor, KU Leuven, Belgium

Hua Ge, Professor, Concordia University, Canada

Wahid Maref, Professor, École de Technologie Supérieure, Canada

Umberto Berardi, Professor, Toronto Metropolitan University, Canada

Dominique Derome, Professor, Université de Sherbrooke, Canada

Carey J. Simonson, Professor, University of Saskatchewan, Canada

Phalguni Mukhopadhyaya, Professor, University of Victoria, Canada

Li Liu, Associate Professor, Tsinghua University, China

Jan Tywoniak, Professor, Czech Technical University in Prague, Czech Republic

Robert Cerný, Professor, Czech Technical University in Prague, Czech Republic

Pavel Kopecky, Researcher, Czech Technical University in Prague, Czech Republic

Kamil Staněk, Researcher, Czech Technical University in Prague, Czech Republic

Anna Marszał-Pomianowska, Associate Professor, Aalborg University, Denmark

Birgitte Andersen, Associate Professor, Aalborg University, Denmark

Ernst Jan de Place Hansen, Senior Researcher, Aalborg University, Denmark

Jørgen Rose, Senior Researcher, Aalborg University, Denmark

Kim B. Wittchen, Senior Researcher, Aalborg University, Denmark

Kirstine Meyer Frandsen, Ph.D. Researcher, Aalborg University, Denmark

Martin Morelli, Senior Researcher, Aalborg University, Denmark

Nickolaj Feldt Jensen, PostDoc Researcher, Aalborg University, Denmark

Olena Kalyanova Larsen, Associate Professor, Aalborg University, Denmark

Per Heiselberg, Professor, Aalborg University, Denmark

Ruut Hannele Peuhkuri, Research Director, Aalborg University, Denmark

Tessa Kvist Hansen, Assistant Professor, Aalborg University, Denmark

Torben Valdbjørn Rasmussen, Senior Researcher, Aalborg University, Denmark

Anne Sørensen, Associate Professor, Aarhus University, Denmark

Mikkel K. Kragh, Professor, Aarhus University, Denmark

Steffen Petersen, Associate Professor, Aarhus University, Denmark

Morten Hjorslev Hansen, Researcher, Byg-Erfa, Denmark

Thor Hansen, Researcher, Danish Technological Institute, Denmark

Lies Vanhoutteghem, Researcher, Danish Technological Institute, Denmark

Carsten Rode, Professor, Technical University of Denmark, Denmark

Christian Anker Hviid, Associate Professor, Technical University of Denmark, Denmark

Eva Møller, Professor, Technical University of Denmark, Denmark

Jørn Toftum, Professor, Technical University of Denmark, Denmark

Menghao Qin, Associate Professor, Technical University of Denmark, Denmark

Ongun Berk Kazanci, Associate Professor, Technical University of Denmark, Denmark

Toke Rammer Nielsen, Associate Professor, Technical University of Denmark, Denmark

Emil Engelund Thybring, Associate Professor, University of Copenhagen, Denmark

Muhyiddine Jradi, Associate Professor, University of Southern Denmark, Denmark

Nebojsa Jakica, Associate Professor, University of Southern Denmark, Denmark

Lucile Sarran, Researcher, Velux, Denmark

Aime Ruus, Associate Professor, Tallinn University of Technology, Estonia

Alo Mikola, Researcher, Tallinn University of Technology, Estonia

Anti Hamburg, Researcher, Tallinn University of Technology, Estonia

Endrik Arumägi, Senior Researcher, Tallinn University of Technology, Estonia

Jaanus Hallik, Researcher, Tallinn University of Technology, Estonia

Jarek Kurnitski, Professor, Tallinn University of Technology, Estonia

Kalle Kuusk, Senior Researcher, Tallinn University of Technology, Estonia

Martin Thalfeldt, Assistant Professor, Tallinn University of Technology, Estonia

Paul Klõšeiko, Researcher, Tallinn University of Technology, Estonia

Targo Kalamees, Professor, Tallinn University of Technology, Estonia

Xiaoshu Lü, Professor, Aalto University, Finland

Miia Pitkäranta, Senior Researcher, AFRY Buildings Finland Oy, Finland

Pauli Sekki, Ph.D. Researcher, AFRY Buildings Finland Oy, Finland

Mikko Koskivuori, Development Manager, AFRY Buildings Finland Oy, Finland

Juha Vinha, Professor, Tampere University, Finland

Jukka Lahdensivu, Associate Professor, Tampere University, Finland

Jérôme Le Dréau, Associate Professor, La Rochelle University, France

Johann Meulemans, Senior Researcher, Saint-Gobain, France

Florence Collet, Professor, University of Rennes, France

Florian Antretter, Researcher, C3RROLUTIONS GMBH, Germany

Andreas Nicolai, Research Assistant, Dresden University of Technology, Germany

Peggy Freudenberg, Researcher, Dresden University of Technology, Germany

John Grunewald, Professor, Dresden University of Technology, Germany

Klaus Peter Sedlbauer, Professor, Technical University of Munich, Germany

Enrico Fabrizio, Associate Professor, Politecnico di Torino, Italy

Marco Perino, Professor, Politecnico di Torino, Italy

Shuichi Hokoi, Professor, Kyoto University, Japan

Anatolijs Borodinecs, Professor, Riga Technical University, Latvia

Andra Blumberga, Professor, Riga Technical University, Latvia

Andrius Jurelionis, Professor, Kaunas University of Technology, Lithuania

Jurga Kumžienė, Researcher, Kaunas University of Technology, Lithuania

Karolis Banionis, Researcher, Kaunas University of Technology, Lithuania

Raimondas Bliūdžius, Professor, Kaunas University of Technology, Lithuania

Rosita Norvaišienė, Researcher, Kaunas University of Technology, Lithuania

Mari Sand Austigard, Researcher, Mycoteam, Norway

Arnkell Jonas Petersen, Associate Professor, Norwegian University of Science and Technology, Norway

Francesco Goia, Professor, Norwegian University of Science and Technology, Norway

Gabriele Lobaccaro, Associate Professor, Norwegian University of Science and Technology, Norway

Hans Martin Mathisen, Professor, Norwegian University of Science and Technology, Norway

Laurent Georges, Associate Professor, Norwegian University of Science and Technology, Norway

Tore Kvande, Professor, Norwegian University of Science and Technology, Norway

Dimitrios Kraniotis, Associate Professor, OsloMET, Norway

Aileen Yang, Researcher, SINTEF, Norway

Berit Time, Chief Scientist, SINTEF, Norway

Lars Gullbrekken, Research Manager, SINTEF, Norway

Peng Liu, Senior Researcher, SINTEF, Norway

Petra Rütther, Research Manager, SINTEF, Norway

Roberta Moschetti, Researcher, SINTEF, Norway

Silje Kathrin Asphaug, Researcher, SINTEF, Norway

Steinar Grynning, Senior Business Developer, SINTEF, Norway

Stig Geving, Professor, SINTEF, Norway

Sverre Bjørn Holøs, Senior Researcher, SINTEF, Norway

Dariusz Gawin, Professor, Lodz University of Technology, Poland

Dariusz Heim, Associate Professor, Lodz University of Technology, Poland

Manuela Almeida, Associate Professor, University of Minho, Portugal

Nuno Ramos, Associate Professor, University of Minho, Portugal

Peter Matiašovský, Deputy Director, Slovak Academy of Sciences, Slovak Republic

Angela Sasic Kalagasidis, Professor, Chalmers University of Technology, Sweden

Pär Johansson, Associate Professor, Chalmers University of Technology, Sweden

Dennis Johansson, Researcher, Lund University, Sweden

Lars-Erik Harderup, Associate Professor, Lund University, Sweden

Kristina Mjörnell, Adjunct Professor, Research Institutes of Sweden (RISE); Lund University, Sweden

Lars Olsson, Researcher, Research Institutes of Sweden (RISE), Sweden

Folke Björk, Professor, Royal Institute of Technology (KTH), Sweden

Thomas Olofsson, Professor, Umeå University, Sweden

Tor Broström, Professor, Uppsala University, Sweden

Jan Wienold, Researcher, École Polytechnique Fédérale de Lausanne (EPFL), Switzerland

Matthias Haase, Professor, Zurich University of Applied Sciences, Switzerland

Ekaterina Petrova, Assistant Professor, Eindhoven University of Technology, The Netherlands

Hector Altamirano, Associate Professor, University College London, UK

Valentina Marincioni, Lecturer, University College London, UK

Yasemin Didem Aktas, Assistant Professor, University College London, UK

Parham Mirzaei Ahranjani, Assistant Professor, University of Nottingham, UK

André Desjarlais, Program Manager, Oak Ridge National Laboratory, USA

Mikael Salonvaara, Senior Researcher, Oak Ridge National Laboratory, USA

Samuel V. Glass, Researcher, U.S. Forest Products Laboratory, USA

List of Sponsors



AIRMASTER



List of all Technical Papers

- B. Sagaiyaraj (2023). **Increasing Energy Efficiency of Central Cooling Systems with Engineered Nanofluids**. In H. Johra (Ed.), *NSB 2023 - Book of Technical Papers: 13th Nordic Symposium on Building Physics* (Vol. 13) [100]. Department of the Built Environment, Aalborg University. <https://doi.org/10.54337/aau538344493>.
- H. Johra, A.R. Hansen & L. Rohde (2023). **Do International Building Researchers Mostly Work Right Before the Deadline? Yes, According to Empirical Data**. In H. Johra (Ed.), *NSB 2023 - Book of Technical Papers: 13th Nordic Symposium on Building Physics* (Vol. 13) [103]. Department of the Built Environment, Aalborg University. <https://doi.org/10.54337/aau541562346>.
- M. Dolgunovas & R. Norvaišienė (2023). **Analysis of Hybrid Timber Construction by Multiple Criteria Decision-Making Method**. In H. Johra (Ed.), *NSB 2023 - Book of Technical Papers: 13th Nordic Symposium on Building Physics* (Vol. 13) [128]. Department of the Built Environment, Aalborg University. <https://doi.org/10.54337/aau541025944>.
- H.P. Tuniki, G. Bekö & A. Jurelionis (2023). **Using Adaptive Behaviour Patterns of Open Plan Office Occupants in Energy Consumption Predictions**. In H. Johra (Ed.), *NSB 2023 - Book of Technical Papers: 13th Nordic Symposium on Building Physics* (Vol. 13) [144]. Department of the Built Environment, Aalborg University. <https://doi.org/10.54337/aau541563857>.
- D. Bjelland & B.D. Hrynyszyn (2023). **Energy retrofitting of non-residential buildings with effects on the indoor environment: a study of university buildings at NTNU in Trondheim, Norway**. In H. Johra (Ed.), *NSB 2023 - Book of Technical Papers: 13th Nordic Symposium on Building Physics* (Vol. 13) [151]. Department of the Built Environment, Aalborg University. <https://doi.org/10.54337/aau541564763>.
- J. Tywoniak, K. Sojková & Z. Malik (2023). **Building Physics in Living Lab**. In H. Johra (Ed.), *NSB 2023 - Book of Technical Papers: 13th Nordic Symposium on Building Physics* (Vol. 13) [152]. Department of the Built Environment, Aalborg University. <https://doi.org/10.54337/aau541565072>.
- B.H. Høegh, L. Vanhouttegehem & T. Hansen (2023). **Documentation of moisture reduction up to two years after refurbishment of moisture damaged exterior basement wall**. In H. Johra (Ed.), *NSB 2023 - Book of Technical Papers: 13th Nordic Symposium on Building Physics* (Vol. 13) [158]. Department of the Built Environment, Aalborg University. <https://doi.org/10.54337/aau541578714>.
- G. Kayo & N. Suzuki (2023). **Measurement of air change behaviour at Finnish apartment rooms**. In H. Johra (Ed.), *NSB 2023 - Book of Technical Papers: 13th Nordic Symposium on Building Physics* (Vol. 13) [165]. Department of the Built Environment, Aalborg University. <https://doi.org/10.54337/aau541579038>.
- R.C. Veloso, C. Dias, A.R. Souza, J. Maia, N.M.M. Ramos & J. Ventura (2023). **Improving the optical properties of finishing coatings for façade systems**. In H. Johra (Ed.), *NSB 2023 - Book of Technical Papers: 13th Nordic Symposium on Building Physics* (Vol. 13) [179]. Department of the Built Environment, Aalborg University. <https://doi.org/10.54337/aau541592743>.
- Z. Ai & Z. Jia (2023). **Accurate CFD prediction of respiratory airflow and dispersion through face mask**. In H. Johra (Ed.), *NSB 2023 - Book of Technical Papers: 13th Nordic Symposium on Building Physics* (Vol. 13) [186]. Department of the Built Environment, Aalborg University. <https://doi.org/10.54337/aau541592930>.
- L. Giroux-Gauthier, A. Kubilay, A. Maheu, S. Wood, J. Carmeliet & D. Derome (2023). **Modelling of rain interception by trees in outdoor urban climate**. In H. Johra (Ed.), *NSB 2023 - Book of Technical Papers: 13th Nordic Symposium on Building Physics* (Vol. 13) [198]. Department of the Built Environment, Aalborg University. <https://doi.org/10.54337/aau541594014>.
- M. Zygmunt & D. Gawin (2023). **Residents' thermal comfort and energy performance of a single-family house in Poland: a parametric study**. In H. Johra (Ed.), *NSB 2023 - Book of Technical Papers: 13th Nordic Symposium on Building Physics* (Vol. 13) [209]. Department of the Built Environment, Aalborg University. <https://doi.org/10.54337/aau541595604>.

- J. Brozovsky, O. Oksavik & P. Rüther (2023). **Temperature measurements in the air gap of highly insulated wood-frame walls in a Zero Emission Building**. In H. Johra (Ed.), *NSB 2023 – Book of Technical Papers: 13th Nordic Symposium on Building Physics* (Vol. 13) [212]. Department of the Built Environment, Aalborg University. https://doi.org/10.54337/aau541595903_2.
- R. Moschetti, L. Gullbrekken & J. Maia (2023). **Accelerated climate aging tests of structural insulated panels with waste-based core materials**. In H. Johra (Ed.), *NSB 2023 – Book of Technical Papers: 13th Nordic Symposium on Building Physics* (Vol. 13) [225]. Department of the Built Environment, Aalborg University. <https://doi.org/10.54337/aau541597546>.
- A. Borodinecs, A. Zajacs & A. Palcikovskis (2023). **Modular retrofitting approach for residential buildings**. In H. Johra (Ed.), *NSB 2023 – Book of Technical Papers: 13th Nordic Symposium on Building Physics* (Vol. 13) [230]. Department of the Built Environment, Aalborg University. <https://doi.org/10.54337/aau541598583>.
- B. Paule, F. Flourentzou, T.D. Kerchove d'Exaerde, J. Boutillier & N. Ferrari (2023). **PRELUDE Roadmap for Building Renovation: set of rules for renovation actions to optimize building energy performance**. In H. Johra (Ed.), *NSB 2023 – Book of Technical Papers: 13th Nordic Symposium on Building Physics* (Vol. 13) [238]. Department of the Built Environment, Aalborg University <https://doi.org/10.54337/aau541614638>.
- S.V. Glass, S.L. Zelinka, C.R. Boardman & E.E. Thybring (2023). **Promoting advances in understanding water vapor sorption in wood: relegating popular models and misconceptions**. In H. Johra (Ed.), *NSB 2023 – Book of Technical Papers: 13th Nordic Symposium on Building Physics* (Vol. 13). [239] Department of the Built Environment, Aalborg University. <https://doi.org/10.54337/aau541615744>.
- N. Dumas, F. Flourentzos, J. Boutillier, B. Paule & T.D. Kerchove d'Exaerde (2023). **Integration of smart building technologies costs and CO2 emissions within the framework of the new EPIQR-web application**. In H. Johra (Ed.), *NSB 2023 – Book of Technical Papers: 13th Nordic Symposium on Building Physics* (Vol. 13). [246] Department of the Built Environment, Aalborg University. <https://doi.org/10.54337/aau541616188>.
- E. Vereecken, M. Prignon, A. Tilmans & T.D. Mets (2023). **HAMSTER Test Facility – Features and future Potential of a unique bi-climatic Chamber**. In H. Johra (Ed.), *NSB 2023 – Book of Technical Papers: 13th Nordic Symposium on Building Physics* (Vol. 13). [253] Department of the Built Environment, Aalborg University. <https://doi.org/10.54337/aau541620389>.
- P. Sekki, E. Saleva & P. Laamanen (2023). **Study of ventilated low-slope and large span wooden element roofs in the current and future climate**. In H. Johra (Ed.), *NSB 2023 – Book of Technical Papers: 13th Nordic Symposium on Building Physics* (Vol. 13). [275] Department of the Built Environment, Aalborg University. <https://doi.org/10.54337/aau541620957>.
- C. Roy, D. Derome & C. Frenette (2023). **Modelling hygrothermal performance of wood assemblies exposed to fungi growth**. In H. Johra (Ed.), *NSB 2023 – Book of Technical Papers: 13th Nordic Symposium on Building Physics* (Vol. 13). [277] Department of the Built Environment, Aalborg University. <https://doi.org/10.54337/aau541621854>.
- N.M.M. Ramos, J. Maia, R.C. Veloso, A.R. Souza, C. Dias & J. Ventura (2023). **Envelope systems with high solar reflectance by the inclusion of nanoparticles – an overview of the EnReflect Project**. In H. Johra (Ed.), *NSB 2023 – Book of Technical Papers: 13th Nordic Symposium on Building Physics* (Vol. 13). [282] Department of the Built Environment, Aalborg University. <https://doi.org/10.54337/aau541621982>.
- U. Ruisinger & H. Sonntag (2023). **Internal insulation: two condensed guidelines for beginners**. In H. Johra (Ed.), *NSB 2023 – Book of Technical Papers: 13th Nordic Symposium on Building Physics* (Vol. 13). [296] Department of the Built Environment, Aalborg University. <https://doi.org/10.54337/aau541623517>.
- A. Witzig, C. Tello, F. Schranz, J. Bruderer & M. Haase (2023). **Quantifying energy-saving measures in office buildings by simulation in 2D cross sections**. In H. Johra (Ed.), *NSB 2023 – Book of Technical Papers: 13th Nordic Symposium on Building Physics* (Vol. 13). [317] Department of the Built Environment, Aalborg University. <https://doi.org/10.54337/aau541623658>.
- N.F. Björk (2023). **Studies of hygrothermal processes in a façade by long term high resolution measurements**. In H. Johra (Ed.), *NSB 2023 – Book of Technical Papers: 13th Nordic Symposium on Building Physics* (Vol. 13). [332] Department of the Built Environment, Aalborg University. <https://doi.org/10.54337/aau541637898>.
- A. Kubilay, J. Bourcet, J. Carmeliet & D. Derome (2023). **How to predict wind driven rain in a changing climate?** In H. Johra (Ed.), *NSB 2023 – Book of Technical Papers: 13th Nordic Symposium on Building Physics* (Vol. 13). [334] Department of the Built Environment, Aalborg University. <https://doi.org/10.54337/aau541649835>.

- P. Liu & C. Iba (2023). **Influence of Energy-saving Renovation Plan on the Hygrothermal Distribution Inside Kyo-machiya Soil Walls Considering their Moisture Buffering Effect.** In H. Johra (Ed.), *NSB 2023 - Book of Technical Papers: 13th Nordic Symposium on Building Physics* (Vol. 13). [341] Department of the Built Environment, Aalborg University. <https://doi.org/10.54337/aau541650556>.
- M. Salonvaara & A. Desjarlais (2023). **The impact of the solar absorption coefficient of roof and wall surfaces on energy use and peak demand.** In H. Johra (Ed.), *NSB 2023 - Book of Technical Papers: 13th Nordic Symposium on Building Physics* (Vol. 13). [350] Department of the Built Environment, Aalborg University. <https://doi.org/10.54337/aau541650886>.
- E. Tanaka, R. Schwerd, W. Hofbauer & D. Zirkelbach (2023). **Laboratory tests on decay of natural fibre insulation materials suggest a more differentiated evaluation and higher RH thresholds.** In H. Johra (Ed.), *NSB 2023 - Book of Technical Papers: 13th Nordic Symposium on Building Physics* (Vol. 13). [370] Department of the Built Environment, Aalborg University. <https://doi.org/10.54337/aau541651346>.
- P. Mukhopadhyaya, M. Mahmoodzadeh, V. Gretka & I. Lee (2023). **Use of Thermography for Quantitative Building Envelope Thermal Performance Analysis.** In H. Johra (Ed.), *NSB 2023 - Book of Technical Papers: 13th Nordic Symposium on Building Physics* (Vol. 13). [383] Department of the Built Environment, Aalborg University. <https://doi.org/10.54337/aau541985169>.
- T. Kauppinen, M. Hienonen & F. Fedorik (2023). **The co-operation between the University and the Industry association in the application of building physics results to practice.** In H. Johra (Ed.), *NSB 2023 - Book of Technical Papers: 13th Nordic Symposium on Building Physics* (Vol. 13). [396] Department of the Built Environment, Aalborg University. <https://doi.org/10.54337/aau541651956>.
- F. Meißner, H. Sonntag & A. Morandell-Meißner (2023). **Water uptake measurement for thermal renovations – comparison between non-destructive method, the Karsten tube, and automatic laboratory measurements.** In H. Johra (Ed.), *NSB 2023 - Book of Technical Papers: 13th Nordic Symposium on Building Physics* (Vol. 13). [407] Department of the Built Environment, Aalborg University. <https://doi.org/10.54337/aau541652209>.
- M. Duan, L. Liu, G. Da, Y. Wang & E. Géhin (2023). **Assessing the relative importance of Mucosal exposure and inhalation exposure to airborne particles.** In H. Johra (Ed.), *NSB 2023 - Book of Technical Papers: 13th Nordic Symposium on Building Physics* (Vol. 13). [10001] Department of the Built Environment, Aalborg University. <https://doi.org/10.54337/aau541653952>.
- Y. Fu, S. Liu, W. Chen, G. Ruan & L. Liu (2023). **Assessing the impact of ventilation on the potential airborne infection risk in hospital lung function room.** In H. Johra (Ed.), *NSB 2023 - Book of Technical Papers: 13th Nordic Symposium on Building Physics* (Vol. 13). [10002] Department of the Built Environment, Aalborg University. <https://doi.org/10.54337/aau541663876>.
- P.V. Nielsen, C. Zhang & L. Liu (2023). **Airborne transmission of disease in stratified flow.** In H. Johra (Ed.), *NSB 2023 - Book of Technical Papers: 13th Nordic Symposium on Building Physics* [10003] Department of the Built Environment, Aalborg University. <https://doi.org/10.54337/aau541985833>.
- H. Qian, J. Ma & P.V. Nielsen (2023). **Exploring the Role of Ambient Temperature in Exhaled Jet Related to Cross Infection between Individuals by CFD.** In H. Johra (Ed.), *NSB 2023 - Book of Technical Papers: 13th Nordic Symposium on Building Physics* (Vol. 13). [10004] Department of the Built Environment, Aalborg University. <https://doi.org/10.54337/aau541987560>.
- S. Mousavi, B. Rismanchi, S. Brey, L. Aye (2023). **Experimental evaluation of PCM embedded radiant chilled ceiling for efficient space cooling.** In H. Johra (Ed.), *NSB 2023 - Book of Technical Papers: 13th Nordic Symposium on Building Physics* (Vol. 13). [333] Department of the Built Environment, Aalborg University. <https://doi.org/10.54337/aau609928685>.

Compilation of all Technical Papers



Aalborg Universitet

AALBORG UNIVERSITY
DENMARK

Increasing Energy Efficiency of Central Cooling Systems with Engineered Nanofluids

Sagaiyaraj, Bernard

DOI (link to publication from Publisher):
[10.54337/aau538344493](https://doi.org/10.54337/aau538344493)

[Link to publication from Aalborg University](#)

Citation for published version (APA):
Sagaiyaraj, B. (2023). Increasing Energy Efficiency of Central Cooling Systems with Engineered Nanofluids. In H. Johra (Ed.), *NSB 2023 - Book of Technical Papers: 13th Nordic Symposium on Building Physics* Department of the Built Environment, Aalborg University. <https://doi.org/10.54337/aau538344493>

Increasing Energy Efficiency of Central Cooling Systems with Engineered Nanofluids

Bernard Sagaiyaraj

Blue Snow Energy

bernard@bluesnowenergy.com

Abstract: Buildings consume about 40% of the world's energy consumption and of that, 65% is dedicated to cooling (or heating) systems. Central building cooling uses water as the main heat transfer medium. The nanoparticle fluid suspension exhibits thermal properties superior to water. The goal was to achieve the highest possible thermal properties with just the right amount of nanoparticles in a uniform and stable dispersion and suspension in water. This engineered nanofluid contains a uniform and stable suspension of graphene nanoparticles (GNP) in water. Using covalent functionalization, centrifugation and high-speed dispersion, the GNP remains in a stable suspension indefinitely. The nanofluid is applied to the closed loop of the chilled water system, where the heat transfer enhancement occurs at the fluid tubes within the evaporator and the tubing in the chilled water coils within the Air Handling Units (AHUs). The Proof of Concept (POC) completed in 2019 using laboratory-derived nanofluid resulted in energy savings that averaged at 32% compared with the baseline fluid (water). In 2022, a Scaled-Up mini plant produced GNP nanofluids in a commercial process environment, showing an average energy savings of 21%. These results were further verified and validated on small chilled water plants outside of the Scaled-Up plant with 25% and 29% average savings.

1. Introduction

High-performance cooling is one of the most vital needs of many industries. All past efforts to improve cooling technology were made by improving systems and equipment but with very little focus on heat transfer fluids. Liquids are used in cooling systems to help dissipate heat or maintain an even temperature. A nanofluid coolant would significantly enhance this process to benefit a range of industries, such as refrigeration systems, data centre cooling and battery cooling. As illustrated in Figure 1, graphene is an allotrope of carbon consisting of a single layer of atoms arranged in a two-dimensional honeycomb lattice.

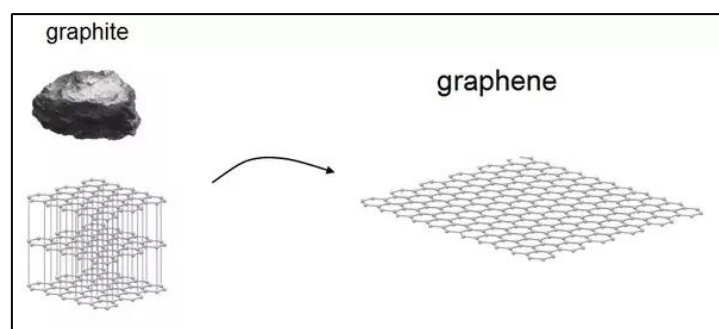


Figure 1: Graphene vs Graphite (From Graphene: The Material That Is Changing The World by Charlotte Brown 2021[1])

Each atom in a graphene sheet is connected to its three nearest neighbors by a σ or sigma bond, and contributes one electron to a conduction band (the $2p_z$ orbital) that extends over the whole sheet and makes graphene a semimetal with unusual electronic properties. Graphene conducts both heat and electricity very efficiently along its plane. It also strongly absorbs light of all visible wavelengths and that is why it appears black, but a single graphene sheet is nearly transparent because it is extremely

thin. The material is also about one hundred times stronger than would be the strongest steel of the same thickness.

Although graphene has various excellent properties, the one that is of main interest in this paper is its thermal properties. Thermal transport in graphene is still an active area of research, which has attracted attention because of the potential for thermal management applications.

1.1 Graphene Nanofluid

The basic concept of dispersing solids in fluids to enhance thermal conductivity is not new; solid particles were added in the past because they conduct heat much better than liquids. The major problem with the use of microparticles is the rapid settling of these particles in fluids. Other problems include abrasion and clogging. These problems are highly undesirable for many practical cooling applications. Nanofluids overcome these problems by stably suspending nanometer-sized particles in base fluids. Nanoparticles stay suspended much longer and possess a much higher surface area. The surface/volume ratio of nanoparticles is one thousand times larger than that of microparticles. The high surface area of nanoparticles enhances the thermal conductivity of nanofluids since heat transfer occurs on the surface of the particle.

These unique properties of nanoparticles are exploited to develop nanofluids for heat transfer systems possessing extreme stability and ultrahigh thermal conductivity. Other benefits of nanofluid include decreased demand for pumping power, reduced inventory of heat transfer fluid (through initial design) and significant energy savings. Stable suspension of minuscule quantities of nanoparticles makes the base fluid cool faster and thermal management systems smaller and lighter.

This is a technical paper built on applied research on graphene nanofluids by which the production method is the subject of a patent filed by this author [2]. The patent filed was for the laboratory method production of the nanofluid and this paper focuses on the application and the validation of the performance of the nanofluid in commercial chilled water plants. The laboratory-produced nanofluid [2] gave an average of 32% savings compared with the baseline using water but this was tested on a laboratory-scale chilled water system.

2. Work Done and Results

2.1 Nanofluid Production - Lab Scale Proof of Concept Stage (2018 - 2019)

A version of the Two-Step Method was used to produce the nanofluid at our facility and our formulation is patent pending. These nanoparticles in themselves are hydrophobic and are repelled by the molecules of water [2]. The nanoparticles were functionalized using a method called covalent functionalization.

Functionalization makes the GNPs hydrophilic. The final nanofluid is prepared by dispersing the functionalized GNP in water. Once this is complete, agglomeration issues become almost non-existent. To further complete the process to decrease the aggregation and enhance the dispersion capability, the f-GNP is dispersed in an ultrasonic bath and an ultrasonicator.

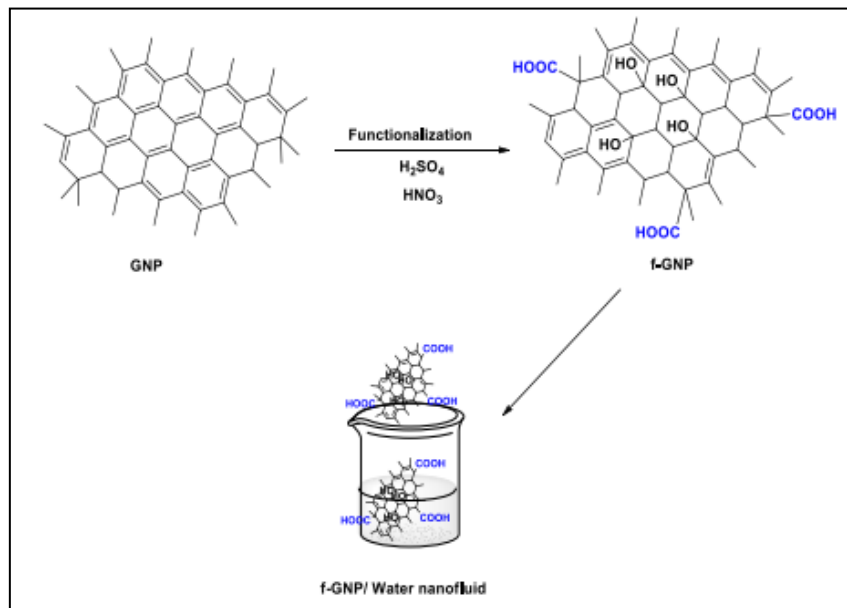
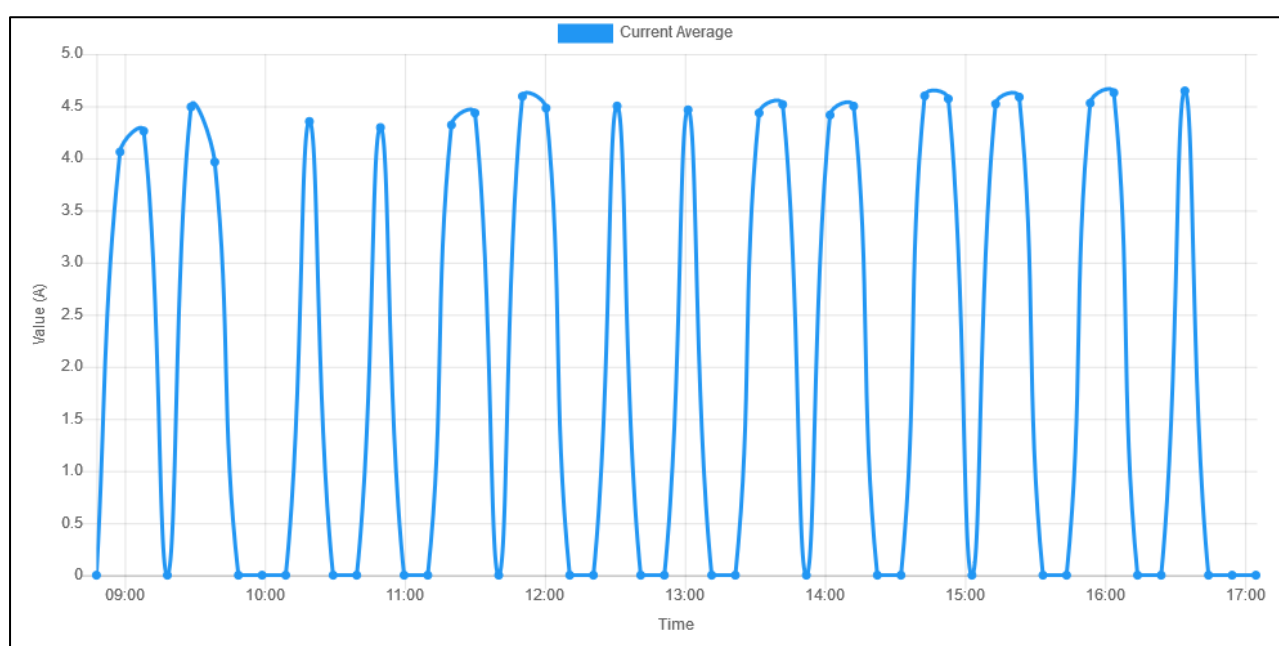
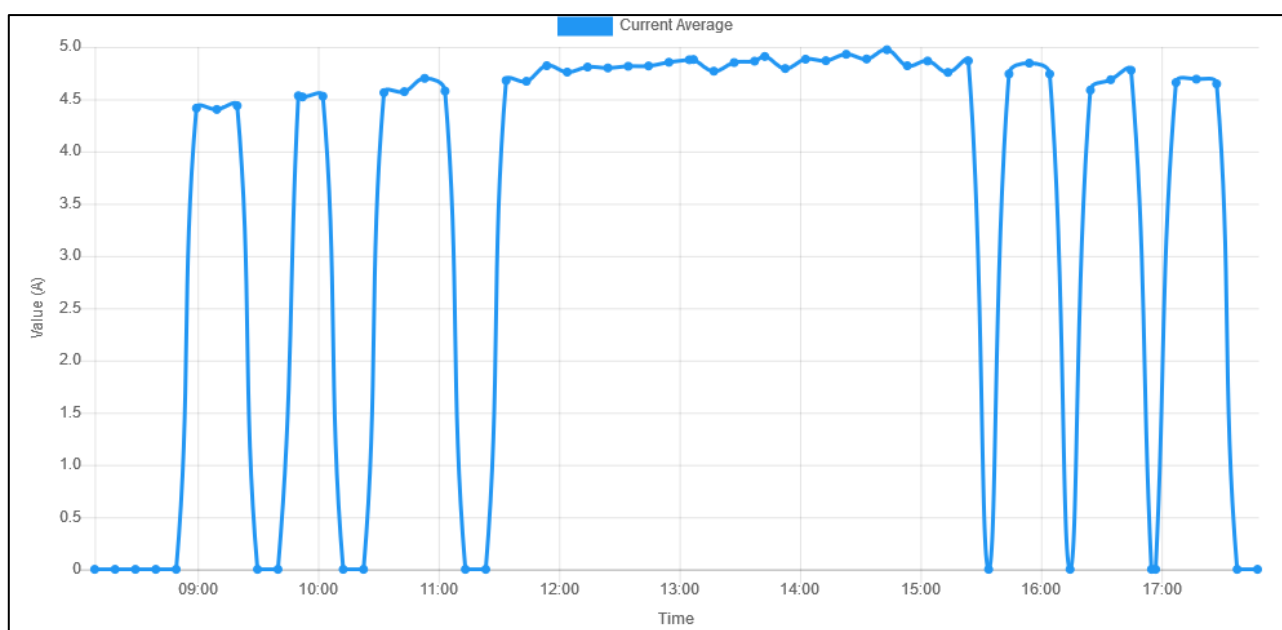


Figure 2: Method of Nanofluid Production

2.2 The POC Test Rig POC (2018-2019)

The GNP nanofluid was tested in a small 1.5 RT (Refrigeration Tons) cooling system. The test rig was connected to a room adjacent to it where the room dry bulb temperature (T) and relative humidity (RH%) and the ambient T and RH% were regularly measured. This was to ensure that both tests i.e., with water or the baseline fluid and with the nanofluid were measured under the same internal and external conditions.

Lower compressor runtimes were observed with the nanofluid. This meant the nanofluid had a better thermal performance compared to water. The 'valleys' in the Figures below represent the time when the compressor cuts off.



The area under the curve (A-s) has a direct relationship to the energy consumed. This was calculated by integrating the curve function between limits (in this case the time signatures). The savings ranged between 18% to 46.1% (average of 32 %). Although this was an excellent result in the world of energy efficiency, the real task ahead was replicating this success in a small industrial-scale manufacturing system, and this was carried out at the Scale-Up stage.

2.3 The Scale-Up Production (2021-2022)

In 2021, the Scale Up lab was designed and installed to produce the nanofluid on a small industrial scale and then test it on a chilled water system to try to replicate the POC results.

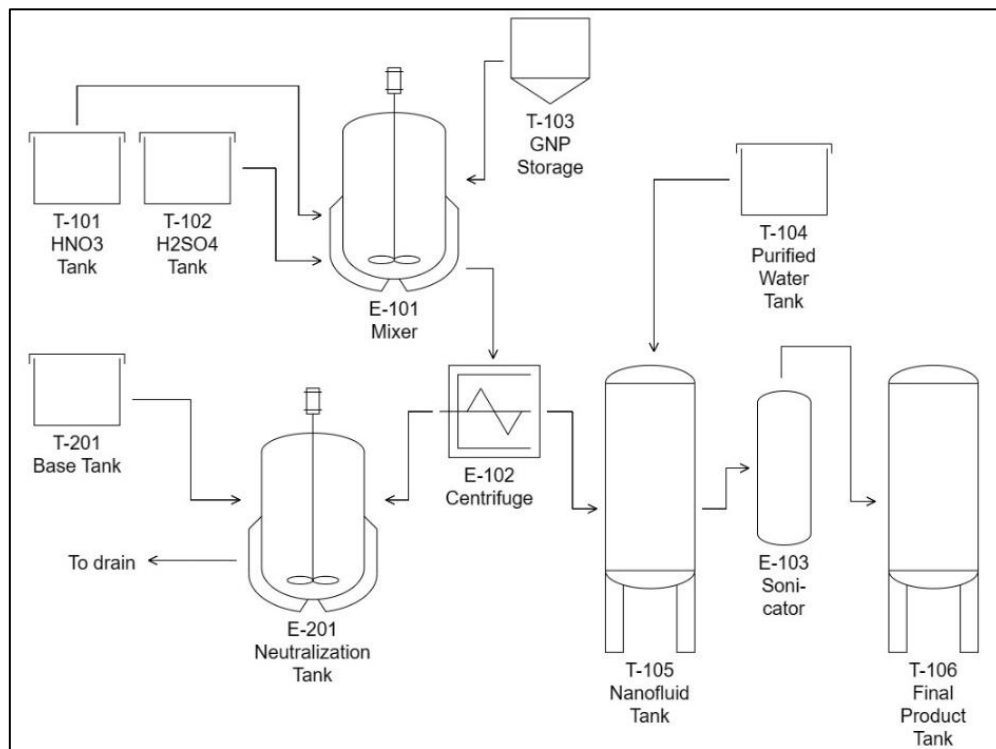


Figure 6: Process flow diagram of production of the nanofluid

Once homogenous mixing is complete, the f-GNP was then sent to centrifuge to produce the f-GNP retentate. Once the desired dispersion was achieved, the nanofluid was stored in a product tank, from which it was pumped into the Scale-Up test rig (Figure 8) for performance testing.

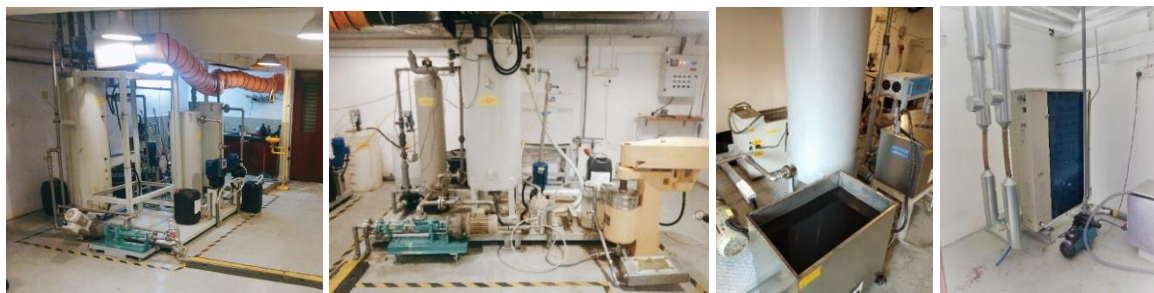


Figure 7: (a) Functionalization (b) Centrifugation (c) Dispersion (d) Test Rig

2.4 The Scale-Up Test Rig

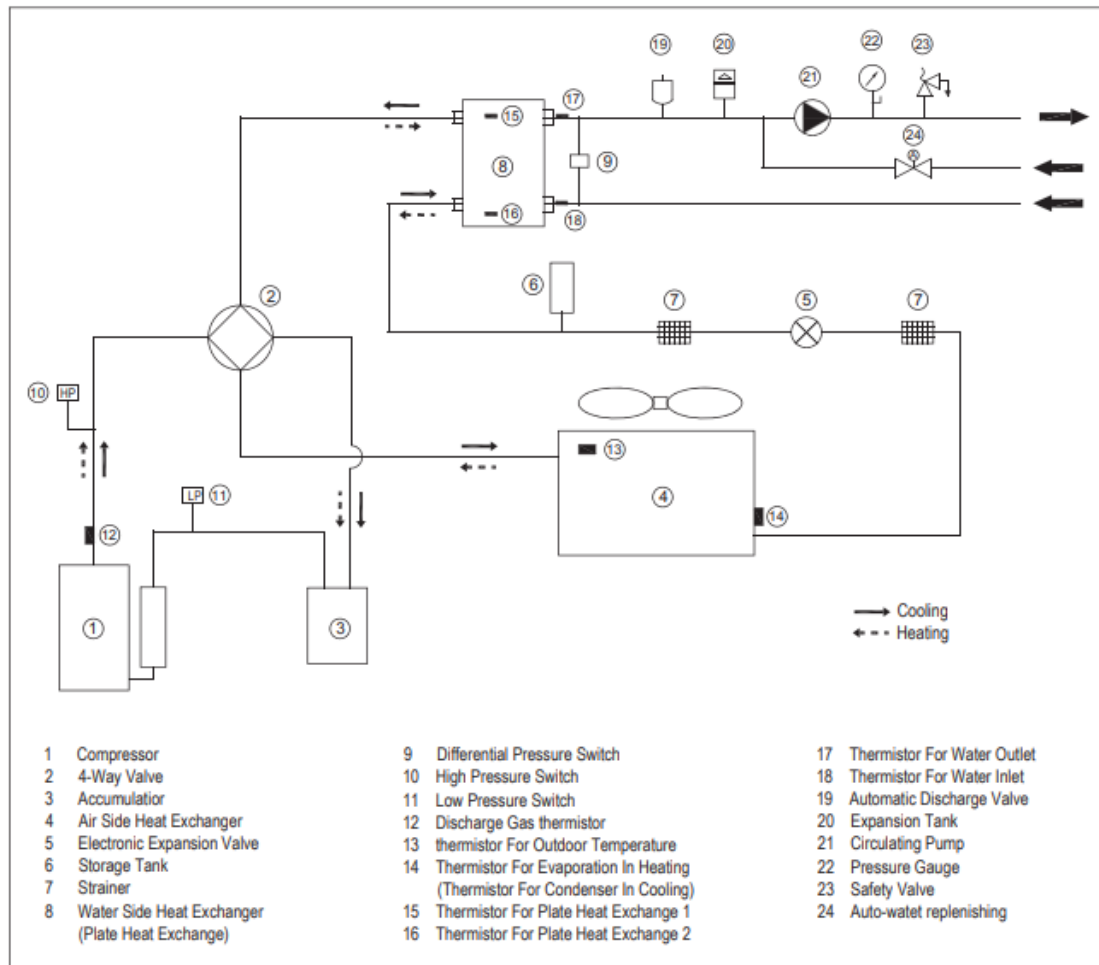


Figure 8: Cooling Test Rig Schematic

To compare both the energy consumed and the heat load, a duration of **330 minutes** were taken for all runs, and this was typically between 9 am and 5.30 pm every day after removing sensor anomalies.

Average Water Run (Nov 21 – Dec 21)	Average Nanofluids Run (Feb 22 – Mar 22)	Savings
1.16	1.14	2%
1.47	1.21	18%
1.67	1.26	24%
1.78	1.23	31%
1.46	1.21	17%
1.87	1.32	30%
1.68	1.23	27%
1.59	1.34	16%
1.58	1.17	26%
1.63	1.23	25%
1.76	1.29	27%
1.35	1.20	11%
Average savings		21%

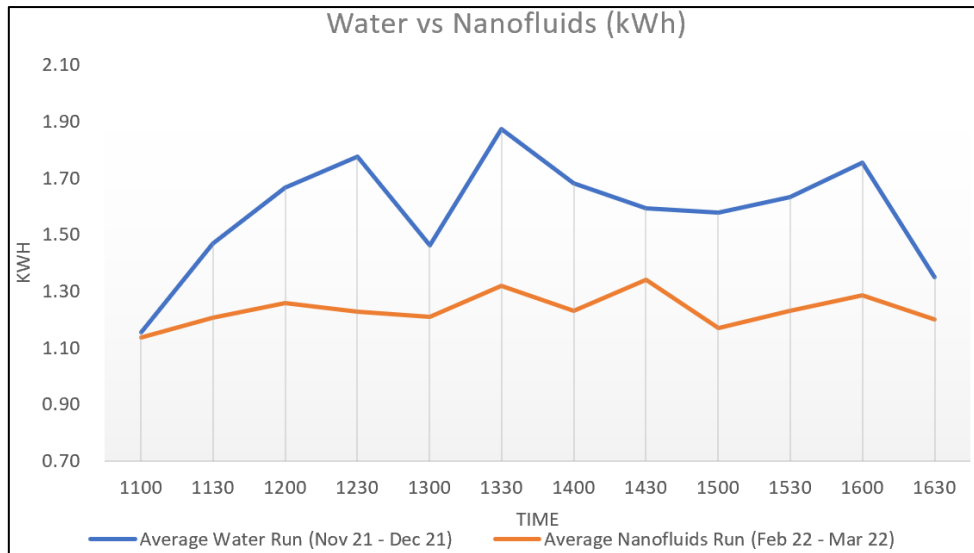


Figure 9: Scale-Up Lab Test Results

The conclusion is that there is an **average energy (kWh) reduction of 21%**.

2.5 Other Outside Lab Results

2.5.1 MFI (Malaysia France Institute) – part of UniKL (Universiti Kuala Lumpur)

An energy performance validation exercise was conducted at Universiti Kuala Lumpur - Malaysia France Institute (UniKL MFI), Bangi. This was conducted from the end of July 2022 to early September 2022. At the HVAC laboratory, the water in the chilled water system was replaced by the nanofluid to observe and measure energy performance improvement.

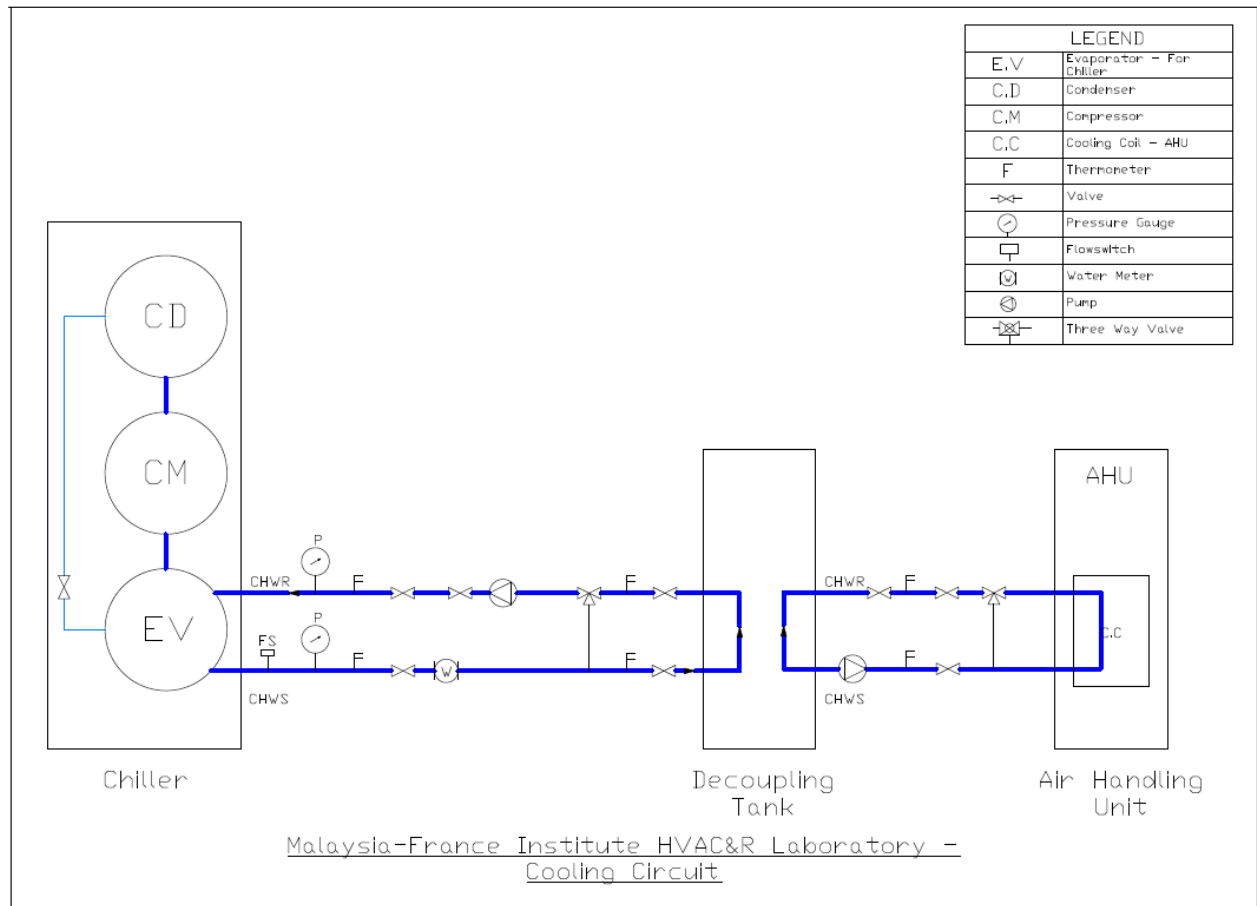


Figure 10: MFI Chiller Plant Set-Up

A duration of **446 minutes** was taken for all runs (between 9 am and 5.30 pm every day).

The following tables are summaries:

Water				
Date	kW	RT	kW/RT	kWh
24 08 2022	12.89	11.34	1.10	95.50
26 08 2022	10.63	10.02	0.96	80.51
Average	11.76	10.68	1.03	88.01
Nanofluid				
Date	kW	RT	kW/RT	kWh
30 08 2022	11.20	11.51	0.86	82.47
10 9 2022	10.92	13.28	0.76	80.89
20 9 2022	12.99	14.98	0.81	96.35
Average	11.69	13.25	0.83	86.88

If based on this result only, energy savings is only 1.3% (86.88 kW vs 88.01 kW). The compressor in this chiller could not modulate except to switch between compressors and that switching capability was unavailable during the testing period.

Water			
kW	RT	kW/RT	kWh
11.76	10.68	1.03	88.01
Nanofluid			
kW	RT	kW/RT	kWh
11.69	13.25	0.83	86.88
Comparison			
kWh	RT	kW/RT	kWh
-1%	24%	-22%	-1.3%

But since that heat load was not constant, the energy consumption needs to be normalized against the variance in the heat load.

Note that the average RT (Refrigeration Tons or the heat load) has increased by 24% during the nanofluid run but the kW/RT or system efficiency has improved by 22%. Using this 24% difference in the RT to normalize the energy consumption, the real energy savings can be obtained as follows:

Normalized			
KWh Nanofluid	82.47	80.89	96.35
KWh Nanofluid (N)	62.59	61.39	73.12
% Saving	-28.9%	-30.2%	-16.9%
Average	-25.3%		

This exercise proved that the nanofluid increased the plant efficiency by **25.3%**

2.5.2 Astana Palace in Kuching

The subsequent energy performance validation exercise was conducted at Astana Palace (Governor's Residence) at Kuching, Sarawak. The validation exercise was conducted over a period of 6 weeks from 29th November 2022 to 17th December 2022.

The measurements were taken between 10.50 am to 5.20 pm and on some days the durations were longer than others because this was an operational building with events running on some of those days (event days: 2 chillers running; normal days: 1 chiller running). To have an unbiased comparison, the period between 12.30 pm and 3.40 pm was selected where energy, load and temperature data was available, a duration of **190 minutes** every day for the 9 days.

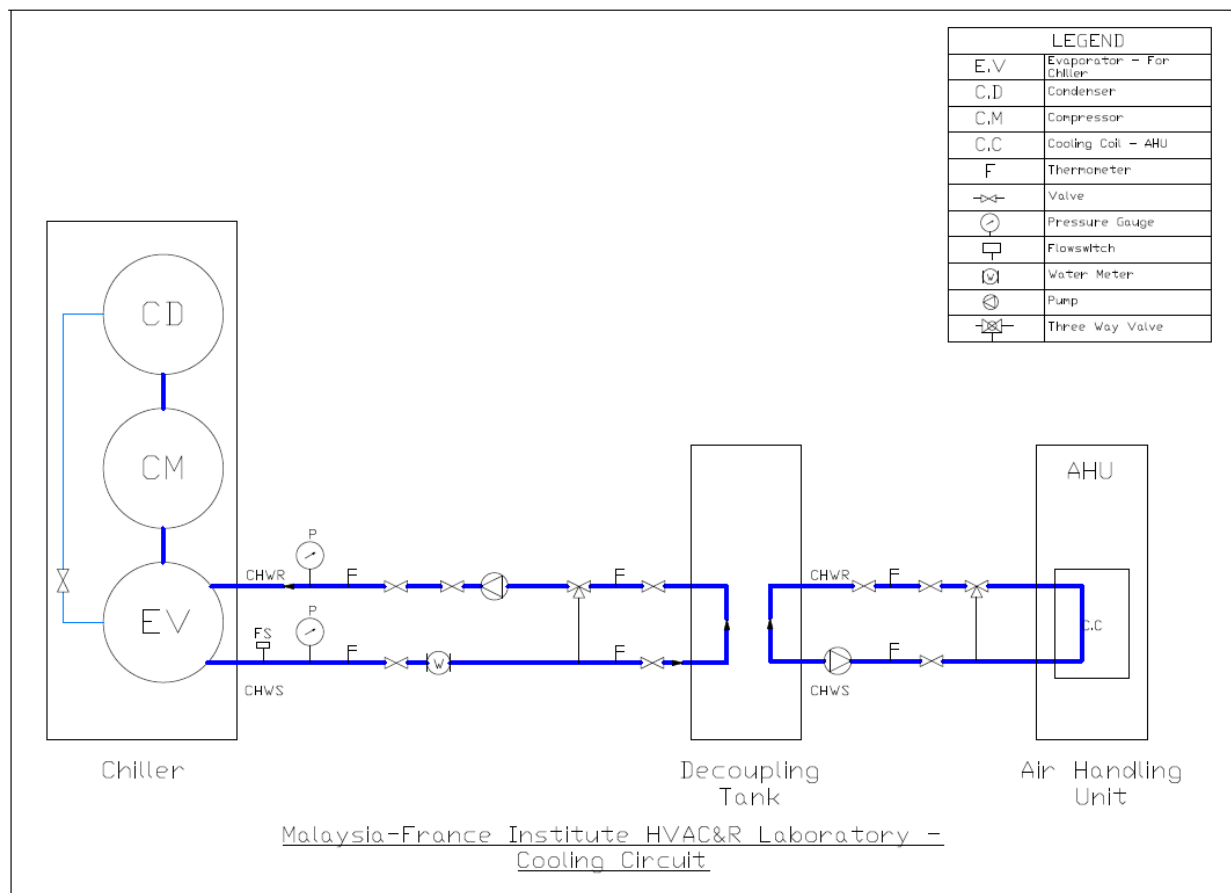


Figure 11: Astana Chiller Plant Set-Up

The following table is a summary of the results:

WATER						
		Average kW	Average RT	Average kW/RT	Average Outdoor Deg C	Nos of Chiller in Operation
Water	30th Nov 2022	85.98	58.03	1.60	35.03	1
Water	1st Dec 2022	86.20	64.49	1.37	35.03	1
Water	2nd Dec 2022	76.39	31.22	2.76	33.70	2
	<i>Average</i>	<i>82.86</i>	<i>51.25</i>	<i>1.91</i>	<i>34.59</i>	

NANOFLUID						
		Average kW	Average RT	Average kW/RT	Average Outdoor Deg C	Nos of Chiller in Operation
Nanofluid	7th Dec 2022	81.66	68.21	1.23	32.53	1
Nanofluid	8th Dec 2022	98.60	60.46	1.70	28.45	2
Nanofluid	12th Dec 2022	103.94	80.42	1.29	30.23	2
Nanofluid	13th Dec 2022	92.42	70.99	1.31	29.95	2
Nanofluid	15th Dec 2022	75.80	82.86	0.91	33.65	1
Nanofluid	19th Dec 2022	83.71	85.84	0.98	32.93	1
<i>Average</i>		<i>89.35</i>	<i>74.80</i>	<i>1.24</i>	<i>31.29</i>	

Normalizing for the 3.3 C average temperature drop, the efficiency improvement was **29.0%**.

3. Discussion

All the tests and measurements were done and taken at the chilled water plant side while maintaining the indoor (occupied) space conditions and normalizing for any outdoor weather conditions. The focus is on the chilled water plant as this is the component in the air-conditioning system that consumes the most energy. The GNP Nanofluid increases the energy efficiency of the chilled water system. The only unknown now is how long will the GNP stay suspended in the closed loop. With stationary samples in a closed container, there does not seem to be any sedimentation or agglomeration observed and logically since a chilled water system is consistently agitated, there is no reason to see this happening in an actual functioning system. However, the nanofluid samples in the installed systems will be removed and tested from time-to-time

Why does the nanofluid show these savings and what value do the nanoparticles add to the base fluid that increases the system efficiency by such a significant %? The answers lie within research done by many scientists in this field, and it is mainly due to the higher convective heat transfer performance [3] at the heat exchangers of these systems. The reason for the increased heat transfer performance is that the nanoparticles cause disturbances in the boundary layer. The Brownian motion of the nanoparticles causes turbulences delaying the process of the boundary layer formation thereby increasing the scope for heat transfer [4]. The nanofluids show a shear thinning (non-Newtonian) rheological behaviour and this decreases the viscosity at the boundary layer leading to superior flow properties and enhanced heat transfer. The nanoparticles also increase the thermal conductivity of the nanofluid, and this gets better at higher concentrations [5] but somehow the heat transfer performance hits a plateau after a certain concentration and with this, we can infer that an extremely high concentration of nanoparticles reverses the advantages of the Brownian motion and shear thinning advantages at the boundary layer.

4. Application

In the above tests, the system's energy performance was measured while the base fluid (water) was circulating. After that, the system is stopped, base fluid drained and the system is replaced with the nanofluid, and the energy performance is tested. While this is possible with small plants with small fluid volumes, in a real operating environment, plant shutdown is almost impossible. Furthermore, large commercial plants have a few hundred thousand to more than a million litres of water (and even more for large district energy plants) and that is a major logistics issue. We have devised a system that converts the water in an operating system to a nanofluid of the required performance without disrupting

the operations of the plant. This system has been successfully tested and will be used in the application to commercial plants worldwide. This will be the material of a future technical paper.

5. Conclusion

This nanofluid applied to the built environment can provide substantial energy efficiency improvements over conventional cooling. This is because the nanofluid is a heat transfer fluid that exhibits thermal properties superior to water.

References

- [1] Brown, Charlotte, 2021. Graphene: The Material That Is Changing The World
- [2] Nanomalaysia Berhad and Blue Snow Consulting and Engineering Sdn Bhd. 2020. Patent filing: 22965MY00031/PM/AQI/smi
- [3] Yarmand, H., Zulkifli, N.W.B.M., Gharehkhani, S., Shirazi, S.F.S., Alrashed, A.A., Ali, M.A.B., Dahari, M. and Kazi, S.N., 2017. Convective heat transfer enhancement with graphene nanoplatelet/platinum hybrid nanofluid. *International Communications in Heat and Mass Transfer*, 88, pp.120-125.
- [4] Barai et al., 2019, Bahnvase et al., Radkar et al., 2019. Intensified convective heat transfer using ZnO nanofluids in a heat exchanger with helical coiled geometry at constant wall temperature. *Mater. Sci. Energy Technology*. 2, 161-170
- [5] Hojjat, M., et al., 2011. "Thermal conductivity of non-Newtonian nanofluids: experimental data and modeling using neural network." *International Journal of Heat and Mass Transfer* 54.5-6 (2011): 1017-1023.



Aalborg Universitet

AALBORG UNIVERSITY
DENMARK

Do International Building Researchers Mostly Work Right Before the Deadline? Yes, According to Empirical Data

Johra, Hicham; Hansen, Anders Rhiger; Rohde, Lasse

DOI (link to publication from Publisher):
[10.54337/aau541562346](https://doi.org/10.54337/aau541562346)

[Link to publication from Aalborg University](#)

Citation for published version (APA):

Johra, H., Hansen, A. R., & Rohde, L. (2023). Do International Building Researchers Mostly Work Right Before the Deadline? Yes, According to Empirical Data. In H. Johra (Ed.), *NSB 2023 - Book of Technical Papers: 13th Nordic Symposium on Building Physics* [103] Department of the Built Environment, Aalborg University. <https://doi.org/10.54337/aau541562346>

Do International Building Researchers Mostly Work Right Before the Deadline? Yes, According to Empirical Data

Hicham Johra^{1*}, Anders Rhiger Hansen¹, Lasse Rohde¹

¹ Department of the Built Environment, Aalborg University, Thomas Manns Vej 23, DK-9220, Aalborg Øst, Denmark

* Corresponding author: hj@build.aau.dk ORCID ID: 0000-0003-4177-9121

Abstract. Academic work is characterised as increasingly time-pressured and deadline-driven. Moreover, increased use of online tools underpins flexible working hours. Does this make researchers work just before a deadline or a meeting (perceived as an intermediate deadline)? The "imminent deadline-driven work habit" hypothesis seems intuitively plausible since the research and academic world is notorious for heavy workloads and multiple parallel tasks and projects. The current article investigates the activity of several collaborative online documents from international building research projects as a function of the distance to a deadline or coordination meeting. A similar analysis is conducted on the submission data of an international conference on building physics. This empirical analysis supports the "imminent deadline-driven work habit" hypothesis. Finally, the article discusses the possible reasons behind the latter and the ensuing practical implications and recommendations for the management of collaborative research/academic work in energy, building physics and indoor environment.

1. Introduction

Academic working practices used to be seen as a comparatively low-stress working environment [1], but in recent decades, a development from "Thought-time" to "Money-time" [2] has increased time pressure and hurriedness [3]. It has contributed to new demands for the temporal order of academic work [4], deadline-driven research [5], and emerging difficulties in balancing work, leisure, and everyday life with a focus on productivity [6].

Digital and online tools have provided flexibility for researchers to organize their work but also brought drawbacks, such as increased stress and time pressure. A typical observation made by the authors and other members of the international building research community is that a few hours before a coordination meeting or a submission deadline, most collaborators of a shared document related to the latter are online working on that document. This intuitively leads to the hypothesis that researchers tend to work right before a deadline, right after, or both (when the deadline is, e.g., a coordination meeting). This "working under pressure" or "cramming" habit with looming deadlines may be perceived by some as a productive way to focus and prioritize tasks. However, it can also contribute to high-stress working environments with time-pressured deadlines and an imbalance between work and everyday life. One of the unintended consequences of these work practices is the deadline-driven workload. The flexibility and "freedom" of academic collaboration might lead to time-squeeze and time-pressure with increasing risks of the precariousness of non-tenured academics [7] and, in general, counter-productivity, poorer result quality and reduced work satisfaction.

The current study aims to test the hypothesis above with empirical data from the international building research community, i.e., the temporal distribution relative to a deadline of the activity level in collaborative working documents, the submission of abstracts to a conference and the submission of abstract reviews to a conference, respectively. This article focuses on a particular professional community that has not been studied before by providing and analysing quantitative data that cannot be found in the existing literature.

2. Materials and methodology

To test the hypothesis of whether or not a deadline significantly influences the workload of researchers from the international building community, empirical data has been collected from working processes

with deadlines in which contributions and progress can be monitored over time: 1) the activity of collaborative scientific documents by small teams; 2) the abstract submission rate to a building physics conference; 3) the review of abstracts to the same conference.

For the analysis of collaborative scientific work, the writing activity was monitored on 6 shared working documents from international projects over 24 evaluation periods in 2021 and 2022, each comprising a coordination meeting. These regular coordination meetings report on the progress of a task or document and plan the follow-up action, but also serve as intermediate deadlines. The daily activity level is assessed by counting the number of versions and edits recorded on the shared document and normalized by the total number of versions and edits recorded over the whole evaluation period.

It is assumed that most of the work on the collaborative documents directly changes the latter's content. However, some of the actual work might require additional activities that are not recorded in the activity level of these collaborative documents. Similarly, submission and reviewing of abstracts to a conference necessitate some work before uploading the contribution on the online platform. Nonetheless, the contributions and work for these activities usually consist of short texts or editing. It can thus reasonably be assumed that the latter is elaborated shortly before the recorded submission or activity. Consequently, the authors are confident that the recorded activities are a good indicator of the whole process timing.

The data collected for this study has been anonymized and is open-access: it can be downloaded from <https://doi.org/10.54337/aau507456682> [8].

3. Results and discussion

One can observe the activity dynamics and temporal distribution of the three investigated processes in the following figures. Regarding the daily submission rate of abstracts to the conference, one can observe in Figure 1 that there is almost no contribution prior to 5 days before the original deadline. Most abstracts are submitted in the last few days before that deadline. Moreover, extending the original deadline by 5 additional days has increased the number of submitted abstracts by +97%. The impact of the imminent deadline on the activity level is thus very clear. One can also notice that Sunday has a very low activity, which corresponds to leisure and family-focused time in most western countries.

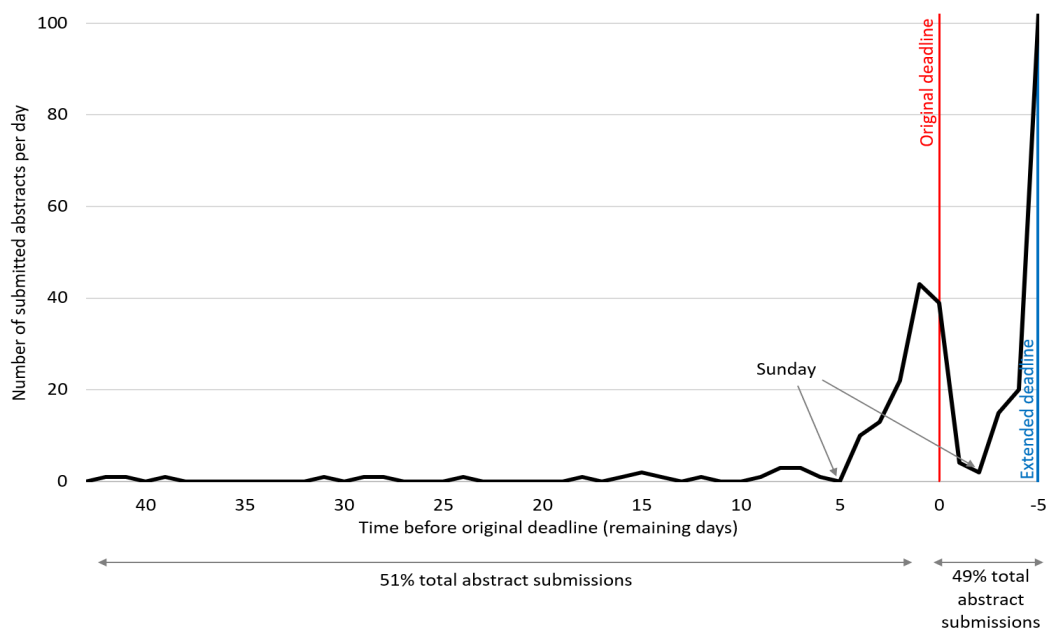


Figure 1. Daily abstract submission rate to an international conference as a function of remaining time before the original (first) submission deadline.

Focusing on the last 24 hours before the final deadline, one can see in Figure 2 similar dynamics: most of the submissions occur after working hours, with a sharp activity increase in the very last hours before the deadline. 27% of all 300 submissions occurred in the last 8 hours before the final deadline, with 8.5% of them in the final hour (between 23:00 and 23:59 CEST). Moreover, 6% of all submissions even occurred after the final deadline (authors directly sending their contributions by email to the conference

organizers). Very similar dynamics can also be observed for the abstract review process of that conference. Despite having 15 days to complete the assessment of 6 abstracts, most of the work is carried out in the last few days with an accelerating increase of activity when approaching the deadline.

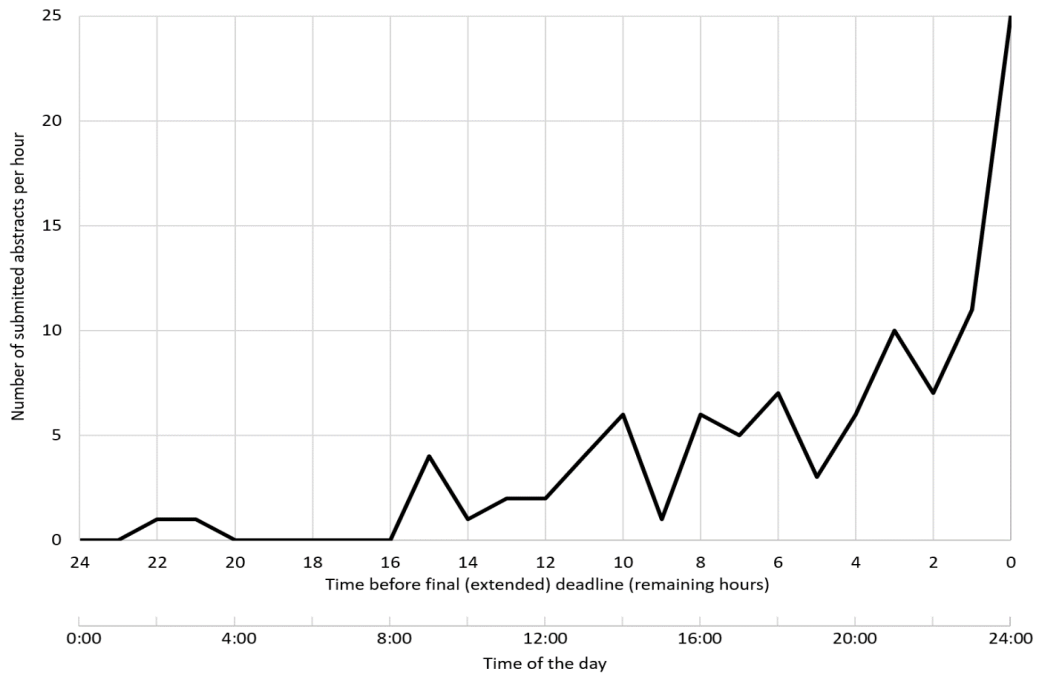


Figure 2. Hourly abstract submission rate to an international conference on the last day before the final (extended) deadline as a function of remaining time before this deadline.

These two processes were closed by a single (sometimes extended) deadline with, in principle, no activity possible after this deadline. The third process studied here concerns collaborative documents with recurrent coordination meetings serving as intermediate deadlines. Because each intermediate deadline does not end the process, one can thus examine if the activity on these collaborative documents occurs mostly right before the deadline and if it extends after the latter.

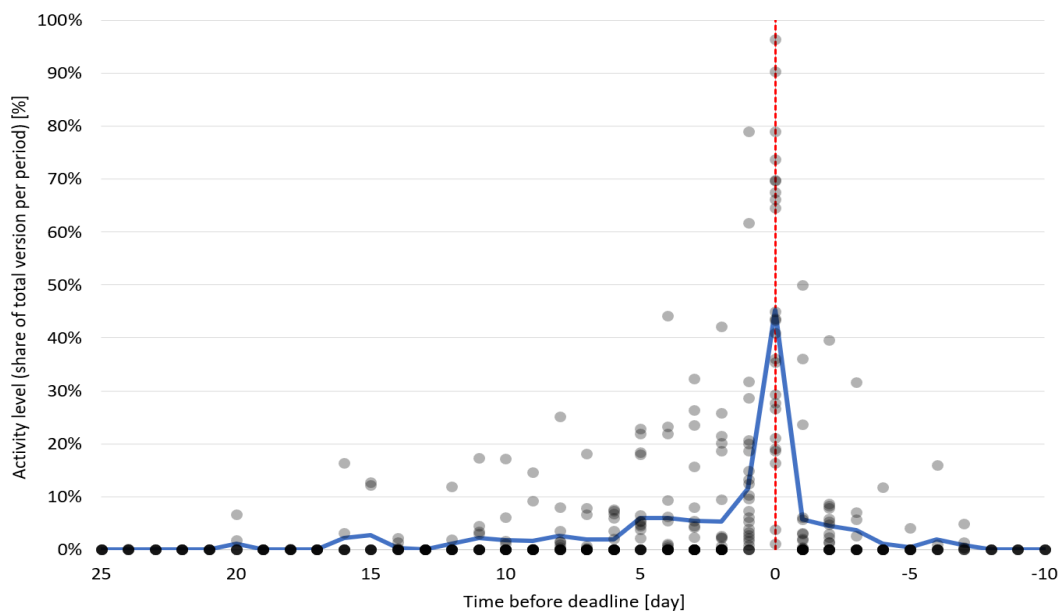


Figure 3. Daily activity level of shared working documents as a function of remaining time before the deadline (coordination meeting). The scattered points represent the activity level of a specific document for a given evaluation period. The blue line is the average activity level of all documents.

Figure 3 presents the daily activity of 6 collaborative documents aggregated over 24 evaluation periods, each comprising a recurrent coordination meeting/intermediate deadline. Similarly to the two first processes, one can observe that most of the activity is concentrated on the day of the deadline. Some moderate activity can be observed a few days prior to the deadline, but it quickly drops to zero after 2-3 days pasted the deadline. While there is almost no activity at all beyond 10 days prior to the deadline and 4 days after the deadline, one can clearly see that nearly 50% of the activity (work) on the collaborative document is carried out on the day of the deadline, mainly just a few hours before the coordination meeting begins.

4. Conclusions and recommendations

This paper set out to investigate whether researchers in the field of building physics tend to place workloads closer to deadlines. The empirical data analysis indicates that, indeed, working practices within this specific field tend to be strongly deadline-driven, and this might apply to other research fields as well. Most of the work is performed a few days before the deadline or on the day of the deadline. In the case of collaborative work document with recurrent deadlines/coordination meetings, the activity rapidly falls right after the deadline, and no significant contributions is made until a few days or hours before the next deadline. The hypothesis of this study - "do international building researchers mostly work right before the deadline?" - is thus clearly validated by the empirical data. The current findings are in line with and reinforce the literature describing how academic working practices are categorized as time-pressured, flexible and deadline-driven [5][9].

The results suggest that regular meetings act as a deadline-pressure mechanism pushing people to contribute significantly. One can thus discuss the reasons behind regular coordination meetings being an effective pressure mechanism. Although often perceived as a way to motivate collaborators and set new goals and directions to continue working on the current process, the activity on shared documents falls immediately after the meeting. The actual occurrence of the coordination meeting itself does not seem to have a sustained effect, it only serves as an imminent deadline driving contributions. This could be explained by negative drivers such as "the fear of consequences from project leaders", "the shame of not having contributed to a collaborative endeavour", or "the fear of losing face among peers and ruining future work collaboration opportunities". This could also be enhanced by systematic forgetfulness and procrastination in a work environment flooded with a constant flow of multiple deadlines, meetings and parallel heterogeneous tasks.

Regarding conference processes, the research community is accustomed to systematic deadline extensions coupled with the relatively low repercussion of missing a deadline. Indeed, the reviewing process in the scientific community is usually volunteer-based and without significant retribution or career impact. In addition, conferences on building physics occur regularly and often overlap. A researcher who is too short on a deadline can thus easily redirect his/her work to another conference if a deadline extension is not granted. This might partly explain the widely observed "last-minute submission" culture and the massive increase in contributions after a deadline extension.

The depicted situation is far from ideal and may be the worrying symptom of a research community being systematically overloaded and "slave of their own calendar". The work prioritization is then only driven by the most imminent threatening deadlines, which favours work-related stress and the detrimental effects associated with it. This can lead to a decrease in the quality of the research outputs and the well-being of a significant part of society. For instance, it has been commonly noticed during the conference process that authors and reviewers failed meeting the deadlines because of unforeseen events occurring in the last few days or hours when the contribution was planned to be made. This resulted in reviews not being submitted on time, authors' dropout, some poor-quality and uncomplete submissions rushed as the last moment, and complaints from participants having to compromise with their private life to meet deadlines.

From the observations made in this study, the authors would like to suggest some recommendations. For the organization of conferences, the organizers should be aware of the submission dynamics and should not expect much activity during the call for abstracts and review process up to the last week and few days before the deadline, even if announcements are made months beforehand. Being aware of that might alleviate some worries and pressure to the organizers and help them adjust the time needed for each phase of the conference process. In addition, sending or publishing a reminder one week before the deadline and then two days before the deadline is an effective way to stimulate contributions.

Announcing a deadline extension by one extra week a couple of days before the original deadline is a common practice that is shown to be very effective to boost abstract and paper submissions. Overwhelmed researchers might thus put the extra effort to finalize their contribution for the new deadline rather than giving up and resubmitting to another conference. However, this contributes to maintaining the "last-minute deadline rush" culture.

For collaborative projects, the project leaders are invited to pay more attention to the (hidden) consequences of specific deadlines and adjust the latter and the coordination meetings accordingly. To improve the quality of research contributions and the well-being of participants, one should take more interest in the temporal organization of workloads and consider factors such as preparation time and alternative working schedules that take into account *when*, *where*, and *how* team members work best. For instance, forwarding a text, figure, slide or another piece of work to collaborators to see a couple of days ahead of a meeting is good timing to re-activate focus and activity on that project.

Senior researchers participating in multiple parallel projects often do not have dedicated time to prepare for meetings. One solution to mitigate that is to allocate a specific working period (30 minutes to 1 hour) at the beginning of the meeting: "before the meeting actually begins, let us leave our email box for 30 minutes, and all do our assignments by reading, commenting and contributing to the document that is the point of discussion of today's meeting". This dedicated working time could also be placed at the end of a meeting to start contributing directly to the tasks elaborated on during the discussions. However, participants tend to jump out earlier from a meeting to catch another overlapping one, or discussions might last longer than expected and trim the working phase. One should also think about whether or not clearly announcing this working phase in the meeting agenda as it might give an opportunity to skip it. Given the common load of parallel tasks undertaken by researchers in the community, it is suggested that scheduling short coordination meetings (30 minutes to 1 hour) every two weeks is the best trade-off to keep a reasonable activity level on collaborative projects/documents without overwhelming the participants.

Finally, the authors advocate for systemic changes in working structures formed by universities or governmental policies, funding instruments and publication systems so that the negative impacts of overwork and deadline-driven research have on productivity, creativity, health and well-being are recognized and accounted for.

References

- [1] Kinman G 2014 Doing more with less? Work and wellbeing in academics *Somatechnics* **4** 219–235
- [2] Noonan J 2015 Thought-time, money-time, and the temporal conditions of academic freedom *Time & Society* **24** 109–128
- [3] Southerton D 2020 *Time, consumption and the coordination of everyday life* Palgrave Macmillan
- [4] Ylijoki O H and Mäntylä H 2003 Conflicting time perspectives in academic work *Time & Society* **12** 55–78
- [5] Wing J M and Guzdial M 2009 CS woes: deadline-driven research, academic inequality *Communications of the ACM* **52** 8–9
- [6] Bartlett M J, Arslan F N, Bankston A and Sarabipour S 2021 Ten simple rules to improve academic work–life balance *PLOS Computational Biology* **17** e1009124
- [7] Petrina S, Mathison S and Ross E W 2015 Threat convergence: The new academic work, bullying, mobbing and freedom *Workplace: A Journal for Academic Labor* **24** 58–69
- [8] Johra H 2022 Datasets on the work habits of international building researchers *DCE Technical Report No. 305, Department of the Built Environment Aalborg University*
- [9] Woolston C 2017 Workplace habits: Full-time is full enough *Nature* **546** 175–177



Aalborg Universitet

AALBORG UNIVERSITY
DENMARK

Analysis of Hybrid Timber Construction by Multiple Criteria Decision-Making Method

Dolgunovas, Markas; Norvaišienė, Rosita

DOI (link to publication from Publisher):
[10.54337/aau541025944](https://doi.org/10.54337/aau541025944)

[Link to publication from Aalborg University](#)

Citation for published version (APA):
Dolgunovas, M., & Norvaišienė, R. (2023). Analysis of Hybrid Timber Construction by Multiple Criteria Decision-Making Method. In H. Johra (Ed.), *NSB 2023 - Book of Technical Papers: 13th Nordic Symposium on Building Physics* (Vol. 13). [128] Department of the Built Environment, Aalborg University.
<https://doi.org/10.54337/aau541025944>

Analysis of Hybrid Timber Construction by Multiple Criteria Decision-Making Method

Markas Dolgunovas, Rosita Norvaišienė

Kaunas University of Applied Engineering Sciences, Tvirtovės av. 35, 50155 Kaunas, Lithuania

rosita.norvaisiene@edu.ktk.lt

Abstract. When selecting materials for a building, designers should not only think about structural requirements but also to the sustainability of the selected materials. The article presents a study of a single building using methods that comprehensively evaluate alternative design solutions. The approach is based on the complex system of criteria allowing a comprehensive evaluation of alternative solutions at an early design stage, combining life cycle assessment (LCA) and multi-criteria decision analysis (MCDA).

This study evaluates the environmental impact of five alternative types of building components (reinforced concrete, hybrid wood elements), while determining the most rational alternative solutions according to the specified criterion (price, CO₂ emissions, human time consumption, envelope thicknesses).

The results show that, when the columns, ceilings and beams are made of reinforced concrete and the external envelope comprises SIP panels, the version of building structures ranks in the second place in terms of theoretical significance (81 points) and in the first place in terms of subjective significance (79 points).

Keywords: Multiple Criteria Decision-Making Method, Life Cycle Analysis, Hybrid Timber, One Click

1. Introduction

Modern buildings and structures consist of mainly masonry, steel, and concrete. Reinforced concrete possesses especially good overall stability - it combines high compressive strength of concrete with high tensile strength of steel. Reinforced concrete is extremely durable, even under dynamic weather conditions. However, it also has its drawbacks such as huge amounts of manufacturing energy, process and subsequently recycle reinforced concrete, which causes large amounts of CO₂ emissions [1-2]. The construction industry is liable for huge amounts of energy-related CO₂ emissions (39%) [3]. Noha Ahmed [4] found that reinforced concrete has a significant negative impact on ecosystems, as it accounts for 78% of all carbon dioxide emissions.

Hafner's [5] life cycle assessment (LCA) calculation indicated that building's operational phase accounts between 45% and 80% of total CO₂ emissions, while the materials used in construction account for 20-55% of total CO₂ emissions. Sizirici et al. [6] found that the application of alternative additives/materials in construction (planning, design and construction) or methods/systems can reduce the CO₂ due to material use up to 90%.

The European Union supports the construction sector's emissions reduction initiative to increase the target from 29% to 40% reduction by 2030. The amount of GHG emissions from buildings can be influenced by the selection of building materials. Because the use of timber structures can help in

reducing the concentration of greenhouse gases, such as CO₂, Europe is increasingly moving towards timber-based constructions [8-11]. In recent years, wood has been considered as an alternative source of building materials because of its sustainability and design efficiency, but the cost-competitiveness of timber buildings is still under investigation because of reduced information.

Engineering timber products for construction (EWD - Engineered Wood Products) are used for load-bearing elements, or for interior or exterior fittings, usually in the form of panels or lumber. These products are formed from small cross-sections of securely interconnected blanks, allowing for the balance between building products, forest resources and the required working capacity and dimensions, while improving their mechanical properties in a targeted way [12].

Multiple studies [13-14] demonstrated that, when compared to concrete or steel, using wood or its engineered product derivatives such as Glued-Laminated Timber (GLT), Cross Laminated Timber (CLT), Laminated Veneer Lumber (LVL) and so on, presents a favorable environmental balance.

The combined energy and ecological efficiency of modern buildings increasingly depend not only on the technology of their construction and the quality of manufacturing, but also on the selection of building materials. The latter can be assessed by LCA and supplemented by multi-criteria analysis. This study proposes a common algorithm - the selection of a rational solution, combining LCA and multi-criteria analysis methods for selecting the structural elements of the building to achieve energy efficiency and reduce CO₂ emissions. The proposed algorithm can be used on a large-scale with the support of building information modeling (BIM) and can be applied to different types of buildings in different locations. The environmental impact of five alternative types of building components (reinforced concrete, hybrid wood elements), is evaluated, and the most rational alternative solutions according to the specified criterion (price, CO₂ emissions, human time consumption, envelope thicknesses) are determined.

2. Methods

Methods used for the building analysis combines LCA and Multiple Criteria Decision-Making Method (MCDM).

One Click LCA software can calculate and compare the embodied carbon footprint impact of a building project and the performance of the used materials. The tool considers the 10 most important building materials (concrete, steel, cement, bricks, glass, gypsum, insulation, wood) and provides access to global, up-to-date databases, including Environmental Product Declarations (EPDs), which describe the environmental impact of different products. One Click LCA provides extensive integration capabilities for software and file formats such as Autodesk Revit, Simple BIM and Naviate Simple BIM 5.0, Excel and DesignBuilder 5.1 or later.

Multiple Criteria Decision Making (MCDM) methods stand out from other optimization methods. These tasks set a solution objective: selecting the best alternative from a range of options proposed or ranking alternatives in relation to the assessment objective. Multi-criteria methods are based on a decision matrix, which includes statistics on the criteria characterizing the evaluation objective, or the values of expert judgements on these criteria.

Determining the significance of evaluation criteria using the theoretical entropy method. The objective weight entropy method is among the most used, although multivariate regression models and other ideas may also be used. The increase in entropy weight is related to the degree of dominance of one criterion value among all alternatives.

Determination of the significance of the assessment criteria using an expert ranking method. Ranking is a procedure in which the most important criterion is given the highest rank equal to a unit, the second in importance is given the rank two, etc., the last in terms of importance is given the rank m, where m - is the number of criteria compared. Equivalent criteria shall be given the same value, the arithmetic mean of the ordinal ranks.

3. Analysis of building design options

A conventional 2-storey building of 26x21m was selected for the study. The building has 30 reinforced 400 x 400 mm concrete columns, 8 m height, floor area - 518.16 m², roof covering is made of multilayer Sandwich panels, 200 mm thick reinforced concrete slabs as ceilings (building A, Table 1). Building was analyzed according to 5 criteria - wall and roof thickness, construction cost, CO₂ emissions and labor costs - and compared with buildings modeled using hybrid timber construction. The criteria were chosen based on realistic criteria that could be held important when constructing a building, meaning most often are accented by clients.

Table 1. Design options for buildings

Building constructions	Building A (Original)	Building B	Building C	Building D	Building E
Columns	Reinforced concrete	Reinforced concrete	Reinforced concrete	Glulam	Glulam
Overlays	Reinforced concrete	Reinforced concrete	Reinforced concrete	CLT	OSB
Beams	Reinforced concrete	Reinforced concrete	Reinforced concrete	Glulam	Glulam
Walls	sandwich	CLT	SIPs	CLT	Timber frame
Roof	sandwich	sandwich	SIPs	CLT	OSB

The 4 hybrid timber building variants are shown in Table 1 (Buildings B, C, D and F).

Selecting the system of evaluation criteria and calculating their values (based on which criterion is selected).

Wall thickness (K1) at $U = 0.17 \text{ W/(m}^2\text{K)}$, mm. The wall thickness criterion shows the thickness of an outer wall when U is at a value of $0.17 \text{ W/(m}^2\text{K)}$.

Roof thickness (K2) at $U = 0.15 \text{ W/(m}^2\text{K)}$, mm. The roof thickness criterion indicates the thickness of a roof when U is at U value of $0.15 \text{ W/(m}^2\text{K)}$.

Price (K3), thousand Eur. The price criterion shows the approximate price that will have to be paid for the materials to build this building using the appropriate option of structures. The price will be determined by assessing the prices of the main structural elements of the building (walls, roof, ceilings, columns).

CO₂ emissions (K4), tCO₂e. The CO₂ emissions criterion shows how many tons of CO₂e are released into the atmosphere during the production of building materials. CO₂ emissions are calculated using the „One click LCA“ software.

Human time consumption per hour (K5). The human time consumption criterion shows how many labor hours the construction process will take, considering the installation of columns, ceilings, walls, and roof. This measurement was taken out of the official construction normative. It is calculated based on the average time it takes one person to complete a certain construction task.

The main factor when comparing different external wall structures is the heat transfer coefficient, which is defined as $U=0.17 \text{ (W/m}^2\text{K)}$ - currently the wall is subject to the requirement for energy performance class A++ for public buildings in Lithuania. The external walls, roof, overlay structures of the building are designed from different structural materials - CLT, multilayer panels "Sandwich", SIP panels with layers of thermal insulation.

Building construction option A. The building is designed with a reinforced concrete frame. The ceilings are made of reinforced concrete slabs 200 mm thick. Walls and roof are constructed of 135 mm and 120 mm thick Sandwich panels. Estimated building cost is 115818 EUR. Based on the „One click LCA“ the building produces 106 tCO₂e. Estimated human hour consumption is 1256 hours.

Building construction option B. The building is designed with a reinforced concrete frame. The ceilings are made of reinforced concrete slabs 200 mm thick. The walls are made from CLT panels (Figure 1). Roof is constructed out of sandwich panels. Estimated building cost is 119932 EUR. Based on the „One click LCA“ the building produces 112 t CO₂e. Estimated human hour consumption is 1191 hours.

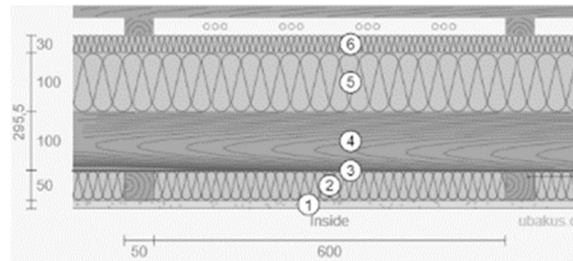


Fig.1. CLT panel wall construction (1 - plasterboard 15 mm; 2 - mineral wool 50 mm; 3 - vapor barrier 0.5 mm; 4 - cross laminated timber 100 mm; 5 - mineral wool 100 mm; 6 - hard mineral wool 30 mm)

Building construction option C. The building is designed from a reinforced concrete frame. The ceilings are made of reinforced concrete slabs 200 mm thick. The walls and roof are 205 mm and 224 mm thick and are made of SIP panels. Estimated building cost is 119932 EUR. Based on the „One click LCA“ the building produces 112 t CO₂e. Estimated human hour consumption is 1197 hours.

Building construction option D. The building is designed from glued timber (Glulam) columns. The walls, roof and ceilings are made of CLT. Estimated building cost is 119932 EUR. Based on the „One click LCA“ the building produces 121 t CO₂e. Estimated human hour consumption is 3251 hours.

Building construction option E. The building is designed from glued timber (Glulam) columns. Ceilings from OSB panels. The walls and roof - timber frame panel construction (Figures 2 and 3) are 255.5 mm and 273 mm thick. The ceilings are made of OSB panels. Estimated building cost is 90465 EUR. Based on the „One click LCA“ the building produces 101 t CO₂e. Estimated human hour consumption is 2525 hours.

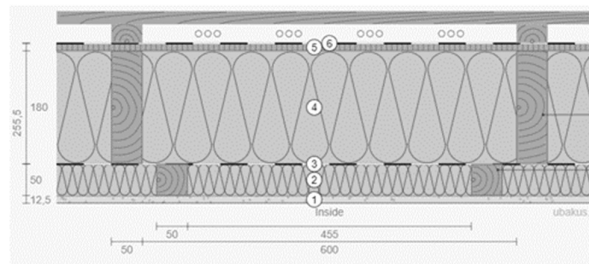


Fig.2. Timber frame panel construction - wall (1 - plasterboard 12.5mm; 2 – mineral wool 50 mm; 3 - vapor barrier 0.5mm; 4 - mineral wool 180 mm; 5 - OSB 12mm; 6 - windproof film)

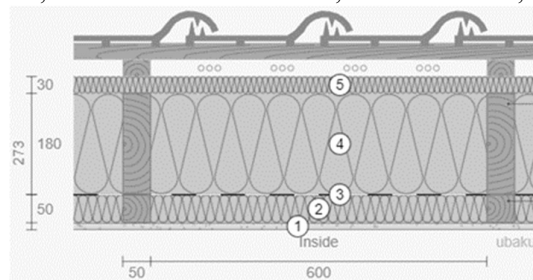


Fig.3. Timber frame panel construction - roof (1 - plasterboard 12.5 mm; 2 – mineral wool 50 mm; 3 - vapor barrier 0.5 mm; 4 - mineral wool 180 mm; 5 - hard mineral wool 30 mm)

When making engineering decisions, it is important to consider the main aspects affecting the function of the buildings and to evaluate all available options and their ability to fulfill their purpose. For this assessment, a single-criteria cost-effectiveness assessment will not reveal and evaluate the most important parameters of materials and engineering systems. Therefore, a multi-criteria approach is chosen, which allows the evaluation of the engineering solutions according to the chosen system of evaluation criteria and their significance. An expert judgement method is used to determine the subjective significance of the criteria.

The numerical values of the evaluation criteria are shown in Table 2.

Table 2. Numerical values of the evaluation criteria

Options	Criteria Wall thickness (K1) at $U = 0.17$ $W/(m^2K)$, mm	Roof thickness (K2) at $U = 0.15$ $W/(m^2K)$, mm	Price (K3), Thousand Eur	CO ₂ emissions (K4), tCO ₂ e	Human time consumption per hour (K5)
A	135	120	116	106	1256
B	296	120	120	112	1191
C	205	224	156	41	1197
D	296	308	127	121	3251
E	256	273	91	101	2525

3.1. Determining the theoretical significance of criteria using the theoretical entropy method

The entropy method is a method for determining the theoretical significance of criteria, based on mathematical calculations using numerical values to determine the significance of the criteria.

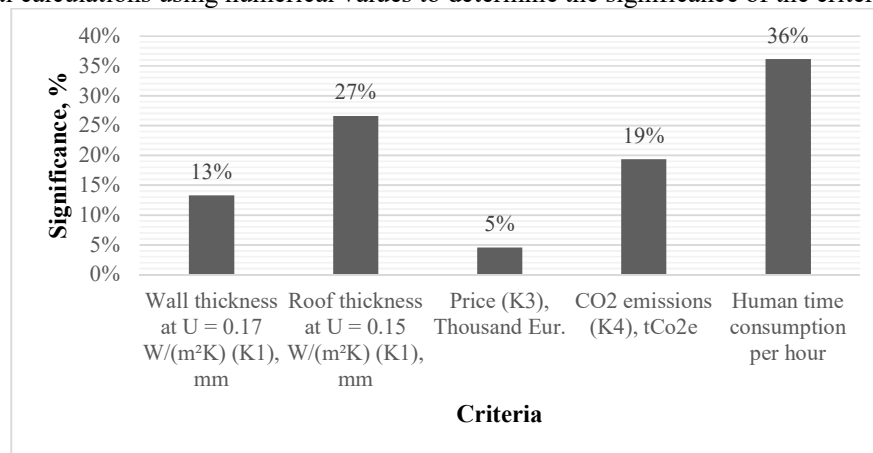


Fig. 8. Theoretical significance of the criteria using the theoretical entropy method

The calculations showed that the human time criterion (K5) has the highest theoretical significance with a theoretical significance of 36.16%, followed by roof thickness with $U = 0.15$ $W/(m^2K)$ criterion (K2) with a theoretical significance of 26.63%, the third place was taken by the criterion of CO₂ emissions (K4) with a theoretical significance of 19.37%, the fourth place was taken by the criterion of the thickness of the wall at $U = 0.17$ $W/(m^2K)$ (K1) with a theoretical significance of 13.30%. According to the theoretical significance calculations, Price (K3) is the least significant, with a significance of only 4.55%.

3.2. Determining the significance of evaluation criteria using the expert pair-wise comparison method

The expert pair-wise comparison method allows the significance of the criteria to be determined, considering the subjective views of the stakeholder groups. The criteria are ranked in order of priority: $K3 > K4 > K5 > K1 = K2$. The criteria are compared in pairs according to the priority ranking, with the more important criterion receiving 2 points and the less important criterion receiving 0 points. If the criteria are approximately equal, they shall be awarded one point each. The results of the calculation are shown in and Figure 4.

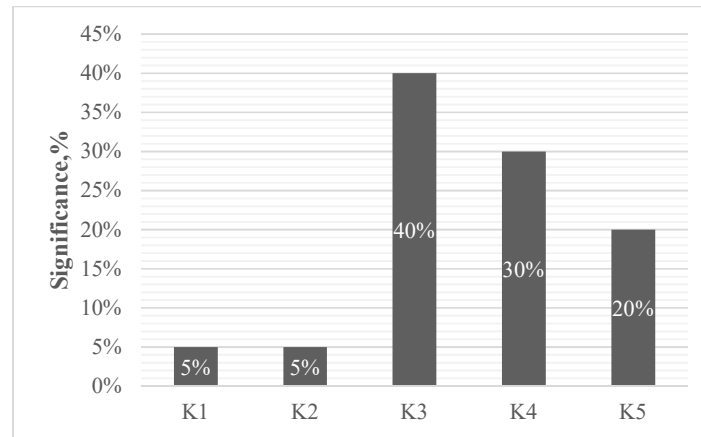


Fig. 4. Subjective significance of the criteria using the expert pair-wise comparison method

The calculations indicated that price (K3) has the highest subjective significance, with 40% of the significance. CO₂ emissions (K4) was the second most significant indicator with 30% of the subjective importance. Human time consumption (K5) is a fairly important indicator, with 20% significance. Wall thickness at 0.17 W/(m²K) and roof thickness at 0.15 W/(m²K) each scored 5% significance, showing that these indicators are almost irrelevant for the subjective choice of building design when compared to the other criteria.

3.3. Determining a rational solution using a multi-criteria utility value approach

This method identifies a rational engineering solution in the following sequence:

1. Based on the calculation data in Table 1, the initial data matrix P is constructed, the optimality of the criteria is determined, and the best value is found.
2. The matrix is normalized to a dimensionless matrix. The criteria to be maximized are normalized and the criteria to be minimized are normalized.
3. A rating scale is selected [0;100], the utility score for each criterion is calculated to determine the rational solution, i.e., the solution with the most useful criteria. Based on the results of the calculation, a priority queue of building design options is created.
4. The criteria values are scored, considering the theoretical and subjective significance of the criteria.

The priority lines and results of the building design options are shown graphically (Figure 4).

The most important criterion in the theoretical significance approach was the "human time cost criterion (K5)" and the order of priorities was as follows: $K5 > K2 > K4 > K1 > K3$.

In the subjective pair-wise comparison method, the most important criterion was "cost per m² (K3)" and the order of preference was: $K3 > K4 > K5 > K1 = K2$.

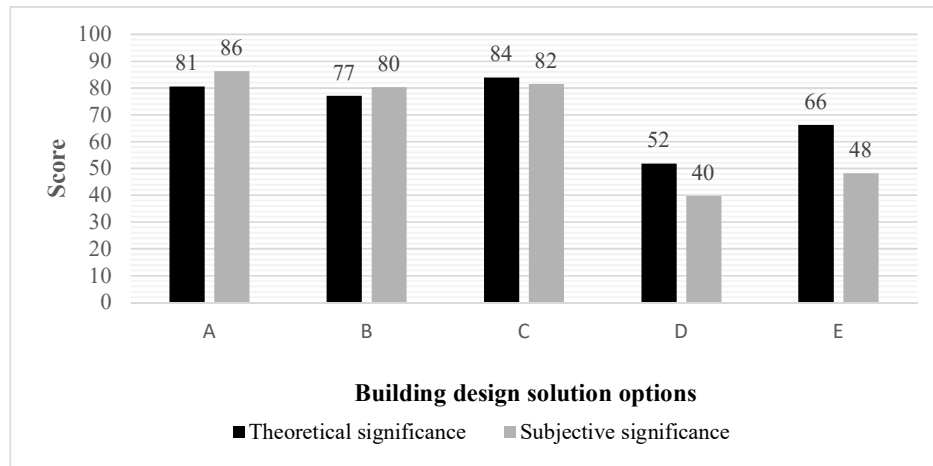


Fig.4. Usefulness of building design solutions when the theoretical and subjective significance of the criteria is assessed

The theoretical and subjective significance assessment produced the following results: Option A of the building design is ranked second in terms theoretical of significance (81 points) and first in terms of subjective significance (86 points) (Fig.4).

In terms of subjective (80 points) and theoretical (77 points) significance, building design option B is third. Building design option C is ranked first in theoretical significance (84 points) and second in subjective significance (82 points). Building design option E is ranked fourth in terms of theoretical (66 points) and subjective (48 points) significance. Building design option D is the least optimal in terms of theoretical (52 points) and subjective (40 points) significance.

4. Conclusion

The article represents the approach based on the complex system of criteria that allows comprehensive evaluation of the alternative solutions on an early design stage combining the life cycle assessment (LCA) and the multi-criteria decision analysis (MCDA).

When making engineering decisions, it is important to consider the main aspects that affect the function of the building and to make a targeted assessment of all available options and their ability to fulfill their purpose. The multi-criteria approach, which allows the evaluation of engineering solutions according to a selected system of evaluation criteria and their significance, has been chosen, and it has been found that the criterion of human time consumption (K5) has the highest theoretical significance with a theoretical significance of 36%. According to the theoretical significance calculations, price (K3) is the least significant with a significance of only 6%.

The theoretical and subjective significance assessment produced the following results: option A is ranked second in terms of theoretical significance (81 points) and first in terms of subjective significance (86 points). Building design option D is the least optimal in terms of theoretical (52 points) and subjective (40 points) significance.

The third option (building C) was the most environmentally friendly according to the data obtained by the „One click LCA“ software: the building was constructed out of a reinforced concrete frame, ceilings from 200 mm thick perforated reinforced concrete panels; walls and roof designed of SIP panels.

The results obtained in this study can be applied to the design of various buildings by altering the criteria to be in line with the priority of design decisions. Criteria can be selected based on what goals need to be met while designing the building. This allows for a levelheaded, concise approach in

evaluation and selection of building parameters that is not possible otherwise. The methodology used can be further improved if needed, by introducing more complex calculative multi-criteria decision-making comparisons.

Acknowledgments

This material is based upon the activities supported by the framework Erasmus+ Call 2020 EC Project Number 2020-1-FR01-KA203-080308 “Sustainable, High-Performance Hybrid Timber Building Construction”.

References

- [1] Andrew, R. M.: Global CO₂ emissions from cement production, *Earth Syst. Sci. Data*, 10, 195–217, <https://doi.org/10.5194/essd-10-195-2018>, 2018.
- [2] EU responses to climate change
Source: <https://www.europarl.europa.eu/news/en/headlines/society/20180703STO07129/eu-responses-to-climate-change> [viewed 2022-06-09].
- [3] World green building council. <https://www.worldgbc.org/> [viewed 2022-06-12].
- [4] Noha Ahmed, Mohamed Abdel-Hamid, Mahmoud M. Abd El-Razik, Karim M. El-Dash. Impact of sustainable design in the construction sector on climate change. *Ain Shams Engineering Journal* Volume 12, Issue 2, June 2021, Pages 1375-1383
<https://www.sciencedirect.com/science/article/pii/S2090447920302446>
- [5] Hafner, A. Contribution of timber buildings on sustainability issues. In *Proceedings of the World Sustainable Building 2014*, Barcelona, Spain, 28–30 October 2014.
- [6] Sizirici, B.; Fseha, Y.; Cho, C.-S.; Yildiz, I.; Byon, Y.-J. A Review of Carbon Footprint Reduction in Construction Industry, from Design to Operation. *Materials* **2021**, 14, 6094.
- [7] EU responses to climate change. Source: <https://www.europarl.europa.eu/news/en/headlines/society/20180703STO07129/eu-responses-to-climate-change> [viewed 2022-06-12].
- [8] Ritter, M.; Skog, K.; Bergman, R. Science Supporting the Economic and Environmental Benefits of Using Wood and Wood Products in Green Building Construction; General Technical Report FPL-GTR-206; U.S. Department of Agriculture, Forest Service, Forest Products Laboratory: Madison, WI, USA, 2011; pp. 1–9.
- [9] Lolli, N.; Fufa, M.S.; Wiik, M.K. An assessment of greenhouse gas emissions from CLT and glulam in two residential nearly zero energy buildings. *Wood Mater. Sci. Eng.* **2019**, 14, 342–354. [CrossRef]
- [10] Lukic, I.; Premrov, M.; Leskovic, Ž.V.; Passer, A. Assessment of the environmental impact of timber and its potential to mitigate embodied GHG emissions. *IOP Conf. Ser. Earth Environ. Sci.* **2020**, 588, 1.01–1.05. [CrossRef]
- [11] Shafayet, A.; Arocho, I. Analysis of cost comparison and effects of change orders during construction: Study of a mass timber and a concrete building project. *Journal of Building Engineering*. Volume 33, January 2021, 101856
<https://www.sciencedirect.com/science/article/pii/S2352710220334896?via%3Dihub>
- [12] Timber products for construction. Source: https://www.ekspertai.lt/medines_konstrukcijos/straipsniai/statybinis_medienos_produkta [viewed 2022-07-20].
- [13] Wooden structures - the future of high-rise buildings. Source: https://issuu.com/statybairarchitektura/docs/sa_2021_n1/s/11750521 [viewed 2022-07-21].
- [14] Building the future with cross-laminated timber (CLT).
<https://www.storaenso.com/en/products/wood-products/massive-wood-construction/clt>



Aalborg Universitet

AALBORG UNIVERSITY
DENMARK

Using Adaptive Behaviour Patterns of Open Plan Office Occupants in Energy Consumption Predictions

Tuniki, Himanshu Patel; Bekö, Gabriel; Jurelionis, Andrius

DOI (link to publication from Publisher):
[10.54337/aau541563857](https://doi.org/10.54337/aau541563857)

[Link to publication from Aalborg University](#)

Citation for published version (APA):

Tuniki, H. P., Bekö, G., & Jurelionis, A. (2023). Using Adaptive Behaviour Patterns of Open Plan Office Occupants in Energy Consumption Predictions. In H. Johra (Ed.), *NSB 2023 - Book of Technical Papers: 13th Nordic Symposium on Building Physics* (Vol. 13). [144] Department of the Built Environment, Aalborg University. <https://doi.org/10.54337/aau541563857>

Using Adaptive Behaviour Patterns of Open Plan Office Occupants in Energy Consumption Predictions

Himanshu Patel Tuniki^{1*}, Gabriel Bekö², Andrius Jurelionis¹

¹Faculty of Civil Engineering and Architecture, Kaunas University of Technology, Kaunas, Lithuania

²International Centre for Indoor Environment and Energy, Department of Environmental and Resource Engineering, Technical University of Denmark, Lyngby, Denmark

*Corresponding author: himanshu.tuniki@ktu.edu

Abstract. One of the factors that affects energy consumption in buildings is the level of control that occupants have over their environment, as well as their adaptive behaviour. The aim of this study was to focus on the adaptive clothing behaviour pattern, and to analyse its impact on energy consumption when integrated into a dynamic energy prediction tool. A questionnaire survey was conducted in an office building to collect the occupant behaviour data. The occupant clothing levels and the window opening behaviour were integrated into the dynamic energy performance prediction software, IDA ICE. The results of the simulations showed that the impact of adaptive clothing behaviour on energy consumption is relatively small, but it can meaningfully improve thermal comfort. Including adaptive behaviour in energy simulations can help in improving the accuracy of the energy performance and comfort predictions.

Keywords: adaptability; open plan office; clothing adaptation; window-opening behaviour; building energy consumption.

1. Introduction

As buildings contribute to about 40% to the global CO₂ emissions, it is an ever increasingly important task to make them energy efficient [1]. Occupant behaviour meaningfully contributes to the building's energy consumption. Energy performance simulation tools enable energy consumption predictions, however, the accuracy of the simulation results is often different from the real energy consumption. This difference is termed the energy performance gap, which needs to be addressed to make prediction results more accurate [2]. One of the main challenges in building modelling and energy studies has been to study and develop new ways to reduce the performance gap to an acceptable margin of error. An investigation of 23 buildings revealed a 34% higher actual energy consumption value than the predicted, with a standard deviation of 55% [3]. Studies reveal that the actual building energy consumption could be up to two times higher than the predicted value [4]. There are a couple of underlying causes for this gap, which were identified in a review [3], such as deterioration of the building systems, occupant behaviour, equipment malfunctioning, limitations in the measurement system, etc. Among these causes, the factor having a considerable impact on the energy predictions is the occupant behaviour. As behaviour is a subjective quantity, it varies depending on the region or location of the building, purpose of the building, income disparity and a wide range of other factors. To analyse this, various methods and tools have been employed, which include stakeholder collaboration [5], Post-Occupancy Evaluation studies [6], etc. But the most common tool used for behaviour studies are the occupant surveys, which could be conducted to understand the energy consumption patterns that can be attributed to occupant behaviour. These patterns, if identified and transferred into the building energy performance predictions,

could have a meaningful impact on the performance. Additionally, occupant behaviour patterns can help in making better energy related decisions for the facilities managers. There are several patterns that impact the energy consumption of the building, such as, lighting usage, temperature preferences, HVAC usage, etc. In most office buildings, the energy demand is higher due to increased number of occupants indoors. Studies show that the impact of the window opening behaviour on the energy use is comparatively low [7]. But, in general, it is not common to operate the windows in central air-conditioned buildings [8]. This study aims to quantify the effect of occupant behaviour patterns on the predicted energy consumption, with focus on clothing adaptation and window opening behaviour.

2. Methodology

The field study was conducted in a mechanically ventilated office in the south Indian city of Hyderabad. The building was located 20 km away from the city centre. The study was conducted in the summer season in the month of May 2022. The office on the third floor of the building which was run by an architecture firm with a seating capacity of 90 occupants with workstations and about 15 visitors per day. Since the office required the employees to work on computers, their physical activity level within the office was low. As per ASHRAE 55 [9], their MET value was between 1.2 and 1.4. The office had a Variable Refrigerant Flow (VRF) HVAC system installed for the open office spaces. The specifications and the details of the office are summarized in Table 1.

Table 1. Description of the analysed office

Area	700 m ²
Energy consumed for the month of May 2022 (as per energy meter)	14,446 kWh
No. of workstations	90
Equipment	Computers, 3D Printers, Laser printers
Cooling capacity of the HVAC system	<ul style="list-style-type: none"> • 30 kW VRF system for the open plan area • 19 kW VRF system for the cabins

2.1. Questionnaire survey

An online questionnaire survey was sent to all the occupants in the office floor, and about 62 responses were received from the occupants. The survey was designed to collect information about indoor air quality perception and comfort, thermal sensation, thermal comfort, and thermal preferences of the occupants, Sick-Building Syndrome (SBS) symptoms, etc. The questions were framed following the guidelines specified in the ASHRAE 55 standard [9]. Possible answer choices varied from “Very uncomfortable” to “Very comfortable”, “Very hot” to “Very cold”, etc. depending on the type of the question. The first page of the survey contained questions related to the basic details of the occupants (age, gender, working hours, etc.). The second page of the survey contained questions about the occupants’ current perception of the indoor environment at the time of filling the survey. The same questions were repeated on the third page of the survey, but with respect to the whole year, considering seasonal variations (winter, summer, autumn, and monsoon). The final page consisted of questions regarding the adaptive behaviour of the occupants; the questions focussed on the adjustments that the occupants prefer to undertake when feeling uncomfortable and on the frequency of the adaptation.

2.1.1. Dynamic simulation software

The software IDA ICE (Indoor Climate and Energy) v5.0 was used for the building energy simulations. It has been validated by the European Committee for Standardization (CEN) EN 15265-2007 and EN 15255-2007 [10] [11]. The office floor used for the simulations has been designed in IDA ICE as shown in Figure 1. The model was calibrated using the detailed information available regarding the office, and it was validated with the electricity meter readings. The energy consumption of the office for May 2022 was 14,446 kWh, while the simulated value was 14,872 kWh. The simulated value was within 3% of the actual energy consumption [6].

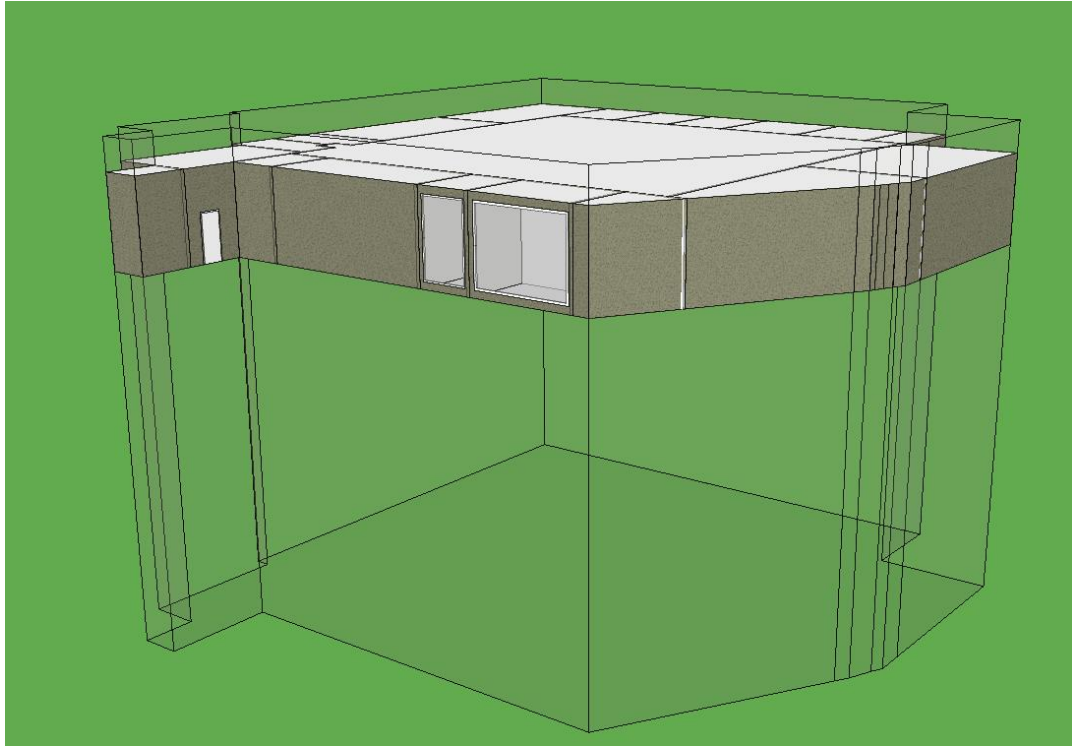


Figure 1. IDA ICE 5.0 model of office O1.

The base case simulation was run by using the information collected from the building. The occupancy profiles were designed in the model as per the obtained survey data. As mentioned by the occupants, the working hours of the office were from 9:30 AM to 6:30 PM. Since the office belonged to an architecture firm and all the occupants had a desk job, the activity level was set to 1.2 MET. The internal gains including lights and the equipment were also added to the model, as specified in Table 1. The temperature was maintained between 24°C–25°C [12]. Occupant clothing level was obtained from visual observations and was used for the base case simulation. There was no strict dress code as per the company policy, but formal attire was expected of the employees. The most observed attire for the occupants was business casual which can be calculated to 0.85 +/- 0.25 CLO (clothing is adjusted between these limits to obtain comfort).

The next simulation was run with a change in the CLO value of the occupants in the open plan office area. Since they did not have direct access to the windows, the clothing adaptation was assumed as the adaptation of choice for this simulation. The only change made to this simulation was the CLO value which was set to 0.6 +/- 0.25, for the open plan area.

For the third simulation, the window opening behaviour was considered for selected small offices (cabins), but all the remaining parameters were kept the same as the base case (Table 2). Only the occupants in the cabins had access to the windows. A graphical script was developed within IDA ICE which would allow for partially opening the windows when the indoor temperature is higher than the outside temperature, and the PPD value within the cabins would rise above 20%.

Table 2. Simulation cases

Simulation 1 (Base case)	Simulation 2	Simulation 3
CLO = 0.85 +/- 0.25	CLO = 0.6 +/- 0.25	CLO = 0.85 +/- 0.25
-	-	Window opening based on outdoor temperature and PPD

3. Results and discussion

Of the 62 responses received, 52% of the employees reported to be thermally uncomfortable, 48% were thermally comfortable during the summer season (Figure 2). The higher rate of discomfort among the occupants could have been a result of the lower capacity of the VRF system installed in the office, which was insufficient for the space and the number of occupants. The unknown performance, maintenance, and general condition of the VRF system adds to the uncertainty which is a limitation of this study. For the question about thermal preference, 81% of the respondents preferred to have cooler environment during the summer season (Figure 3). Note that the survey was conducted in the summer season; the results for other seasons reflect answers by recall.

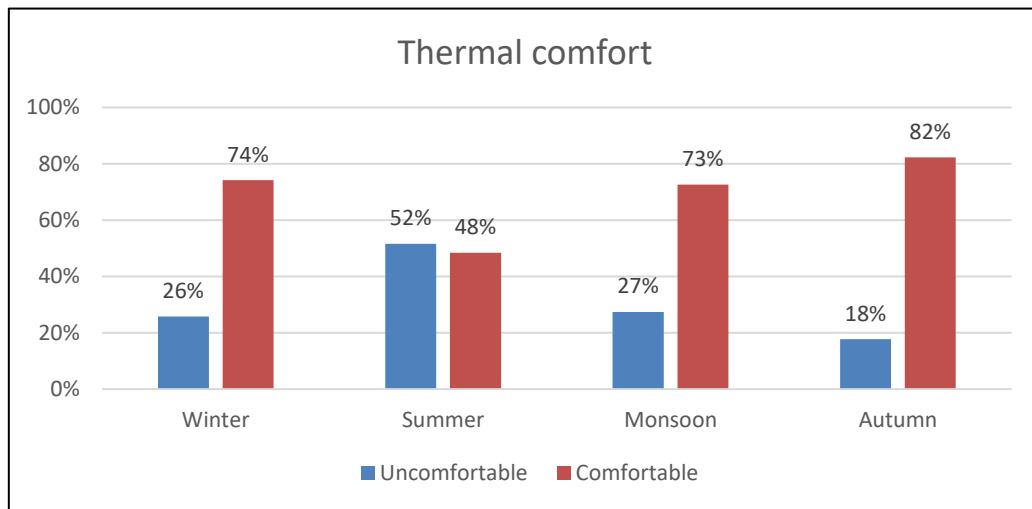


Figure 2. Thermal comfort responses for each season

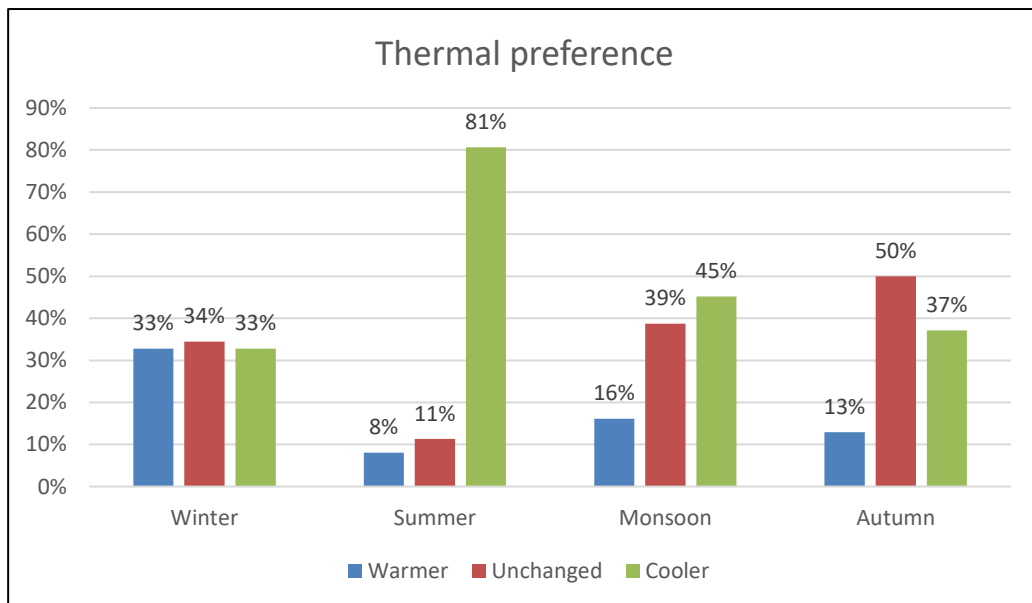


Figure 3. Thermal preference of occupants for each season

Based on all the information gathered from the office, the base case simulation was run, and it resulted in 14,872 kWh of energy consumed for the month of May 2022. The whole year simulation showed that the energy consumption by the office for the year of 2022 was 127,736 kWh with a maximum PPD of 31% in the open plan area. Simulation 2 showed a negligible 1 kWh increase with the

whole year consumption to be 127,737 kWh, but the maximum PPD decreased to 18% in the open plan area, indicating that clothing adaptation can improve the comfort without a considerable impact on the energy consumption. Various simulations were run with different CLO values and the results did not show any change in the energy consumption but changes in the comfort levels were noticed (Table 4).

Simulation 3 revealed that in the zones where window opening behaviour was allowed, the comfort level remained unaffected. This behaviour increased the annual energy consumption by 79 kWh (Table 3).

Table 3. IDA ICE Simulation results

	Simulation 1 (Base case)	Simulation 2	Simulation 3
CLO value	0.85 +/- 0.25	0.6 +/- 0.25	0.85 +/- 0.25
Window opening behaviour	No	No	Yes
Annual energy consumption (kWh)	127,736	127,737	127,815

Table 4. Results of the PPD predictions under different CLO values

CLO value	CLO value (limits)	PPD
0.85 +/- 0.25	0.6 – 1.1	31%
0.7 +/- 0.25	0.55 – 0.85	28%
0.6 +/- 0.25	0.35 – 0.85	18%
0.6 +/- 0.15	0.45 – 0.75	23%

4. Conclusion

Since the beginning of the COVID pandemic, most organizations adopted remote and/or flexible working hours. This has resulted in buildings being occupied for fewer hours per day or with fewer occupants at any given time. The occupant behaviour studies can help in predicting the building's energy performance more accurately, for making better energy-related decisions. This paper focussed on the occupants' adaptive actions such as, clothing adaptation and the window opening behaviour. The simulation results showed that the clothing adaptation improved the comfort without affecting energy consumption, and the simulated comfort level depended on greater flexibility with regards to clothing. On the other hand, if the clothing adaptation were to be ignored, a higher level of target comfort maybe desirable which would require increased energy use. The window opening behaviour increased the energy consumption level while not affecting the comfort of the occupants. These adaptive behaviour patterns can help in improving the accuracy of energy performance predictions. It is essential to maintain the balance between the adaptive behaviours and the total energy consumption of the building. Also, the pandemic has underscored the importance of healthy indoor environment and practicing energy efficient strategies. Occupant behaviour studies can help in implementing these measures more effectively.

References

- [1] P. H. Shaikh, N. B. M. Nor, P. Nallagownden, I. Elamvazuthi, and T. Ibrahim, "A review on optimized control systems for building energy and comfort management of smart sustainable buildings," *Renew. Sustain. Energy Rev.*, vol. 34, pp. 409–429, Jun. 2014, doi: 10.1016/J.RSER.2014.03.027.
- [2] M. S. Geraldini and E. Ghisi, "Building-level and stock-level in contrast: A literature review of the energy performance of buildings during the operational stage," *Energy Build.*, vol. 211, p. 109810, Mar. 2020, doi: 10.1016/J.ENBUILD.2020.109810.
- [3] C. van Dronkelaar, M. Dowson, C. Spataru, and D. Mumovic, "A Review of the Regulatory Energy Performance Gap and Its Underlying Causes in Non-domestic Buildings," *Front. Mech. Eng.*, vol. 1, no. January, pp. 1–14, 2016, doi: 10.3389/fmech.2015.00017.

- [4] B. Bordass, A. Leaman, and P. Ruyssevelt, "Assessing building performance in use 5: Conclusions and implications," *Build. Res. Inf.*, vol. 29, no. 2, pp. 144–157, 2001, doi: 10.1080/09613210010008054.
- [5] P. X. W. Zou and M. Alam, "Closing the building energy performance gap through component level analysis and stakeholder collaborations," *Energy Build.*, vol. 224, p. 110276, Oct. 2020, doi: 10.1016/J.ENBUILD.2020.110276.
- [6] A. C. Menezes, A. Cripps, D. Bouchlaghem, and R. Buswell, "Predicted vs. actual energy performance of non-domestic buildings: Using post-occupancy evaluation data to reduce the performance gap," *Appl. Energy*, vol. 97, pp. 355–364, Sep. 2012, doi: 10.1016/J.APENERGY.2011.11.075.
- [7] R. Jack, D. Loveday, D. Allinson, and K. Lomas, "Quantifying the Effect of Window Opening on the Measured Heat Loss of a Test House," *Sustain. Ecol. Eng. Des.*, pp. 183–196, 2016, doi: 10.1007/978-3-319-32646-7_13.
- [8] S. Chen, G. Zhang, X. Xia, Y. Chen, S. Setunge, and L. Shi, "The impacts of occupant behavior on building energy consumption: A review," *Sustain. Energy Technol. Assessments*, vol. 45, p. 101212, Jun. 2021, doi: 10.1016/J.SETA.2021.101212.
- [9] "Thermal Environmental Conditions for Human Occupancy," *ANSI/ASHRAE 55-2017*, vol. 2017, p. 66, 2017, doi: ISSN 1041-2336.
- [10] EQUA, "Validation of IDA Indoor Climate and Energy 4.0 with respect to CEN Standards EN 15255-2007 and EN 15265-2007." [Online]. Available: http://www.equaonline.com/iceuser/validation/CEN_VALIDATION_EN_15255_AND_15265.pdf.
- [11] J. Carlander, B. Moshfegh, J. Akander, and F. Karlsson, "Effects on Energy Demand in an Office Building Considering Location, Orientation, Façade Design and Internal Heat Gains—A Parametric Study," *Energies*, vol. 13, no. 6170, p. 22, 2020, doi: 10.3390/en13236170.
- [12] B. of E. Efficiency, "Frequently Asked Questions on BEE recommendations on temperature setting of Air Conditioners," New Delhi, 2018. [Online]. Available: <https://pib.gov.in/PressReleaseIframePage.aspx?PRID=1537124#:~:text=Typically%2C room temperature is set,is 24-25 degree Celsius>.



Aalborg Universitet

AALBORG UNIVERSITY
DENMARK

**Energy retrofitting of non-residential buildings with effects on the indoor environment:
a study of university buildings at NTNU in Trondheim, Norway**

Bjelland, David; Hrynyszyn, Bozena Dorota

DOI (link to publication from Publisher):
[10.54337/aau541564763](https://doi.org/10.54337/aau541564763)

[Link to publication from Aalborg University](#)

Citation for published version (APA):

Bjelland, D., & Hrynyszyn, B. D. (2023). Energy retrofitting of non-residential buildings with effects on the indoor environment: a study of university buildings at NTNU in Trondheim, Norway. In H. Johra (Ed.), *NSB 2023 - Book of Technical Papers: 13th Nordic Symposium on Building Physics* (Vol. 13). [151] Department of the Built Environment, Aalborg University. <https://doi.org/10.54337/aau541564763>

Energy retrofitting of non-residential buildings with effects on the indoor environment: a study of university buildings at NTNU in Trondheim, Norway

David Bjelland¹ and Bozena Dorota Hrynyszyn¹

¹ Department of Civil and Environmental Engineering, NTNU, 7491 Trondheim, Norway
E-mail: david.bjelland@ntnu.no

Abstract. The year 2050 is considered the deadline for achieving the European climate goal of net zero emissions, an essential sustainability milestone. Current strategies ask for higher retrofitting rates in the building sector, as most of today's buildings will still be standing and be used in 2050, and longer. However, retrofitting strategies must consider energy and emissions reductions alongside social sustainability, targeting not only the building but also its users. Historically, the focus has been on indoor environmental quality, while other aspects of human well-being such as the quality of views were not addressed as frequently. Educational buildings can function as lighthouse projects, profiting from its many users as communicators. This article presents the retrofitting potential of the central building complex of the Gløshaugen campus of the NTNU in Trondheim in terms of energy, as basis to study the impact of retrofitting strategies on the indoor environment. The study consists of a selection of details, their building physical assessment, and a proposal of retrofitting measures. The results highlight the importance of human-centric definitions in the early (re-)design stages. Human-centric planning aspects can have diverse positive influences on the building's users, especially in educational and other highly cognitive settings. Their impact however is strongly dependent on the selection of measures and their implementation. Interactions of the many aspects of well-being that can be addressed during retrofitting must be studied further as their interdependencies are often unclear and case specific. Human-centric retrofitting can function as a guide for upcoming mass retrofits throughout Europe for the sustainable achievement of climate goals.

Keywords: Energy retrofitting; Indoor environment; Indoor comfort; Occupant well-being; Non-residential buildings

1. Introduction

This section explains the motivation of the case study. It contains a description of the climate goals of 2050 concerning the built environment and links these efforts to the two fields of indoor comfort and well-being.

1.1. Climate goals of 2050 and the role of non-residential building retrofit

The European Commission aims to reach climate neutrality by the year 2050 [1]. To achieve this goal, the “European Green Deal”, aligned with the Paris Agreement, was initiated [2]. The Green Deal is dedicated to improving the “well-being and health of citizens and future generations”, supporting among others renovated and energy efficient buildings in “A Renovation Wave for Europe” [3].

The main argument for retrofitting instead of building new and highly efficient buildings is the prediction that 85 – 95 % of today's buildings will still be standing and used in 2050, when climate-neutrality is wanted to be achieved. Existing buildings consume currently about 40 % globally, emitting 36 % of global climate gas emissions. [4] As all economic sectors aim to reduce energy consumption and related emissions, the relative share of the building and construction industry might get less insightful, which is why absolute values must be looked at. The International Energy Agency (IEA) states for 2021 that energy use in buildings increased to about 135 EJ (+ 17% compared to 2010) and associated emissions to about 9.9 Gt CO₂ (+10 % compared to 2010) and concludes that the building industry currently is not on track when it comes to set goals. Intermediate reductions due to Covid19 restrictions did not sustain, and lead to a rebound effect. [5]

Within the Renovation Wave, the three priorities are (1) energy poverty and worst-performing buildings, (2) public buildings, and (3) decarbonization of heating and cooling [3]. By targeting public buildings, the European Commission aims to establish role models for private buildings. Incentives are highly needed, as currently only 0.2 % of the building stock undergoes deep energy retrofit annually. The year 2030 represents an intermediate milestone for retrofits, where the European Commission aims for a 55 % reduction of emissions that cannot be achieved without the help of the building industry [4].

To align with the Renovation Wave, this case study focuses on a public, non-residential, university building complex which has a poor energy performance as typical for buildings that were built more than 50 years ago. The goal is to inspire other building retrofits and focus on buildings of educational usage with high energy demands.

1.2. Indoor environment

Indoor environmental quality ideally refers to the overall question whether a building or a room affects the comfort and well-being of the occupants. Its components traditionally include factors such as air quality, lighting, temperature, humidity, acoustics, and ergonomics. Widely accepted models exist for all those factors, making an integration relatively straight forward. However, it can be argued that aspects of well-being such as the quality of views and the effect on productivity that can and should be addressed are missing in most projects. To gather information on overall well-being that can be addressed in buildings, Hanc et al. performed a scoping review, where they established the eight themes of (1) subjective well-being, (2) eudaimonic well-being, (3) social well-being, (4) productivity, (5) environmental quality, satisfaction, and comfort, (6) mental health, (7) physical health, and (8) other [6]. All these themes have sub-themes that can be addressed in design such as the feeling of control (e.g., deployment of a sunshade) within eudaimonic well-being, the sick building syndrome (e.g., contamination, noise etc.) within physical health, and many more. The assumed biggest challenge of including parameters of human well-being, outside of established comfort parameters, is that that often introduces conflicts and contradictions especially among subjective aspects. Such an instance is easily demonstrated through the case of planning window areas (mostly) in new buildings. Here, it is desired to increase the areas as much as possible (under privacy constraints) to introduce natural daylight and stimulating views of the outdoors for enhanced productivity and learning, less stress etc. At the same time, depending on location, the risk for overheating versus the heat

transmission's loss demands a more optimized and balanced design of components, which often ends with window openings as small as possible. This simplified example shows the importance of the ability to compromise between contradicting requirements. Standards, such as the Norwegian building code TEK17 often don't provide guidance for issues like that for non-residential buildings [7]. In retrofits, the conflicts are limited by whatever is kept of the original structure and materials etc. Another difficulty is the interdisciplinary and already mentioned subjective nature of well-being that might include fields such as philosophy, social sciences, medicine, and psychology [8].

This case study aims to include aspects that exceed traditional factors of indoor environmental quality. As the buildings are mostly occupied by students and academic staff, the focus lies on the well-being theme of productivity. According to Hanc et al., the theme of productivity includes the sub-themes of (1) productivity and performance, (2) learning, and (3) cognitive performance. Large window areas for example can lead to higher test scores and increased learning speed for students by provision of daylight [9,10], while views of the outside can increase mental function and memory [11].

Despite not being able to focus on more aspects of well-being the authors believe that every (retrofit) project should assess what aspects of indoor comfort and well-being can be addressed additionally. With this study, the authors aim to contribute to combining previous and current research on an educational building case study in Norway, including social aspects with energy ambitions.

2. Method

Different methods and materials were used for the case study analysis of this paper. The introduction section is based on literature on climate goals and the role of energy-related building retrofit in that context, as well as scientific literature such as the mentioned review by Hanc et al. on the topics of indoor comfort and occupant well-being. The case study description within the ongoing FEM ZEN (Research Centre on Zero Emission Neighbourhoods in Smart Cities) research project is based on building information that was obtained in archives and through monitoring of the buildings' actual energy use. Hygro-thermal building physical simulations in the results section were then performed using the tools THERM [13] and WUFI [14] to build a basis for the retrofit measures proposed in the results section. The hygro-thermal analyses were performed on detailed level (mm scale), for representative building components, while the energy analyses represent the entire building complex using monthly and annual data.

2.1. Case study

This section contains a description of the research project, as well as the construction of the buildings looked at, their heritage value, energy, and the resulting retrofitting potential.

2.1.1. Project description

The building complex looked at in this paper is part of a pilot project by the "Research Centre on Zero Emission Neighbourhoods in Smart Cities" (FME ZEN) [15] that looks at the "Knowledge Axis" including the NTNU university campus in Trondheim, Norway. The research centre follows the zero-emission goal on neighbourhood level and contributes with its own definitions, KPIs, and active research on pilot projects [16]. Its predecessor, "The Research Centre on Zero Emission Buildings", builds the basis for the bigger neighbourhood scale. That is comprised of the categories (1) GHG Emissions, (2) Energy, (3) Power, (4) Mobility, (5) Spatial Qualities, and (6) Economy [17]. Even though the research centre focuses on Norwegian projects, it contributes very much to European goals and developments through its definitions and research cooperations. The "Knowledge Axis" project of NTNU, however, focuses mostly on the three categories of (1) GHG Emissions, (2) Energy, and (5) Spatial qualities. The central building complex on campus, as displayed in Figures 1 and 2 is the subject of this paper.

Apart from being part of the FME ZEN pilot, studying the building complex additionally aims to contribute to the "Campus development" project, in which the university strives for a unified campus

including both new and retrofitted buildings [18]. The development project is currently in the design phase in which a mapping of the retrofit potential of existing buildings plays a crucial role.

The chosen complex of buildings is comprised of two high-rise buildings with three adjacent/connecting buildings. The complex is, for the sake of the following analysis, divided into two parts: central buildings 1 (southern low-rise, southern high-rise, and central low-rise) and central buildings 2 (northern high-rise and the northern low-rise), see Figures 1 and 2.



Figure 1. Campus Gløshaugen of NTNU in Trondheim, Norway with the central building complex as case study (circle).
[Google Maps]



Figure 2. Campus Gløshaugen Central building complex
Foreground: southern low-rise building, background: two high-rise buildings and the central low-rise building.
[photo by the authors]

2.1.2. Construction

To analyse the existing structure, old documentation was retrieved from multiple archives throughout Norway. It revealed probable construction types, but the results were non-conclusive. The current state represented in this paper is therefore comprised of a combination of multiple sources and assumptions: archived information, previous renovation documentation, and recent maintenance efforts. Details on the main construction type and materials used can be found in Table 3 in the results section 3. All buildings of this case study are built with prefabricated concrete elements above ground level and a poured concrete under ground level, with interior insulation along the external walls. The construction type is considered typical and representative for many similar university buildings of the 1960's.

A WUFI analysis (simulation software for heat and moisture transiency) was performed to assess the assumed current state of the construction. The results indicate a risk for condensation and thereby a risk for mold in the existing, external wall construction, as shown in Figure 3. That is indicated by the points above the limit's lines, with the dashed line as limit for biodegradable substrates and the grey line as limit for non-biodegradable substrates. The analysis was performed for multiple wall variations due to uncertainties related to materials used. The risk for mold must be addressed in present and future considerations as the building documentation indicates the use of organic materials between two vapor-tight layers. These findings have a significant impact on the following retrofit propositions described in the results section 3.

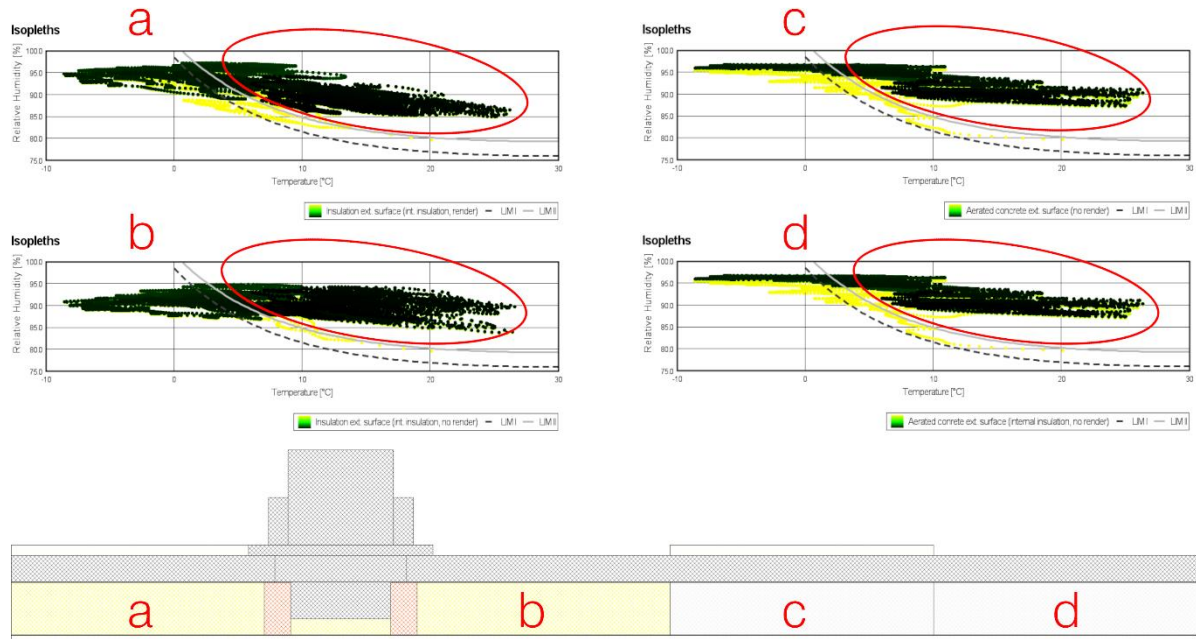


Figure 3. Hygro-thermal WUFI analysis of case study construction alternatives including mineral wool insulation (a,b) vs. porous concrete (c,d) and exterior render (a,c). Points above the limit lines (marked with red) indicate mold risk (with the dashed line as limit for biodegradable substrates and the grey line as limit for non-biodegradable substrates). [analysis by the authors]

2.1.3. Heritage value

The entire complex of central buildings built in the 1960's has heritage value and is classified as protection class C, which means that there might be restrictions to what can be done to the exterior aesthetic of the buildings. The entire campus "Gløshaugen", shown in Figures 1 and 2, is part of the ongoing and extensive process of the campus development described in section 2.1.1. This is relevant for this study, as even rebuilding measures on buildings of the highest heritage value class A (such as the main building, the northern most building colored dark red in Figure 4) have recently been approved by the Directorate of Cultural Heritage [19]. As the building complex looked at here is part of the same axis and therefore the established architectural landscape, proposed retrofitting measures have a significant potential to be approved. Especially as the entire campus, as neighbourhood, could be pushed one step closer toward a ZEN (Zero Emission Neighbourhood), improving occupant's overall well-being and sharing energy gains saved and generated between buildings.

Considering possible restrictions, proposed measures include solutions with exterior insulation (alternative 1) and a combination of both exterior and interior insulation (alternative 2), both of which must be considered under heritage value constraints. The alternatives will be further investigated and presented as separate studies after consulting the Norwegian Directorate of Cultural Heritage.

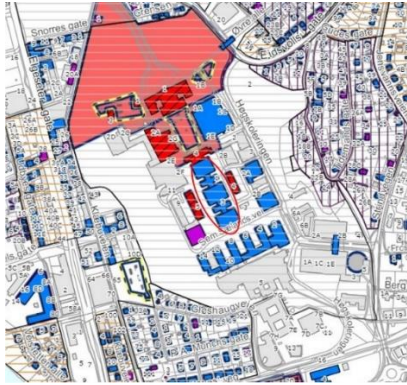


Figure 4. Campus Gløshaugen of NTNU in Trondheim, Norway with buildings of heritage value, the case study has value category C (red circle) [Byantikvaren].

Protection class A (red): Very high heritage value.

Protection class B (purple): High heritage value.

Protection class C (blue): Heritage value.

Buildings having overall values and potential as a cultural environment.

Unclassified: Value of protection.

2.1.4. Energy use

Monitored energy usage data from the year 2021 was retrieved as basis for energy-related retrofit analyses. The data has a time-step resolution of one hour and is divided into energy carrier. Table 1 shows that the main carrier was electricity, followed by the local heating system on campus which, to some degree, allows for energy sharing between buildings already now.

Table 1. Energy use of the case study buildings in 2021.

	Electricity [kWh/a]	Local heating [kWh/a]	District heating [kWh/a]	Total energy [kWh/a]	Area [m ²]	Energy per area [kWh/(m ² ·a)]
Central buildings 1	1864024	1390830	508724	3763578	17387	216
Central buildings 2	1460759	1164880	8706	2634345	12149	217

The choice of looking at the year 2021 was made for reasons of availability. Implications that the choice might have, are discussed in the discussion section 4.

3. Results

3.1. Retrofitting potential

As the retrofitting potential is hard to quantify, it was important to start with comparing the current measured energy consumption incl. heating and electricity to the Norwegian building standard TEK 17 [7]. In its current form, the regulation requires university buildings/high schools to have a maximum net energy consumption of 125 kWh/(m²·a). For the chosen case study this means that the energy consumption must be reduced by about 92 kWh/(m²·a) to reach the minimum energy requirements. That equals to a minimum needed energy reduction of about 42 %. When compared to both international and national retrofitting projects, a cut of about 42 % is realistic and can even be exceeded with extended retrofitting measures. A typical Austrian retrofit is reported to cut about 43 % of energy, while a reduction of up to 87 % was shown to be possible after the retrofit of a university building in Vienna [20]. A renovation study of Norwegian office buildings, on the other hand, showed that both a reduction of 50 % and 75 % is achievable [21]. Following Figure 5 shows the amount of energy that can be saved totally in different scenarios ranging from a minimum to an ambitious reduction of 80 %, equalling to a save of 2.69 to 5.12 GWh/a.

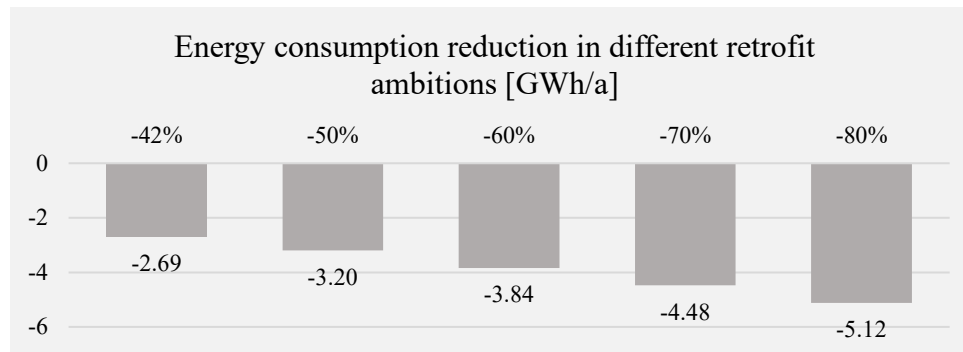


Figure 5. Saving potential of different levels of retrofitting ambitions for the entire complex comparing measured consumption to minimum requirements (-42 %), and more ambitious scenarios. [figure by the authors]

In Norway, both new buildings and total renovations must meet the minimum energy requirements, according to the Norwegian building code, TEK17 [7], which therefore also applies to the chosen case. If necessary, an exception must be requested and approved by authorities. The currently valid minimum energy requirements are based on maximum allowed U-values for components of a building envelope and shortly presented in Table 2. Additionally, applying to university buildings, the total net energy demand must be $\leq 125 \text{ kWh}/(\text{m}^2 \cdot \text{a})$, heated area (BRA).

Table 2. Minimum energy requirements, Norwegian building code, TEK17.

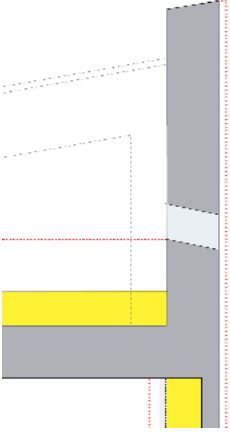
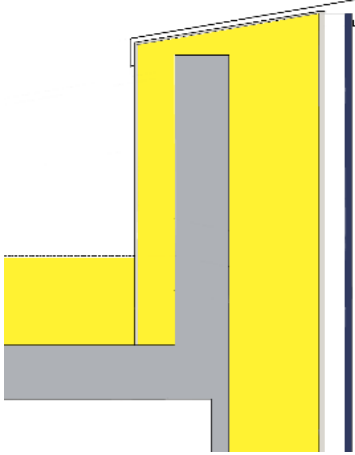
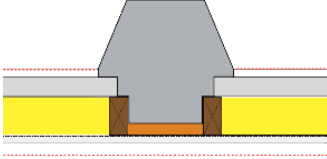
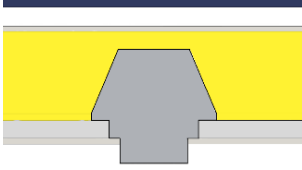
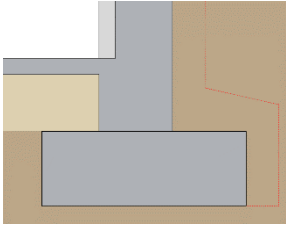
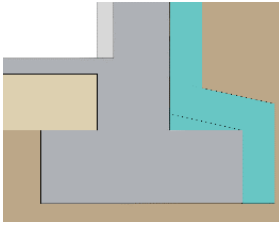
Floor	External wall	Roof	Window/Door	Airtightness
$\leq 0.18 \text{ W}/(\text{m}^2 \cdot \text{K})$	$\leq 0.22 \text{ W}/(\text{m}^2 \cdot \text{K})$	$\leq 0.18 \text{ W}/(\text{m}^2 \cdot \text{K})$	$\leq 1.2 \text{ W}/(\text{m}^2 \cdot \text{K})$	$\leq 1.5 \text{ l/h}$

Two main façade retrofitting alternatives were selected to be investigated. Both include the removal of some of the existing structures and materials used, the installation of new façade components, and the exchange of the current windows, as described in the following two sections.

3.2. Alternative 1, Exterior insulation

The first retrofit alternative with exterior insulation shown in Table 3, was selected based on the primary studies, and supported by simulations carried out in the thermal simulation tool THERM. The table shows detail drawings for both the existing construction and proposed changes. The choice of materials and their thickness, however, is a subject of further investigations and optimizations. This approach was considered the most usual and is expected to be the best performing (building physically). The minimum energy requirements given by the Norwegian building code, TEK17 [7] can easily be achieved. Constraints are given by the fact that additional materials are placed on the exterior surface of the existing façade that might be under heritage protection.

Table 3. Retrofit alternatives.

Description existing	Details existing (+ Alternative 2 marked “red”)	Details retrofit Alternative 1	Description retrofit
<p>Detail 1a: Roof</p> <p>Prefabricated concrete; exterior/interior insulation; mineral wool; vapor barrier between concrete and insulation; wooden construction on the top of the roof.</p>			<p>Detail 1b: Roof</p> <p>Exterior insulation; vapor barrier inside in the roof construction only; no wooden construction on the top of the roof.</p>
<p>Detail 2a: External wall</p> <p>Prefabricated concrete; interior insulation; mineral wool; cellulose based divider between concrete/insulation; vapor barrier inside.</p>			<p>Detail 2b: External wall</p> <p>Exterior insulation; no interior insulation; no cellulose-based divider; no wooden construction or cork materials inside; no vapor barrier inside; climate screen outside.</p>
<p>Detail 3a: Floor</p> <p>Poured concrete; interior insulation; mineral wool; no radon/moisture barrier.</p>			<p>Detail 3b: Floor</p> <p>Exterior insulation of the wall only; radon/moisture barrier in the floor only; no interior insulation.</p>

3.3. Alternative 2, Interior insulation combined with exterior insulation

Interior insulation is often considered “unwanted” (as unusual and expected to be a difficult approach) but sometimes a necessity due to exterior constraints such as the heritage value. Following measures (mostly on the interior) are proposed as “heritage-friendly alternative”, as only some of the measures are applied to the exterior surface:

- Existing interior insulation must be increased by additional insulation in the existing external wall, as shown with a red dot-line in details existing, in Table 3.
- Interior insulation must be completed by a thin layer of material with insulation function externally, as well, to meet the minimum energy requirements and, considering heritage requirements, unifying the visual appearance of the existing prefabricated concrete plates. Preferably and probably necessarily, the external prefabricated façade-plates of concrete

should be replaced with new components, such as alkali-activated concrete (ACC), with insulation function.

- Cellulose-based material must be removed from the external wall construction and replaced with a non-organic and well-performing material to avoid risk for condensation between concrete and interior insulation after retrofitting.
- The existing vapor-barrier must be removed and replaced with an another one made of flexible and well-performing material, such as a smart-vapor-barrier, after investigating this solution theoretically first.

This is where it is appropriate to mention that additional insulation can contribute to a lower quality of indoor environment in terms of access to daylight and views as mentioned in the introduction. This issue is rather poorly addressed in the Norwegian technical requirements TEK17 (Chapter 13 Indoor climate and health, paragraph 13-8) where only generally formulated requirements regarding access to daylight and view can be found [7]. However, the occupant's well-being, including both physical and mental comfort, is depending on a sense of connection and a feeling of security within the exterior environment, including a view of the three layers of sky, built and natural environment, and ground [22], which is not specified further in Norwegian regulations where it is only specified that sufficient quality of views must be ensured.

4. Discussion

Looking back at the ambition of the European Green Deal to improve human health and well-being, among others through the Renovation Wave, this study aims to link a case of energy retrofitting to the indoor environment. Typically, retrofitting projects are associated with a windows' change, in the first step, while by installing new windows in the same position the outcome can be negative, as additional insulation might reduce views and daylight. Exterior façade design should therefore aim for more flexible solutions, including window size, to achieve better performance and benefit for the new materials and components used. Other aspects to consider are the façade's orientation as that might require multiple façade solutions, as well as other relevant conditions including the protection of aesthetical and heritage values. Increasing the rate of retrofitting projects can be considered the most usual and efficient (also, in many cases, economically) approach to achieve significant energy, climate gas and demolition-related waste reduction, in long term. However, these kinds of projects are often impeded or opted out due to missing detailed solutions, recommendations, and reference projects. Especially, the concrete-based constructions potential of retrofitting having heritage constraints should not be underestimated and wasted. Both alternatives displayed depend on the addition of insulation material. The added thickness can lead to decreased views of the outdoor, that in turn can influence productivity. Window openings in both alternatives must therefore at least be of the same quality as in the current stage. The German code DIN EN 17037 [22] as example gives guidance on how to assess and ensure good quality of view as a combination of horizontal and vertical angles and layers of view, and the distance of views. This also depends on the elevation of the individual floors and room, resulting in lower quality of the low-rise buildings of this case. Alternative 1 and external insulation in general is considered favourable due to less risk for moisture within the construction, while alternative 2 must be considered if heritage restrictions apply only. It is more difficult to achieve due to the significant risk for condensation inside the existing external wall construction what can lead to a mold growth. This could result in a significant reduction of the indoor air quality and might introduce health-problems for long-term users. The complex showed to have great energy-related retrofitting potential of 2.69 GWh/a (-42 %) meeting Norwegian regulations, and up to 5.12 GWh/a (-80 %) according to very ambitious goals as found in reference projects.

To test whether the year 2021 is a representative year, the two months January and February were compared for 2021 and 2022 to see if large unknown Covid-19-related deviations show. This initial comparison showed no major difference in energy consumption. For the entire complex, the 2022 usage was at 102 % in January 2022 and at 97 % in February 2022 compared to the same months in 2021, see Figure 6.

That in mind, used 2021 energy data might be slightly higher than during other years but is considered sufficient for the estimates performed here. These two months of 2022 were the only ones available for comparison. Other parameters such as indoor temperature, outdoor weather conditions, and data from more years must be included to establish a reference year.

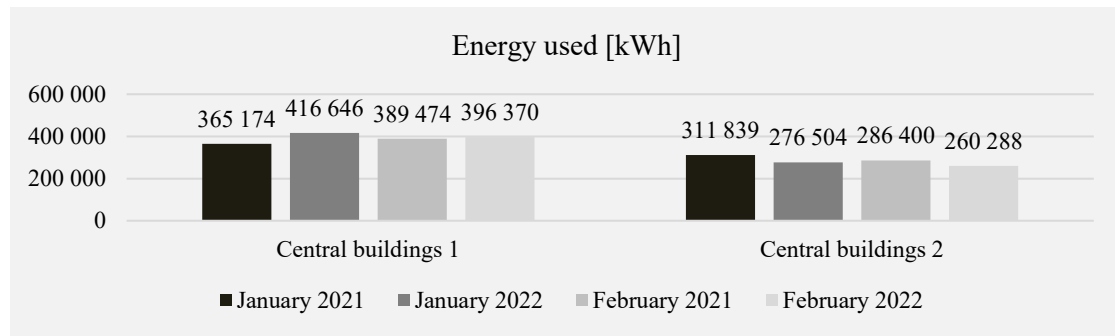


Figure 6. Energy use in the entire complex, comparison between January and February in 2021 and 2022. [figure by the authors]

Future retrofit propositions will be done in cooperation with other departments at NTNU to establish detailed HVAC definitions and will include user surveys. The fact that the user group is already known is considered an advantage of retrofit projects, as it is easier to compare pre and post-retrofit surveys and user participation in general. Both proposed alternatives are subject to ongoing analysis. More information and detailed drawings will be presented in separate studies after consulting the Directorate of Cultural Heritage. Some retrofit requirements must be met regardless of the chosen alternative. As mentioned in the introduction, good and ideally increased productivity of the occupants is one of the main goals, apart from energy and emission reductions. During the replacement of windows and providing additional insulation, following requirements must be met:

- Same or larger window openings, especially regarding Alternative 1, as smaller windows or reduced effective windows' area restrict both the access to natural daylight, views of the outdoors, and ventilation openings which is expected to decrease productivity.
- Windows of at least the same physical quality as worse windows negatively impact visual tasks and thermal conditions of the interior which is expected to decrease productivity.

Acknowledgements

We thank all students and colleagues involved in the research presented in this paper.

This article has been written within the Research Centre on Zero Emission Neighbourhoods in Smart Cities (FME ZEN). The authors gratefully acknowledge the support from the ZEN partners and the Research Council of Norway (project no. 257660)

References

- [1] "2050 long-term strategy." https://climate.ec.europa.eu/eu-action/climate-strategies-targets/2050-long-term-strategy_en (accessed Jan. 14, 2023).
- [2] "A European Green Deal." https://commission.europa.eu/strategy-and-policy/priorities-2019-2024/european-green-deal_en (accessed Jan. 14, 2023).
- [3] "Renovation wave." https://energy.ec.europa.eu/topics/energy-efficiency/energy-efficient-buildings/renovation-wave_en (accessed Jan. 14, 2023).
- [4] European Commission, "Communication from the Commission to the European Parliament, the European Council, the Council, the European Economic and Social Committee and the Committee

- of the Regions: A Renovation Wave for Europe - greening our buildings, creating jobs, improving lives.” European Commission, Oct. 14, 2020. Accessed: Mar. 01, 2022. [Online]. Available: <https://eur-lex.europa.eu/legal-content/EN/TXT/?qid=1603122220757&uri=CELEX:52020DC0662>
- [5] IEA, “Tracking Buildings 2021,” Paris, 2021. Accessed: Jan. 14, 2023. [Online]. Available: <https://www.iea.org/reports/tracking-buildings-2021>
- [6] Hanc M, McAndrew C, and Ucci M, “Conceptual approaches to wellbeing in buildings: a scoping review,” *Build. Res. Inf.*, vol. 47, no. 6, pp. 767–783, Aug. 2019, doi: 10.1080/09613218.2018.1513695
- [7] “Byggeteknisk forskrift (TEK17).” <https://dibk.no/regelverk/byggeteknisk-forskrift-tek17/> (accessed Jan. 14, 2023).
- [8] Orii L, Alonso L, and Larson K, “Methodology for Establishing Well-Being Urban Indicators at the District Level to be Used on the CityScope Platform,” *Sustainability*, vol. 12, no. 22, p. 9458, Nov. 2020, doi: 10.3390/su12229458.
- [9] Nicklas M and Bailey G, “Analysis of the Performance of Students in Daylit Schools,” Innovative Design, Inc., North Carolina, ERIC Number: **ED458782**, 1996. Accessed: Sep. 29, 2021. [Online]. Available: <https://files.eric.ed.gov/fulltext/ED458782.pdf>
- [10] Hesong L, “Daylighting in Schools An Investigation into the Relationship Between Daylighting and Human Performance Condensed Report,” 1999, doi: 10.13140/RG.2.2.31498.31683.
- [11] Hesong L, Aumann D, Jenkins N, Suries T, and Therikelsen R L, “Windows and offices: a study of office worker performance and the indoor environment,” California Energy Commission, California Energy Commission, P500-03-082-A-9, 2003. Accessed: Sep. 29, 2021. [Online]. Available: <https://newbuildings.org/resource/windows-and-offices-study-office-worker-performance-and-indoor-environment/>
- [12] Kamarulzaman N, Saleh A A, Hashim S Z, Hashim H, and Abdul-Ghani A A, “An Overview of the Influence of Physical Office Environments Towards Employee,” *Procedia Eng.*, vol. 20, pp. 262–268, 2011, doi: 10.1016/j.proeng.2011.11.164.
- [13] “THERM” | Windows and Daylighting. Accessed: Mar. 03, 2023 [Online]. Available: <https://windows.lbl.gov/software/therm>
- [14] “WUFI” | Home. Accessed: Mar. 03, 2023 [Online]. Available: <https://wufi.de/en/>
- [15] “NTNU Campus, Knowledge Axis Trondheim – FME ZEN.” <https://fmezen.no/knowledge-axis-trondheim/> (accessed Mar. 08, 2022).
- [16] Backe S, Bø L A, Askeland M, and Junker E, “ZEN Annual Report 2022.”
- [17] Wiik M R L et al., Zero Emission Neighbourhoods in Smart Cities. Definition, key performance indicators and assessment criteria: Version 3.0. SINTEF akademisk forlag, 2022. Accessed: Aug. 01, 2022. [Online]. Available: <https://sintef.brage.unit.no/sintef-xmlui/handle/11250/2997415>
- [18] “Campus development - NTNU.” <https://www.ntnu.edu/campusdevelopment> (accessed Jan. 14, 2023).
- [19] Hanger M R and Javorovic B E, “Riksantikvaren har godkjent ny byggeplan for Hovedbygningen,” Jan. 09, 2023. <https://www.universitetsavisa.no/campusprosjektet-hovedbygget-ntnu/riksantikvaren-har-godkjent-ny-byggeplan-for-hovedbygningen/373878> (accessed Jan. 14, 2023).
- [20] T. Wien, “energy innovation austria 5/2016,” Das Plus-Energie-Bürohochhaus der TU Wien Gebäudeinnovationen in der Praxis, May 2016. https://nachhaltigwirtschaften.at/resources/nw_pdf/eia/eia_165_de.pdf (accessed Jan. 14, 2023).
- [21] “LECO Rehabilitering av kontorbygg til faktor 2 og 4 SINTEF Bokhandel.” https://www.sintefbok.no/book/index/902/leco_rehabilitering_av_kontorbygg_til_faktor_2_og_4 (accessed Jan. 14, 2023).
- [22] DIN Deutsches Institut für Normung e.V., *Daylight in buildings: German version EN 17037:2018*, vol. 91.160.01. Berlin, Heidelberg: DIN Deutsches Institut für Normung e.V., 2019.



Aalborg Universitet

AALBORG UNIVERSITY
DENMARK

Building Physics in Living Lab

Tywoniak, Jan; Sojková, Kateřina; Malík, Zdenko

DOI (link to publication from Publisher):
[10.54337/aau541565072](https://doi.org/10.54337/aau541565072)

[Link to publication from Aalborg University](#)

Citation for published version (APA):
Tywoniak, J., Sojková, K., & Malík, Z. (2023). Building Physics in Living Lab. In H. Johra (Ed.), *NSB 2023 - Book of Technical Papers: 13th Nordic Symposium on Building Physics* (Vol. 13). [152] Department of the Built Environment, Aalborg University. <https://doi.org/10.54337/aau541565072>

Building Physics in Living Lab

J Tywoniak, K Sojková and Z Malík

Czech Technical University in Prague, Faculty of Civil Engineering,
Dep.Architectural Engineering, Thákurova 7, 166 29 Prague, Czech Republic

tywoniak@fsv.cvut.cz

Abstract. Team from Czech Technical University in Prague participated in prestigious international contest Solar Decathlon Europe 21-22. The topic of its FIRSTLIFE project was an extension of student dormitory by adding of new floors on the building together with a retrofit of the existing part. The paper deals with the pedagogical context of this activity. Students got an extraordinary opportunity to actually implement their theoretical proposals based on calculations. They also received feedback on the extent to which detailed designs are feasible in normal construction practice. New knowledge can be applied in future better estimation of the effect of imperfections, for example in calculations of heat conduction, the effect of thermal bridges, leaks for moisture transport and air tightness. Information about future research in Living Lab is given at the end of the paper.

1. International contest

Team from Czech Technical University in Prague (CTU) participated in prestigious international contest Solar Decathlon Europe 21-22 [1]. The topic of its FIRSTLIFE project [2] was an extension of student dormitory from the 1960s by adding of new floors on the building together with a retrofit of existing part. The overall solution was focused on compliance with the principles of sustainable construction, which includes very low energy consumption, use of renewable energy sources, ensuring comfort, use of nature based and recycled materials, integration of urban and social context, etc.

Within almost two years of activities, the student team delivered architectural and technical documentation and physical models of both, overall solution of the building retrofit and of functional unit (House Demonstration Unit, HDU – small house being an extraction of the overall solution). HDU was built by students supported by technicians of University Centre for Energy Efficient Buildings (UCEEB) CTU [3] during approximately 6 weeks. As a next step, the HDU being ready to approx. 60 % was disassembled and transported to the competition plot in Wuppertal. A time for final assembly and setting the HDU in operation was extremely short, only 227 hours.

After the end of the competition (3rd place in the Comfort category and 5th place in the House functioning category for the Czech team), and end of the exhibition being visited by 115.000 people, the HDU remains in place.

2. Tests and monitoring

2.1. First evaluations

As a part of the contest evaluation the organizers performed measurement of several parameters (temperatures, daylight, etc.) in one-minute step according to a detailed manual within contest rules [1]. Teams received data on-line and as a reaction had to choose an appropriate strategy to maintain indoor

comfort and maximize the HDU performance (opening/closing windows, setting up the regulation of mechanical ventilation and shading system etc.). The Comfort Contest has been evaluated without active cooling, heating or lighting.

The Temperature Sub-Contest used a slightly modified EN 15251 [4] approach and points were awarded based on the time in which the internal environment fulfilled the requirements of individual comfort classes. This meant, that each day the optimal interior temperature was different, based on the sliding weighted average of the outdoor temperature in the past seven days. 100 % of the points could have only been awarded, if all the measured indoor air temperatures were in the range of ± 2 K around the optimal indoor air temperature for a given day. At the same time, the free-floating relative humidity has been constantly measured and the maximal points could only have been awarded if all the measured values were in the range from 35 % to 65 %. The HDU has been fully operational during these measurements: the teams had to do laundry, let it dry, cook, simulate showering, prepare meals for other teams and also host dinners.

Organizers performed a set of short co-heating tests. The student teams then obtained the measured data – outdoor conditions, supplied energy and measured indoor conditions. Their task was to minimize the performance gap of previously set-up energy simulation models within the SimRoom software when compared with measured data. They were allowed to only adjust the basic model properties to account for the as-built state: areas of envelope components with U-values, thermal bridge surcharge ΔU_{TB} , glazing properties, shading and usable storage mass. They also could adjust the air tightness at n_{50} , to assume the envelope quality. They, however did not know the blowerdoor test results at the time of these calculations.

The relative air tightness was measured then [5]. The Czech team reached here the overall best result with n_{50} value of 0.89 h^{-1} . If we consider the extremely short construction time without the possibility of corrections, we accept it as a very satisfactory value.

External experts carried out a measurement of the air sound insulation of the perimeter wall [6] (the one with the largest proportion of windows and balcony doors was selected), where the Czech HDU also showed a very good result (41 dB), mainly thanks to the very high performing windows and the well-executed details of the connection to opaque parts.

2.2. Living Lab as a second step

Together with other seven HDUs, the Czech house becomes part of the newly emerging Living Lab, where it will be possible to monitor real properties under controlled conditions for at least the next 3 years, coordinated by University of Wuppertal (BUW) [7]. Data from the operation of technical systems, climatic data and data from the interior of the building will be used, among other things, for comparison with complex and simplified simulation calculations.

These may include overall building performance modelling using single-zone and multizone building models, investigation of accuracy of different floor-heating modelling approaches, analysis of windows and glazing performance, dedicated building energy systems simulations. Tools considered for these comparisons are assumed to be EnergyPlus based packages, such as OpenStudio, Ladybug Tools or Climate Studio. Furthermore, TRNSYS simulations and use of university-developed simulation algorithms are considered.

Operation in various modes is assumed, including repeated co-heating tests and free-floating situations. BUW increased its team by 5 new doctoral students focusing on the Living Lab and related sustainability agenda.

3. Education

3.1. Overall pedagogical context

The Czech team comprised bachelor's, master's and doctoral students from several study programs. The preparatory stages were integrated into the teaching in the design studio.

Students of architecture, architectural engineering and similar take classes in individual subjects from the field of building physics. They then apply the partial knowledge in the design studio subjects and in the final theses. However, the teaching is usually very theoretical. Participation in the competition, where in addition to conceptual questions and construction details, the actual implementation of the design is also solved, has an extraordinary benefit for students.

The students thus get a better idea of the properties of the materials and components they used in the design, if they are in a situation where they have to actually implement what they have drawn. Another important effect is the necessity to work in a team with students of different study programs, discuss proposals in variants and reach a final decision in each matter.

3.2. Increased practical knowledge in building physics

In the field of building physics, we can specifically mention as a possible permanent benefit for students the following:

- (a) For some of them, the first real physical contact with the insulating material – getting a feel for how it is realistic to implement a specific detail, seal joints, etc. under real construction conditions.
- (b) Getting a feel for what kind of imperfection needs to be accounted for in realistic calculations of heat conduction, moisture transport, soundproofing, etc. Let's mention, for example, an increase in thermal conductivity, linear and punctual thermal bridges, increase of thermal transmittance, increase of water vapour diffusivity due to not properly connected tight layers, reachable level of air-tightness used in calculation of efficiency of heat recovery and heat demand.
- (c) Overall feedback from the analyses of the measured values in HDU in operation, especially for doctoral students.
- (d) Detailed information about the technical solution is used as illustrative material in the lectures.

4. Concluding remarks

During the preparatory period the team organized a workshop for younger colleagues in a specialized design studio. After the end of the contest, an exhibition was organized in the premises of the university followed by a lecture, both presenting approaches of all 16 teams in the contest.

Practical lessons learned will be applied in the upcoming semester of teaching in the next specialized design studio: adding new floors to another student dormitory in Prague using the experience from the contest building.

Data obtained in the next 3 to 5 years in the Living Lab will also be interpreted in theoretical lectures. A cooperation among key persons from universities participating there is under preparation.

Moreover, there is a discussion among teaching staff about how to include practical (physical) construction work in the standard education, apparently using the UCEEB facilities [3].

In conclusion, it can be stated that in all respects the very demanding work of the students and the pedagogical management in the SDE contest brings a long-term positive effect. Of course, the ideal concrete result of our project would also be the real implementation of the extension of the student dormitory using the knowledge gained.

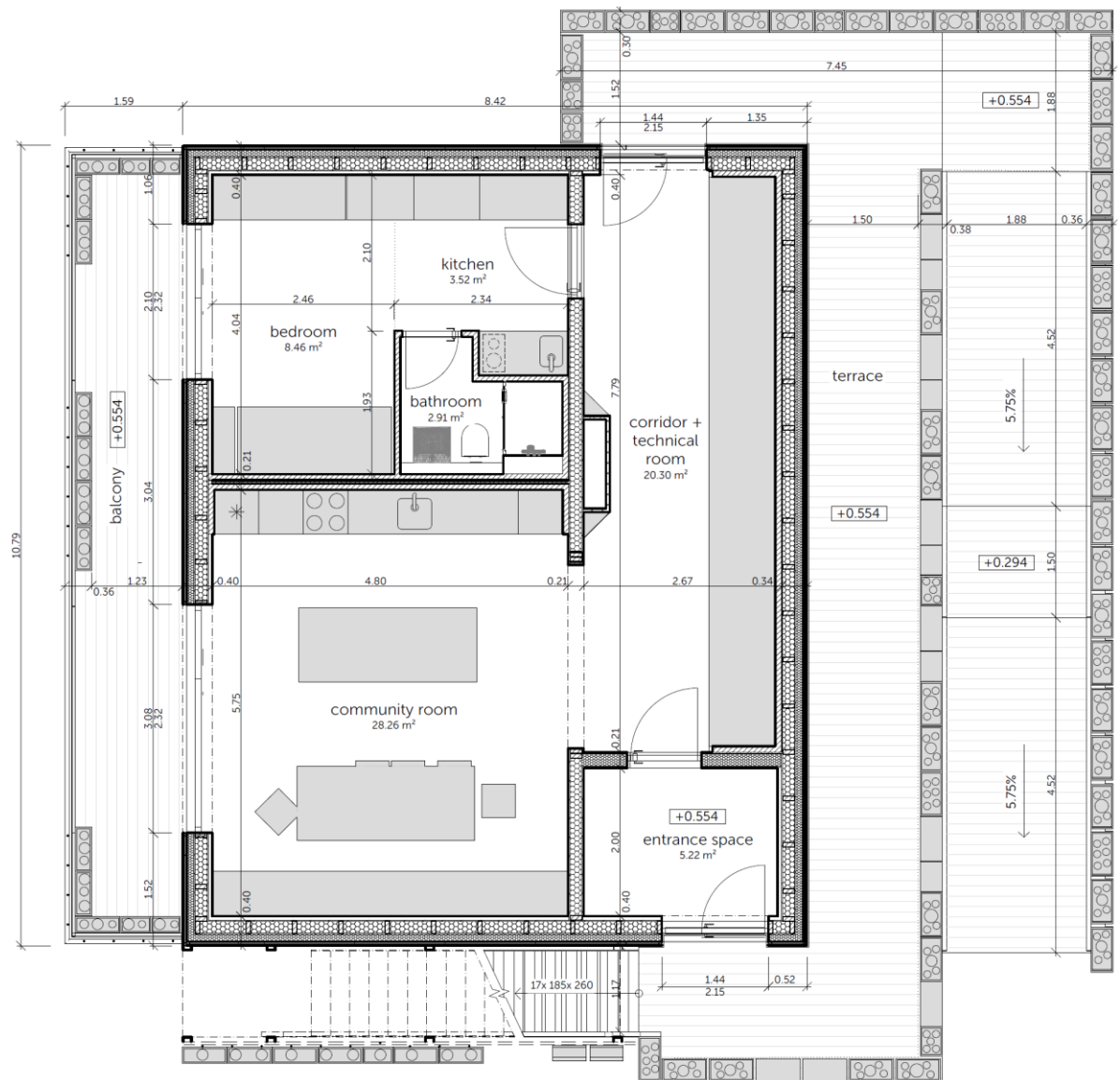


Fig. 1 HDU floor plan.

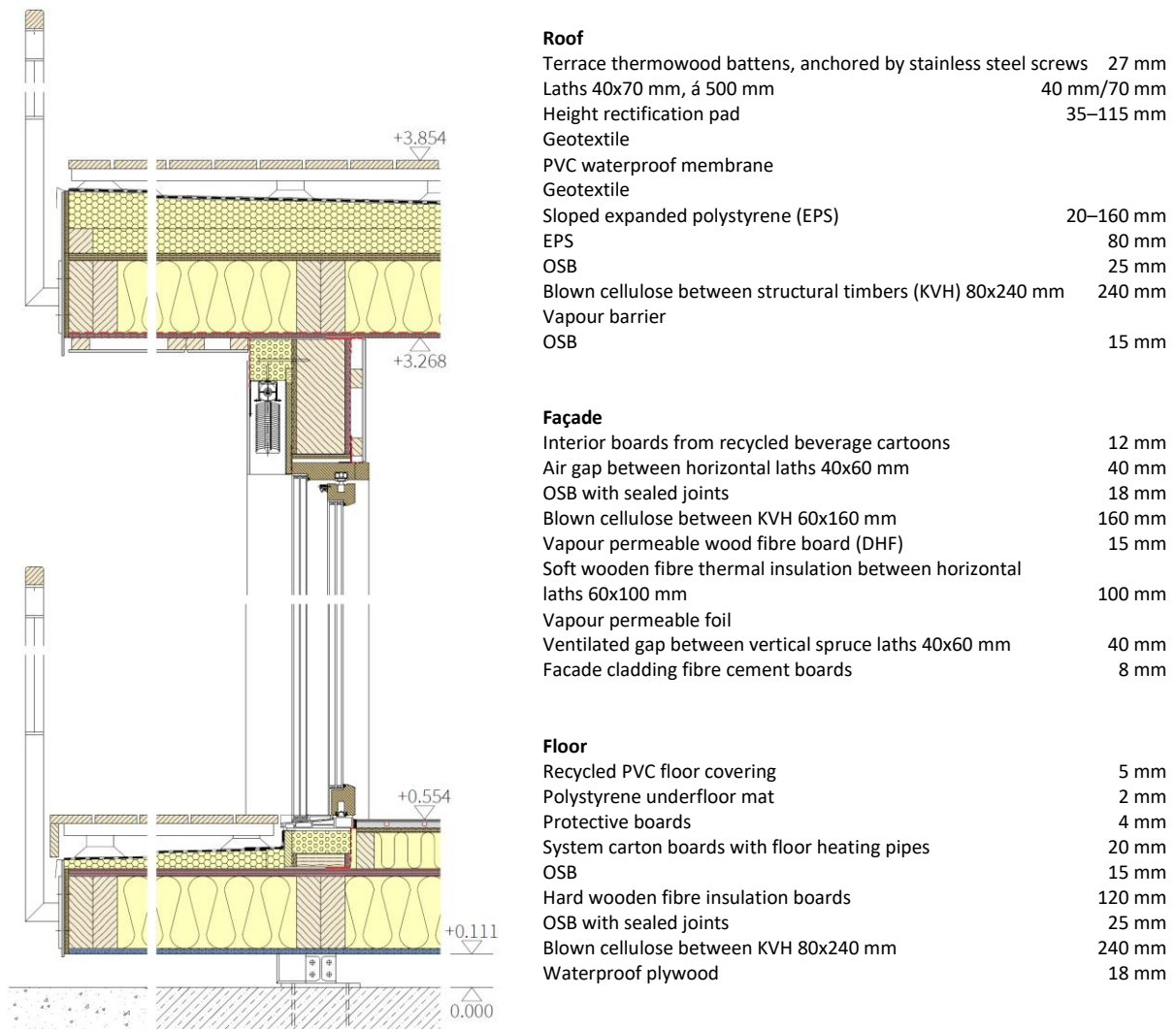


Fig. 2 Construction detail (east façade) and structure compositions.



Fig. 3 Air tightness measures carried out precisely by the team members – the construction phase was the first practical experience with structural detail implementation for most of the students.



Fig. 4 Finished Czech HDU at the competition plot in Wuppertal, Germany.

References

- [1] <https://sde21.eu>
- [2] <http://firstlife.cz>
- [3] <https://www.uceeb.cz/en/home/>
- [4] sw SimRoom. www.ingefo.de/Werkzeuge/SimRoom/
- [5] EN 13829 Thermal performance of building – Determination of air permeability of buildings – Fan pressurization method, CEN 2000
- [6] EN ISO 16283-3 Acoustics – Field measurement of sound insulation in buildings and of building elements – Part 3: Façade sound insulation, CEN 2017
- [7] <https://www.btga-arch.uni-wuppertal.de>



Aalborg Universitet

AALBORG UNIVERSITY
DENMARK

Documentation of moisture reduction up to two years after refurbishment of moisture damaged exterior basement wall

Høegh, Britt Haker; Vanhouttegehem, Lies; Hansen, Thor

DOI (link to publication from Publisher):
[10.54337/aau541578714](https://doi.org/10.54337/aau541578714)

[Link to publication from Aalborg University](#)

Citation for published version (APA):

Høegh, B. H., Vanhouttegehem, L., & Hansen, T. (2023). Documentation of moisture reduction up to two years after refurbishment of moisture damaged exterior basement wall. In H. Johra (Ed.), *NSB 2023 - Book of Technical Papers: 13th Nordic Symposium on Building Physics* (Vol. 13). [158] Department of the Built Environment, Aalborg University. <https://doi.org/10.54337/aau541578714>

Documentation of moisture reduction up to two years after refurbishment of moisture damaged exterior basement walls

B H Høegh¹, L Vanhouttegehem¹ and T Hansen¹

¹ Danish Technological Institute, Gregersensvej 1, 2630 Taastrup, Denmark.

brh@teknologisk.dk

Abstract. In Denmark, many old buildings are constructed with massive masonry basement walls. Originally, these basements were used for storage or as boiler room. Hence moisture in the basement walls was not considered a problem, and moisture protection of basement constructions was not considered necessary. However, leaving older buildings basement walls exposed to moisture from the surrounding soil, results in a high risk for damage and mould growth on the interior surface of the exterior basement walls. Today, many of these basements are used for daily purposes. Accordingly, moisture problems in the basements are no longer acceptable. Therefore, drainage systems in combination with external insulation of the basement walls are installed in many buildings. Traditionally, insulation materials with a high water vapour resistance are used as external insulation for basement walls in Denmark. However, theoretical approach and field experiences indicate that application of insulation materials with a low water vapour diffusion resistance, results in a larger reduction of the moisture content in the masonry of the basement's exterior walls. This paper documents moisture measurements from a basement, in which external insulation with low vapour diffusion resistance was applied to the external basement walls. Additionally, at the bottom of the basement walls a horizontal moisture barrier and perimeter drain were installed, as well as heating and natural ventilation of the basement. After one year, a noticeable reduction in moisture content was measured compared to the moisture content before installation, while no further reduction was seen after the second year.

1. Introduction

Many basements in Denmark are affected by moisture from surrounding soil and rising damp. This results in a high risk for damages and mould growth, not only on the interior surface of the exterior basement walls, but also in wooden beam ends of the joist floor above the basement, and on the interior and exterior surface of the exterior walls above terrain. Especially buildings from the late 18th and early 19th century, which are typically constructed with brick walls [1], are in risk, as the capillary suction in masonry walls with lime mortar can be several meters high.

Still, the residents use the basement e.g., as laundry or bike storage. To reduce the risk of mould growth and associated odour problems, measures to reduce the moisture content in the basement's exterior walls are often installed. These include for example the installation of a drainage system. As the earth around the building is dug up for installing the drainage system, this is usually combined with exterior insulation of the basement walls. Exterior insulation has a positive impact on the moisture conditions on the inner surface of the basement walls and on the building's energy consumption.

In Denmark, the exterior surface of the basement walls is typically tightened with a waterproof membrane, and an insulation material with a high water vapour resistance is used, to cut off soil

dampness from the outside [2]. However, the masonry basement walls of buildings established before the 1980's are normally not only affected by soil dampness from the outside. In masonry walls, rising damp from underneath the building constitutes another significant moisture source, that cannot be stopped by the installation of a drainage system and by tightening the outside of the basement walls. At the same time, the use of water and diffusion tight materials prevents moisture transport from the masonry to the outside.

To allow for this moisture transport, insulation materials with a low vapour diffusion resistance should instead be used as external insulation of basement walls. A theoretical study on the effect of exterior insulation of basement walls with an insulation material with low water vapour resistance has shown that this results in a lower moisture level in the basement walls and in a higher drying speed of the masonry [3]. However, the use of water vapour open materials on the outside of the basement walls still requires that the basement walls and the subjacent foundations are protected from ground water by use of perimeter drains, sometimes complemented with sub-slab drainage or a horizontal moisture barrier. In this paper, field experiences and moisture measurements with different measurement methods are presented for a case study building, in which insulation with a low vapour diffusion resistance was used for external insulation of the basement walls.

2. Description of the case building and the installed moisture reduction measures

The case building is a multi-story building established in 1906, situated next to a lake in Copenhagen city, where the ground water level is high. The basement has a floor area of 166 m² and a clear height of 140 cm. The joist floor above the basement starts approximately at terrain level.

The basement's exterior brick walls are 500-610 mm thick and placed directly on clay ground. The partition brick wall to the neighbouring building is 360-480 mm thick. Originally, the exterior basement walls were treated with asphalt on the outside, which is typical for the building period in Denmark. The inside rendering (lime mortar) of the basement walls appeared with efflorescence and peeling.

The existing ground slab in the basement consists of a non-reinforced concrete ground slab (ca. 5 cm) placed on a layer of pebbles. In the pebbles layer, sub-slab drainage pipes were placed along the inside of the brick wall foundations and connected to a well. The pipes were silted up. On the outside of the basement walls, a perimeter drain was installed in the early 2000's.

In June 2016, a first series of moisture measurements was performed with the Troxler gauge (see chapter 3.2) to investigate the moisture content and the height of rising damp in the exterior walls of the basement and the first floor. From the measurements, it was concluded that the moisture level in the exterior basement walls and in the lower parts of the exterior walls on the first floor was quite high. Therefore, the building-owner's association decided to implement measures to reduce the moisture level in the exterior basement walls and the walls on the first floor to avoid mould growth on the internal surface of the walls and to protect the wooden beam ends in the joist floor above the basement from dry rot. Following measures were installed in 2020 (completed November 2020), see also Figure 2:

- The asphalt layer on the outside of the exterior basement walls was removed.
- 100 mm insulation with low vapour diffusion resistance was installed on the outside of the exterior basement walls. The insulation consists of a bitumen glued expanded polystyrene with 35 % pore volume and thermal conductivity of $\lambda = 0,039 \text{ W/(m}\cdot\text{K)}$. Measurements for water vapour resistance of the product are not available, but as the material is not airtight and water can run through the material, the water vapor resistance of the material is assumed to be low.
- A geotextile with a low vapour diffusion resistance was mounted on the outside of the insulation.
- New perimeter drainage was laid on the outside of the exterior basement walls.
- The sub-slab drainage pipes were cleaned, and two new wells were established.
- A horizontal moisture barrier of stainless steel was established in the masonry on top of the first course over the basement ground slab. In the exterior basement walls, the barrier was placed over the total thickness of the wall, except behind the boiler, where the barrier was established from the outside, covering only about 75 % of the thickness of the exterior walls. In the partition

wall to the neighbouring building, the horizontal barrier was stopped ca. 20-50 mm from the inner surface in the neighbouring building, to avoid damage.

- All render was removed from the inner surfaces of the exterior basement walls. Afterwards, the surfaces remained untreated.
- Heating was installed in the basement, and the indoor temperature kept at 16-18 °C year-round.
- Natural ventilation was established in the basement to continuously remove moisture from the indoor air. The air outlets were formed as a gooseneck, to lift them over terrain level.

3. Description of measurement methods, measurement positions and time of measurements

This chapter describes the measurement positions and the time of the measurements, as well as the two methods used for moisture measurements in the exterior basement walls. The first method uses the Troxler gauge, the second method uses a hf-sensor.

Measurement positions and time of measurements

For each number marked on the basement plan (Figure 1), measurements were taken at 3 different heights (Figure 2): MH1 at 20-40 cm, MH2 at 60-80 cm and MH3 at 110-130 cm above the ground slab.

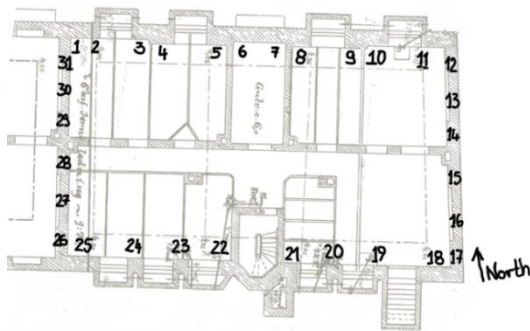


Figure 1. Basement plan with measurement positions. Figure 2 shows measurement heights (MH).

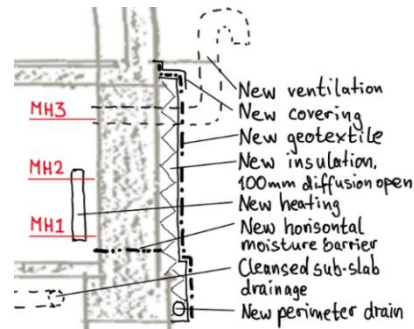


Figure 2. Exterior basement wall with indication of measurement heights (MH) and moisture reduction measures.

The first series of measurements were performed with the Troxler gauge in June 2016, before any moisture reduction measures were applied. As the basement was divided in small storage rooms, no measurements at the interior surfaces of the exterior basement walls in east and west orientation could be performed. In January 2022, one year and two months after the completion of the moisture reduction measures, the second measurement series with the Troxler gauge were performed. At that time, all interior surfaces of the exterior basement walls, except behind radiators and the boiler, were accessible. A third measurement series was performed in November 2022, two years after completion of the moisture reduction measures, using both the Troxler gauge and the hf-sensor.

Moisture measurement with Troxler gauge

Measurements with the Troxler gauge are non-destructive. In most constructions, depending on the included materials, the Troxler gauge registers the moisture content up to a depth of 100-150 mm. The presence of salts or air gaps in the investigated materials or constructions does not influence the moisture measurement. Measurements can be performed at temperatures under 0 °C. [4]

The Troxler system [4,5] is based on a moisture gauge with a small radioactive source. This calibrated neutron source emits a steady stream of fast neutrons into the measured construction. The neutrons are reflected by collision with the atomic nuclei in different materials in the construction. The velocity of the neutrons is reduced significantly in collision with the light hydrogen nuclei bound in both water and in other materials, while heavy atomic nuclei reduce the velocity of the neutrons only slightly upon return. The Troxler gauge counts only the slow neutrons, that are reflected by hydrogen nuclei, and gives

a result called the Troxler digit count. The content of bound hydrogen in a material usually varies little. Thus, variations of digit counts, when measuring on the same type of material, reflect variations of moisture content. According to practical experience of the authors, Troxler digit counts on masonry in the range of 8-12 indicate a moisture content of up to 0,8 weight %, digit counts over 50 indicate a moisture content of more than 10 weight-%.

Moisture measurement with hf-sensor

The third series of moisture measurements included moisture measurements with a hf-sensor [4,6]. Different surface sensing heads allow measurements at different depths in a material. In this case, the surface sensing heads MOIST-R2M and MOIST-PM were used, allowing measurement depths of 7 cm and 30 cm, respectively. As with the use of the Troxler gauge, the presence of salts in the investigated materials or constructions does not influence the measurements. However, surface roughness and air gaps have a great impact on measured moisture content. Moreover, metallic objects in the construction must be avoided, and a temperature above 0 °C is required for measurements.

The hf-sensor uses a dielectric moisture measurement method. As water is a polar molecule, water molecules can be forced to orientate in a preferred direction by an electric field. By applying an alternating electromagnetic field, the water molecules will start rotating with the frequency of the field. This rotation (orientation polarization) is described by the dielectric constant (also permittivity). At high frequencies, there will occur dielectric losses. As the dielectric effect of water is much stronger than the dielectric effect of most solid building materials, the dielectric losses of water can be measured as an indication of even small amounts of water in the measured material. The instrument provides the results as moisture content in weight-% for the chosen material.

4. Results

The results of the moisture measurements with the Troxler gauge are shown in Figure 3. The variation of the Troxler digit counts at the different measurement dates and at different heights above the ground slab are shown separately for each of the three exterior basement walls (North, East and South) and for the neighbouring partition wall (West).

The individual results of the basement walls showed a larger moisture reduction in the middle of a wall section e.g., at measurement positions 2, 10, 13, 16, 19 or 23, while the moisture reduction was less

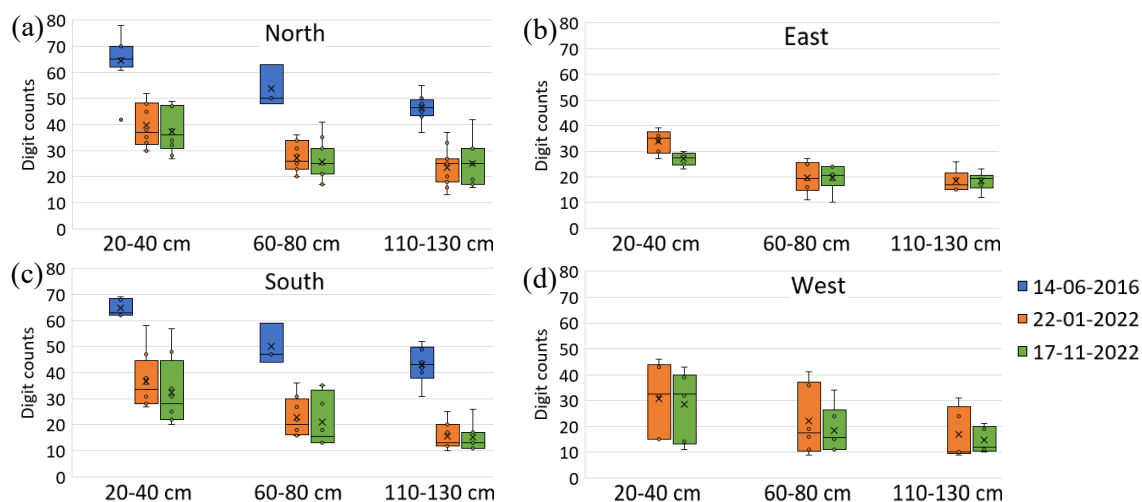


Figure 3. Troxler measurement results on the interior surface of the exterior basement walls at different heights over the ground slab before (blue series), 1 year 2 months after (orange series) and 2 years after (green series) installation of the moisture reduction measures. Graphs a), b), c) and d) represent the three exterior basement walls and the neighbouring partition wall.

in wall areas close to exterior wall corners (positions 11, 12, 17 and 18), close to intersections with partition walls (positions 1, 6, 7, 21, 22, 25, 26 and 31), or at level MH1 behind the boiler (position 9).

In Figure 4 the results of the moisture measurements with the two hf-sensor surface sensing heads are shown separately for each of the three exterior basement walls (North, East and South) and for the neighbouring partition wall (West). The individual results showed higher moisture content in the same wall areas, as for the measurements with the Troxler system i.e., close to outer wall corners, intersections with partition walls and at level MH1 behind the boiler.

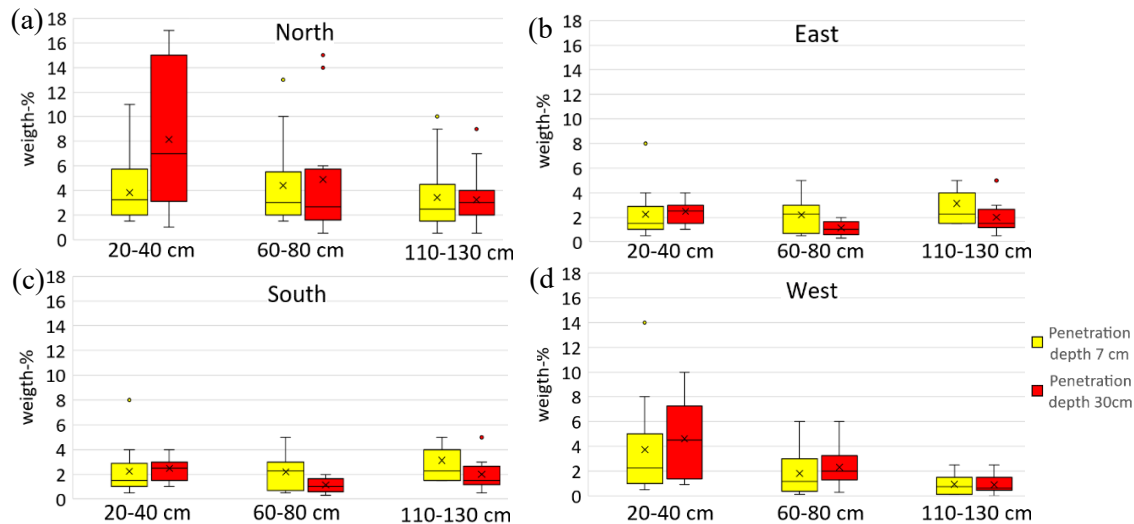


Figure 4. Hf-sensor measurement results at 7 cm depth (yellow) and 30 cm depth (red) on the interior surface of the exterior basement walls at different heights over ground slab, performed 2 years after installation of the moisture reduction measures. Graphs a), b), c) and d) represent the three exterior basement walls and the neighbouring partition wall.

5. Discussion

One year and two months after the installation of the moisture reduction measures, measurements with the Troxler system showed a noticeable reduction of the moisture level at all measurement heights for the exterior basement walls towards north and south (Figure 3, a) and c)). In the following 10 months, no further significant moisture reduction was measured, neither in these walls, nor in the eastern wall (Figure 3, b)) or the neighbouring partition wall (Figure 3, d)).

Comparing the individual results for each wall after the implementation of the moisture reduction measures, a variation in moisture content was seen, which indicates varying moisture reduction in the different parts of each wall. Lowest reduction was seen close to corners, in areas with adjacent partition walls or behind the boiler, where the horizontal moisture barrier only covered 75 % of the thickness of the exterior wall.

Two years after the installation of the moisture reduction measures a moisture content in the exterior basement walls of 0,5-17 weight-% was registered with the hf-sensor. The highest moisture content was measured at height MH1 over the ground slab. At height MH3, close to the joist floor above the basement, a moisture content of 0,5-4 weight-% was measured. To avoid dry rot, the acceptable moisture content in the wooden beam ends should at maximum be 20 weight-%, corresponding to a relative humidity (RH) of 87 % [4]. In equilibrium with 87 % RH, masonry has a moisture content of less than 0,6 weight-% [7]. This criterium was still exceeded in most of the masonry right under the joist floor.

Measurements with the hf-sensor showed similar moisture levels with both sensor heads, indicating the same moisture level at both penetration depths. Only in the northern wall at height MH1 over the ground slab, the results indicate a larger moisture reduction in the surface of the wall than in its core.

Furthermore, measurements with the hf-sensor showed a wider range in measured moisture content,

with more outliers in all measurement positions, than measurements with the Troxler gauge. This could be due to the structure of masonry walls. Masonry joints, especially the butt joints, are not totally filled up with mortar when erecting a masonry wall, resulting in remaining air gaps in the structure. Both these air gaps and the roughness of the surface of masonry walls are considered to affect the measurements with the dielectric moisture measurement method used by the hf-sensor, resulting in a larger variation of results.

6. Conclusions

Moisture measurements one year and two months after the completion of the moisture reduction measures showed a remarkable reduction of the moisture content in the masonry of the basement's exterior walls. Although no noticeable moisture reduction was registered in follow-up measurements after 2 years, further moisture reduction is expected, but at a lower speed. Compared to the results of the study in [3], the moisture reduction in this case was faster and more effective. We assume that the fast moisture reduction is related to the installation of heating in the basement, as the elevated indoor temperature in the basement induces the necessary gradient in vapour pressure over the exterior basement wall construction. We assess that this gradient was the driving force for water vapour transport from the masonry, through the exterior vapour diffusion open insulation material, to the surrounding ground. To investigate this further, we suggest hygrothermal simulations of the case-study.

At the same time, the results indicated a positive effect on the moisture reduction by the installation of a horizontal moisture barrier of stainless steel at the bottom of the exterior basement walls and neighbouring partition wall. The effect was though slightly reduced at positions, where the horizontal moisture barrier did not penetrate the whole wall thickness.

The achieved moisture content in the exterior basement walls right under the joist floor above the basement at height MH3, was still higher than expected for masonry walls under normal indoor conditions, and in general still giving conditions for development of dry rot. Thus, moisture protection measures for the wooden beam ends in the joist floor above the basement are still required.

Comparing both measurement methods, we suggest more measurement positions in a smaller measurement grid, when using a hf-sensor compared to the Troxler-gauge, in order to reduce the influence of air gaps in the masonry joints and obtain reliable measurement results.

7. Acknowledgments

Measurements were performed partly on demand of the building-owner's association and partly as activity in a project supported by the Ministry of Higher Education and Science. Thanks to the building-owner's association and especially to Max Lord for consenting to supplementary measurements and to the publication of the results of the project.

References

- [1] Engelmark J 1983 *Københavnsk Etageboligbyggeri 1850-1900. En Byggeteknisk Undersøgelse* (Hørsholm: Statens Byggeforskningsinstitut) pp 135 ff.
- [2] Brandt E, et al. 2022 *SBi-anvisning 279 Fugt – Bygningsdele* (Danmark: BUILD, Aalborg Universitet)
- [3] Geving S, Kvalvik M and Martinsen E 2011 Rehabilitation of basement walls with moisture problems by the use of vapour open exterior thermal insulation *9th Nordic Symposium on Building Physics* (vol 1) (Amsterdam: North-Holland/American Elsevier) pp 323-300
- [4] Brandt E, et al. 2022 *SBi-anvisning 277 Fugt – Teori, beregning og undersøgelse* (Danmark: BUILD, Aalborg Universitet)
- [5] 2006 *Instruction Manual Model 3216 Roof Moisture Gauge* (Troxler Electronic Laboratories, Inc.: Durham, NC, USA)
- [6] hf sensor GmbH, Leipzig, Tyskland located at www.hf-sensor.de
- [7] Kielsgaard Hansen K 1986 *Technical Report 162/86 Sorption Isotherms A Catalogue* (Danmark: The Technical University of Denmark)



Aalborg Universitet

AALBORG UNIVERSITY
DENMARK

Measurement of air change behaviour at Finnish apartment rooms

Kayo, Genku; Suzuki, Nobue

DOI (link to publication from Publisher):
[10.54337/aau541579038](https://doi.org/10.54337/aau541579038)

[Link to publication from Aalborg University](#)

Citation for published version (APA):
Kayo, G., & Suzuki, N. (2023). Measurement of air change behaviour at Finnish apartment rooms. In H. Johra (Ed.), *NSB 2023 - Book of Technical Papers: 13th Nordic Symposium on Building Physics* (Vol. 13). [165] Department of the Built Environment, Aalborg University. <https://doi.org/10.54337/aau541579038>

Measurement of air change behaviour at Finnish apartment rooms

Genku Kayo¹, Nobue Suzuki²

¹ Tokyo City University, Japan

² Freelance

genku@tcu.ac.jp

Abstract. While the expectation for natural ventilation is increasing under the context of COVID-19, fresh air at residential houses in Finland is basically guaranteed by mechanical ventilation systems. It means that natural ventilation is not considered as an available potential of ventilation in Finnish building regulation. Even if the mechanical ventilation system handles the air quality, the natural ventilation by window opening is expected to be a supportive measure. However, there is not enough measured data about how much air change is fulfilled by window opening. The article describes the evaluation of fresh air accessibility by window openings at six Finnish apartments. To understand the behaviour of air change, CO₂ mass balance equation model was applied. The results of summer season clarified that the actual number of air changes are 0.85 to 1.54 times per hour with one-side opening. The CO₂ mass balance model for apartments, which is a kind of tracer gas decay method, is an effective way to estimate the actual number of air changes without preventing occupants' daily living. Since some buildings, such as residential, school, churches, are affected by the moisture problems, the management of moisture behaviour by both natural and mechanical ventilation is essential.

1. Introduction

1.1. Importance of ventilation

Currently, the residential built environment faces two big risks; one is related to the heat waves and cold waves threat caused by the climate crisis, and another is indoor infection risk under the context of COVID-19 crisis. Therefore, enhancing ventilation is one of the key measures for coping with these risks. REHVA, ASHRAE or SAGE-EMG publish the guidelines for epidemic [1, 2, 3]. These guidelines show the acceptable limitation of CO₂ concentration rate for managing safe indoor air quality, such as under 1000 ppm in ASHRAE or 1500 ppm in REHVA. CO₂ concentration rate can be the appropriate key indicator to monitor indoor air quality. However, these guidelines don't show the air change rate as an indicator. In case of Japanese guideline for COVID-19 based on SHASE (the Society of Heating, Air-Conditioning, and Sanitary Engineers of Japan) [4], the air change rate is also shown as one of indicators. In addition, enhancing natural ventilation is strongly recommended. Natural ventilation cannot guarantee the appropriate amount of air change, because it is unstable and the efficiency is affected by local situation such as window layout, surrounding of building, wind profile or occupants' behavior. In case of Finland, fresh air at residential houses in Finland is basically guaranteed by mechanical ventilation systems and the natural ventilation is not considered as an available ventilation

solution in the Finnish building regulation. That's why a centralized ventilation system controls the indoor air quality of rooms in apartment building. Especially in the context of infection control under the COVID-19, ventilation is getting more important than ever. Even if the mechanical ventilation system handles the air quality, natural ventilation by window opening is expected to be a supportive measure. However, there is not enough measured data about how much air change is fulfilled by window opening.

1.2. Objectives

To clarify the potential of natural ventilation for air change under Finnish climate condition, the article describes the evaluation of fresh air accessibility by window openings at rooms of Finnish apartments.

2. Methodology

2.1. Investigated apartment rooms

The authors measured the indoor environment factors (air temperature, relative humidity, and CO₂ concentration rate) in both summer and winter in 2022. The article reports the evaluation results of summer investigation. The number of air changes was estimated with several patterns of opening window combination, closed condition, one-side opening condition, and cross-opening condition. The details of investigated cases is summarized in Table 1.

Table 1. Detail of investigated cases

		Case 1	Case 2	Case 3	Case 4	Case 5	Case 6
Number of Rooms		4	3	5	5	4	4
Number of Adults		4	4	4	2	3	4
Number of Child		2	2	3	0	0	2
Volume	m ³	119.6	120.2	123.6	209.4	130.8	125.0

2.2. Layout of openings

Fig 1 shows the pictures of openings a living room. The opening consists of three parts, door for accessing balcony, small window for ventilation, and large window. The large window is usually closed and only open when cleaning the glass. In summer season, the occupants of investigated room manage the door for accessing balcony for ventilation because it is large and easy to open. Fig 2 shows the layout of openings of the apartment rooms. Every living room connects to the balcony and kitchen and bedroom are located the opposite side. When the occupants handle cross ventilation by opening kitchen or bedroom together with openings at living room.

2.3. CO₂ mass balance equation

The methodology for measuring ventilation rate Mass balance equation model regarding CO₂ concentration was applied to estimate the behavior of air change.

$$V_o C_o dt + m G dt = V_r dC_r + V_o C_r dt \quad (\text{Eq 1})$$

V_o Ventilation rate [m³/s]

G CO₂ generation rate from body
[mg/s/person]

V_r Room volume [m³]

m Number of people [person]

C_r CO₂ concentration rate, indoor [mg/m³]

C_o CO₂ concentration rate, outdoor [mg/m³]



Fig 1. Openings at the living room

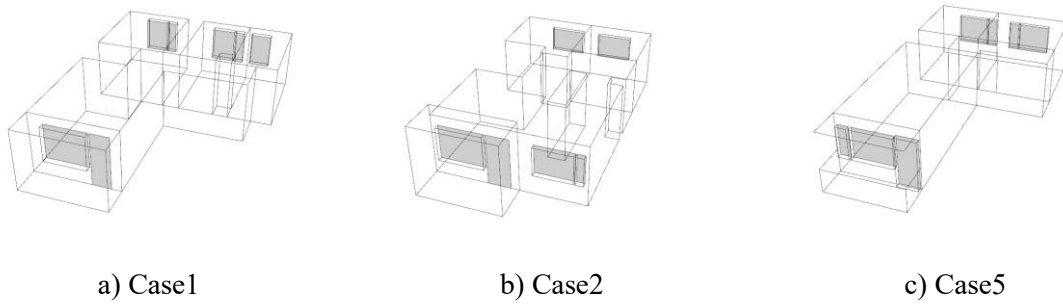


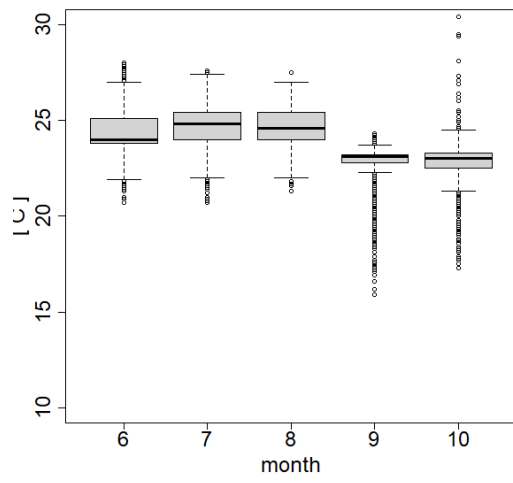
Fig 2. Openings at the living room

3. Results and Discussions

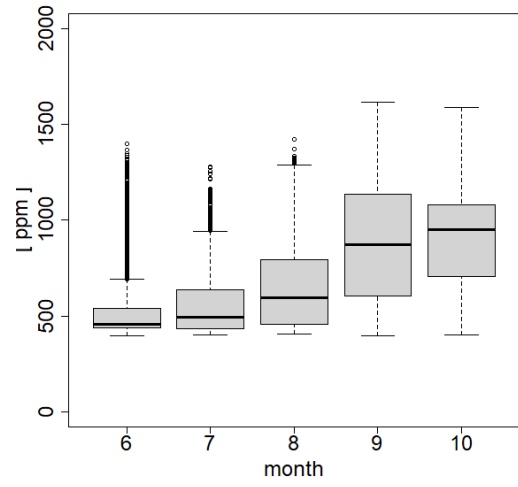
3.1. Trend of indoor environment

Fig 3 shows the monthly boxplots of indoor air temperature and CO₂ concentration in Case 1. The range between the first and third quartiles is 2 to 3°C and the range of monthly indoor air temperature are quite small. The monthly average indoor air temperature dropped approximately 1°C from August to September while the average outdoor air temperature decreased around 9°C. Through the months, the level of CO₂ concentration gradually increased from summer to autumn. It is because that the opportunity of window openings gets decreased through outdoor air temperature dropping down. In other word, window opening for natural ventilation worked well in summer season to keep CO₂ concentration level low.

Fig 4 shows the series of hourly CO₂ concentration trends in each month from July to October. In summer season, the CO₂ concentration was low through the day, it means that the occupants managed the level of CO₂ concentration by window opening. By shifting to the autumn season, the level of CO₂ concentration increased especially in night-time. The CO₂ generation from occupants' body was higher than exhausting CO₂ by ventilation system. The results shows that window opening as occupant behaviour has potential to manage CO₂ concentration level.

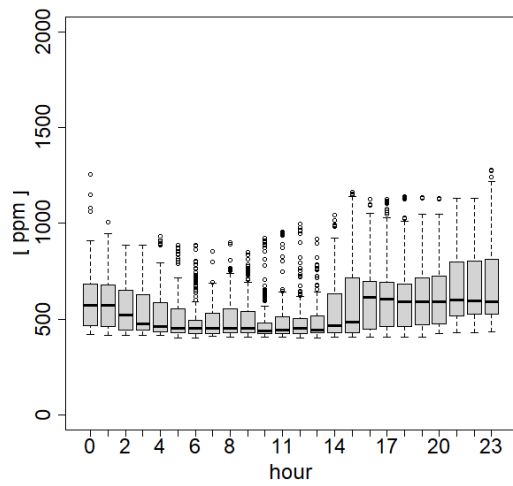


Indoor air temperature

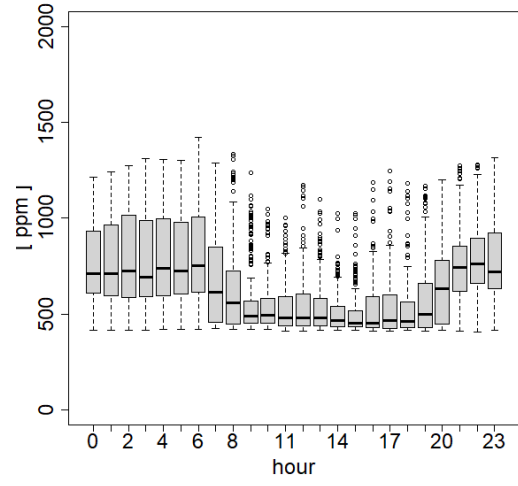


CO₂ concentration

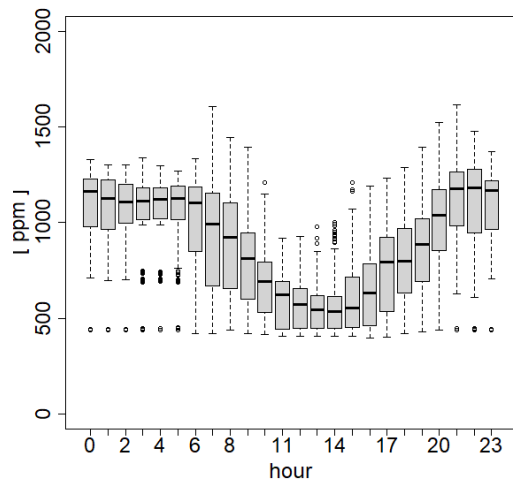
Fig 3. Monthly boxplots of measured values, Case 1



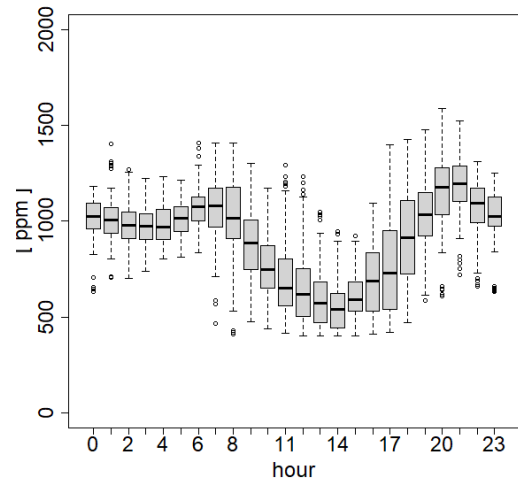
July



August



September



October

Fig4. Hourly trends of CO₂ concentration at Case 1

3.2. Ventilation rate at one-side opening

Fig. 5 shows the trend of CO₂ concentration rate during the measurement of Case 1. The CO₂ concentration rate changed between 500 and 900 ppm by reputation of window open and close. By closing windows, CO₂ concentration increased from 500 ppm to 850 ppm in 15 minutes in the apartment room with three adults. By opening one window, the CO₂ concentration decreased from 850 ppm to 480 ppm in 15 minutes. The maximum level did not exceed the limitation suggested by the guideline as 1000 ppm. The window opening can be a supportive measure to control indoor air quality under the limitation suggested by the guidelines. Fig. 6 shows the air change volume rate during the measurement and the dark grey bars indicate a one-side opening case. Case 1 has potential to change the amount of air 104 L/s on average, which is equivalent to 3.13 times per hour when the opening at balcony opened as the occupants usually do in summer. In the case of the apartment flat of Case 2, it has air exchange of 81.6 L/s on average, which is equivalent to 2.44 times per hour when the opening at balcony opened. And the case of apartment flat of Case 5, the air of 28.4 L/s in average, which is equivalent to 0.85 times per hour, is changed when the opening at bedroom opened.

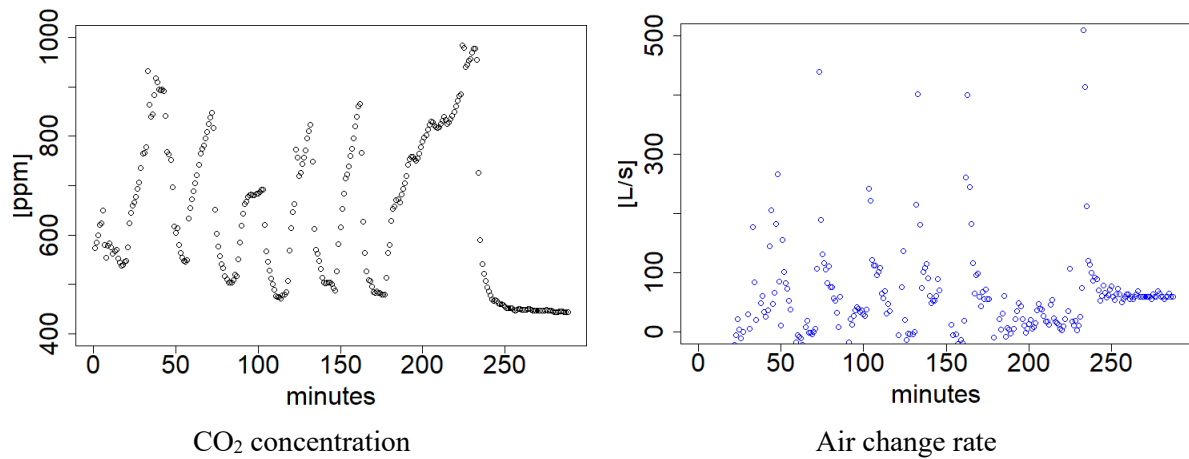


Fig 5. Trends of value during the measurement at Case 1

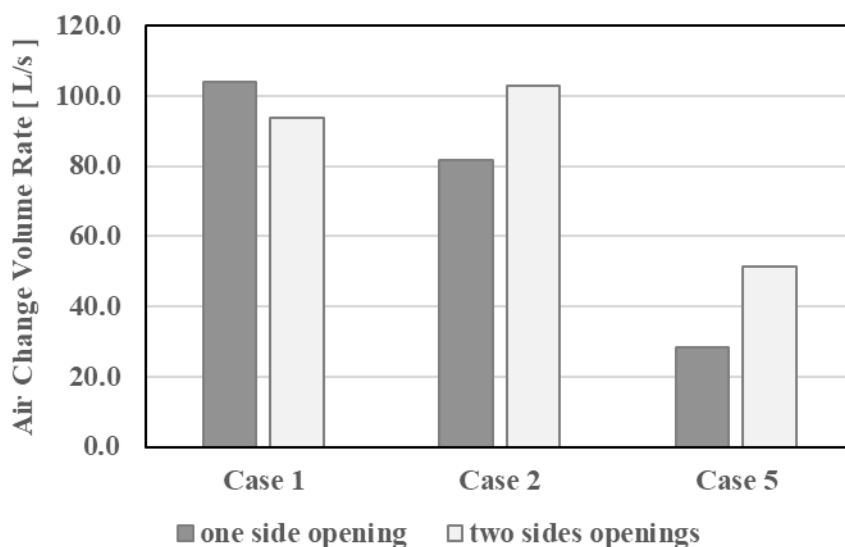


Fig 6. Air change volume rate

3.3. Ventilation rate at cross ventilation

Light grey bars in Fig 6 indicate the air change volume rate in two-side openings which means cross ventilation was implemented. In addition to the opening opened at one-sided study, which is mentioned in 3.2, the result of cross-ventilation was 93.9 L/s in average, which is equivalent to 2.82 times per hour in Case 1. The result of Case 2 was 103 L/s on average, which is equivalent to 3.10 times per hour, at cross ventilation. And 51.4 L/s, which is equivalent to 1.54 times per hour in Case 5. Compared with one-side opening, cross ventilation increased the air change volume 26% in Case 2 and 81% improvement in Case 5. On the other hand, the amount of air change in Case 1 decreased by 10%. The performance of ventilation is affected by not only occupant behavior but also wind profile. Therefore, it is needed to investigate more long-term and reputation of measurement in different wind situations in order to get more accurate result.

4. Conclusions

The results of summer season clarified that the actual number of air changes are 0.85 to 1.54 times per hour with one-side opening and it reaches up to 3.12 when cross ventilation. The measured apartment rooms are all available to apply cross-ventilation across living room to bedroom. Since some buildings, such as residential, school, churches, are affected by the moisture problems, the management of moisture behavior by both natural and mechanical ventilation is essential. The observation of air change with the CO₂ mass balance model can be an effective method also for the problem. The CO₂ mass balance model for apartments, which is a kind of tracer gas decay method, is an effective way to estimate the ventilation rate without preventing occupants' daily living.

Acknowledgement

This work was supported by the Scandinavia-Japan Sasakawa Foundation (GA22-JPN-0067).

References

- [1] REHVA, COVID-19 GUIDANCE Ver.4.1, 15 April 2021
- [2] ASHRAE, COVID-19: ONE PAGE GUIDANCE DOCUMENTS, 24 June 2021
- [3] SAGE-EMG, Role of Ventilation in Controlling SARS-CoV-2 Transmission, 23 October 2020
- [4] Kurabuchi T, Yanagi U, Ogata, M, et al. Operation of air-conditioning and sanitary equipment for SARS-CoV-2 infectious disease control. *Jpn Archit Rev.* 2021;00:1–13.
<https://doi.org/10.1002/2475-8876.12238>



Aalborg Universitet

AALBORG UNIVERSITY
DENMARK

Improving the optical properties of finishing coatings for façade systems

Veloso, Rita Carvalho; Dias, Catarina ; Souza, Andrea Resende; Maia, Joana ; Ramos, Nuno M. M.; Ventura, João

DOI (link to publication from Publisher):
[10.54337/aau541592743](https://doi.org/10.54337/aau541592743)

[Link to publication from Aalborg University](#)

Citation for published version (APA):

Veloso, R. C., Dias, C., Souza, A. R., Maia, J., Ramos, N. M. M., & Ventura, J. (2023). Improving the optical properties of finishing coatings for façade systems. In H. Johra (Ed.), *NSB 2023 - Book of Technical Papers: 13th Nordic Symposium on Building Physics* (Vol. 13). [179] Department of the Built Environment, Aalborg University. <https://doi.org/10.54337/aau541592743>

Improving the optical properties of finishing coatings for façade systems

Rita Carvalho Veloso^{1, 2*}, Catarina Dias¹, Andrea Resende Souza², Joana Maia², Nuno M. M. Ramos² and João Ventura¹

¹IFIMUP –Departamento de Física e Astronomia, Faculdade de Ciências, Universidade do Porto, Rua do Campo Alegre s/n, 4169–007 Porto, Portugal

²CONSTRUCT-LFC-Departamento de Engenharia Civil, Faculdade de Engenharia, Universidade do Porto, Rua Dr. Roberto Frias, 4200-465 Porto, Portugal

*up201001431@up.pt

Abstract. The need to improve energy efficiency of the building stock has led to a continuous increase in the implementation of exterior thermal insulation systems, such as ETICS. Progressively, these systems are being applied with darker colours, increasing the concern for hygrothermal behaviour and durability. Despite the significant developed studies, very few reports regarding their optical properties are available. The optical and catalytic capacity turns nanomaterials into excellent candidates for use in finishing coatings with high solar reflectance with dark colours without affecting the aesthetic characteristics, thus improving the durability of such coatings. Our study targeted the development of innovative envelope systems by increasing their solar reflectance through new finishing coatings formulations with the inclusion of nanoparticles. For that, it is necessary to develop and optimize nanoparticles formulations to achieve a high near-infrared reflectance. Here, we studied how the incorporation of reflective nanomaterials influence the optical behaviour of a black colourant for a finishing coating, varying the concentration in the coating from 0 to 20%. Such optical performance was experimentally evaluated through spectral reflectance calculations using a modular spectrophotometer, which allowed an understanding of the relation between these properties and the morphological and structural characteristics of the nanoparticles. The results from such studies can help formulate new finishing coatings with increased near-infrared reflectance of buildings façades, using, for instance, more than one type of nanoparticle.

1. Introduction

Nowadays, the construction of new buildings and rehabilitation of existing ones must consider thermal requirements, safeguarding the thermal comfort conditions in summer and winter, and reducing the heating and cooling energy loads [1]. One of the key factors for achieving such goal aims to reduce the excessive solar radiation absorbed by buildings and the consequent heat gains that leads to large necessity cooling demands to preserve indoor thermal comfort [2].

When designing an energy-efficient building, one important tool is the application of thermal insulation systems, as for example ETICS. Research and development of ETICS is well established but such studies focused mainly on the hygrothermal performance of the system [3]. Fewer studies are directed to the importance of the finishing layer for the durability of these systems. Besides, there is an increasing tendency to use dark tones and colors on façades with ETICS for aesthetic reasons [4], leading to higher temperature values of surfaces exposed to solar radiation. These high thermal oscillations to

which façades are subjected can cause anomalies and a reduction in their service life, particularly in regions with large climate amplitudes. Such fluctuations can provoke dimensional variations and consequently deformation and cracking.

To attenuate this effect, it is possible to integrate high reflectance pigments that are characterized by having high solar reflectance and high infrared emittance, in their finishing coatings [5]. For instance, Bishara et al. [6] tested four different black finishing coatings: two conventional organic and inorganic coatings and two coatings with NIR reflective pigments concluding that the surface temperature can be reduced by around 10 K using such reflective materials. Experimental studies performed by Ramos et al.[4] evaluated the natural degradation of the coloured finishing coating with NIR reflective pigments, in ETICS systems. The authors concluded that the incorporation of those pigments in the finishing coatings can increase the durability of the system, consequently improving the thermal performance, without comprising the aesthetic characteristics.

Although several solutions with high reflective materials are widespread in the scientific community, the literature review shows that the research emphasis on maximizing the reflectance without considering the visual aesthetic. Also, this technology is mainly applied on roofs, instead of building façades.

As such, this work focuses on the incorporation of nanomaterials with improved reflectance in a commercial black colorant used on ETICS system for façades. An assessment of the optical properties of the doped samples were carried out to analyse the adequacy of such formulations in the finishing coating for the system application.

2. Materials & methods

2.1. Incorporation of the nanoparticles in the commercial black colorant

Selected commercial nanoparticles (Table 1) were combined with the black commercial colourant in different proportions to obtain different concentrations (1, 3, 5, 8, 12, 16 and 20% w/w) in order to study the effect of their properties on the optical performance of the colourant, particularly in the near-infrared region. The black commercial colourant is black iron (II, III) oxide-based dispersion with a colour index PBk11 and 48% pigment content. All samples were mixed in a beaker at room temperature until a homogeneous mixture was obtained and applied with the aid of a spatula on 35×35×3 mm³ acrylic substrates. The visual aspect of all samples is shown in **Figure 1**.

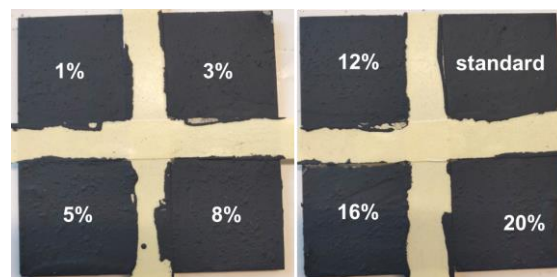


Figure 1: Visual aspect of the colourant-doped samples.

Table 1: Reflective nanomaterials properties used to dope the conventional black colourant.

Nanomaterial	Diameter (nm)	Crystalline phase	R _{Total}	R _{NIR}
TiO ₂ Anatase	25,1000	Tetragonal	0.79-0.81	0.72-0.80
TiO ₂ Rutile	50, <5000		0.65-0.90	0.63-0.83
ZnO	10-30, 500	Hexagonal	0.70-0.88	0.69-0.84
Al ₂ O ₃	13, 300	Trigonal	0.83-0.88	0.74-0.87

2.2. Optical properties evaluation

The optical properties, such reflectance and colour properties, were carried out using the “ASTM E903-Standard Test Method for Solar Absorptance, Reflectance and Transmittance of Materials Using Integrating Sphere”[7]. According to the procedure, the Solar Reflectance (SR) of the materials was calculated based on:

$$SR = \int_{280}^{1650} RI_{\lambda}d\lambda / \int_{280}^{1650} I_{\lambda}d\lambda \quad (1)$$

while the NIR Solar Reflectance (SR_{NIR}) was calculated using:

$$SR_{NIR} = \int_{700}^{1650} RI_{\lambda}d\lambda / \int_{700}^{1650} I_{\lambda}d\lambda \quad (2)$$

Where R is the measured spectral reflectivity by the spectrophotometer, and I_{λ} the spectral irradiance of the sun at the earth surface ($W/(m^2nm)$), according to the ASTM Standard G197 [8] to a vertical surface. A modular spectrophotometer was used to continuously assess such measurements in the 200-1650 nm range. Each sample was measured six times at different locations to calculate the spectral reflectance based on Table X2.1 100 ordinates Direct Normal Irradiance A.M. 1.5 of ASTM G173 [9].

As for the colorimetric analysis, the color coordinates of all samples were determine using the UV-Vis region with same equipment. The CIE L^*a^*b color coordinates, was used as recommended by the Commission Internationale de l'Eclairage (CIE) [10] in the 200–1650 nm range using ten standard observed angle, D65 illumination and after calibration with a white standard (Spectralon®). The colour difference (ΔE) is the colour variation between two materials (1, 2) and it can be calculated using:

$$\Delta E^*_{ab} = [(\Delta L^*)^2 + (\Delta a^*)^2 + (\Delta b^*)^2]^{1/2} \quad (4)$$

3. Results and Discussion

3.1. Reflectance evaluation

The optical properties of the samples were assessed by measuring the reflectance and determining the colorimetric parameters. The calculated total and near infrared reflectances are presented in Figure 2Figure 3, respectively, versus the nanoparticle concentration for the different diameters. As showed in Figure 2, the reflectances of the sample are below 0.20. Although the values are lower than the limit considered for reflective coatings (0.65)[11], it is still an interesting result considering we are using a black tone colourant. As verified, all samples present a similar performance (as expected) by partially absorbing the visible light, characteristic of a dark tone coating. Although all nanoparticles improve the total reflectance, the best performance was attributed to the TiO_2 Rutile 50 nm size [Figure 2(b)], especially for concentrations between 5% and 12%. A similar behaviour is observed for the alumina particles [Figure 2(d)]. However, the results are not better than the ones found for dioxide titanium.

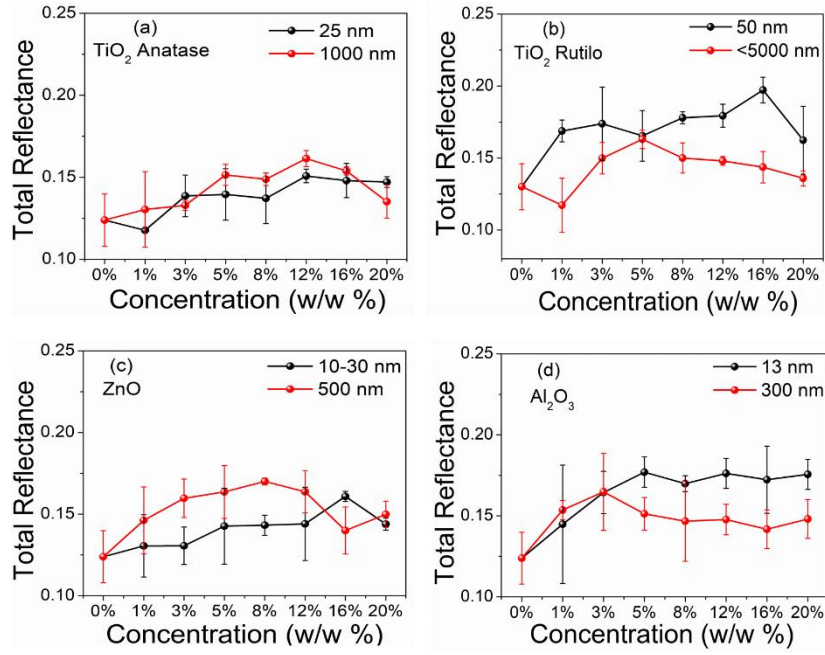


Figure 2: Calculated total average reflectance using ASTM E903 of the of conventional black colourant samples doped with (a) TiO_2 Anatase, (b) TiO_2 Rutile, (c) ZnO, (d) Al_2O_3 .

Analysing Figure 3, it is possible to notice that in the near-infrared region the doped samples present distinguished differences, showing enhanced reflectance when compared to the conventional one. The most promising result was obtained for the TiO_2 nanoparticles, particularly in the rutile phase [Figure 3(b)], with an overall maximum reflectance of 22% at 16% of concentration, when compared to only 12% of the conventional black colourant.

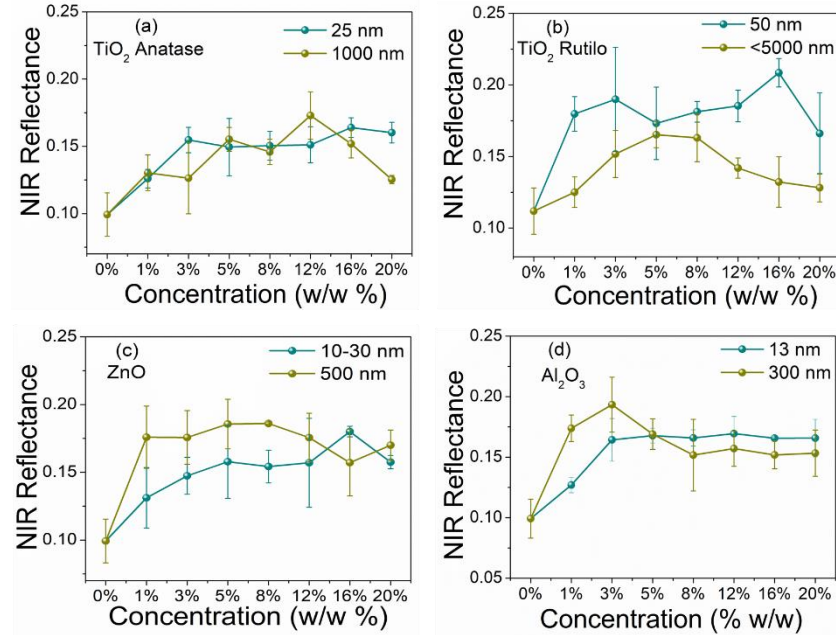


Figure 3: Calculated NIR average reflectance using ASTM E903 of the of conventional black colourant samples doped with (a) TiO_2 Anatase, (b) TiO_2 Rutile, (c) ZnO, (d) Al_2O_3 .

3.2. Colourimetric assessment

If we look closer to the results obtained, almost all samples show a ΔE above 3, being considered perceptible or very perceptible. Thereby, the inclusion of nanomaterials can have an increase in the lightness of the doped samples, turning them lighter than the conventional black colourant. One of the possible causes of this effect is related to the poor dispersion of the nanomaterials in the matrix, turning the samples greyish. Nevertheless, there are interesting results and possible candidates that can be used as dopants in colourants without significantly influence the visual aesthetic and simultaneously improving the reflectance, as is the case of the titanium dioxide samples.

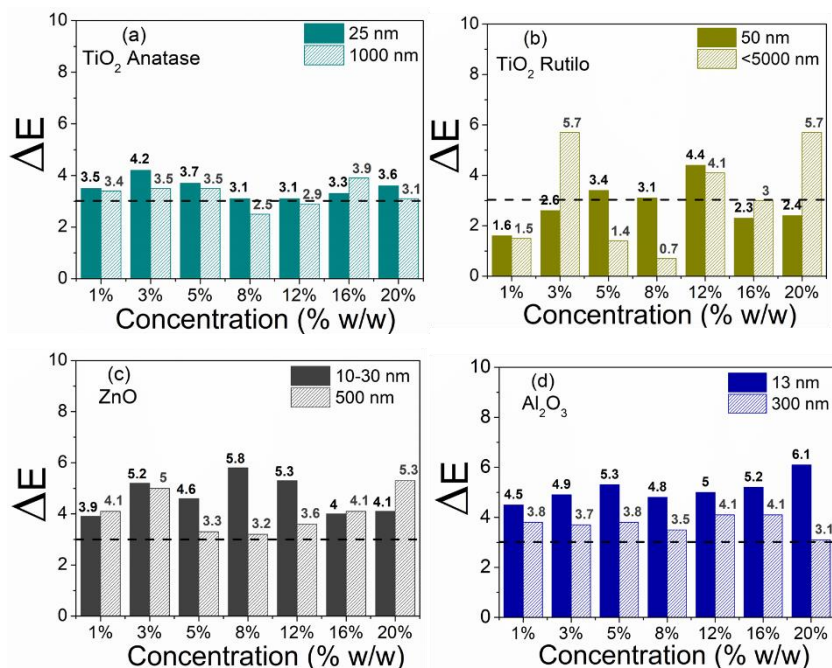


Figure 4: Colour lightness difference of nanoparticle-doped black samples when compared with the conventional colorant.

To establish a balance between the colour difference and the experimental measured reflectance of the doped samples, it was considered that the best nanoparticle, from the tested group, to be further used as dopant is the TiO_2 50 nm in rutile phase. Such nanoparticles show ΔE below 3 for the concentrations between 1-3% and 16%-20%, which makes them suitable candidates to dope finishing coatings without significantly affecting the colour.

4. Concluding Remarks

This study aimed to analyse the impact nanoparticles inclusion on the optical properties of black colourant and their suitability for a façade finishing coating. Several studies in the literature, such as the study conducted by Synnefa et al. [12], indicate that façades exposed to solar radiation can reach 70°C on the hottest days in summer. As such, by reducing the quantity of absorbed radiation, the inclusion of reflective nanomaterials in finishing coatings can be an approach towards a decrease in thermal oscillations, minimizing degradation and improving the service life.

To achieve this goal, commercial nanoparticles were used as dopants in a commercial black colourant. It was possible to observe that the most adequate nanoparticle to be used are the titanium dioxide, with an overall total reflectance of around 20% (50 nm size, 16% concentration) when compared to only 12% of the non-doped colourant. Regarding the colour assessment, it was found that increasing the concentration of the nanoparticles, one observes an increase in the colour difference

affecting the perception of lightness, turning the sample greyish. However, we also show that it is possible to enhance the performance of nanomaterials in the NIR region, compared to conventional materials, providing a similar visual aesthetic.

Further research includes new formulated coatings with nanoparticle-doped black colourant and perform laboratorial and accelerated ageing tests for analysing the suitability of these improved finishing coatings for façades system, as well as, the bio susceptibility of such coatings, once we can use nanomaterials that have dual function, reflective and anti-microbial activity.

Acknowledgements

This work was financially supported by project PTDC/ECI-CON/28766/2017—POCI-01-0145-FEDER-028766—funded by FEDER funds through COMPETE2020—Programa Operacional Competitividade e Internacionalização (POCI) and by national funds (PIDDAC) through FCT/MCTES, project Circular 2B – 37 CALL#2 – Circular Construction in Energy-Efficient Modular Buildings, financed under the Environment, Climate Change and Low Carbon Economy Programme, and within the scope of the European Economic Area Financial Mechanism – EEA Grants 2014-2021 and by Base Funding—UIDB/04708/2020 of the CONSTRUCT—Instituto de I&D em Estruturas e Construções—funded by national funds through the FCT/MCTES (PIDDAC). R. C. Veloso and A. Souza would like to acknowledge the support of FCT—Fundação para a Ciência e Tecnologia for the funding the doctoral grant SFRH/BD/148785/2019 and DFA/BD/8418/2020, respectively.

References

- [1] Brambilla A, Salvalai G, Imperadori M and Sesana M M 2018 Nearly zero energy building renovation: From energy efficiency to environmental efficiency, a pilot case study *Energy and Buildings* **166** 271-83
- [2] Santamouris M, Synnefa A and Karlessi T 2011 Using advanced cool materials in the urban built environment to mitigate heat islands and improve thermal comfort conditions *Solar Energy* **85** 3085-102
- [3] Barreira E and de Freitas V P 2013 Experimental study of the hygrothermal behaviour of External Thermal Insulation Composite Systems (ETICS) *Building and Environment* **63** 31-9
- [4] Ramos N M M, Maia J, Souza A R, Almeida R M S F and Silva L 2021 Impact of Incorporating NIR Reflective Pigments in Finishing Coatings of ETICS *Infrastructures* **6**
- [5] Veloso R C, Souza A, Maia J, Ramos N M M and Ventura J 2021 Nanomaterials with high solar reflectance as an emerging path towards energy-efficient envelope systems: a review *Journal of Materials Science* **56** 19791-839
- [6] Bishara A, Kramberger-Kaplan H and Ptatschek V 2017 Influence of different pigments on the facade surface temperatures *11th Nordic Symposium on Building Physics (Nsb2017)* **132** 447-53
- [7] ASTM 2020 ASTM E903: Standard Test Method for Solar Absorptance, Reflectance, and Transmittance of Materials Using Integrating Sphere. (West Conshohocken, PA, USA: ASTM International)
- [8] ASTM 2021 ASTM G197-14: Standard Table for Reference Solar Spectral Distributions: Direct and Diffuse on 20° Tilted and Vertical Surfaces. (West Conshohocken, PA, USA: ASTM International)
- [9] ASTM 2020 ASTM G173: Standard Tables for Reference Solar Spectral Irradiances: Direct Normal and Hemispherical on 37° Tilted Surface. (West Conshohocken, PA, USA: ASTM International)
- [10] ISO/CIE 2007 ISO/CIE 11664: Colorimetry - Part 4: CIE 1976 L*a*b* Colour space. (Brussels: European Committee for Standardization)
- [11] Gobakis K, Meier, H., Kolokotsa, D., Synnefa, A., Evans, R., Santamouris, M., 2016 Cool Roofs in the European context *REHVA Journal* **04** 19-24
- [12] Synnefa A, Santamouris M and Livada I 2006 A study of the thermal performance of reflective coatings for the urban environment *Solar Energy* **80** 968-81.



Aalborg Universitet

AALBORG UNIVERSITY
DENMARK

Accurate CFD prediction of respiratory airflow and dispersion through face mask

Ai, Zhengtao; Jia, Zhongjian

DOI (link to publication from Publisher):
[10.54337/aau541592930](https://doi.org/10.54337/aau541592930)

[Link to publication from Aalborg University](#)

Citation for published version (APA):
Ai, Z., & Jia, Z. (2023). Accurate CFD prediction of respiratory airflow and dispersion through face mask. In H. Johra (Ed.), *NSB 2023 - Book of Technical Papers: 13th Nordic Symposium on Building Physics* (Vol. 13). [186] Department of the Built Environment, Aalborg University. <https://doi.org/10.54337/aau541592930>

Accurate CFD prediction of respiratory airflow and dispersion through face mask

Zhengtao Ai and Zhongjian Jia

Department of Building Environment and Energy, Hunan University, Changsha, 410082, China

Abstract. This study develops an accurate modelling framework of flow and dispersion through face mask based on computational fluid dynamics (CFD) theory and method. The influence of grid division, time step size, and turbulence model on simulation accuracy were investigated. The result shows that the viscous resistance coefficient and inertial resistance coefficient of face masks (surgical masks) were 3.65×10^9 and 1.69×10^6 , respectively. The cell size on the surface of face masks should not be larger than 1.0 mm; the height of the first layer cells near the face masks should not be larger than 0.1 mm; and the time step sizes discretizing the breathing and coughing periods should not be more than 0.01 s and 0.001 s, respectively. The results given by LES model show closer agreement with the experimental data than RANS models, with approximately 10% relative deviation for the air speed near the face mask. Overall, the SST k- ω model performs the best among the RANS models, especially for the air speed. The findings obtained form a CFD modelling framework for an accurate prediction of airflow and dispersion problems involving face masks.

1. Introduction

Statistics show that the COVID-19 pandemic could result in a monthly global consumption and waste of 129 billion face masks. In addition, even during the non-pandemic period, face masks are the basic consumables of hospitals. However, the performance of face mask, in terms of protective efficacy and negative health effect to users, has not been well understood. As one of common evaluation methods, experimental measurement has usually been adopted in the study of face masks. However, it is difficult for experimental methods to measure accurately the respiratory airflow and dispersion through a face mask. Alternatively, numerical simulation is an important method to increase the understanding of the health effect of face masks and to develop high-performance ones. However, the accuracy of CFD technology depends largely on the user's knowledge of fluid dynamics and the experience and skills of using numerical technology, specifically and particularly being influenced by the selection of turbulence model, time step size, grid generation, and boundary conditions etc. There is so far no an accurate modelling framework of flow and dispersion through face mask based on CFD theory and method. This study aims to address this problem. The value and significance of this study is to establish a modelling framework for accurate CFD prediction of face masks under using status and in turn to promote further studies and improvements on face masks and other face shield technologies.

2. Methodology

Methodology includes the following four parts. First, the filtering performance of commonly used surgical masks was experimentally tested to obtain the boundary conditions for CFD simulations. Then, the air speed and concentration through the face mask when its user is breathing and coughing were measured via human subject experiments, so as to validate CFD modelling framework. Finally, based on the porous media model, the influence of turbulence model, grid distribution, and time step size on

the simulation accuracy of respiratory airflow and dispersion through face mask under different expiratory activities (breathing/coughing) was investigated. The computational geometry and boundary conditions are described as follows and other parts of methodology are omitted.

A full-scale test room with dimensions of 4 m-length \times 3 m-width \times 2.6 m-height was employed. The floor, ceiling, and walls around the room were set to be no-slip, stationary, and adiabatic, with the internal emissivity to be 0.95. The ventilation mode of the room was mixed ventilation, where an air inlet with dimensions of 0.4 m-length \times 0.2 m-height was located at the bottom of the side wall and an air outlet with the same dimensions was located at the top of the same side wall, as shown in Figure 1. A 3D computational thermal manikin (CTM) wearing a face mask, with a height of 1.72 m and a total surface area of 1.66 m², was located in the middle of the room and facing the wall with air inlet and outlet.

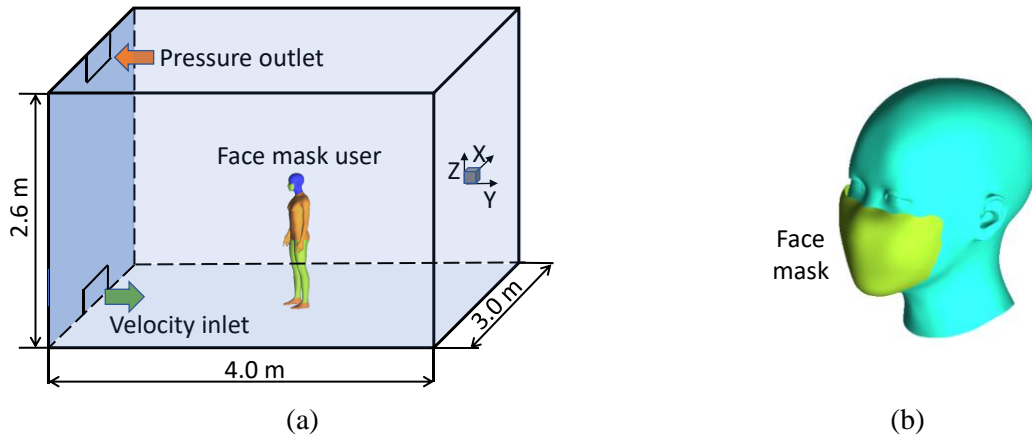
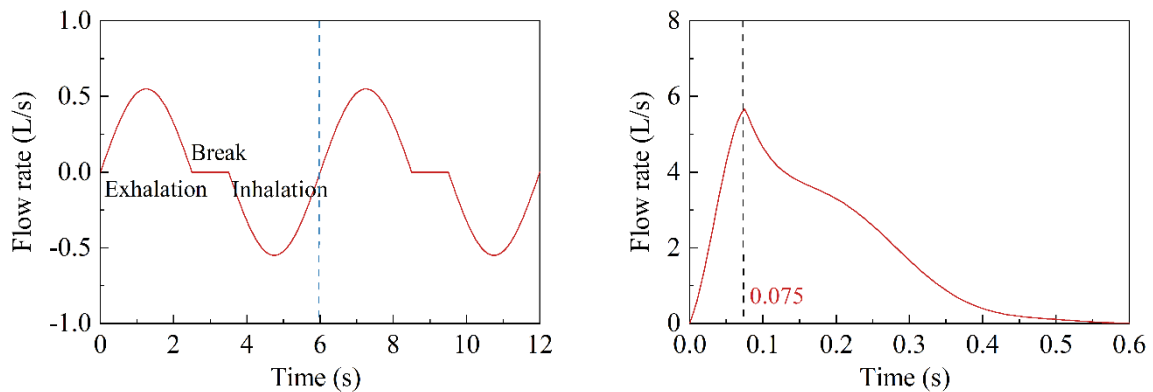


Figure 1. Geometrical model: (a) test room and (b) human head wearing a face mask.

In the present study, the surface of the CTM was divided into different parts with different skin temperatures, and detailed information can be found in our previous study. In addition, the heat transfer between human body and surrounding air through both convection and radiation was considered. According to the study by Murakami et al., the internal emissivity of human skin was defined as 0.98. Two typical expiratory activities including breathing and coughing were investigated. The airflow patterns under different expiratory activities are shown in Figure 2. During normal breathing, the opening area of mouth was about 120 ± 52 mm², but exceeded 400 ± 95 mm² during coughing. Hence, the mouth opening area was defined to be 132 mm² and 360 mm² for breathing and coughing, respectively. In the breathing process, the pulmonary ventilation rate was set to be 9 L/min, representing light-level activities in sitting and standing postures. The exhaled air and ambient air were considered as incompressible ideal gas to simulate buoyancy effect. The tracer gas, carbon dioxide (CO₂) widely representing the exhaled pollutants, was released from the mouth with a fraction of 4.5%.



(a)

(b)

Figure 2. Airflow patterns under different expiratory activities: (a) breathing and (b) coughing.

The lace of face mask was omitted in the simulations. In order to make the face mask fit the face perfectly, the shape of face mask has to be adjusted when wearing in practice. In the present study, a geometrical model of face mask was developed according to the adjusted shape under using status. The thickness of the face mask was set to be 1.0 mm based on the present measurement and those reported in previous studies, namely, 0.5-2.3 mm, depending on the type of face mask. It was reported that the gap size between the face mask and face was around 4-14 mm, influenced by the wearer's face shape and wearing habits. In the present study, the largest gap size was less than 10.0 mm, which was located on the top of face masks. Overall, the geometrical model of face mask developed in the present study is close to the reality.

3. Conclusions

The findings from the present study allow the following conclusions to be drawn.

- (1) The boundary conditions of surgical masks required by the porous media model were determined by experimental test and mathematical fitting, where the viscous resistance coefficient and the inertial resistance coefficient are 3.79×10^9 and 1.69×10^6 , respectively.
- (2) The cell size on the surface of face masks should not be larger than 1.0 mm, and the height of the first layer cells near the face mask should not be higher than 0.1 mm.
- (3) The time step sizes discretizing the breathing and coughing periods are better to be kept no more than 0.01 s and 0.001 s, respectively.
- (4) The LES model is more accurate than RANS models in predicting respiratory airflow and dispersion through face mask, with approximately 10% relative discrepancies for the air speed near the face mask from the experimental data.
- (5) Compared with LES model, the SST $k-\omega$ model performs best among the RANS models, especially for air speed, with 5.1-20% relative deviation.

References

- [1] Jia Z J, Ai Z T, Yang X H and Mak C M 2022 Towards an accurate CFD prediction of airflow and dispersion through face mask Build. Environ. Accepted.



Aalborg Universitet

AALBORG UNIVERSITY
DENMARK

Modelling of rain interception by trees in outdoor urban climate

Giroux-Gauthier, Léopold; Kubilay, Aytaç; Maheu, Audrey; Wood, Sylvia; Carmeliet, Jan; Derome, Dominique

DOI (link to publication from Publisher):
[10.54337/aau541594014](https://doi.org/10.54337/aau541594014)

[Link to publication from Aalborg University](#)

Citation for published version (APA):
Giroux-Gauthier, L., Kubilay, A., Maheu, A., Wood, S., Carmeliet, J., & Derome, D. (2023). Modelling of rain interception by trees in outdoor urban climate. In H. Johra (Ed.), *NSB 2023 - Book of Technical Papers: 13th Nordic Symposium on Building Physics* (Vol. 13). [198] Department of the Built Environment, Aalborg University. <https://doi.org/10.54337/aau541594014>

Modelling of rain interception by trees in outdoor urban climate

Léopold Giroux-Gauthier¹, Aytaç Kubilay², Audrey Maheu³, Sylvia Wood⁴, Jan Carmeliet², Dominique Derome¹

¹ Department of Civil and Building Engineering, Université de Sherbrooke, Sherbrooke, QC J1K 2R1, Canada

² Chair of Building Physics, Swiss Federal Institute of Technology ETHZ, Leonhardstrasse 27, 8092 Zürich, Switzerland

³ Institute of Temperate Forest Sciences (ISFORT), Université du Québec en Outaouais, 58 rue principale, Ripon, QC J0V 1V0, Canada

⁴ Habitat, 5818 Boulevard Saint-Laurent, Montréal, QC H2T 1T3, Canada
Leopold.Giroux-Gauthier@Usherbrooke.ca

Abstract. Studies in building and urban physics can benefit from detailed modelling of outdoor climate conditions. Up to two-thirds of the rain, which a tree is exposed to, can be intercepted by tree foliage, branches and stem and evaporate without reaching the ground. However, the interception of rainwater by trees has not yet been considered in wind-driven rain studies of local urban climate. The aim of our work is to model rain interception by trees and implement it into a microclimate modelling suite (urbanMicroclimateFoam) based on OpenFOAM, in order to consider the outdoor environmental conditions more accurately. Field measurements are performed on a red oak for validation. Numerical results performed with the modelling tool which does not consider rain interception shows an overestimation of rain deposition on the ground, compared to measurements for two rain events of 2022 summer. Ongoing work leads to the addition of sink and source terms to account for interception and to close the presented gaps.

1. Introduction

Building and urban physics studies can benefit from detailed modelling of outdoor climate conditions. Trees in urban environment provide shading, extract sensible heat from the air to transpire water vapor, and reduce wind velocity. As such they provide avenues for heat mitigation, especially during heat wave events. Certain CFD-based (computational fluid dynamics) numerical tools can support such studies of thermal comfort assessment in urban settings, which can help evaluate mitigation measures for heat waves [1]. The modelling suite, urbanMicroclimateFoam, can take into account the influence of vegetation [2]. WindDrivenRainFoam, a related solver can simulate rain deposition on solid surfaces.

Rain interception is a physical phenomenon that has been studied mostly in the field of hydrology and can be also relevant in urban microclimate. Up to two-thirds of the rain can be intercepted by tree foliage, branches and stem and evaporate without reaching the ground. Intercepted rain refers thus to the amount of rain that is caught by tree leaves and that is returned to the atmosphere by evaporation before it can fall onto the ground. Only few analytical models [3] exist to assess rain interception by trees, and some are specialized specifically for trees in cities [4]. It would be of interest to simulate wind-driven rain in urban environments that contain trees and to consider rain interception. The impact

of moisture redistribution due to rain interception by foliage on local microclimate and on rain redeposition onto facades of buildings adjacent to trees could then be studied.

In this study, we present the numerical and experimental work done towards the implementation of rain interception by trees into urbanMicroclimateFoam, a suite of numerical models that involves CFD, heat, air and moisture (HAM) transport processes radiation exchanges and wind-driven rain.

Experimental work consists in field measurements of rain interception on an isolated tree in an open field on the Université de Sherbrooke campus during the 2022 summer. Experiments are performed to measure characteristics of the tree and to provide a dataset for validation. Measurement campaign results are presented and compared with simulation performed with OpenFOAM v6 [5]. This simulation is, for now, only performed with windDrivenRainFoam.

2. Methods

2.1. Experimental method

Measurements occurred through the summer of 2022. Five rain events are measured. A meteorological station at Université de Sherbrooke, 350 m from the studied trees, provides wind direction, velocity, air temperature and relative humidity.

Water reaching the soil under the tree is measured during multiple rain events, using a combination of an array of 2 L containers ($0,021 \text{ m}^2$ receiving area per container) and an array of rain gauges (0.019 m^2 receiving area per gauge) (Onset RG3-M, USA) of 0.2 mm resolution, positioned under a red oak, on Université de Sherbrooke campus. For this campaign, we have a maximum of 9 rain gauges and 20 containers. The tree is around 20 years old, and isolated from neighboring trees and thus, could be representative of most urban street trees, which are planted at a distance from each other. In contrast with urban environments, no building is in the immediate vicinity of the tree and the ground is mostly covered with grass. Figure 1 shows the site of the measurement campaign on Université de Sherbrooke campus.

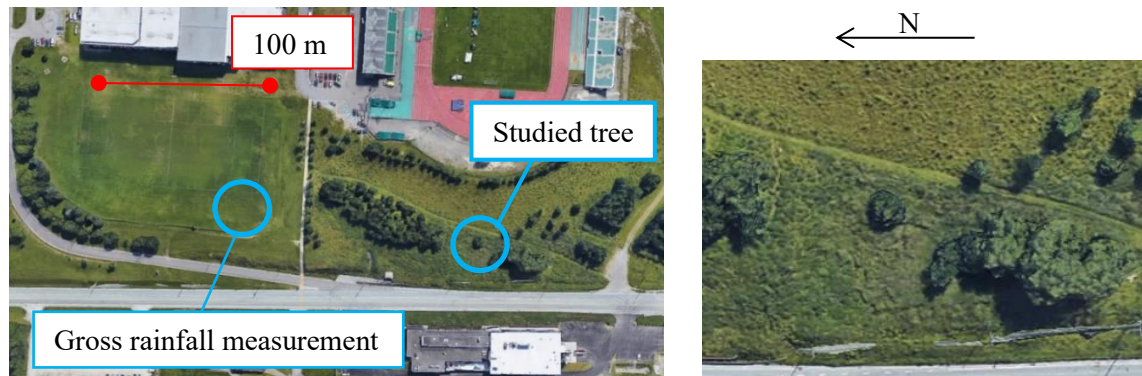


Figure 1 – Measuring campaign site (images from google.earth)

The area of interest under the tree canopy (100 m^2) is delimited with twine to form a 4×4 matrix, forming 16 sections as shown in figure 2. Measurement equipment is positioned arbitrarily within these sections. Each section has one container in it (total of 0.332 m^2 measurement area). However, the positions of the 9 rain gauges (0.167 m^2 measurement area) are selected considering wind direction. We conducted a few measurements using both systems concurrently for comparison purposes.

In addition, one gauge and one container are positioned in an open area, approximately 150 m from the studied tree, and provide the gross rainfall in the open environment as reference (see figure 1).



Figure 2. Division of measurement area into 16 sections under tree canopy

As rain is intercepted by the foliage, part of rainwater runs down the systems of branches to reach the trunk. To measure the amount of this water, a PVC hose, cut in half longitudinally to form a gutter, is fixed around the trunk, just below the crown of the tree. Water that flows from the stems to the trunk ends in this pipe, which is then connected to a rain gauge or to a water container on the ground [6].

As we measured the rain that fell through the foliage or down the stem, rain interception is measured indirectly. The water measured with the rain gauges or containers on the ground is called throughfall, which is the sum of rain that drips from the leaves to the ground after being caught by the leaves and the rain that manages to go through the leaves without hitting them (free throughfall). Rain interception, which is defined as the part of water that is caught by the leaves of a tree, and that will be evaporated from there, is the difference between the reference gross rainfall and the sum of the measured throughfall and stemflow quantities.

2.2. Simulation method

Rain is simulated with windDrivenRainFoam. Numerical model solves an isothermal wind flow with Reynolds-averaged Navier Stokes (RANS) equations and turbulence model k- ϵ . It also performs wind-driven rain calculations with an Eulerian multiphase approach [7].

In CFD, trees are considered as porous zones with momentum source for drag [8], linked to the leaf area density (LAD). The momentum source is considered in momentum equation in the following way:

$$s_u = -\rho c_d a |\bar{u}| \bar{u} \quad (1)$$

Where c_d is the leaf drag coefficient of 0.2, a is LAD, ρ is air density (1.225 kg m^{-3}) and \bar{u} is the main velocity vector, in m s^{-1} .

To compare simulation results with experimental data, a domain of $180 \times 300 \text{ m}^2$ is created with a mesh close to 1.7 million cells. A patch of trees, similar to a small urban forest with several trees, and the studied red oak are included in the domain. The geometry used for the patch of trees is a 15 m high trapezoidal prism, with a foliage that starts approximately at a height of 1.5 m above the ground. The red oak is represented with a pyramid shape that has a $7 \times 7 \text{ m}^2$ base and a 5.8 m height. The foliage starts at a height of 1.5 m above the ground. An LAD value of 1.5 m^2 of leaves per m^3 is used for foliage density, based on a measured value for the same tree species [9]. The same LAD value is used also for the patch of trees. Figure 3 shows geometrical features of trees, the domain and the mesh.

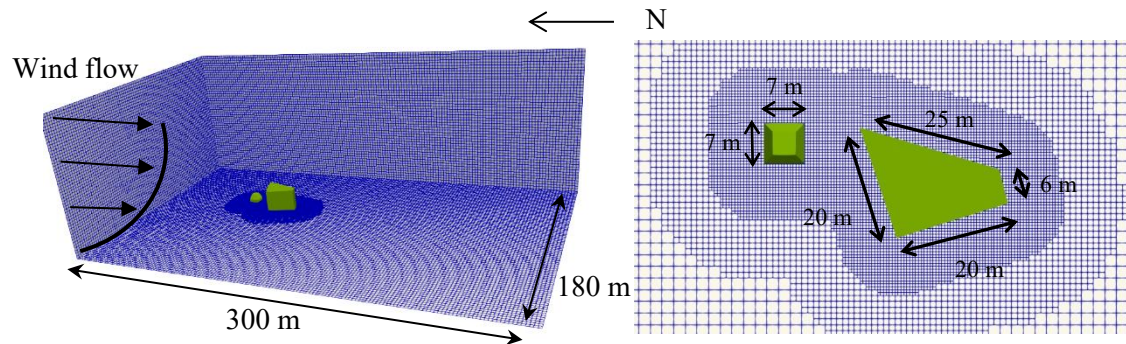


Figure 3. Computational domain in OpenFoam v6

3. Results

3.1. Measurement campaign results

We present the rain event of June 9th and August 8th. During the event of June 9th, both rain gauges and containers are used. Wind is from north with a velocity that reaches approximately 2 m s^{-1} at 2.5 m. Air temperature is around 15°C and relative humidity is close to 95 %.

For the event of August 8th, only rain gauges are used. Wind is from north and with very low mean speed, showing some gusts of 0.5 m s^{-1} at 2.5 m. Air temperature is 19°C and relative humidity 96 %.

Comparison of results from rain gauges and containers is done in sections 6, 13, 16, and in the open area. Throughfall quantities measured over time for those sections show some important differences between the two measuring techniques (close to 35 % of rain amount at the end of the event). Figure 7b in a following section of the paper support this affirmation.

Throughfall measurements of June 9th (in mm h^{-1}) at the 16 sections after two time frames during the rain event are presented in figure 4, at approximately 2:45 pm and 3:50 pm. These are measured from containers and measurements are done every 20 minutes. Spatial differences are due to combined effects of wind on rain deposition but are also strongly linked to the tree variability. Wind seems to yield a rain intensity that is higher on the two sections at the western corners under the tree canopy. The throughfall quantities also decrease towards the southeast corner.

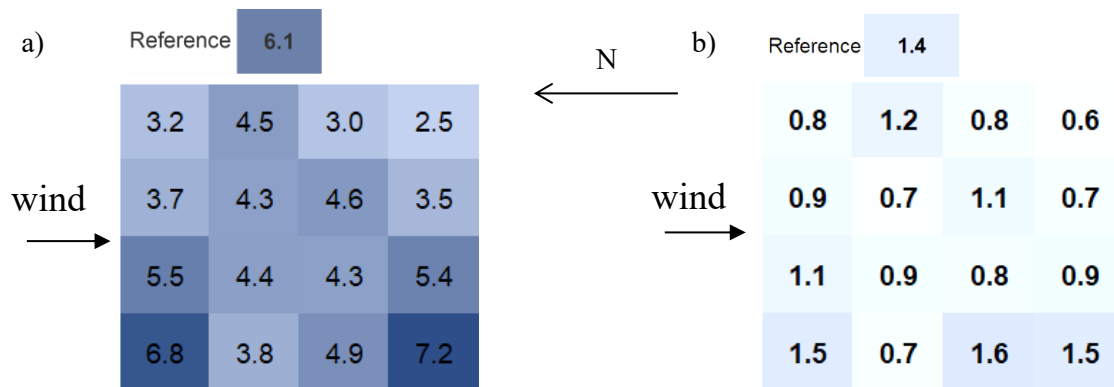


Figure 4. Rain intensity (mm h^{-1}) in the 16 slots and at reference location at a) 2:45 pm and b) 3:50 pm

3.2. Simulation results

In a first step, we simulate rain deposition on the ground, without rain interception and, thus, using the wind-driven rain solver as it is now. Therefore, only the disturbance of wind caused by tree leaves is considered. Figure 5 shows wind flow field, at 2.5 m. The approaching wind speed is 2 m s^{-1} at 2.5 m height for the event of June 9th (a) and 0.5 m s^{-1} at same height for the event of August 8th. For both simulation a constant wind flow from north is assumed.

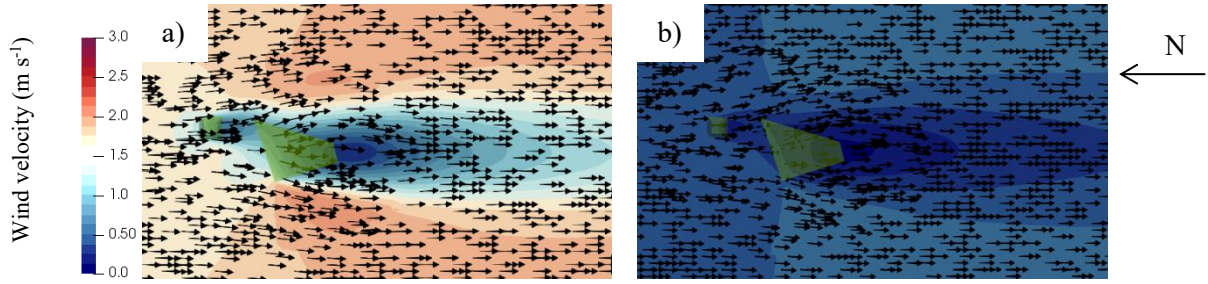


Figure 5. Wind velocity in a horizontal plane at a height of 2.5 m in a pure WDR simulation (i.e. no interception) for rain event of a) June 9th and b) August 8th 2022

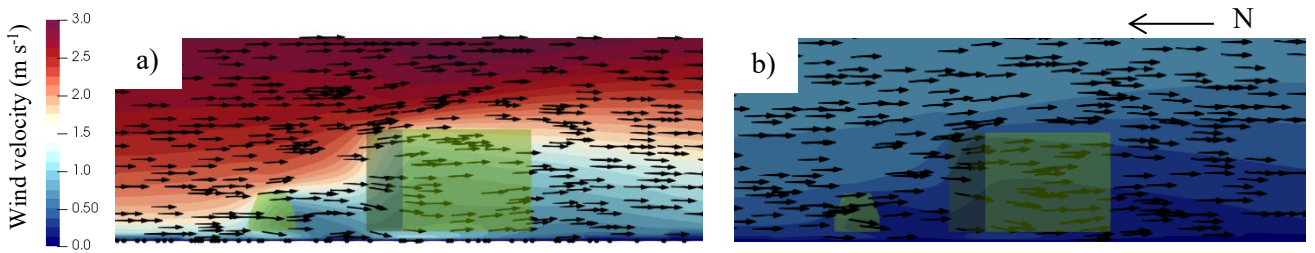


Figure 6. Wind velocity in a vertical plane going through the trees in a pure WDR simulation for rain event of a) June 9th and b) August 8th 2022

Figure 5 shows that for the event of June 9th (a), the wind speed falls below 1 m s⁻¹ in the wake of the isolated tree. The following patch of trees is subjected to a slower wind flow, as a zone below 0.5 m s⁻¹ is created. For a wind coming from the north, the patch of trees does not create a blockage effect windward that affects the flow around the single tree.

For the event of August 8th (b), the area where the flow velocity is slowed by the trees follows a similar pattern, but the zone with low wind speed is larger. For both events, the wind flow deviates from its main trajectory due to the presence of trees, but no recirculation zone is seen.

For its part, figure 6 presents a vertical 2D slice through the trees during the event of June 9th (a) and August 8th (b). In both cases, the reference velocity (i.e. 2 m s⁻¹ and 0.5 m s⁻¹) is observed at the trees top. The extent of the blockage on the windward side of trees is also limited. The trajectory of flow is slightly affected by the trees, but without any important vertical motion and recirculation zone.

The wind flow disturbance in the region of interest yields a particular catch ratio distribution on the ground. Catch ratio is the rainfall intensity at locations on the ground surface divided by the reference rainfall intensity, away from the trees. Figure 7a and 7c shows such a pattern for a rain intensity of 2 mm h⁻¹ for the two presented rain events. From the catch ratio values, accumulated amount of water over time can be calculated. Catch ratio time gross rainfall gives water amount, which can be compared with field measurements. Figure 7b and 7d compare preliminary numerical results with measurements.

In figure 7a below, the distribution of catch ratio is distinctly separated under the single tree canopy. Higher values of catch ratio (~1.02) are obtained windward, and lower values are obtained leeward (~0.97). The higher catch ratio zone, in red, is concentrated while the lower catch ratio zone, in blue, spreads in the direction of the wind. Results under the patch of trees present a similar pattern (figure 7c), but values get higher windward (~1.04) and lower leeward (~0.96). The difference in the spatial extent of the catch ratio values zone is also magnified.

Figure 7b and 7d shows that without any source and sink terms to account for rain interception, the pure WDR simulation overestimates rain deposition on the ground. In figure 7b, the rise in rainfall amounts in rain gauges is reduced compared to the one of reference rainfall, while numerical results yield a similar curve than the reference one. In figure 7d, the slopes are much different for measurements below the canopy and at the reference location around 11:30 pm and 00:10.

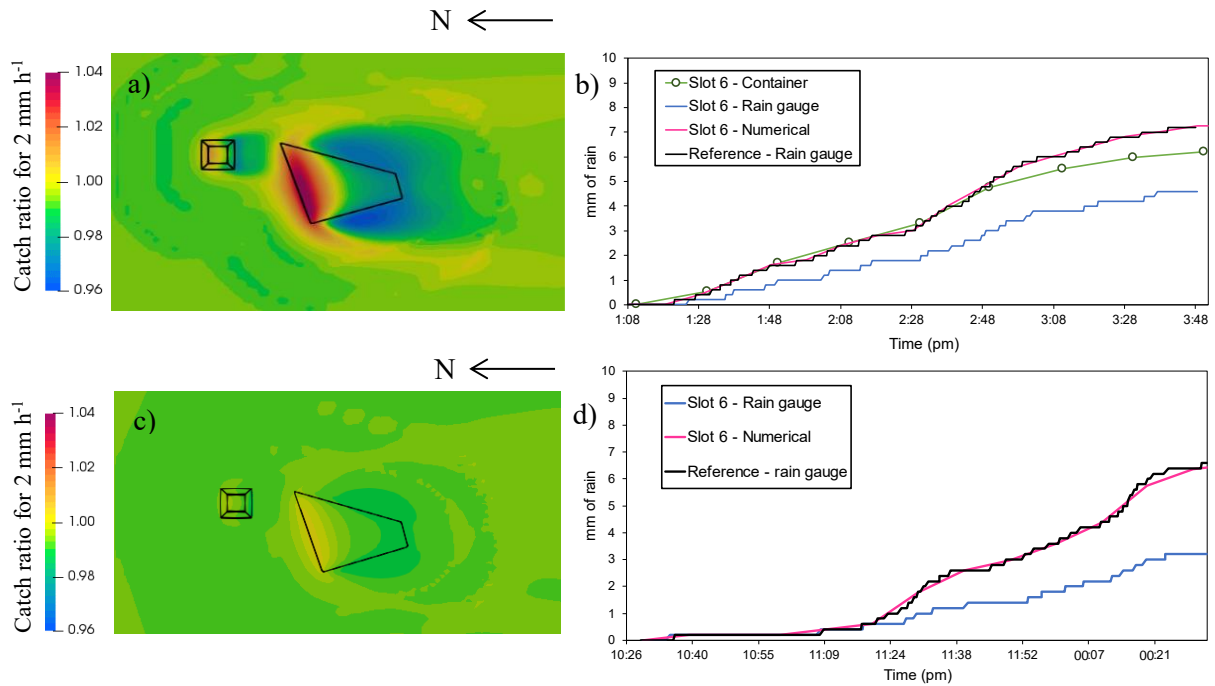


Figure 7. Numerical results of throughfall comprising catch ratio distribution on the ground for rain intensity of 2 mm h^{-1} and amount of rain in mm calculated from simulation for rain event of June 9th (a,b) and August 8th (c,d)

4. Conclusion

In this paper, we show the experimental and numerical methods developed toward implementation of a new capability, rain interception by trees, in the microclimate computational tool urbanMicroclimateFoam. Numerical and experimental results are presented for a red oak on Université de Sherbrooke campus. An initial comparison between experimental and numerical results is shown.

Our next steps consist in adding source and sink terms in wind-driven rain conservation equations to represent both storage of rainwater on leaves and dripping of stored rainwater on the ground and determining their magnitude. Such terms would likely change catch ratio on the ground, and on near facades in urban setups. Because water would be stored and then evaporates in the environment, trees would become a moisture source. The understanding of their impact on post-rain drying conditions is an important potential outcome of this study. The conference presentation will include the latest developments of this project.

In our future work, the modelling of this phenomenon should be applied in the urban environment. A numerical simulation could be performed to understand where the rainwater goes, where surfaces can dry, and how moisture damaged risk evolves on buildings near vegetation. We could then give more insights whether tree sheltering and evaporation can have impacts on a building facade.

References

- [1] Mughal MO, Kubilay A, Fatichi S, Meili N, Carmeliet J, Edwards P and Burlando P 2021 *Urban Clim.* **39** 100939
- [2] Kubilay A, Derome D and Carmeliet J 2018 *Urban Clim.* **24** 398–418
- [3] Muzylo A, Llorens P., Valente F, Keizer JJ, Domingo F and Gash JHC 1997 *J. Hydrol.* **370** 191-206
- [4] Xiao Q and McPherson EG 2002 *Urban Ecosyst.* **6** 291-302
- [5] Greenshields C 2016 *OpenFOAM v6 User Guide*
- [6] Eliades M, Bruggeman A, Djuma H, Christou A, Rovanias K and Lubczynski MW 2022 *Agric. For. Meteorol.* **313** 108755.
- [7] Kubilay A, Derome D, Blocken B and Carmeliet J 2013 *Build. Environ.* **61** 69–81
- [8] Manickathan L, Defraeye T, Allegrini J, Derome D and Carmeliet J. 2018 *Agric. For. Meteorol.* **248** 259–74.
- [9] Wang YS, Miller DR, Welles JM and Heisler GM 1992 *For. Sci.* **38** 854-65



Aalborg Universitet

AALBORG UNIVERSITY
DENMARK

Residents' thermal comfort and energy performance of a single-family house in Poland: a parametric study

Zygmunt, Marcin; Gawin, Dariusz

DOI (link to publication from Publisher):
[10.54337/aau541595604](https://doi.org/10.54337/aau541595604)

[Link to publication from Aalborg University](#)

Citation for published version (APA):
Zygmunt, M., & Gawin, D. (2023). Residents' thermal comfort and energy performance of a single-family house in Poland: a parametric study. In H. Johra (Ed.), *NSB 2023 - Book of Technical Papers: 13th Nordic Symposium on Building Physics* (Vol. 13). [209] Department of the Built Environment, Aalborg University.
<https://doi.org/10.54337/aau541595604>

Residents' thermal comfort and energy performance of a single-family house in Poland: a parametric study

Marcin Zygmunt^{1,2} and Dariusz Gawin¹

¹ Lodz University of Technology, Department of Building Material Physics and Sustainable Design, Lodz, Poland

² KU Leuven, Department of Building Physics and Sustainable Design, Leuven, Belgium

Abstract. Building energy and environmental efficiency is presently one of the most important research subjects due to global climate change and the actual geopolitical situation. Residential buildings should provide a comfortable environment for the occupants while they spend up to 90% of their life indoors. Moreover, a comfortable indoor environment should be provided efficiently and affordably. Thus, the examination of the correlated factors of buildings' energy efficiency and occupants' comfort is highly anticipated. This field can be analyzed using various methods, where computational simulations are the most comprehensive technique. Unfortunately, buildings' simulated energy demands usually differ from the actual use. There are numerous uncertainties impacting buildings' energy demand, likewise, those parameters are usually strongly correlated. Therefore, parametric analyses are a valuable approach allowing us better understanding of various phenomena occurring in buildings. This article shows some preliminary results of the case study analysis for a residential building in Poland examining the impact of residents' thermal comfort on the buildings' energy performance. This study will be continued and expanded to fully understand the occupants' behavior impact on building energy performance. Studies like this are helpful for future building design, following the paradigm of sustainable development.

1. Introduction

People spend up to 90% of their life in buildings. Residential buildings should assure a comfortable environment for the occupants, provided in an efficient way. Building energy and environmental efficiencies are presently one of the most important research subjects due to the global climate change and the actual geopolitical situation. Buildings and their energy improvement are an essential part of the numerous long-term strategies for a more sustainable environment in the future, especially the ambitious EU strategies towards an environmentally neutral society by 2050 [1]. Yet, buildings consist of approximately one-third of energy demand and approximately 40% of total greenhouse gas (GHG) emissions [2]; thus, their impact on the ongoing global energy transformation is crucial.

Building energy performance, as well as occupants' thermal comfort can be analyzed using various methods, assuming different complexity of the applied model. Computational simulations (white-box modeling) are usually the most appropriate and comprehensive technique, while for some studies gray-box or black-box (e.g. Artificial Intelligence) modeling is found to be sufficient [3-6]. White-box modeling allows us to receive very precise outputs, which can be furtherly analyzed. The obtained outputs are not only assessing buildings' performance but also allow us to examine variable in time phenomena occurring in the examined objects, such as residents' comfort. Unfortunately, this method has several disadvantages. White-box modeling is always challenging, where detailed input data and expert knowledge are required. Also, computational simulations are time-consuming, and licenses of the applied software (e.g. Design Builder) are typically payable. Despite all the disadvantages, if

performed appropriately, the computational simulations and parametric studies are a valuable source of knowledge on the examined field: the correlation between energy performance and occupants' thermal comfort [7-9].

Unfortunately, buildings' simulated energy demands usually differ from the actual energy use [10,11]. Out of numerous uncertainties impacting buildings' energy demand (e.g. its geometry, construction, systems applied, or weather data), the residents' impact seems to be usually neglected or underestimated. The role of occupants in the energy performance of buildings is still not fully investigated, let alone standardized. The occupants' impact on the building's energy efficiency has recently attracted much academic attention. It is highly probable, that occupants' impact, due to various feeling of thermal comfort, can be one of the main causes of the energy performance gap between predicted and actual building energy use [12]. The above-mentioned statement is especially valid for modern buildings, which are usually highly energy efficient and often with building management systems, where users can control the parameters of the indoor environment by adjusting the settings of HVAC and lighting systems.

In this article, we try to estimate the influence of some parameters, which affect both occupants' thermal comfort and building energy performance. This analysis is performed using white-box modeling, executed by means of parametric simulations obtained out of Energy Plus software. This study is performed for a case study designed as a prototype moveable single-family house. In total, 6600 computational simulations were performed, each with the hourly calculation step. A comprehensive outputs database was obtained, allowing us to examine the impact of exterior climate conditions (6 scenarios: 3 locations, 2 weather files each), building orientations (4 scenarios), and its' thermal insulation (11 scenarios), as well as set-point temperatures for heating and cooling purposes (5 scenarios each). Building energy performance was examined based on the calculated annual energy demands, while thermal comfort was evaluated based on discomfort hours obtained following the ASHRAE 55 standard [13]. Those types of studies might be helpful for future buildings design, considering sustainable development basis, focusing on the social, environmental, and economic aspects of buildings operation. Additionally, some of the obtained results might be helpful in terms of explanation for the potential performance gap between the predicted and actual energy use of buildings.



Figure 1. The examined portable residential house: (a) design visualization and (b) floor plan view in Design Builder.

2. The transportable portable house

The examined building is a transportable prototype house, which can be easily moved from one place to other. It has no basement, and its placement is usually performed on concrete blocks/frame, limiting contact with the ground. It is an energy-efficient building, providing all residential conveniences and various zones. The prototype building was in depth examined in 2022 to assess its energy efficiency, as well as users and environmental friendliness.

The examined building has a 78.3 m² useable floor area, consisting of a large living zone with a kitchen (46.1 m²), two bedrooms (12.7 m² and 14.8 m²), and a bathroom (4.7 m²), as well as an unoccupied attic. The total glazing area is 10.8 m², distributed on two opposite walls. The building enclosure is designed with highly energy-efficient sandwich panels (R-value equals 5.58 m²K/W) with an additional XPS layer (thermal conductivity $\lambda=0.032$ W/mK) as thermal insulation. An additional

5 cm of XPS was added to external walls, and 10 cm to ceilings and ground floor providing thermal transmittance (U-value) of 0.13 W/m²K and 0.11 W/m²K, accordingly for both ceilings and ground floor. This building has a complex HVAC system, consisting of electric radiators, split units, as well as supply and exhaust fans with heat recovery. Air conditioning is provided for all zones excluding the bathroom. It also has an energy-efficient lighting system with LEDs and standard housing appliances. The hot water system was not analyzed. All the above-mentioned information are based on the measurements of the prototype building. Within the performed measurements, the blower door test, thermography imaging, the U-value evaluations, as well as thermal and lighting comfort assessments were done following the national regulations and standards. Additionally, despite the fact, that this building is designed to be a moveable house, it fulfills all the Polish regulations for residential buildings.

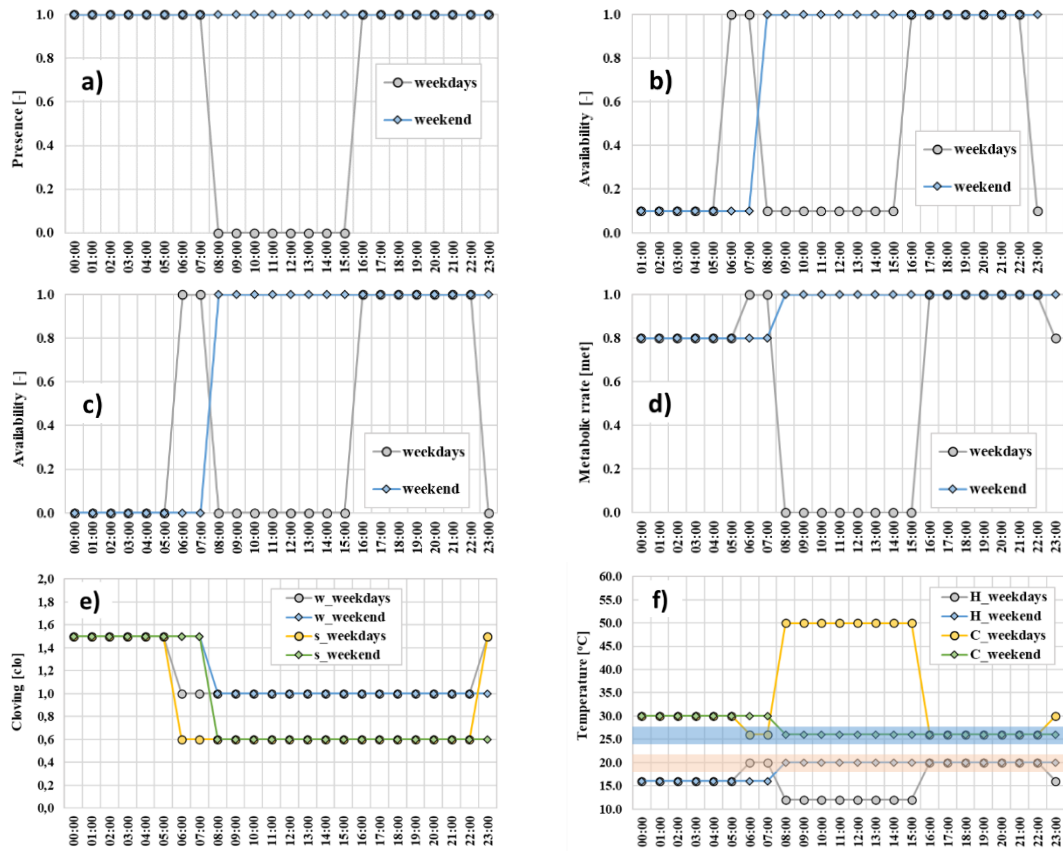


Figure 2. The assumed schedules for the examined house: (a) occupancy, (b) equipment availability, (c) lighting availability, (d) metabolic rate, (e) occupants' clothing, and (f) temperature setpoints for living zones.

The examined house was modeled using Design Builder software providing high conformity with the actual building (see Figure 1). Building enclosure, as well as the HVAC system were input in detail. Additionally, the nominal capacity of heating and cooling coils, as well as provided air flows and fan efficiencies were assumed respectively for each zone. The air infiltration rate was simplified as constant throughout the whole year, with the n_{50} index equal to 0.76 1/h (the result of the performed blower door test). The examined building enclosure is highly airtight (thermal bridges impact is marginal according to the performed thermography). The lighting system (power density and target illuminance) was assumed out of the performed measurements, adequately for each zone. Moreover, in the performed computation analyses, detailed hourly operation schedules were assumed (see figure 2) in order to precisely define the occupants' presence. It was set, that the family of 4 has a regular weekly schedule, assuming working/school on weekdays from 8:00 AM to 4:00 PM. The housing

equipment is used following the people's presence, with marginal demands during nights and working hours. A similar schedule was assumed for the availability of the lighting system; it is controlled based on the natural lighting, by the 3-step control/switch (off/half-on/on). The human-related factors, in particular, metabolic rate and clothing were assumed precisely, with high consideration of the daytime, where 0 represents the time that people are outside. The metabolic rate considers occupants' activity throughout the day: light activity during daytime (equals 1.00 met), and relaxation during nighttime (sleeping, equals 0.80 met). The thermal resistance of the cloths depends on the day period, as well as the time of the year. The winter outfit was set as 1.00 clo, and summer as 0.60 clo, while throughout the whole year in the nighttime, it was set as 1.50 clo (occupants under the duvet).

Finally, schedules for heating and cooling setpoints were set for each zone. The default temperatures for all living zones were set as 20/16/12°C for heating and 26/30/50°C for cooling, accordingly for occupied/sleeping/unoccupied periods. The temperature management for the bathroom is much more limited: there is no air conditioning (no cooling setpoints), while heating setpoints differ only for occupied/unoccupied periods, with 24/12°C temperatures.

3. Methods applied

The performed analyses were made using a computational simulation approach. The white-box model approach was considered the most appropriate for this study due to the needs and requirements of designers, as well as the availability of a large set of input data.

Firstly, the examined portable house was defined by means of Design Builder software, in accordance with the technical documentation, as well as measurement data (see more in section 2). The complex input data, as well as information from numerous consultations with designers, were used. Next, computational outputs were validated with all the available data. Finally, the obtained model was accepted, considering it sufficiently accurate.

Secondly, the simulation file was exported into Energy Plus format (IDF file) and then furtherly used for parametric calculations. The process was automatic, performed using a script written in Python language, allowing for looping the EP-launch software. The original IDF file was constantly overwritten, assuming a set of the examined parameters (see more in subsection 3.1). Comprehensive outputs out of each simulation were saved, focusing mostly on energy demands and occupants' thermal comfort. Saved results can be furtherly used in future studies, considering especially their granularity (hourly calculation step).

Thirdly, the obtained results were sorted considering their proper data management. This post-processing was performed using additional scripts written in Python language. The sorted outputs allow us to analyze the impact of the examined parameters on the buildings' energy performance, as well as occupants' thermal comfort.

The applied method is an effective approach allowing for complex assessment of various phenomena occurring in buildings. This method can be easily modified, as well as furtherly developed considering the current needs. Unfortunately, advanced computational simulations are time-consuming and require considerable computing power. Furthermore, the simulation outputs cover significant space on a hard drive, thus the range of performed calculations should be well-planned at the early stage.

3.1. Examined parameters

The first of the examined variables is the exterior climate. 3 different localizations were examined: Gdansk (a representative city at the Polish seaside), Lodz (a city located directly in the geographical center of Poland), and Krakow (probably the most tourist city of Poland, located in the South-Eastern part of Poland). This selection covers the most representative climates of Poland, excluding extreme conditions like in mountain regions. For each city, two EPW files [14] were used: the traditional weather files (obtained based on data from years 1970-2000), as well as more recent data (from years 2001-2020). The used EPW files can be found on the web [15]. The distribution of Dry Bulb Temperature (DBT), as well as total monthly solar radiations can be seen in figure 3. It can be seen, that for the all examined localizations the annual average temperature is higher now than in the past. Additionally, the annual amplitude of the temperature is generally shifting upward, observing warmer winters. Solar radiation is now usually greater than in the past. For the examined localizations the solar

radiation growth was as high as approx. 14%. Surprisingly, the total solar radiations decrease for Krakow. Additionally, the sunny hours (a time when solar radiation occurs) for Gdansk increase by up to 15%.

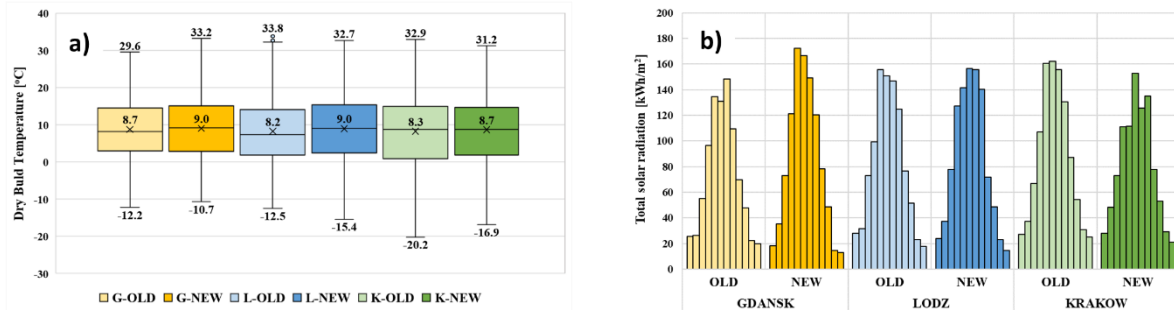


Figure 3. Comparison of the examined exterior climate conditions for the examined locations: (a) DBT distribution and (b) total monthly solar radiation during consecutive months.

The second examined parameter is building orientation. The original one (the same as for the building prototype) had facades with windows oriented East and West. 4 scenarios were assumed, considering the base orientation, as well as 3 positions rotated by 90, 180, and 270 degrees.

The third of the examined parameters is related to the thermal insulation of the main components of this moveable house. All these components (exterior walls, ceilings, ground floor) are based on the prefabricated sandwich panels, with PUR core (the R-value equals 5.6 m²K/W). The examined variability of thermal insulation thickness is related only to the supplementary layer of the XPS added to each component: 5 cm for exterior walls and ground floors, and 10 cm for ceilings. The thickness was analyzed with 1 cm increment, providing 11 different scenarios of the thermal performance of the building enclosure.

The fourth and fifth parameters are temperature setpoints for heating and cooling respectively (see figure 2). For each set of temperatures, only the setpoints (temperatures during the occupied periods) were analyzed, considering the following ranges (changeable by 1°C): for heating in the range from 18°C to 22°C, and from 24°C to 28°C for cooling purposes. Thus, 5 scenarios for heating and 5 scenarios for cooling management were examined.

In total, 6600 parametric simulations were executed, each with an hourly calculation step. Out of all the outputs, the following parameters were collected for further analyses: heating, cooling, fans, and lighting demands (hourly and annual), as well as PMV index (hourly) and hours of discomfort (annual, based on [13]). Moreover, each of the simulated scenarios assumed the detailed schema corresponding to the occupants' behavior, in particular, their activity and how they are dressed; those assumptions are shown in figure 2.

4. Results

Firstly, the obtained results were examined considering the exterior climate conditions; a short summary can be seen in table 1. Energy consumption by lighting system (which maintains relatively constant for all the examined scenarios), as well as fans (depending on ventilation system efficiency, as well as air conditioning usage), are not examined individually. The total energy demand, i.e. heating, cooling, lighting, and fans supply combined (**T** in table 1) varied significantly, regardless the examined localization. The obtained results showed demand as low as 3894 kWh/a (the best thermal insulation, and less demanding setpoint values) and as high as 7065 kWh/a (building without additional thermal insulation and the most demanding setpoint values). The outputs varied even more for heating and cooling demands separately. The cooling demand (**C**) was as low as 256 kWh/a and as high as 1199 kWh/a, while heating demand (**H**) varied in the range of 776 kWh/a and 2621 kWh/a. The best comfort (**COM**) for the occupants was provided with only 1042 dissatisfied hours (out of 6672 occupied hours throughout the year) for the scenario assuming the best thermal insulation and 22°C and 24°C setpoint temperatures accordingly for heating and cooling purposes.

All the above-discussed outputs are also shown in figure 4. Those figures show that the exterior climate conditions have a huge impact on the obtained outputs. It can be concluded that higher comfort can be provided now rather than in the past: the mean and minimal values of dissatisfied hours are lower for outputs with the usage of present weather data (NEW) compared with older ones (OLD). Conclusions for energy demands are not so evident. Heating demands are lower for outputs using present climate data for all the analyzed localizations. Surprisingly, cooling demand for Krakow is lower for outputs with the present climate data, despite the noteworthy increases for Gdansk and Lodz. Additionally, an interesting comparison can be observed for total energy demands. A visible reduction in the observed outputs is noticed for Krakow, while for Gdansk and Lodz, the outputs are maintained at similar levels.

Table 1. Summary of the obtained results: impact of the exterior climate conditions on buildings' energy demand and occupants' comfort.

		GDANSK		LODZ		KRAKOW	
		OLD	NEW	OLD	NEW	OLD	NEW
C [kWh/a] ¹	min	277.6	256.1	342.1	363.9	418.5	315.8
	max	945.9	1103.5	1047.6	1193.0	1199.9	1108.3
H [kWh/a] ²	min	837.5	776.4	964.6	943.9	1117.1	850.8
	max	2154.2	2025.9	2441.5	2307.6	2621.8	2239.7
T [kWh/a] ³	min	3966.5	3894.6	4177.6	4207.8	4407.4	4091.6
	max	6376.0	6308.4	6721.1	6714.1	7065.1	6582.6
COM [h] ⁴	min	1333	1042	1573	1437	1770	1512
	max	4765	4884	5033	4911	5029	4723

¹ Annual cooling demand [kWh/a].

² Annual heating demand [kWh/a].

³ Annual total energy demand (heating, cooling, fans, and lighting combined) [kWh/a].

⁴ Discomfort hours according to ASHRAE 55 standard [h].

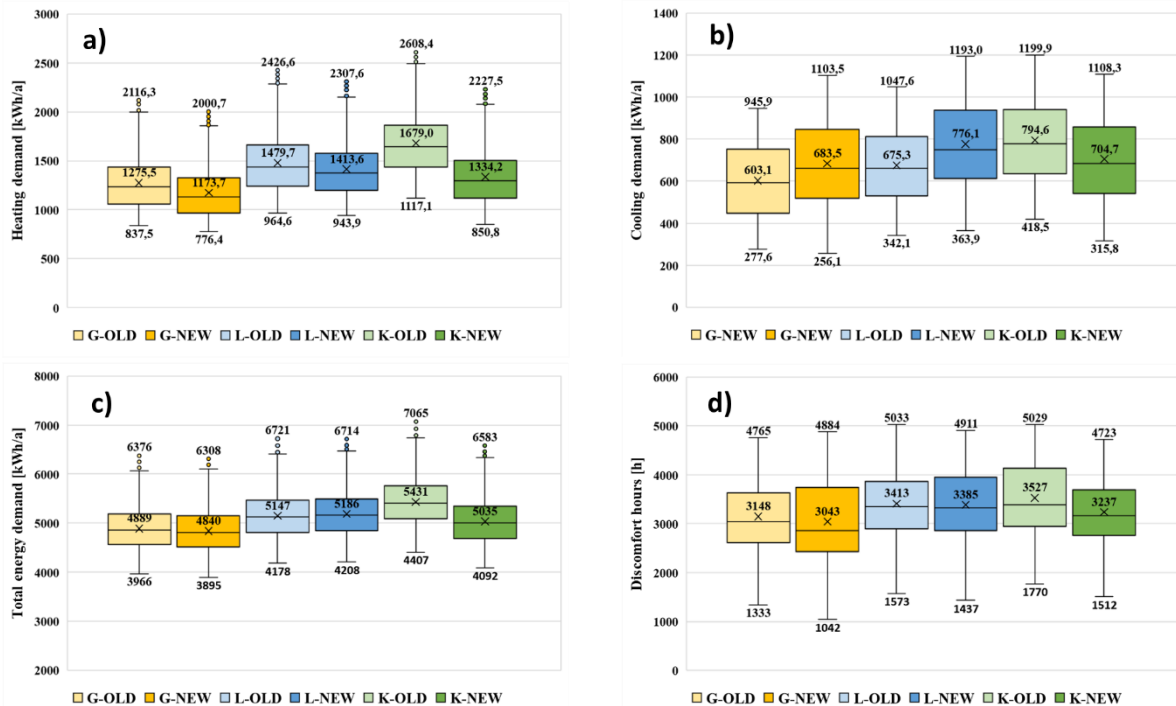


Figure 4. Summary of the obtained results comparing exterior climate conditions: (a) heating demand, (b) cooling demand, (c) total energy demand, and (d) discomfort hours.

Secondly, detailed analyses were performed to investigate each of the examined parameters. The impact of additional thermal insulation on energy demand and occupants' comfort is shown in figure 5,

for all the examined localizations. The impact of thermal insulation on building energy demand is obvious, yet the outputs show, that despite the same parameters of building operation it impacts occupants' comfort as well. The above-mentioned shows the importance of other parameters related to building enclosures, such as thermal mass or temperature distribution on surfaces. The dependencies between occupants' comfort and energy demand are shown in figure 6, based on setpoint temperatures for heating and cooling purposes. It might be seen that the higher temperature for heating, and the lower for cooling, the better the occupants' comfort obtained. The best results, in terms of occupants' comfort, are obtained for setpoint temperatures of 22°C and 24°C respectively for heating and cooling.

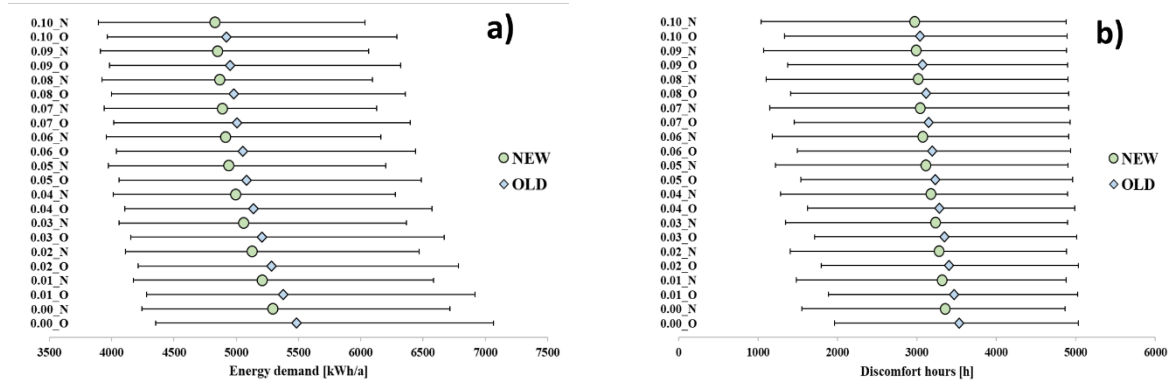


Figure 5. Impact of the additional thermal insulation of building enclosure components on (a) energy demand and (b) occupants' comfort.

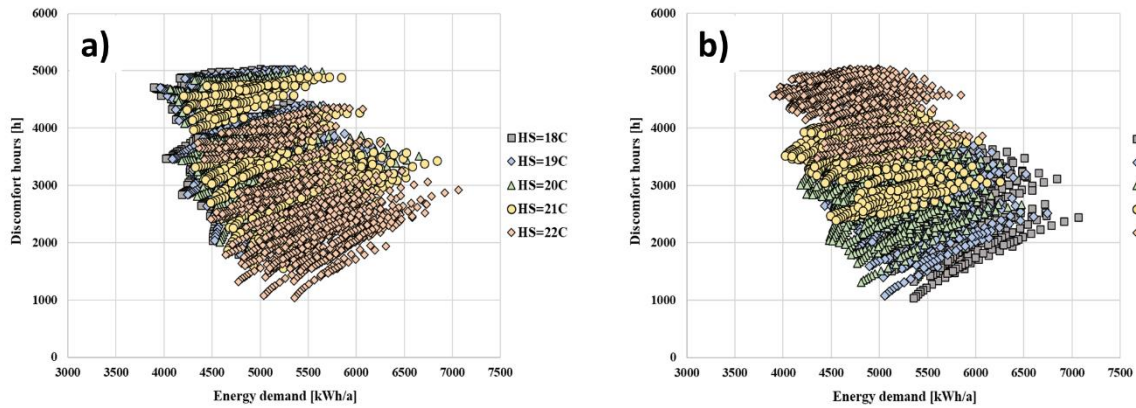


Figure 6. Impact of the setpoint temperatures of (a) heating (HS) and (b) cooling (CS) on energy demand and occupants' comfort.

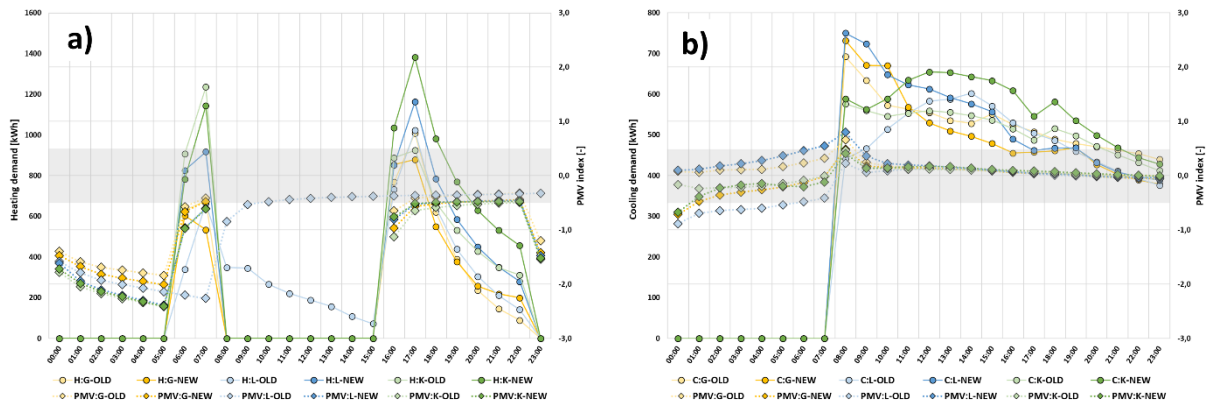


Figure 7. The PMV index distributions for the most demanding days in terms of (a) heating and (b) cooling demands.

Thirdly, the hourly distributions of the PMV-index are shown in figure 7, for the scenarios with the best results in terms of annual discomfort hours (best thermal insulation and 22°C and 24°C setpoint temperatures accordingly for heating and cooling purposes). The PMV values are shown with hourly heating and cooling demands, for a single day period. The selected day is the most demanding day throughout the year in terms of energy consumption (the highest observed demand) for the examined purpose. The range of the 2nd class of thermal comfort, according to [16], is shown in the gray range, screening the PMV values in the range from -0.5 to +0.5. It can be easily concluded, that 24°C during the summer is a perfect temperature for the occupants of this study. Additionally, the 22°C seems to be slightly too low for the occupants during winter with a given activity and outfit. Moreover, during the heating season in the nighttime, the occupants' comfort is not provided, despite the made assumptions. Finally, the ASHRAE standard [13] seems to be less restrictive in terms of occupants' comfort rather than the ISO [16].

5. Conclusions

The presented analyses were performed using computational parametric simulations. The moveable residential building was analyzed, considering several parameters affecting building energy demand as well as occupants' comfort. The above-mentioned parameters include exterior climate conditions, building orientation, and its enclosure parameters, as well as operational schemas. The obtained results show the preferable conditions to provide thermal comfort for the occupants, with the setpoint temperatures of 22°C and 24°C for heating and cooling accordingly. It also showed which parameters can be changed to improve occupants' comfort, simultaneously considering buildings' energy demand. Yet, this study also showed, that the examined field is much more complex, and it is affected by much more variables.

This article should be considered a preliminary analysis of a very comprehensive research subject. Building energy efficiency is now important more than ever, while occupants' thermal comfort is continuously gaining greater attention and importance. Authors will continue this topic throughout their upcoming analyses to examine more parameters and factors related to this subject, in particular, focusing more on occupant-related information, especially the operation patterns variability in order to evaluate the impact of occupants' behavior on the energy performance of a residential building, represented by a single-family house. Those types of studies can help to understand the residents' behavior impact on their thermal comfort and building energy performance.

6. References

- [1] European Commission. *A Roadmap for Moving to a Competitive Low Carbon Economy in 2050*; European Commission: Brussels, Belgium, 2011
- [2] The Our World in Data website, <https://ourworldindata.org> {accessed on 09.01.2023}
- [3] Khan M E and Farneena K A 2012 Comparative Study of White Box, Black Box and Grey Box Testing Techniques *Int. J. Adv. Comput. Sci. Appl.*, 3, 12-15
- [4] Royer S, Thil S, Talbert T and Polit M 2014 Black-box modeling of buildings thermal behavior using system identification *IFAC Proceedings Volumes*, 47 (3), 10850-10855
- [5] Li Y, O'Neill Z, Zhang L, Chen J, and DeGraw J 2021 Grey-box modeling and application for building energy simulations - A critical review *Renew. Sust. Energy Rev.* 146, 111174
- [6] Chen Y, Guo M, Chen Z, Chen Z and Ji Y 2022 Physical energy and data-driven models in building energy prediction: A review *Energy Rep.* 8, 2656-2671
- [7] Paone A and Bacher J P 2018 The Impact of Building Occupant Behavior on Energy Efficiency and Methods to Influence It: A Review of the State of the Art *Energies* 11 (4), 953
- [8] Alsharif R, Arashpour M, Chang V and Zhou J 2021 A review of building parameters' roles in conserving energy versus maintaining comfort *J. Build. Eng.* 35, 102087
- [9] Munoz P, Gonzales C, Recio R and Gencel O 2022 The role of specific heat capacity on building energy performance and thermal discomfort *Case Stud. Constr. Mater.* 17, e01423
- [10] Wilde P 2014 The gap between predicted and measured energy performance of buildings: A framework for investigation *Autom. Constr.* 41, 40-49

- [11] Dronkelaar C, Dowson M, Burman E, and Mumovic D 2016 A Review of the Energy Performance Gap and Its Underlying Causes in Non-Domestic Buildings *Front. in Mech. Eng.* 1, 17.
- [12] Mahdavi A, Berger C, Amin H, Ampatzi E, Andersen R K, Azar E, Barthelmes V M, Favero M, Hahn J, Khovalyg D, et al. 2021 The Role of Occupants in Buildings' Energy Performance Gap: Myth or Reality? *Sustainability* 13, 3146
- [13] ANSI/ASHRAE Standard 55-2020: *Thermal Environmental Conditions for Human Occupancy*
- [14] Abdulsalam Ebrahimpour A and Maerefat M 2010 A method for generation of typical meteorological year *Energy Conversion and Management*, 51 (3), 410-417
- [15] The Energy Plus website, <https://energyplus.net> {accessed on 09.01.2023}
- [16] ISO 7730:2005: *Ergonomics of the thermal environment. Analytical determination and interpretation of thermal comfort using calculation of the PMV and PPD indices and local thermal comfort criteria*



Aalborg Universitet

AALBORG UNIVERSITY
DENMARK

Temperature measurements in the air gap of highly insulated wood-frame walls in a Zero Emission Building

Brozovsky, Johannes; Oksavik, Odne; Rüther, Petra

Published in:

NSB 2023 - Book of Technical Papers: 13th Nordic Symposium on Building Physics

DOI (link to publication from Publisher):

[10.54337/aau541595903_2](https://doi.org/10.54337/aau541595903_2)

Creative Commons License

Unspecified

Publication date:

2023

Document Version

Publisher's PDF, also known as Version of record

[Link to publication from Aalborg University](#)

Citation for published version (APA):

Brozovsky, J., Oksavik, O., & Rüther, P. (2023). Temperature measurements in the air gap of highly insulated wood-frame walls in a Zero Emission Building. In H. Johra (Ed.), *NSB 2023 - Book of Technical Papers: 13th Nordic Symposium on Building Physics* (Vol. 13). [212] Department of the Built Environment, Aalborg University. https://doi.org/10.54337/aau541595903_2

General rights

Copyright and moral rights for the publications made accessible in the public portal are retained by the authors and/or other copyright owners and it is a condition of accessing publications that users recognise and abide by the legal requirements associated with these rights.

- Users may download and print one copy of any publication from the public portal for the purpose of private study or research.
- You may not further distribute the material or use it for any profit-making activity or commercial gain
- You may freely distribute the URL identifying the publication in the public portal -

Take down policy

If you believe that this document breaches copyright please contact us at vbn@aub.aau.dk providing details, and we will remove access to the work immediately and investigate your claim.

Temperature measurements in the air gap of highly insulated wood-frame walls in a Zero Emission Building

J Brozovsky, O Oksavik and P Rüther

Architecture, Materials and Structures, SINTEF Community, 7034 Trondheim, Norway

E-mail: johannes.brozovsky@sintef.no

Abstract. Especially for wooden wall constructions, ventilated rain-screen walls have been used for many decades to prohibit moisture-induced damage. The air gap behind the façade cladding provides drainage, enhances ventilation, and thus facilitates drying of wetted façade components. The conditions in the air gap behind different cladding materials, however, are still an object of research. In the presented study, the interim findings after more than two years of ongoing measurements in the air gap behind different cladding materials of a zero-emission office building in the high-latitude city of Trondheim, Norway are presented. The results provide valuable insight into the temperature conditions in the air gap of ventilated claddings in order to determine the in-use conditions of building materials and develop improved testing schemes. The results indicate that the air and surface temperature in the air cavity of the walls is strongly influenced by the solar radiation incidence on the facades. Both the highest and lowest values were observed on the roof with 81 °C and -21.9 °C, respectively, at the back side of the building integrated photovoltaic modules, resulting in a total temperature range of almost 103 °C.

1. Introduction

Especially for wooden wall constructions, ventilated rain-screen walls have been used for many decades to prohibit moisture-induced damage. The air gap behind the façade cladding provides drainage, enhances ventilation, and thus facilitates drying of wetted façade components. However, the conditions in the air gap behind different cladding materials, are still an object of research. For instance, Girma and Tariku [1] investigated the thermal conditions in ventilated air gaps of different depths behind fibre cement cladding in Burnaby, Canada to evaluate their effect on the thermal performance of the wall in summer conditions. Riahinezhad et al. [2] measured the conditions in the ventilated air gap in a test house in Ottawa, Canada, over 6 years. This was done for the surface temperature on both sides of the air gap in a south-facing brick-cladded façade (back of cladding and top of orientated strand board sheathing) and underneath of the roofing underlayment below asphalt shingles in the roof's air gap. They reported the frequency of occurrence by categorizing the hourly-averaged measurements into 5 °C intervals and average monthly temperatures over the measurement period. Geving et al. [3] took detailed measurements of the hygrothermal conditions in ventilated and unventilated air gaps behind wooden cladding in Trondheim, Norway, over the course of 2 years.

These previous works, however, are either only done for short periods of time as in [1], or only for one façade or roof orientation as in [2] and [3]. In this research, the data from the first 2 years of an ongoing measurement campaign in the air gap behind different cladding materials of a zero-emission office building in Trondheim, Norway (63°24'51" N, 10°24'27" E) are presented. Preliminary results

from the same measurement campaign from November 2019 to February 2020 are shown in an earlier study by Rüther et al. [4] and Brozovsky et al. [5] used the measurements to calibrate a hygrothermal simulation model for future applications. Measurements were taken at in total 21 locations in five different orientations (North, South, East, West, and inclined South-facing roof) of the building envelope with three sensor positions per location: (i) surface of the wind barrier, (ii) middle of the air gap, and (iii) back side of cladding which includes charred wood, building integrated photovoltaics (BIPV), and black aluminium-covered polyethylene (Alu-PE) panels. Thus, in total 63 thermocouples were installed, and the measurements are logged once every 15 minutes starting September 1, 2020.

2. Measurement setup

2.1. ZEB Laboratory

The building that served as a test facility for the experimental data collected in this study is the Zero Emission Building (ZEB) Laboratory (<https://zeblab.no>). Completed in 2020, the ZEB Laboratory was designed and constructed to provide a research facility allowing for testing new environmentally friendly building components, solutions, strategies, and constructions as well as management processes [6–8]. It is a 4-storey, ca. 2000 m² living office laboratory with glued laminated timber columns, cross-laminated timber floors, stiffening internal walls, and insulated wooden framework in the external walls as load-bearing structure. On the façade to the North, charred wood is used as cladding material, BIPV on the roof, and both BIPV and Alu-PE panels on the remaining façades (see figure 1 and figure 2). Unfortunately, no measurements of the optical properties of the cladding materials are available. The determination of which remains subject of further work.



Figure 1. The ZEB Laboratory viewed from the Southeast (a), and Northeast (b). Photos: © Nicola Lolli, 2021.

2.2. Measurements and sensors

There are 21 measurement locations with three sensor positions each, resulting in 63 thermocouples in total. Figure 2 highlights the locations and names of the sensors used in this study, as well as the sensor positions within the air gap. There are in total five sensor locations behind charred wood as façade cladding, 14 behind BIPV, and two behind Alu-PE panels. The wall and roof structures can be seen in figure 3. For this study, measurements starting 01.09.2020 until 31.08.2022 were used. The frequency of logging is 1 every 15 minutes. Thermocouples of type T were used which have a measurement range from -40 to +85 °C and an accuracy of ± 0.5 °C, after an initial calibration. Indoor temperature data is not shown in this work. However, most commonly, it was between 20 and 23 °C. Furthermore, because of high insulation thicknesses of the building envelope, it can be reasonably assumed that small changes in indoor air temperature only have a negligible effect on the conditions in the air gap. The roof has a 30° inclination precisely towards South to maximize BIPV production.

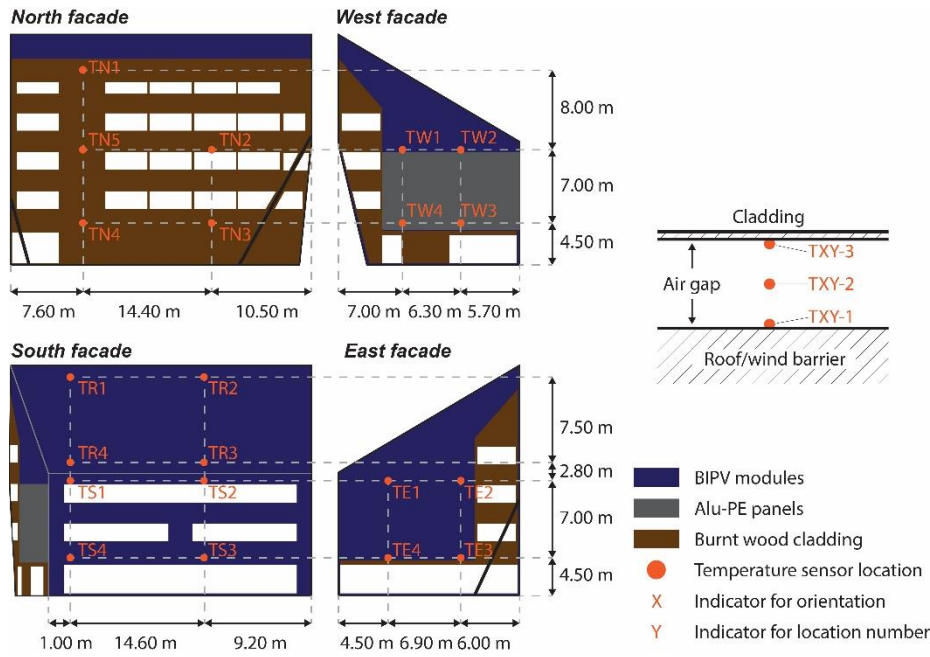


Figure 2. Schematic illustration of the locations of temperature (T) sensors on the five building envelopes: north façade (N), east façade (E), south façade (S), west façade (W), and roof (R) and thermocouple positions in the air gap.

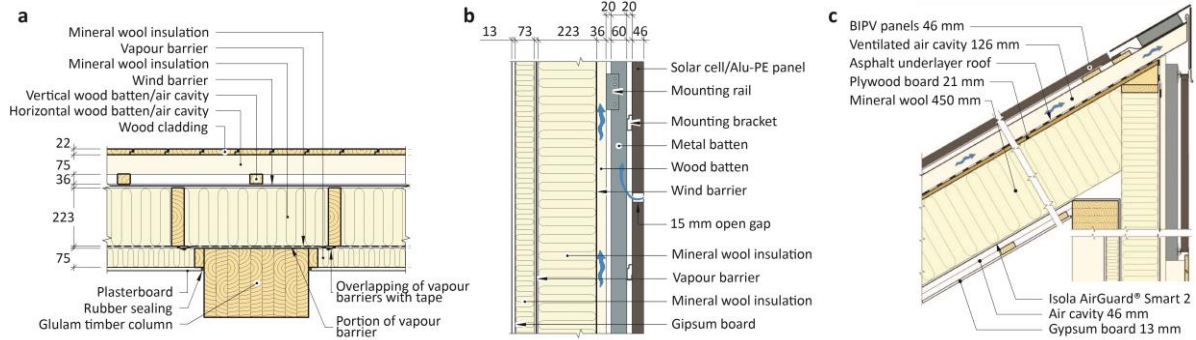


Figure 3. Wall with wood cladding (a), BIPV/Alu-PE panel (b), and BIPV-covered roof (c).

3. Results and discussion

The measured mean hourly temperature in the ventilated air gap ranges from $-21.9\text{ }^{\circ}\text{C}$ ($TR2-3$ on 11.02.2021 at 07:45 CET) up to $81.0\text{ }^{\circ}\text{C}$ ($TR2-3$ on 25.07.2022 at 12:00 CET). Boxplots of the measurements are shown in figure 4. It is noticeable that the $TXY-3$ sensors (at the back of the cladding) recorded both the highest and lowest temperatures at the respective locations. This is the case in every location where complete data is available, except for $TR3$. The minimum temperatures at the wind barrier and in the middle of the air gap are almost identical. This is because they are mostly affected by the outdoor air temperature and convection inside the air gap. The recorded temperatures at the back of the cladding, however, are additionally affected by radiative heat losses of the cladding to the surrounding during cold nights. This leads to the cladding material being colder than the ambient air. During times of solar irradiation, the opposite effect can be observed. Then, the cladding material gets heated up by the sun well above ambient air temperature. Due to that, the cladding material emits longwave radiation energy to the wind barrier surface where this radiation is absorbed, and the second highest maximum temperature of a respective location is measured. In the middle of the air gap, the lowest maximum temperature of a respective location is measured, meaning that it is closest to the ambient air temperature. From figure 4, it is also visible that the median of recorded temperatures is highest at the wind barrier and lowest at the back of the cladding of a respective location where complete data is available. However, there are exceptions to that with $TE4$, $TW3$ and $TW4$. In $TE4$, the missing data for parts of the measurement period is most likely responsible for this

deviation. At the façade to the North, the lowest temperature levels are recorded. At the highest measurement location on this façade (*TN1*), higher temperatures are recorded than at the remaining northern measurement locations due to less shading from surrounding buildings. However, lower heat conductivity of the wood cladding compared to the BIPV and Alu-PE panels might also be a reason for lower temperature levels. At *TR2*, both the absolute maximum and minimum temperatures are recorded, resulting in a total temperature range of almost 103 °C at the back of the cladding, and still 78.2 °C at the wind barrier. This sensor also recorded the largest change between two consecutive measurements with 37.5 °C. But significant differences between two consecutive measurements were also found at the walls, e.g., *TS2-3* with 31.3 °C, *TW3-3* with 27.0 °C, or *TE4-3* with 24.3 °C. According to ISO 15686-1 on *Buildings and constructed assets - Service life planning*, “*extreme levels or fast alterations of temperature*” are among the most common agents affecting the service life of building materials and components. High temperatures are of particular importance, as they increase the reactivity of carbon atoms with oxygen in plastics, followed by further decomposition and reaction of the initial products through many stages [9].

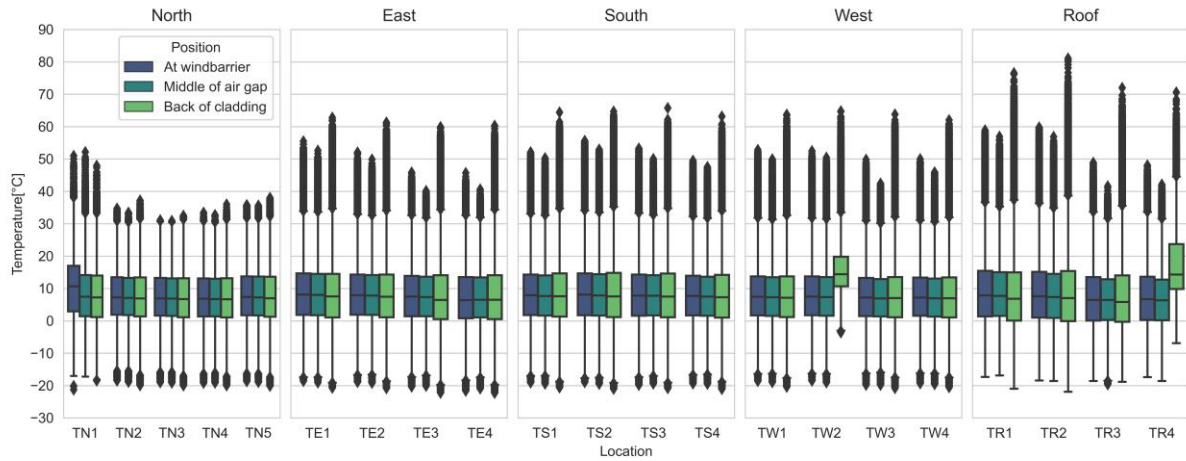


Figure 4. Boxplots of temperature in the air gaps of the different building envelopes at the ZEB Laboratory. Due to sensor malfunctions, there is incomplete data for *TN1-1*, *TE4-2*, *TE4-3*, *TW2-3*, and *TR4-3*.

Figure 5 presents time percentage of the average surface temperature at the wind barrier at the different building envelopes. These have been categorised in time-intervals of 5 °C steps. With 22.5 % on average, the wind barrier surface temperature has mostly been in the temperature interval between 0 and 5 °C. In 60.2 % of the 2-year measurement period from September 2020 to August 2022 it has been between 0 and 15 °C. Moreover, the roof and the façade to the south have the highest share of hours in the temperature categories of 25 °C and above. The surface temperature at the northern façade, on the other hand, rarely rises above 30 °C.

Table 1 shows the distribution of hours in the same time intervals of all sensors at the wind barrier during the measurement period. At the northern façade, the temperature exceeds 40 °C only at the uppermost sensor (*TN1-1*), where the façade is unshaded especially in the morning and evening of the long summer days at Trondheim’s latitude. Due to a large building to the West of the ZEB Laboratory (see also figure 1a on the left), there are comparatively few hours in which high temperatures are recorded on the western façade. Contrary to this, the largely unshaded façade to the East, where solar irradiance is strongest during the morning hours, has a larger share of measured temperatures above 15 °C. As might be expected, the roof and the façade facing South have the largest share of measured temperatures in the upper six temperature intervals. It is noticeable, however, that at the roof there are considerably more hours within the temperature interval between -5 and 0 °C, while there are significantly less in the 5–10 °C interval. This can be explained by longwave radiation losses from the

roof to the sky especially during clear nights so that lower temperatures are recorded than at the less exposed vertical facades.

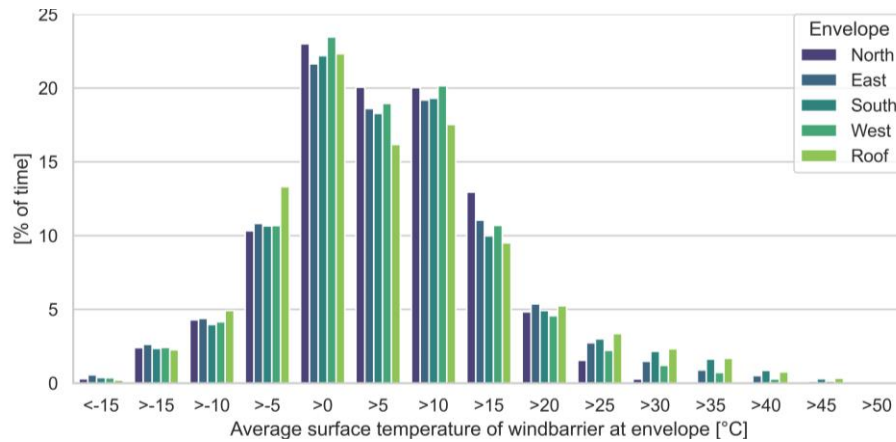


Figure 5. Time percentage of average surface temperature at the wind barrier in the temperature categories at the different building envelopes during the two years of measurements (Sep 2020–Aug 2022).

Table 1. Time distribution in the temperature intervals [°C] of the sensors at the surface of the wind barrier in hours (rounded).

Sensor	<-15	>-15	>-10	>-5	>0	>5	>10	>15	>20	>25	>30	>35	>40	>45	>50	>55
TN1-1^a	5	85	331	1135	2641	2043	2698	2364	1101	448	167	61	10	5	0	0
TN2-1	47	394	721	1825	4137	3461	3607	2268	787	244	29	0	0	0	0	0
TN3-1	63	459	743	1891	4190	3393	3610	2250	736	178	6	0	0	0	0	0
TN4-1	77	458	833	1945	4189	3363	3559	2155	736	187	19	0	0	0	0	0
TN5-1	48	399	746	1883	4074	3350	3458	2294	903	306	57	3	0	0	0	0
TE1-1	51	435	714	1839	3765	3195	3322	1929	1036	537	270	186	131	81	27	0
TE2-1	56	396	713	1817	3828	3330	3373	1930	983	500	259	168	117	47	1	0
TE3-1	134	482	789	1929	3824	3256	3389	1955	896	457	239	128	44	1	0	0
TE4-1	203	487	822	2007	3822	2828	2976	1756	801	425	227	111	35	0	0	0
TS1-1	61	392	685	1840	3895	3239	3392	1729	872	541	376	294	149	51	7	0
TS2-1	56	393	696	1870	3834	3134	3320	1704	856	556	384	313	248	126	32	2
TS3-1	95	432	716	1885	3856	3180	3369	1738	835	522	373	286	165	60	10	0
TS4-1	70	431	717	1838	3951	3256	3513	1801	843	491	336	184	75	15	0	0
TW1-1	52	388	720	1864	4079	3361	3455	1841	792	377	240	187	112	46	8	0
TW2-1	50	391	696	1838	4107	3344	3474	1865	800	400	237	182	95	39	5	0
TW3-1	93	453	752	1910	4098	3340	3605	1894	734	321	162	100	44	17	0	0
TW4-1	72	451	740	1881	4134	3297	3655	1945	742	310	151	90	39	13	0	0
TR1-1	23	266	705	2067	4129	2739	2988	1786	1021	648	430	312	241	104	51	12
TR2-1	43	340	763	2246	3923	2794	2961	1669	985	629	426	315	240	108	60	18
TR3-1	121	498	971	2641	3677	2907	3099	1561	848	550	391	174	74	10	0	0
TR4-1	106	419	1030	2340	3888	2935	3157	1599	863	564	389	159	66	6	0	0

^a Incomplete data (September 2020–April 2021 is missing)

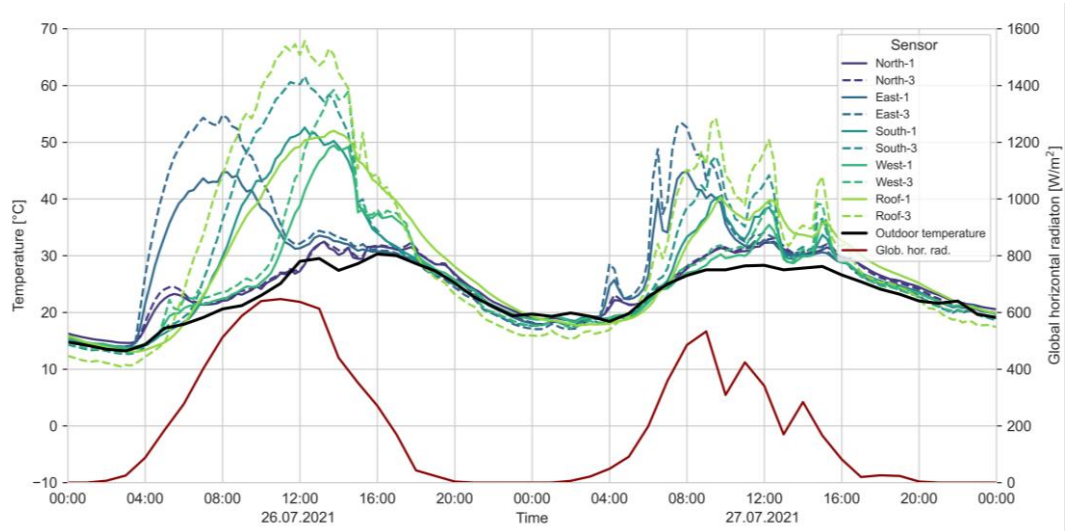


Figure 6. Average surface temperatures of the wind barrier (solid lines) and at the back of the cladding (dashed lines) of all sensors of the different envelopes for the two days with the highest outdoor air temperature during the measurement period (July 26–27, 2021). Outdoor air temperature (black line) and global horizontal radiation (red line) are hourly values and measured in 70 m distance to the studied building.

In figure 6, the measured surface temperatures at the wind barrier and at the back of the cladding are shown for the two warmest days of the measurement period. It is clearly visible, that the temperatures at the back of the cladding are surpassing those at the wind barrier during the day, while they are slightly lower during the night. During the morning hours, especially the façade to the East experiences a strong increase in temperatures. Also, at the façade to the North, a peak in temperatures at the sensor positions can be seen on both days in the morning. On both days, the highest temperatures are recorded at the roof at the back of the cladding. Especially on the second day, it is clearly noticeable how the temperatures in the air gap follow the pattern of solar irradiation that due to cloud coverage is less uniform than on the first day. In Table 2, the largest negative and largest positive difference as well as the median of the difference between the measured temperatures in the air gap and the outdoor air temperature is shown. The results are presented as envelope surface averages, meaning that all sensor data of a particular position (wind barrier, cladding, or wind barrier) are averaged per building envelope surface orientation. The differences can reach up to about 47 °C and can get as low as -13.3 °C at the roof. In the air gap of the façade to the North, the measured temperatures are closest to the outdoor air temperature.

Table 2. Median, largest negative and largest positive difference between the measured envelope surface-averaged temperatures in the air gap (T_{sensor}) and the outdoor air temperature (T_{out}).

Envelope surface	Position	$\min(T_{sensor} - T_{out})$	$\max(T_{sensor} - T_{out})$	Median
North	Wind barrier	-9.2	11.8	0.3
	Cladding	-9.8	14.8	-0.2
East	Wind barrier	-10.3	28.8	-0.1
	Cladding	-11.1	41.5	-0.6
South	Wind barrier	-10.3	30.1	0.0
	Cladding	-11.4	45.0	-0.6
West	Wind barrier	-10.0	23.3	0.0
	Cladding	-10.9	36.3	-0.5
Roof	Wind barrier	-10.6	27.7	-0.1
	Cladding	-13.3	46.8	-1.1

4. Conclusions

The measurements provide valuable insights to the microclimatic conditions in ventilated air gaps and the in-use conditions of air-tightening materials. They are publicly accessible and can be accessed here: <https://zenodo.org/record/7042548> [10]. The results can be used to better design accelerated ageing and durability tests of these materials. To accurately predict the service life of building components, ISO 15686-1 [11] suggests that ideally, “[...] *the microclimate [and] the performance of the component under the intended conditions [...]*” should be known and that this data is not often available. The ongoing work described in this paper aims to fill the knowledge gap regarding these conditions for materials adjacent to or in the ventilated air gap of highly insulated wood frame walls with wood, Alu-PE panels, and BIPV as cladding, as well as BIPV-covered roofs. The presented results are expected to provide useful information for developing durable materials for conditions to be expected in ventilated air gaps in the investigated, subarctic climate of Trondheim, Norway. Particularly, the large temperature range and rapid changes in temperature over relatively short periods of time put significant strain on plastics that are often used as tightening materials. Further measurements and studies should be performed in other locations around the world for a more complete understanding of the exposure of such materials.

Acknowledgements

The authors gratefully acknowledge the financial support by the Research Council of Norway and several partners through the TightEN project [grant number 294894], the Centre of Research-based Innovation Klima 2050 (www.klima2050.no) [grant number 237859], and the ZEB Laboratory project [grant number 245663].

References

- [1] Girma G M and Tariku F 2021 *Build. Environ.* **194** 107710.
- [2] Riahiinezhad M, Eve A, Armstrong M, Collins P and Masson J-F 2019 *Can. J. Civ. Eng.* **46** 969.
- [3] Geving S, Erichsen T H, Nore K and Time B 2006 *Hygrothermal conditions in wooden claddings. Test house measurements* (Oslo, Norway).
- [4] R  ther P, Oksavik O, Nocente A and Gullbrekken L 2021 *J. Phys.: Conf. Ser.* **2069** 12200.
- [5] Brozovsky J, Nocente A and R  ther P 2022 *Build. Environ.* **228** 109917.
- [6] Nocente A, Time B, Mathisen H M, Kvande T and Gustavsen A 2021 *J. Phys.: Conf. Ser.* **2069** 12109.
- [7] Time B, Engeb   A, Christensen M, Dalby O and Kvande T 2019 *IOP Conf. Ser.: Earth Environ. Sci.* **352** 12053.
- [8] Time B, Mathisen H M, F  rland-Larsen A, Ramberg Myhr A., Jacobsen T and Gustavsen A 2019 *ZEB Laboratory - Research Possibilities* (Oslo).
- [9] Pickett J E 2018 *Handbook of environmental degradation of materials* ed M Kutz (Norwich: William Andrew) pp 163–84.
- [10] R  ther P and Oksavik O 2022 *TightEN - ZEB-Laboratory - Temperature behind cladding*. Available at <https://doi.org/10.5281/zenodo.7042548>.
- [11] ISO 15686-1 2011 *Buildings and constructed assets - Service life planning. Part 1: General principles and framework* (Geneva, Switzerland).



Aalborg Universitet

AALBORG UNIVERSITY
DENMARK

Accelerated climate aging tests of structural insulated panels with waste-based core materials

Moschetti, Roberta ; Gullbrekken, Lars; Maia, Joana

DOI (link to publication from Publisher):
[10.54337/aau541597546](https://doi.org/10.54337/aau541597546)

[Link to publication from Aalborg University](#)

Citation for published version (APA):

Moschetti, R., Gullbrekken, L., & Maia, J. (2023). Accelerated climate aging tests of structural insulated panels with waste-based core materials. In H. Johra (Ed.), *NSB 2023 - Book of Technical Papers: 13th Nordic Symposium on Building Physics* (Vol. 13). [225] Department of the Built Environment, Aalborg University. <https://doi.org/10.54337/aau541597546>

Accelerated climate aging tests of structural insulated panels with waste-based core materials

Roberta Moschetti¹, Lars Gullbrekken¹ and Joana Maia²

¹SINTEF Community, Trondheim, Norway

²Civil Engineering Department, Faculty of Engineering of the University of Porto, Portugal

Abstract. One of the challenges of climate change in the building sector is related to the durability of materials, i.e., the resistance to degradation due to weathering over time. The durability of building components can be assessed through long-term natural outdoor climate exposure or appropriate accelerated climate aging in the laboratory. SINTEF Research Centre owns a climate simulator apparatus to perform aging tests according to the Nordtest method NT Build 495:2000. The aim of this article is to show the results from an accelerated climatic aging test performed on three different configurations of a structural insulated panel (SIP), which is characterized by waste-based core materials. The samples were tested for one month, corresponding to about one year of natural outdoor climate exposure. The results from the test performed in the climate simulator include information on the sample changes occurring during the analyzed period, together with the scale of such changes and the time of occurrence. Therefore, the test results are qualitative and based on the fact that a change in the performance properties of the samples corresponds to a change in their appearance during the test. This includes, for instance, signs of degradation, such as cracks, loss of gloss, or delamination.

1. Introduction

The durability of building materials and components has recently gained increasing attention in connection to future climate change challenges. The resistance to degradation due to weathering over time can be assessed through long-term natural outdoor climate exposure or appropriate accelerated climate aging in the laboratory. Several apparatuses can be used in laboratories to subject test samples to various climate exposures with different aging methods and standards [1]. SINTEF Research Centre owns a climate simulator apparatus to perform aging tests according to the Nordtest method NT Build 495:2000 [2].

Structural insulated panels (SIP) are made up of two oriented strand boards (OSB) boards, i.e., wood-based, surrounding the core insulation (usually EPS). Concerning their durability, the biggest problem is exposure to humidity, although a waterproof treatment. Despite that, to study these degradation processes on SIP, the SIPA – Structural Insulated Panel Association carried out a durability assessment on SIP when exposed to distinct moisture conditions. The average results showed no significant loss of mechanical strength compared to the control sample [3].

Nanoparticles significantly affect the thermal behavior of facades through the reduction of the surface temperature. Also, they allow the improvement of the characteristics of materials such as cement, increase the durability of composite materials, allow weight reduction, and confer antimicrobial, anti-corrosive, and self-cleaning properties to facades [4,5,6]

The production of building materials, in particular mortars, and the consequent management of their construction and demolition waste (RCD), has become an important issue worldwide due to the

significant volume of waste generated annually by this industry, with a significant contribution to carbon dioxide emissions into the atmosphere [7]. As such, there has been a growing concern to create new applications for this waste and waste from other industries in developing alkali-activated mixtures (i.e., without incorporating Portland cement). Its reuse alters the status of "waste", thus creating a "sub-product", generating a fundamental step towards waste management and control success and a direct contribution to the circular economy in the construction industry.

Considering a lack of durability assessment on this innovative systems, this article aims to show the results from an accelerated climatic aging test performed on different configurations of SIP characterized by waste-based core materials and dark finishing coatings incorporating nanoparticles with high NIR (Near-Infrared) reflectance. The results focus on the performance of the surface treatment of the samples. This test is performed in connection to the Circular 2B (Circular Construction in Energy-efficient Modular Buildings) project [8] funded by the EEA grants. Circular 2B project aims to optimize a commercial modular envelope solution, a SIP, produced by the consortium's industrial partner by replacing standard original materials with functionally equivalent materials. The project focuses on the development of new waste-based materials, such as the SIP core, by replacing the original insulation slab with an equivalent, incorporating residues, such as plastics, construction and demolition waste, and slag. Also, watertightness was treated by applying an acrylic painting doped with nanoparticles.

2. Methods

We performed artificial climatic aging tests in SINTEF's climate simulator, as described in section 2.1, according to the Nordtest method NT Build 495:2000 [2]. This test was developed by SINTEF about 50 years ago and the method description was developed and later approved as the Nordtest method after many years of experience, including comparisons with natural climatic aging of façade materials [9,10]. The objective of the accelerated climate aging tests was to define the durability of specific variants of the SIP qualitatively.

The samples were subjected to accelerated ageing for 1 month, which corresponds to about 1 year of natural outdoor climate exposure.

Note that the performed tests are not usually run to provide an estimation of the service life expressed in terms of the number of years, as their main purpose is to compare the aging properties of different materials and components.

The results from the tests performed in the climate simulator include information on the changes occurring during the analyzed period, together with the scale of such changes, and the time of occurrence. The main findings are, therefore, qualitative and based on the fact that a change in the performance properties of the samples corresponds to a change in their appearance during the test. This includes, for instance, signs of degradation, such as cracks, loss of gloss, or delamination.

Note that, before and after the aging tests in the climate simulator, the samples will be subjected to other specific tests to examine relevant characteristics of the materials, such as water permeability, adhesion, hard body impact, color and solar reflectance. This will make it possible to examine how the accelerated aging of the materials affects these different characteristics. However, the results of these additional tests are out of the scope of this article.

2.1. The climate simulator

SINTEF's climate simulator is a non-commercial accelerated climate aging apparatus in which test samples are subjected by rotation to four different climate zones, as shown in Figure 1.

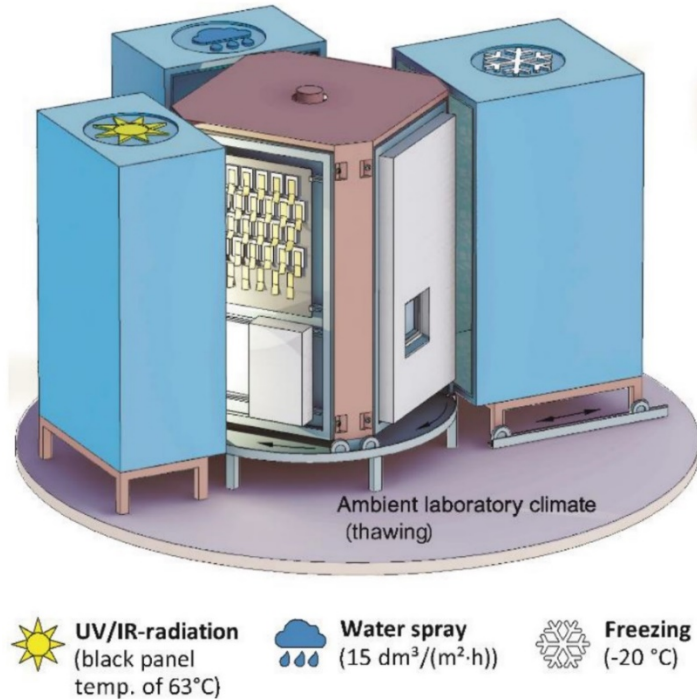


Figure 1 Illustration of SINTEF's climate simulator with the four climate zones used for testing according to NT Build 495. The mid-section is rotating clockwise. Source: [3]

The first zone is an ultraviolet (UV) and infrared (IR) irradiation chamber, where UV radiation is applied using fluorescent UV tubes with a relative spectral distribution in the UV band close to that of global solar irradiance. The black panel's temperature reaches a designated value (normally 63 °C) within 45 minutes of exposure to UV light and heat radiation. The black panel temperature may be chosen as 35±5 °C, 50±5 °C, or 75 ±5 °C, based on ISO 4892 [11]. The temperature is controlled using infrared halogen lamps and the UV intensity can vary at different levels depending on the choice of the UV tubes. For instance, for one specific set of UV tubes, the UVA and UVB intensities are averaged to 15 W/m² and 1.5 W/m², respectively.

The second zone is a water spray zone, where the specimens are wetted with a spray of demineralized water. The suggested strain is 15 dm³/m²/h, but several spraying conditions may be used. Furthermore, to allow water to drip off the examined samples, the spraying is terminated 10 min before the rotation into the third zone.

The third zone is a freezing zone, where an air temperature of -20±5 °C is suggested, but it is also possible to use other air temperatures if registered and reported.

The fourth and last zone is the ambient laboratory thawing zone, where the specimens are thawed at the laboratory climate of 23±5 °C and 50%±10% relative humidity.

The exposure time is 1 hour in each climate zone in the given sequence.

2.2. The tested samples

Three different SIP configurations were tested, as illustrated in Table 1.

Table 1 Main materials of the three tested variants.

	Configuration 1	Configuration 2	Configuration 3
Int.	Oriented strand board (OSB)	Oriented strand board (OSB)	Oriented strand board (OSB)
	Waste-based core	Waste-based core	Waste-based core
	Oriented strand board (OSB)	Oriented strand board (OSB)	Oriented strand board (OSB)
	Commercial basecoat	Commercial basecoat	Commercial basecoat
Ext.	Acrylic paint	Acrylic paint dopped with nanoparticles	-

The samples were prepared by sealing all the lateral faces with epoxy glue, which means the front and back surface will be exposed to the climate simulator. The specimens were positioned in one of the four test faces in the mid-section of the climate simulator. The test was stopped after 30 days.

3. Results and discussion

The test revealed different performances of the surface treatment of the samples. Visual control during and after the test sequence revealed the results showed in Table 2.

Table 2 Results from testing in the climate simulator.

	Configuration 1	Configuration 2	Configuration 3
Start.			02.12.22
11.11.22		09.12.22	Visible cracks in the front face
		Visible cracks in the front face	observed in all the samples
		observed in all the samples	
End	No cracks or delamination	Delamination observed in areas	Delamination observed in
11.12.22	observed	close to the cracks	areas close to the cracks

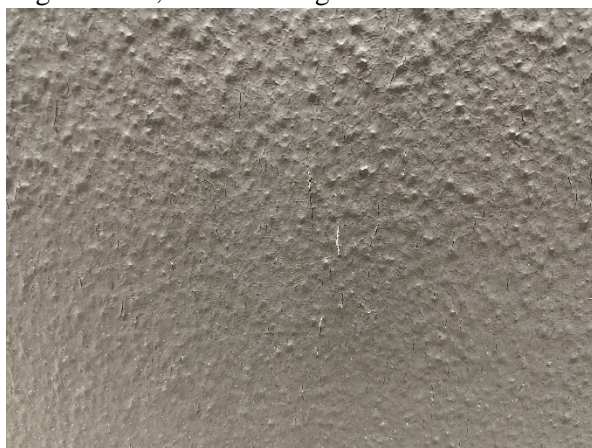
All the samples before testing



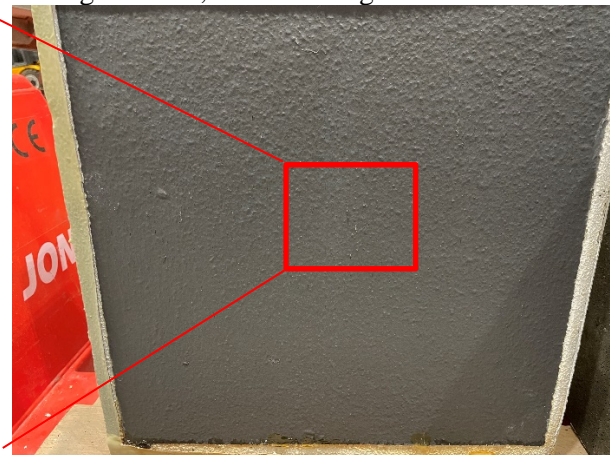
Configuration 1 end of testing



Configuration 2, end of testing



Configuration 2, end of testing



Configuration 3, end of testing



Configuration 3, end of testing

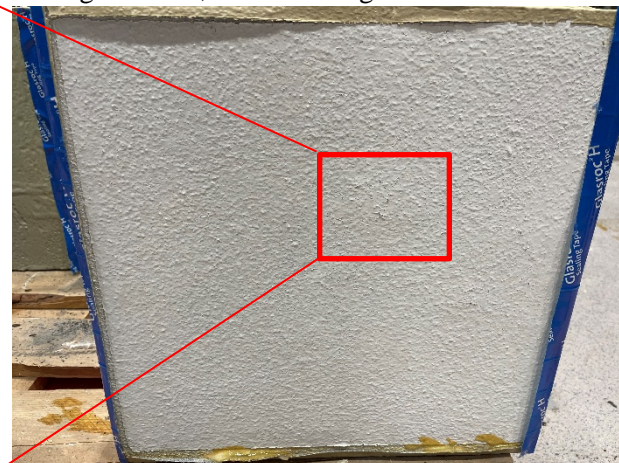


Figure 2 Pictures of the different samples before (upper left corner) and after the testing in the climate simulator.

4. Conclusions

The article presented the results from an accelerated climatic aging test performed on three different configurations of an innovative structural insulated panel (SIP), which is characterized by waste-based core materials.

Visual control of the samples during and after the test sequence indicated a higher performance of configuration 1 compared to configurations 2 and 3. Further developments will include that the samples will be subjected to other specific tests to examine relevant characteristics of the materials, such as water permeability, adhesion, hard body impact, color and solar reflectance. The results will be compared to comparable tests performed before the aging test.

Acknowledgements

This work was financially supported by Project Circular2B - 37_CALL#2 - Circular Construction in Energy-Efficient Modular Buildings financing under the Environment, Climate Change and Low Carbon Economy Programme within the scope of the European Economic Area Financial Mechanism EEA Grants 2014-2021 and by Base Funding—UIDB/04708/2020 of the CONSTRUCT—Instituto de I&D em Estruturas e Construções—funded by national funds through the FCT/MCTES (PIDDAC).

References

- [1] Jelle B P 2012 Accelerated climate ageing of building materials, components and structures in the laboratory *J. Mater. Sci.* **47** 6475–96
- [2] Nordtest Standard 2000 *NT BUILD 495. Building materials and components in the vertical position: Exposure to accelerated climatic strains*
- [3] SIPA 2012 *Durability of SIP's Exposed to Moisture*. Retrieved from https://www.sips.org/documents/SIPA_TB_09_Durability-of-SIPs-Exposed-to-Moisture.pdf
- [4] Broekhuizen F A. v. B J C v 2009. *Nanotechnology in the European Construction Industry - State of the art*
- [5] Papadaki D, Kiriakidis G, & Tsoutsos T 2018 Applications of nanotechnology in construction industry. *Fundamentals of nanoparticles* (pp. 343-370): Elsevier.
- [6] Veloso R C, Souza A, Maia J, Ramos N M M, & Ventura J J J 2021 Nanomaterials with high solar reflectance as an emerging path towards energy-efficient envelope systems: a review. **56**. 36, 19791-19839.
- [7] Secco M P, Brusch G J, Vieira C S, Cristelo N 2022 Geomechanical Behaviour of Recycled Construction and Demolition Waste Submitted to Accelerated Wear. *Sustainability*. **14**. 11. p. 6719.
- [8] WEB-page for the Circular 2B-project accessed at: <https://paginas.fe.up.pt/~circular2b/en/the-project/>
- [9] Kvande T, Bakken N, Bergheim E and Thue J 2018 Durability of ETICS with Rendering in Norway—Experimental and Field Investigations *Buildings* **8** 93
- [10] Asphaug S K, Time B and Kvande T 2021 Moisture Accumulation in Building Façades Exposed to Accelerated Artificial Climatic Ageing—A Complementary Analysis to NT Build 495 *Buildings* **11** 568
- [11] International Organization for Standardization (ISO) 2016 *ISO 4892: Plastics — Methods of exposure to laboratory light sources. Part 1: General guidance* (Geneva, Switzerland: ISO)



Aalborg Universitet

AALBORG UNIVERSITY
DENMARK

Modular retrofitting approach for residential buildings

Borodinecs, Anatolijs; Zajacs, Aleksandrs; Palcikovskis, Arturs

DOI (link to publication from Publisher):
[10.54337/aau541598583](https://doi.org/10.54337/aau541598583)

[Link to publication from Aalborg University](#)

Citation for published version (APA):
Borodinecs, A., Zajacs, A., & Palcikovskis, A. (2023). Modular retrofitting approach for residential buildings. In H. Johra (Ed.), *NSB 2023 - Book of Technical Papers: 13th Nordic Symposium on Building Physics* (Vol. 13). [230] Department of the Built Environment, Aalborg University. <https://doi.org/10.54337/aau541598583>

Modular retrofitting approach for residential buildings

Anatolijs Borodinecs, Aleksandrs Zajacs, Arturs Palcikovskis

Riga Technical University, Kipsalas street 6, Riga, Latvia

anatolijs.borodinecs@rtu.lv

Abstract. Residential buildings are one of the crucial energy consumers. The vast majority of the existing buildings require urgent retrofitting due to the very poor thermal insulation properties of their external building envelope. There are many building retrofitting technologies available on the market. However, thermal insulation technologies, such as rendered and double facades, require large amount of on-site human working hours. One of the most promising technologies is a modular retrofitting.

1. Current situation

According to the Latvian Ministry of Economy, 741 buildings in Latvia were renovated between 2009 and 2015, achieving energy savings of 45% on average. While in almost all cases ventilation systems were not renovated, the natural ventilation systems were left as they were initially designed. Since 2016, 508 projects have been submitted, most of which have not yet been completely built. According to the State Building Control Office, the average specific consumption for heating in multi-apartment dwellings in 2020 was 124.21 kWh/m² per year, similar to 125.59 kWh/m² per year in 2019. These figures also show that renovation is taking place on a small scale and at a slow pace and the overall efficiency of implemented measures is not sufficient to reach general EU targets.

One of the most perspective solutions is modular retrofitting. There are many benefits of this approach [1]. However, one of the main challenges is the higher construction cost in comparison to conventional retrofitting and lack of clear guidance on panel mounting specifics.

2. Lessons learnt from the existing case study

In scope of H2020 MORE-CONNECT project, small multi apartment building was renovated using prefabricated wooden frame panels (Figure 1). It represents a typical brick multi apartment building built in 1960ies. The pilot building is a silicate brick residential house with a lateral bearing system. All wooden frame windows were replaced by PVC windows more than ten years ago.

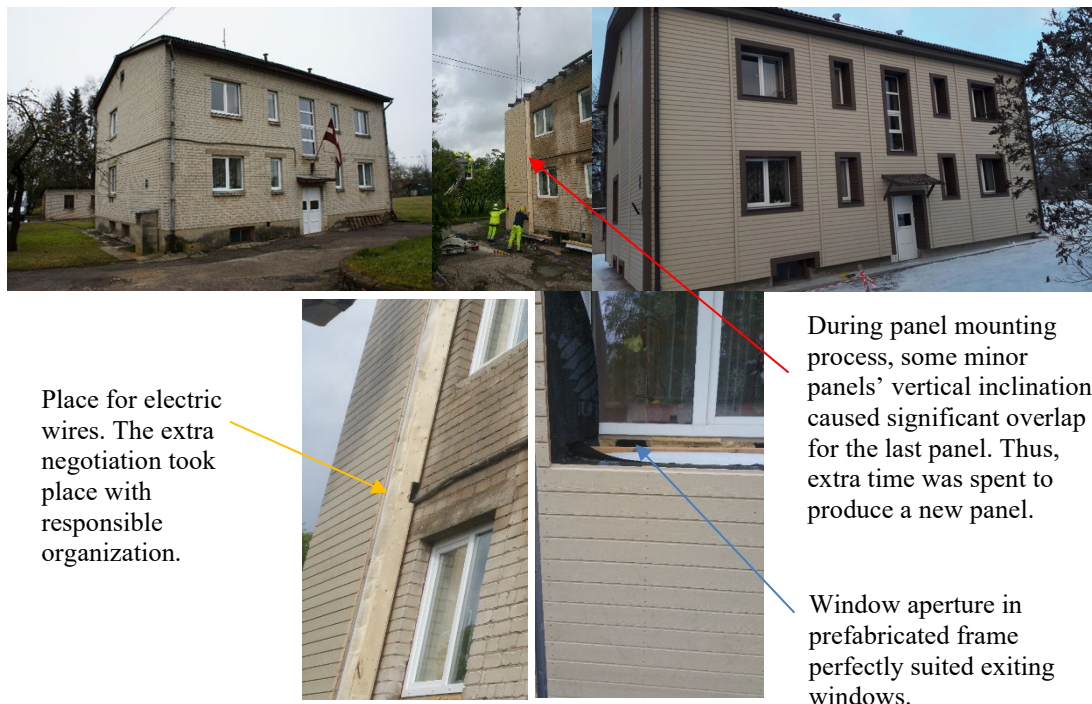


Figure 1 Demonstration case in Latvia

During the project development the delay occurred also due to the owner of electric wires. The initial requirement was to disconnect the wire and to place it on top of the new facade. After some negotiation and calculations, it was allowed to leave it on the exit façade and to embed it into panels.

The main problem for old buildings is a facade vertical deviation. The research made earlier [2] has shown that vertical displacement of external wall could be up to 48mm from foundation level. Thus, unification of prefabricated panels for all buildings requires extra calculation fasteners. The selection of thickness of steel corner brace and steel screws as well as calculation of their number per square meter could require an extra effort during adaptation of prefabricated panel for specific building. Figure 2 (left) represents results of façade 3D scanning. While Figure (right) – solution how wooden frame carcass can be fixed. For demo building point fasteners were used.

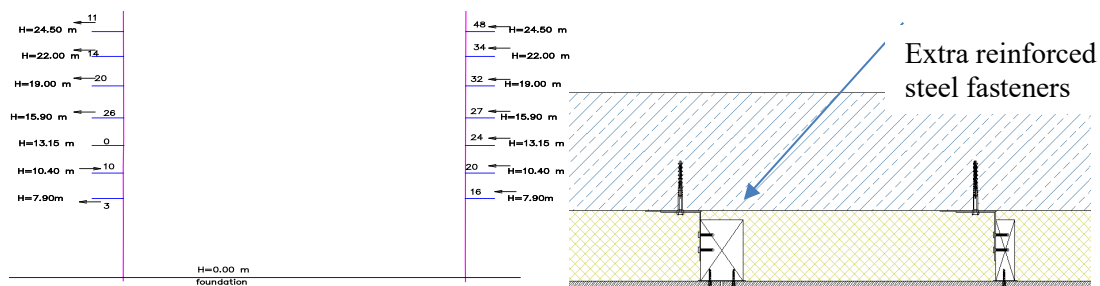


Figure 2 Façade vertical deviations and wooded frame mounting to the wall

Using angles with a thickness of 2 mm, a width of 50 mm and the anchor bolt arrangement shown in Figure 2, these angles need to be placed in 250 mm increments, provided that the vertical beams are in 1200 mm increments. This calculation of angles applies to both the wind loads for the Liepaja region and for Riga. The angles can be increased in increments by increasing their width and thickness. Similar to study [3], even with all necessary data on building technical condition, anchor mounting requires extra effort and time.

The overall project implementation required slightly less than two months. The most time consuming was the development of architectural project including all permissions from the local authorities.



Figure 3 Time frame of renovation project.

The main disadvantage of the proposed modular retrofitting solution is relatively high proportion of linear thermal bridges which has 4.6% higher heat losses in comparison to rendered facades. The critical point are external corners.

Table 1 Review of thermal bridges

Type of thermal bridge	External Ψ_e W/(m ² ·K)	Internal Ψ_i W/(m ² ·K)	Classic rendered facade
			Internal Ψ_i W/(m ² ·K)
Basement/stem wall	0.37	0.4	0.3
External corner	-0.09	0.1	0.05
Wall/attic slab	0.14	0.30	0.24
Panel joint	0.02	0.05	0.00

In addition, initial moisture content [4] of the existing wall has an impact on overall wall assembly hydrothermal performance. However, these data are unique for each building and depend on its location, effect of wind driven rain and technical condition of the building (gutters, roof overhang, etc.) This issue is especially topical for prefabricated panels since they have an OSB on the internal side to ensure straightness during transportation and panel mounting.

3. Conclusion

Retrofitting of multi apartment buildings has many advantages such as construction quality and short on-site construction time.

Existing wall vertical deviation can require extra effort to adapt typical layout of prefabricated panels. It is recommended to pay extra attention to vertical deviation during creation of 3D building model bases on 3D scanning data.

The more extensive study on existing wall moisture content should be performed in Latvia to prepare all necessary data for the fast deployment of prefabricated retrofitting.

Even though prefabricated panel has a bigger share of thermal bridges, its overall impact can be neglected since the major impact refers to heat recovery from exhaust air and overall improvement of energy performance of external building envelope.

References

- [1] P.O. t. Veld, MORE-CONNECT: Development and advanced prefabrication of innovative, multifunctional building envelope elements for modular retrofitting and smart connections, in: Energy Procedia, 2015. <https://doi.org/10.1016/j.egypro.2015.11.026>.
- [2] A. Borodinecs, J. Zemitis, M. Dobelis, M. Kalinka, A. Geikins, Development of prefabricated modular retrofitting solution for post-world War II buildings, in: 10th International Conference on Environmental Engineering, ICEE 2017, 2017. <https://doi.org/10.3846/enviro.2017.252>.
- [3] P. Hejtmánek, K. Sojková, M. Volf, A. Lupíšek, Development of a Modular Retrofitting System for Residential Buildings and Experience from Pilot Installation, in: IOP Conf Ser Earth Environ Sci, 2019. <https://doi.org/10.1088/1755-1315/290/1/012132>.

- [4] P. Pihelo, H. Kikkas, T. Kalamees, Hygrothermal Performance of Highly Insulated Timber-frame External Wall, in: Energy Procedia, 2016. <https://doi.org/10.1016/j.egypro.2016.09.128>.



Aalborg Universitet

AALBORG UNIVERSITY
DENMARK

PRELUDE Roadmap for Building Renovation: set of rules for renovation actions to optimize building energy performance

Paule, Bernard; Flourentzou, Flourentzos; d'EXAERDE, Tristan de KERCHOVE ;
BOUTILLIER, Julien ; Ferrari, Nicolo

DOI (link to publication from Publisher):
[10.54337/aau541614638](https://doi.org/10.54337/aau541614638)

[Link to publication from Aalborg University](#)

Citation for published version (APA):

Paule, B., Flourentzou, F., d'EXAERDE, T. D. KERCHOVE., BOUTILLIER, J., & Ferrari, N. (2023). PRELUDE Roadmap for Building Renovation: set of rules for renovation actions to optimize building energy performance. In H. Johra (Ed.), *NSB 2023 - Book of Technical Papers: 13th Nordic Symposium on Building Physics* (Vol. 13). [238] Department of the Built Environment, Aalborg University. <https://doi.org/10.54337/aau541614638>

PRELUDE Roadmap for Building Renovation: set of rules for renovation actions to optimize building energy performance

**Bernard PAULE, Flourentzos FLOURENTZOU, Tristan de KERCHOVE
d'EXAERDE, Julien BOUTILLIER, Nicolo FERRARI**

Estia SA, EPFL Innovation Park, 1015 Lausanne, Switzerland

paule@estia.ch

Abstract. In the context of climate change and the environmental and energy constraints we face, it is essential to develop methods to encourage the implementation of efficient solutions for building renovation. One of the objectives of the European PRELUDE project [1] is to develop a "Building Renovation Roadmap"(BRR) aimed at facilitating decision-making to foster the most efficient refurbishment actions, the implementation of innovative solutions and the promotion of renewable energy sources in the renovation process of existing buildings. In this context, Estia is working on the development of inference rules that will make it possible. On the basis of a diagnosis such as the Energy Performance Certificate, it will help establishing a list of priority actions. The dynamics that drive this project permit to decrease the subjectivity of a human decisions making scheme. While simulation generates digital technical data, interpretation requires the translation of this data into natural language. The purpose is to automate the translation of the results to provide advice and facilitate decision-making. In medicine, the diagnostic phase is a process by which a disease is identified by its symptoms. Similarly, the idea of the process is to target the faulty elements potentially responsible for poor performance and to propose remedial solutions. The system is based on the development of fuzzy logic rules [2],[3]. This choice was made to be able to manipulate notions of membership with truth levels between 0 and 1, and to deliver messages in a linguistic form, understandable by non-specialist users. For example, if performance is low and parameter x is unfavourable, the algorithm can give an incentive to improve the parameter such as: "you COULD, SHOULD or MUST change parameter x". Regarding energy performance analysis, the following domains are addressed: heating, domestic hot water, cooling, lighting. Regarding the parameters, the analysis covers the following topics: Characteristics of the building envelope. and of the technical installations (heat production-distribution, ventilation system, electric lighting, etc.). This paper describes the methodology used, lists the fields studied and outlines the expected outcomes of the project.

1. Introduction

One of the objectives of the PRELUDE project is to propose ways of reducing the buildings energy consumption while ensuring the comfort of the occupants, which we call Building Renovation Roadmap (BRR)

This implies that, when faced with an existing building, one must be able to qualify the energy performance (consumption), the state of the elements of the envelope (characteristics and level of degradation), the efficiency of the technical installations (technology, adjustments), and to establish a list of actions with priorities for intervention. This includes the possibility to detect malfunctions of the

building either by observing a drift in consumption compared to the objectives, or by reporting complaints from the occupants.

To achieve this objective, we propose a decision process divided into the 5 main steps described in Figure 1 below. The idea is to observe the building status, to detect deviations, to review the potential causes, and to dress a list of actions.

The purpose of this work is to build a set of decision rules based on fuzzy membership functions that allow both deviations and potential causes to be "qualified" and to deliver a list of recommendations in a linguistic form.

As a first approach, we propose to focus the analysis on residential buildings and, more precisely, on collective housing, which represents a considerable stock of buildings in Europe (as an example, this category of building represents about 2/3 of the built area in the State of Geneva).

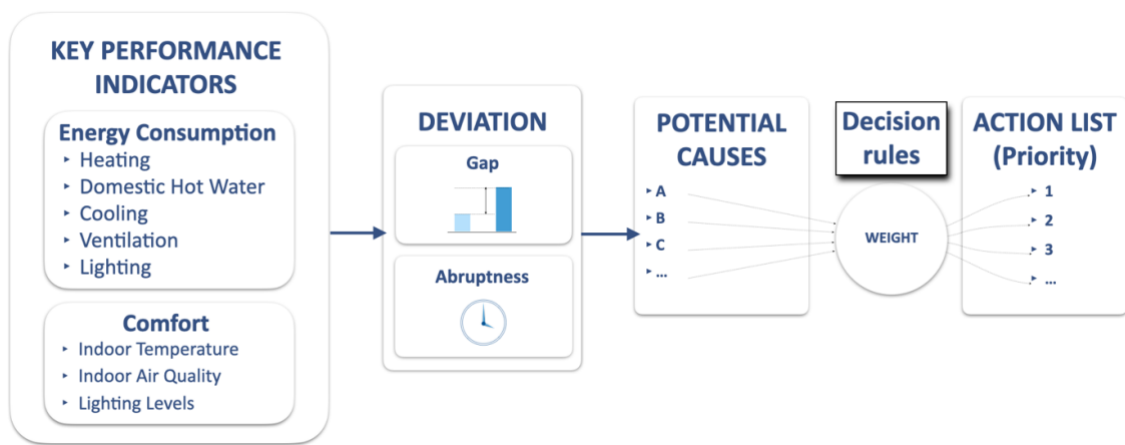


Figure 1: Simplified representation of the decision-making process.

2. Method

As the final objective of BRR is to provide guidance to improve the performance and comfort of buildings, we have chosen to use a method that delivers recommendations in a linguistic and intuitive form. The goal is to target different building stakeholders involved in the renovation process (building owners, architects, building diagnostics experts).

The interface should facilitate the description of the characteristics of the building and its technical installations, in particular:

- Allow for imprecise parameters to be considered:
When diagnosing a building, a certain amount of data cannot be understood in any other way than in vague terms.
- Facilitate the description of the problem:
Working on linguistic concepts allows us to remain as close as possible to the way of thinking of the various actors (diagnosticians, owners, architects, etc.).
- To initiate a process of optimization for the design parameters:
The purpose is to establish a list of actions with integrated priority levels to facilitate decision-making.

2.1. Fuzzy sets, membership functions, linguistic variables

Fuzzy logic allows to consider values inside non-rigid boundaries. The membership of an element u of a universe U to a subset A takes its values in the interval $[0, 1]$; it is described by a "membership function". This indicates the "possibility" that the element u belongs to the subset A .

The uncertainty underlying this notion of membership can, in many cases, be represented using linguistic variables, taken from everyday language. A linguistic variable is defined as a variable whose values are

sentences (or parts of sentences) in a natural or artificial language. If "big", "not big", "very big", etc., are values of height, then height is a linguistic variable.

In the following, we show how to qualify the state of a given parameter by assigning it a degree of belonging to one or other of the linguistic categories that describe the properties of that parameter.

For example, the actual heating energy consumption of a given building, can belong to one of the following categories:

- *Very low, Low, Moderate, High, Very high.*

The membership of each of these categories can also be associated with the potential for improvement that can be expressed with the same linguistic form: A "Very High" consumption indicates that the potential for improvement is also "Very High".

2.2. Key Performance Indicators qualification: Example of the heating energy consumption

We propose to qualify the potential for reducing energy consumption of a given building as a function of its position on the energy class scale. shows the example of Heating demand, where this potential can be qualified as "Very Low" (1), "Low" (2), "Moderate" (3), "High" (4) or "Very High" (5) depending on the energy class of the building.

Dual membership

In addition to the fact that it introduces flexibility in the designation of an element, the notion of gradual membership includes, the possibility of "multiple membership". In the example presented in Figure 2, the heating consumption, which is equal the Limit value +140%, is rated as "Moderate" to "High". The truth levels for each of these two statements are 0.22 and 0.78 respectively.

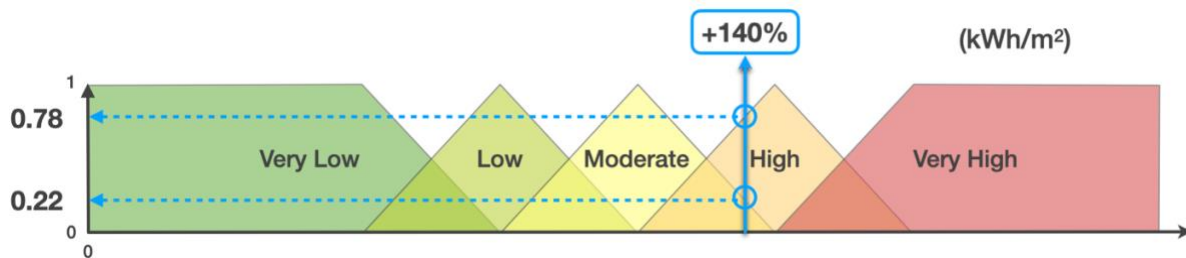


Figure 2: Example of a building with an annual heating consumption equivalent to 140% of the limit.

2.3. Potential causes: Example of the Walls U-Values

Similarly, each of the parameters that influence the energy consumption should be reviewed to determine its potential for improvement. Thus, in the example shown in Figure 3, the Wall's U-value is broken down into 5 fuzzy subsets.

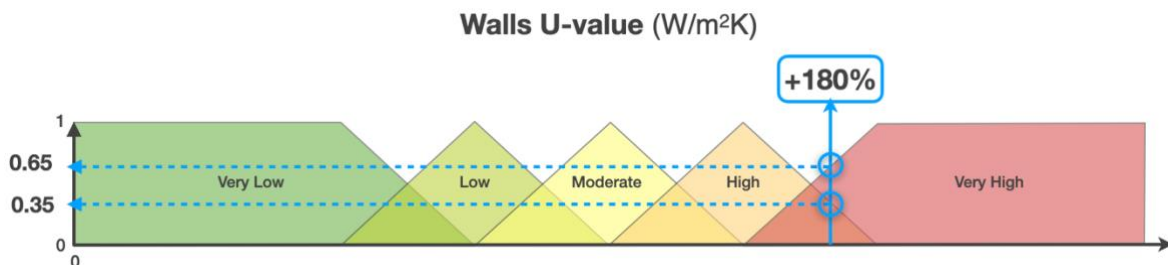


Figure 3: Fuzzy decomposition of the different classes describing the influence of the Walls' U-value to reduce heating consumption.

We propose to use the SIA (Swiss Standard) limit values as [4] a basis and to set the thresholds for membership of the various fuzzy subsets for each deviation steps of +50% from this limit value.

2.4. Incentive levels

Once the potential for consumption improvement has been determined on the one hand, and the potential for improvement of a given parameter on the other, the principle consists in deducing the strength of the incentive level to be delivered to the user.

We propose four distinct levels of prompting, each associated with a verbal injunction:

- Imperative Incentive ➤ You **MUST** (check or modify the parameter)
- Strong Incentive ➤ You **SHOULD** (check or modify the parameter)
- Slight Incentive ➤ You **COULD** (check or modify the parameter)
- None ➤ -

2.5. Aggregation process

If we take the cases mentioned above (cf. Figure 2 & Figure 3) where energy consumption for heating = 140% of the limit value and U-value of the walls = 180% of the limit value), we have 4 incentives that are simultaneously activated, as shown in Figure 4.

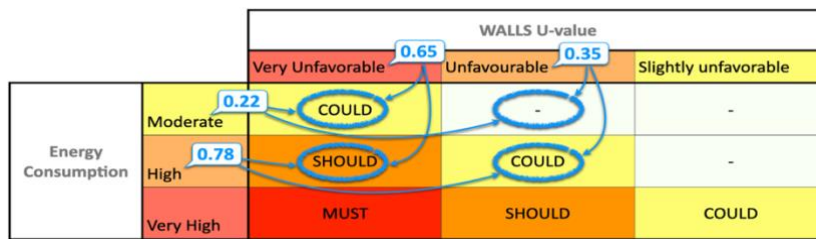


Figure 4: Determination of the incentive levels to be delivered according to the measured performance on the one hand and the potential for improvement associated with a given parameter on the other.

We use the minimum implication process, whereby the lowest truth value is retained for each activated rule. Thus, in the case treated here, the levels of truths for each of the combinations are as follows:

$$E_{\text{Consumption}} = \text{Moderate} (0.22) \quad / \quad \text{U-value} = \text{Very Unfavourable} (0.65) \quad \blacktriangleright \quad \text{COULD} = \text{Min}(0.65, 0.22)$$

$$E_{\text{Consumption}} = \text{Moderate} (0.22) \quad / \quad \text{U-value} = \text{Unfavourable} (0.35) \quad \blacktriangleright \quad \text{NONE} = \text{Min}(0.22, 0.35)$$

$$E_{\text{Consumption}} = \text{High} (0.78) \quad / \quad \text{U-value} = \text{Very Unfavourable} (0.65) \quad \blacktriangleright \quad \text{SHOULD} = \text{Min}(0.78, 0.65)$$

$$E_{\text{Consumption}} = \text{High} (0.78) \quad / \quad \text{U-value} = \text{Unfavourable} (0.35) \quad \blacktriangleright \quad \text{COULD} = \text{Min}(0.78, 0.35)$$

When two identical incentive levels are simultaneously activated (in this case the “COULD” level, i.e. Slight incentive), the levels of truths add up. We thus have the following results:

- NONE: 0.22
- COULD: 0.57 (0.22 + 0.35)
- SHOULD: 0.65

The incentive delivered is the one that gets the highest value, so in this case:

You SHOULD improve the insulation of the walls.

When all the parameters have been reviewed, the list of recommendations is displayed, according to the incentive levels and the degree of truth of each injunction. This presents a list of actions prioritised according to their presumed importance.

3. Considered parameters

At this stage of the project, the parameters mentioned in Table 1 have been characterised with fuzzy membership functions. For the construction of the different membership classes, we relied heavily on recommendations from Swiss practice and standards (e.g. Energo documentation [5]).

Building Characteristics	Form Factor
	Inertia
	Climate related correction (Orientation, Latitude Altitude)
	U-values (Roof, Walls, Floor, Windows, Doors, Blind boxes)
	g-values (Windows, Shading devices)
	Automation (Openings, Shading devices)
Heating Syst. Characteristics	Multiple boilers in a row: Switching process
	Max. temperature, Large & Small Flame Switching
	Heating schedule
	Indoor Set point temperatures (Normal & Reduce)
	Heating curve (Non-Heating point, Design point)
	Heating limits (Day-Night / Winter-Summer Limits)
DHW Syst. Characteristics	Maximum DHW Temperature
	DHW Large & Small flame Switch-ON & OFF
	Circulation pumps: Time Scheduling
	Set-Point Temperatures
	Temperature Hysteresis

Table 1: First list of parameters taken into consideration for the analysis

The following topics are still under development and will be included in the final version of the Building Renovation Roadmap:

- Lighting
- Ventilation
- Cooling
- Renewable Energy Sources

4. Input

The input parameters are divided into the three following categories:

- Main parameters: Mandatory
- Sub-parameters: That make it possible to define the main parameters if they are not know (or no intuitive for the users).
- Advance parameters: Only used and known by experts.

The screenshot displays the 'FACADES PROPERTIES' input interface. At the top, there's a header with a building icon and the title 'FACADES PROPERTIES'. Below this, the 'U-value' is set to '2.3 W/m²'. A question mark icon is placed next to it, with a curved arrow pointing to the 'Insulation Thickness' field, which is set to '25 cm'. Underneath, there are two rows of selection options. The first row, 'Construction Type', includes five icons: 'Concrete / Stone', 'Masonry', 'Bricks', 'Metal', and 'Wood'. The second row, 'Insulation Position', includes three icons: 'Outdoor', 'Intermediate', and 'Indoor'.

Figure 5: Example of an input screen to quickly describe the building.

In the example shown in Figure 5, if the user does not know the U-value of the façade (*Main*), which will happen in most cases, icons allow him to quickly describe his case with *sub-parameters*.

5. Output

The results of the diagnosis are presented in the form of a list of incentives with estimated costs for the corresponding works. These costs come from the EPIQR cost database [6].

Since decision-making is highly dependent on the financial capacity of the actors, it is of high importance to be able to rely on credible costs for renovation, maintenance and improvement works, which together determine the performance of buildings. The updating of this database and the integration of new technologies are an integral part of the PRELUDE project in which the Building Renovation Roadmap is developed.





		The HEATING Consumption is VERY HIGH	
List of potential actions			Estimated costs
	You MUST	⇒ Change the glazings	26'000 €
		⇒ Improve the Ground-Floor insulation	8'500 €
	You SHOULD	⇒ Complete the Pipe insulation	6'000 €
	You COULD	⇒ Install thermostats on radiators	2'700 €

Figure 6: Example of recommended actions issued from the diagnosis

6. Conclusions

Buildings are very complex objects and few people are in a position to master all the subjects that condition their energy and environmental performance. The BRR as we conceive it aims to synthesise a body of disparate knowledge and to propose concrete actions. The ideal framework in which we wish to position this tool is the moment of the realisation of the energy performance certificate. In concrete terms, the tool, which will be available in the form of a web-app, should make it possible to fill in any missing information and to draw up a list of prioritised actions that will help the actors involved in the renovation process to target the most decisive actions.

Acknowledgments

This project has received funding from the European Union's Horizon 2020 research and innovation programme under grant agreement n° 958345 (PRELUDE)

References

- [1] <https://prelude-project.eu/>
Prescient building Operation utilizing Real Time data for Energy Dynamic Optimization
- [2] Lootsman, Freerk A (2011). Fuzzy logic for planning and decision making. OCLC : 752482397. New York ; London : Springer Science & Business Media.
- [3] Paule B (1999). Application de la Logique Floue à l'aide à la décision en éclairage naturel. Thèse N°1916 (1999) EPFL (Swiss Federal Institute of Technology).
- [4] SIA 380/1: 2016 Construction, Besoins de chaleur pour le chauffage. Société Suisse des Ingénieurs et des Architectes, Norme Suisse 520/380/1.
- [5] Enerconseil(2020): Lignes directrices pour optimisation. energo – Groupe Immo Vaud.
- [6] EPIQR: <https://www.epiqrplus.ch/>



Aalborg Universitet

AALBORG UNIVERSITY
DENMARK

Promoting advances in understanding water vapor sorption in wood: relegating popular models and misconceptions

Glass, Samuel V.; Zelinka, Samuel L.; Boardman, Charles R. ; Thybring, Emil Englund

DOI (link to publication from Publisher):
[10.54337/aau541615744](https://doi.org/10.54337/aau541615744)

[Link to publication from Aalborg University](#)

Citation for published version (APA):

Glass, S. V., Zelinka, S. L., Boardman, C. R., & Thybring, E. E. (2023). Promoting advances in understanding water vapor sorption in wood: relegating popular models and misconceptions. In H. Johra (Ed.), *NSB 2023 - Book of Technical Papers: 13th Nordic Symposium on Building Physics* (Vol. 13). [239] Department of the Built Environment, Aalborg University. <https://doi.org/10.54337/aau541615744>

Promoting advances in understanding water vapor sorption in wood: relegating popular models and misconceptions

S V Glass^{1,*}, S L Zelinka¹, C R Boardman¹ and E E Thybring²

¹ Building and Fire Sciences, US Forest Service Forest Products Laboratory, 1 Gifford Pinchot Drive, Madison, WI 53726, USA

² Bioresource Chemistry & Technology, Department of Geosciences and Natural Resource Management, University of Copenhagen, Rolighedsvej 23, DK-1958 Frederiksberg C, Denmark

*Correspondence: samuel.v.glass@usda.gov

Abstract. Water vapor sorption is a fundamental characteristic of wood as a building material. Apart from empirical prediction, models are often used to interpret the time-dependent process of water vapor uptake (sorption kinetics) and equilibrium states of water in wood (sorption isotherms). This paper summarizes our recent investigations into measurement methods and popular models that are widely used for interpreting these physical phenomena. Commonly used criteria for determining equilibrium moisture content with the dynamic vapor sorption technique yield much larger errors than previously thought. A more rigorous equilibrium criterion and a method to reduce data acquisition time are proposed. Evaluation of the parallel exponential kinetics model with improved data and multi-exponential decay analysis indicates that this model is unable to characterize the full sorption kinetic response following a step change in relative humidity. Fitting of common sorption isotherm models to high-quality equilibrium data for wood gives model predicted physical quantities such as monolayer capacity and enthalpy of sorption that are far from agreement with independently measured data. Thus, these models are not valid for water vapor sorption in wood. New theoretical models are needed that correctly describe the physical phenomena.

1. Introduction

The performance of wood as a building material is highly influenced by its interaction with water. Physical properties (dimensions, heat capacity, thermal conductivity) and mechanical properties (strength, stiffness, creep) depend strongly on moisture content. In addition, water is a critical factor in mold growth and fungal decay.

Models are commonly used for empirical prediction of wood moisture content (MC) as a response to environmental conditions, i.e., relative humidity (RH) and temperature. Additionally, theoretical models are used for interpretation of sorption kinetics as well as sorption isotherms. Such interpretation relies on the assumption that the idealized physical system for which the model is derived is an adequate representation of the real physical system. Here we summarize recent work on this topic and highlight three main concerns: the need for reliable measurements and stringency in defining equilibrium (Section 2); the inadequacy of a popular model for sorption kinetics (Section 3); and the failure of well-known sorption isotherm models to accurately predict physical quantities for water in wood (Section 4). The paper concludes with recommendations for advancing the state of the art.

2. Promoting reliable sorption measurements

Experimental measurements provide a foundation for validating sorption models and relating equilibrium states to other physical properties. Several criteria affect the reliability of the data, including the operational definition of equilibrium, the calibration accuracy of mass, temperature, and RH measurements, and the stability of the environmental conditions (temperature and RH) [1]. A mass stability criterion is often used for identifying equilibrium, meaning that the moisture content is assumed to be sufficiently close to equilibrium when the rate of change in mass with time under constant environmental conditions becomes arbitrarily small. Surprisingly, our evaluation of sorption data for wood found that the more reliable measurements were made in the 1960s and 1970s [1].

In the past 15 years, automated sorption balances, also known as dynamic vapor sorption (DVS) analyzers, have become widely used. A commonly reported mass stability criterion for this technique is a rate of change in moisture content less than $0.002\% \text{ min}^{-1}$, or 20 micrograms of water per gram of dry material per minute ($20 \mu\text{g g}^{-1} \text{ min}^{-1}$) over a 10-min period. Although this criterion reduces data acquisition time, it yields much larger errors than previously thought [2], as illustrated for loblolly pine in Figure 1 using our recent DVS data [3] for a solid specimen 1.2 mm thick (longitudinal) with dry mass of ~ 20 mg. These errors in MC are more significant than measurement errors in temperature or RH using DVS analyzers. We defined equilibrium operationally as the point at which the change in mass over 24 hours was within the inherent mass stability of the instrument ($2 \mu\text{g}$). Furthermore, we developed a correction method to account for systematic error from interrupting data collection prior to equilibrium; this method improves data quality while reducing acquisition time [3].

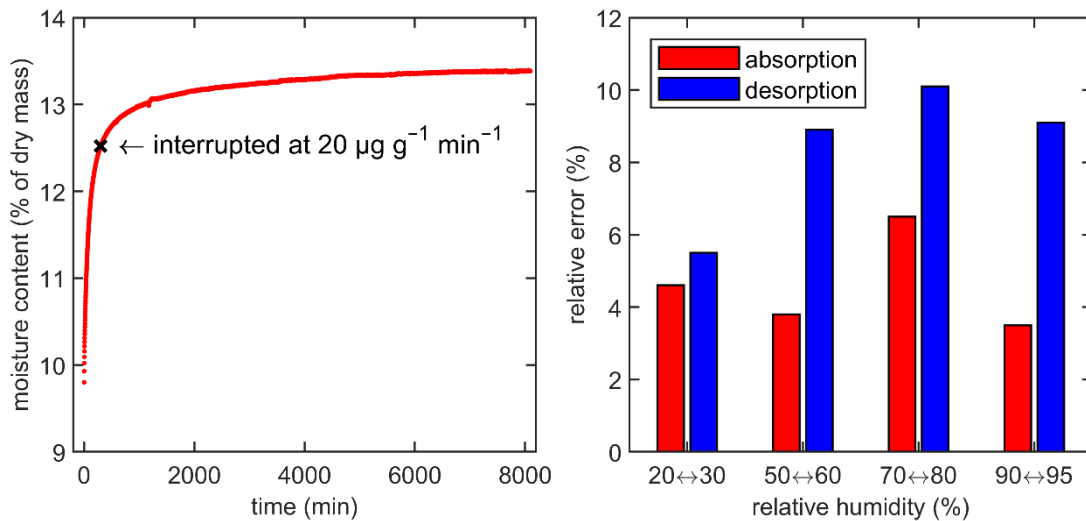


Figure 1. Water vapor absorption in loblolly pine from 70% to 80% RH as moisture content vs. time (left). Relative error in equilibrium moisture content of loblolly pine using the $20 \mu\text{g g}^{-1} \text{ min}^{-1}$ stability criterion for various relative humidity conditions (right). Data replotted from [3].

3. Relegating the parallel exponential kinetics model

The most widely adopted model to interpret the rate of water vapor sorption in wood is the parallel exponential kinetics (PEK) model. Mathematically, this model is the sum of two independent exponential functions, each having a moisture component and a characteristic time constant corresponding to “fast” and “slow” sorption processes [4–6]. Many papers have ascribed physical significance to the model parameters. Although the PEK model yields good curve-fitting statistics, we found that this was an artifact of interrupting the measurements prior to equilibrium (i.e., stopping data acquisition prematurely) [7], as illustrated in Figure 2. When the model was fitted to data collected to

equilibrium (given by the operational definition described above), the parameters changed drastically, the residuals became nonrandom, and the fitting statistics became worse (e.g., Figure 2, right column).

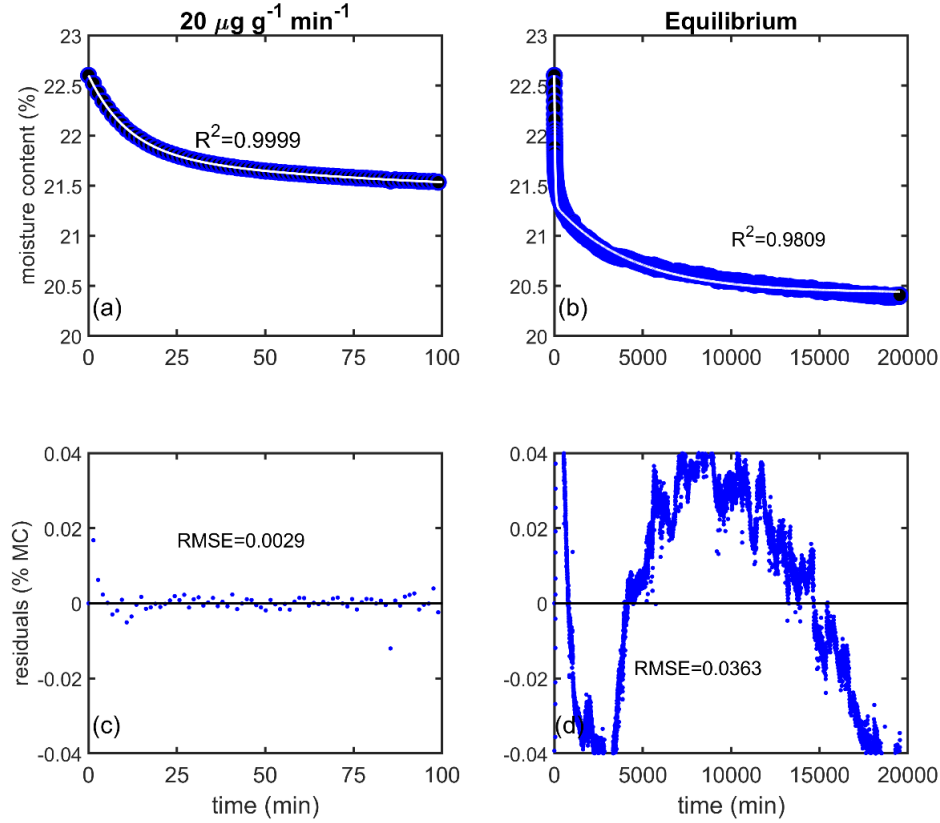


Figure 2. (Top) PEK model (white curve) fitted to scanning desorption data (blue points) from 95% to 90% RH in loblolly pine, for interrupted sorption (left) based on the common mass stability criterion of $20 \mu\text{g g}^{-1} \text{min}^{-1}$ over 10 min and for sorption until equilibrium (right). (Bottom) Residuals from PEK model fits. Data replotted from [7] for solid specimen 1.2 mm thick (longitudinal) with dry mass of ~ 20 mg.

We introduced a new approach for analyzing sorption kinetic data known as multi-exponential decay analysis (MEDEA), which involves fitting a series of hundreds of exponentially decaying functions to normalized sorption data [6–8]. This approach generates spectra indicating the dominant time scales of sorption kinetics after a change in RH until equilibrium is reached. The spectra exhibit between two and six distinct peaks or components, as shown in Figure 3. Most cases have four or more components. This analysis confirms that the PEK model does not capture the full sorption process, and the model parameters cannot be physically meaningful.

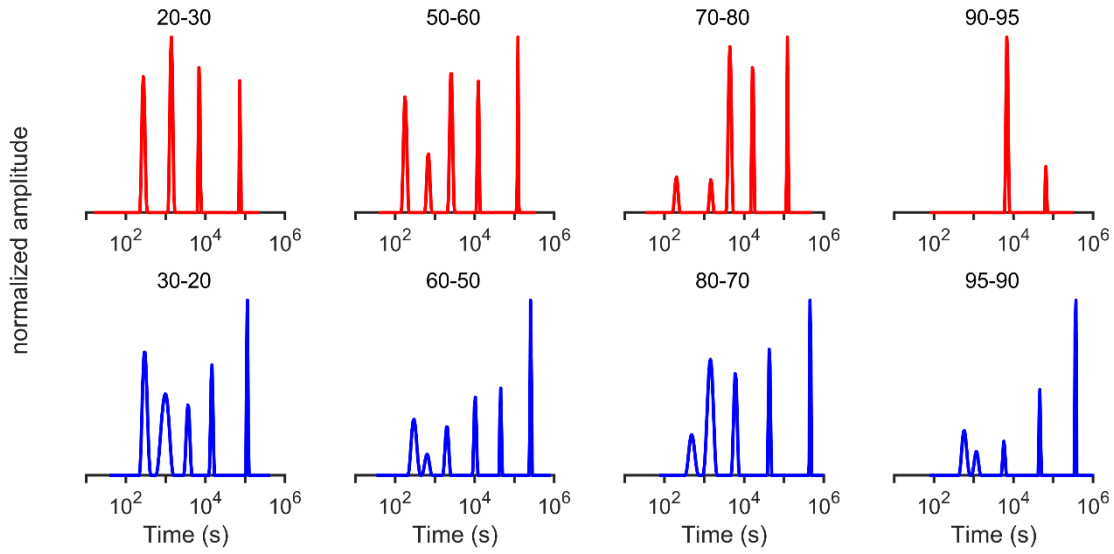


Figure 3. MEDEA spectra for loblolly pine absorption steps (top row) and desorption steps (bottom row). Peaks indicate dominant relaxation times. Numbers above each spectrum indicate the initial and final RH. Data replotted from [8] for solid specimen 1.2 mm thick (longitudinal) with dry mass of ~20 mg.

4. Relegating popular sorption isotherm models

Several sorption isotherm models, including the Brunauer-Emmett-Teller (BET) [9], Dent [10], Guggenheim-Anderson-de Boer (GAB) [11–14], and Hailwood-Horrobin (HH) [15] models, have been widely applied to water vapor sorption in wood. However, these models do not correctly predict the enthalpy of sorption, a key thermodynamic quantity for wood–water interactions [16]. Despite this and further critiques [17–18], the models are often used in the scientific literature to predict properties such as the monolayer capacity, which is a representation of the number of available sorption sites in the material. After identifying high-quality sorption isotherm data for wood at multiple temperatures [1, 19], we fitted the models mentioned above and compared the physical properties predicted by the models with independently measured values [20]. None of the models accurately predicted any of the physical properties. The discrepancy between model predictions of monolayer capacity and measured values of hydroxyl (-OH) groups accessible for water sorption is illustrated in Figure 4. Uncertainty analysis showed that the disagreement between predicted values and experimental measurements could not be attributed to experimental error. These findings demonstrate that the models cannot be considered valid or meaningful for describing wood–water interactions.

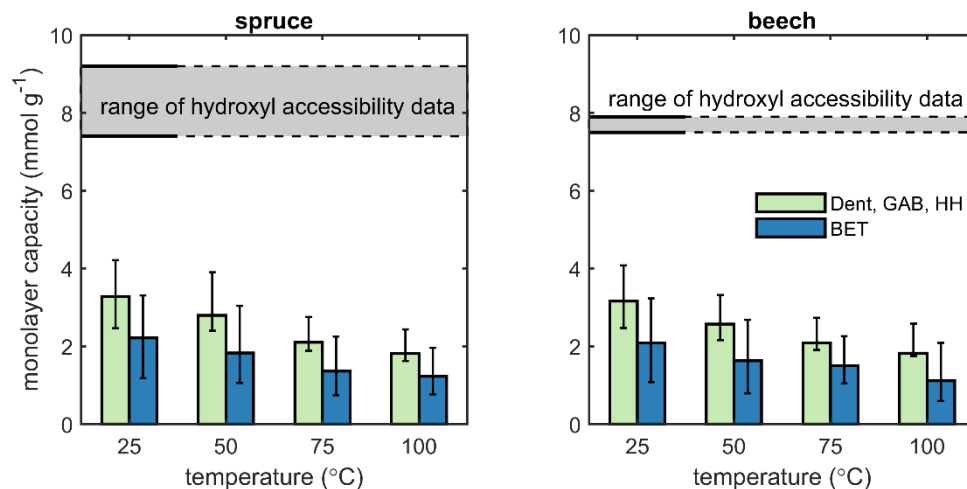


Figure 4. Predicted monolayer capacity from models fitted to sorption data for spruce and beech [19] as a function of temperature, compared to experimental hydroxyl accessibility data. Data replotted from [20] for models mentioned in the body of the paper.

5. Recommendations

This paper highlights the importance of reliable sorption measurements and the invalidity of the parallel exponential kinetics model and popular sorption isotherm models for understanding wood–water interactions. New and improved experimental methods that can probe smaller length scales and refined computational methods are needed to elucidate the complex interactions between water and wood [21]. New modeling approaches are needed that correctly describe the complex physical phenomena involved in the sorption process, including the heat of interaction, moisture-induced swelling, internal stresses, and changes in polymer mobility [6]. Finally, equilibrium models are needed that explain the distinct populations of absorbed water in the cell wall and the origin of sorption hysteresis [20].

References

- [1] Zelinka S L, Glass S V and Thybring E E 2020 Evaluation of previous measurements of water vapor sorption in wood at multiple temperatures *Wood Sci. Technol.* **54** 769–786
- [2] Glass S V, Boardman C R and Zelinka S L 2017 Short hold times in dynamic vapor sorption measurements mischaracterize the equilibrium moisture content of wood *Wood Sci. Technol.* **51** 243–260
- [3] Glass S V, Boardman C R, Thybring E E and Zelinka S L 2018 Quantifying and reducing errors in equilibrium moisture content measurements with dynamic vapor sorption (DVS) experiments *Wood Sci. Technol.* **52**(4) 909–927
- [4] Kohler R, Dück R, Ausperger B and Alex R 2003 A numeric model for the kinetics of water vapor sorption on cellulosic reinforcement fibers *Composite Interfaces* **10** 255–276
- [5] Hill C A S, Norton A and Newman G 2010 Analysis of the water vapour sorption behaviour of Sitka spruce [*Picea sitchensis* (Bongard) Carr.] based on the parallel exponential kinetics model *Holzforschung* **64**(4) 469–473
- [6] Thybring E E, Glass S V and Zelinka S L 2019 Kinetics of water vapor sorption in wood cell walls: state of the art and research needs *Forests* **10**(8) 704
- [7] Thybring E E, Boardman C R, Glass S V and Zelinka S L 2019 The parallel exponential kinetics model is unfit to characterize moisture sorption kinetics in cellulosic materials *Cellulose* **26**(2) 723–735
- [8] Glass S V, Zelinka S L and Thybring E E 2021 Exponential decay analysis: A flexible, robust, data-driven methodology for analyzing sorption kinetic data *Cellulose* **28**(1) 153–174

- [9] Brunauer S, Emmett P H and Teller E 1938 Adsorption of gases in multimolecular layers *J. Am. Chem. Soc.* **60** 309–319
- [10] Dent R W 1977 Multilayer theory for gas sorption. 1. Sorption of a single gas *Text. Res. J.* **47**(2) 145–152
- [11] Anderson R B 1946 Modifications of the Brunauer, Emmett and Teller equation. *J. Am. Chem. Soc.* **68** 686–691
- [12] Anderson R B and Hall W K 1948 Modifications of the Brunauer, Emmett and Teller equation II. *J. Am. Chem. Soc.* **70** 1727–1734
- [13] de Boer J H 1953 The quantity σ : Unimolecular and multimolecular adsorption *The Dynamical Character of Adsorption* ed J H de Boer (Oxford, UK: The Clarendon Press) chapter 5 pp 54–89
- [14] Guggenheim E A 1966 Localized monolayer and multilayer adsorption of gases *Applications of Statistical Mechanics* ed E A Guggenheim (Oxford, UK: The Clarendon Press) chapter 11 pp 186–206
- [15] Hailwood A J and Horrobin S 1946 Absorption of water by polymers: Analysis in terms of a simple model *Trans. Faraday Soc.* **42** B084–B092
- [16] Simpson W 1980 Sorption theories applied to wood *Wood Fiber* **12**(3) 183–195
- [17] Willems W 2015 A critical review of the multilayer sorption models and comparison with the sorption site occupancy (SSO) model for wood moisture sorption isotherm analysis *Holzforschung* **69** 67–75
- [18] Zelinka S L, Glass S V and Thybring E E 2018 Myth versus reality: Do parabolic sorption isotherm models reflect actual wood–water thermodynamics? *Wood Sci. Technol.* **52** 1701–1706
- [19] Weichert L 1963 Investigations on sorption and swelling of spruce, beech and compressed beech wood at temperatures between 20° and 100°C, *Holz als Roh- und Werkst.* **21**(8) 290–300
- [20] Thybring E E, Boardman C R, Zelinka S L and Glass S V 2021 Common sorption isotherm models are not physically valid for water in wood. *Colloids Surf. A Physicochem. Eng. Asp.* **627** 127214.
- [21] Thybring E E, Fredriksson M, Zelinka S L and Glass S V 2022 Water in wood: A review of current understanding and knowledge gaps *Forests* **13** 2051



Aalborg Universitet

AALBORG UNIVERSITY
DENMARK

Integration of smart building technologies costs and CO2 emissions within the framework of the new EPIQR-web application

Dumas, Nathalie; Flourentzos, Flourentzou ; BOUTILLIER, Julien ; Paule, Bernard;
d'EXAERDE, Tristan de KERCHOVE

DOI (link to publication from Publisher):
[10.54337/aau541616188](https://doi.org/10.54337/aau541616188)

[Link to publication from Aalborg University](#)

Citation for published version (APA):

Dumas, N., Flourentzos, F., BOUTILLIER, J., Paule, B., & d'EXAERDE, T. D. KERCHOVE. (2023). Integration of smart building technologies costs and CO2 emissions within the framework of the new EPIQR-web application. In H. Johra (Ed.), *NSB 2023 - Book of Technical Papers: 13th Nordic Symposium on Building Physics* (Vol. 13). [246] Department of the Built Environment, Aalborg University. <https://doi.org/10.54337/aau541616188>

Integration of smart building technologies costs and CO2 emissions within the framework of the new EPIQR-web application

**Nathalie DUMAS, Flourentzos FLOURENTZOU, Julien BOUTILLIER,
Bernard PAULE, Tristan de KERCHOVE d'EXAERDE**

Estia SA, EPFL Innovation Park, 1015 Lausanne, Switzerland

dumas@estia.ch

Abstract. The EPIQR method was developed between 1996 and 1998 within the framework of the European research programme JOULE II and with the support of the Swiss Federal Office for Education and Science. In its first versions, the EPIQR software and EPIQR+ that succeeded it, were desktop tools, allowing a precise diagnosis of the state of deterioration of an existing building and the elaboration of renovation scenarios including the different costs of the necessary works. However, deep refurbishment rate is still low. Climatic emergency state declared by most of the Swiss Cantons makes it necessary to search also for other strategies for urgent reduction of CO2 emissions. As part of the PRELUDE project, a web version of this tool has been developed to integrate both smart technologies and energy optimization actions. Some of them can be considered as soft actions, making it possible to develop a soft renovation roadmap for buildings that are not scheduled for renovation in the short term. As examples, the costs of optimization contracts, intelligent heating control, demand-controlled ventilation, abandonment of heat production from fossil fuels, integration of renewable energies into the building, and communities' creation for self-consumption of photovoltaic production have now been modelled. To help the residential building stock fit with the CO2 reduction of 60% by 2030 compliance and the "2000 W society" energy sobriety target by 2050, the EPIQR-WEB database includes the CO2 indirect emissions of each refurbishment action. Hence, this updated version enables the building diagnosis expert to evaluate and optimise deep refurbishment scenarios, from both financial and environmental point of view. Parallel calculation of CO2 indirect emissions with the calculation of refurbishment cost is done without extra time cost for the user. The paper will show the software new functions, the EPIQR-WEB database expansion and how its overall results can be used to meet the European Union Climate Target through a realistic and comprehensive investment plan.

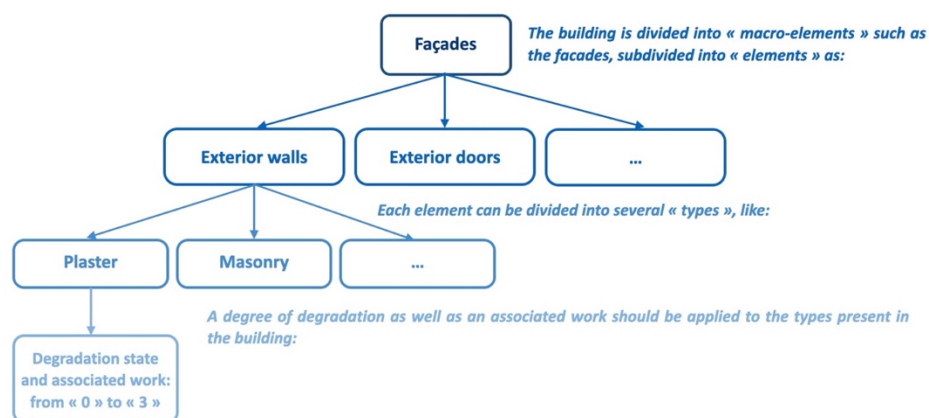
1. Introduction

The cost and financial aspect of refurbishments are often the main obstacle to building's renovation. The lack of clear information between the environmental and energetic requirements of a renovation and the corresponding costs is another issue that slows down building refurbishment, although this is one of the most popular subjects nowadays.

Moreover, reliable tools allowing anyone to understand this relationship through an easy diagnostic should be developed. This is based on this observation linked to the increasing need of having access to informatic instruments from anywhere that the transition from a software platform to a web application for the EPIQR+ method was done. The first PRELUDE development of the EPIQR+ tool therefore

corresponded to this transition from a desktop version to an online version, without changing the initial method or the database philosophy. As a reminder, Figure 1 below resumes the building structure and the coding principle of the EPIQR method:

Figure 1: Simplified representation of the building structure and coding principle of the EPIQR method.



Then, in addition to the already existing costs in the EPIQR software, namely the ones linked to the diagnosis of architectural (interior and exterior) and

technical elements, a non-exhaustive list of expenses needed to make a residential building smarter were included in the EPIQR web-app and currently based on Swiss reference costs. A validation process of the new interface as well as the integration of other European financial data is currently under development within the PRELUDE project.

Finally, CO2 emissions of each refurbishment or optimization action in the database are actually being calculated and integrated to the new application results.

2. EPIQR web interface

The following major improvements can be noted:

- Web access,
- Easier navigation in the tool, especially with the merging of the diagnosis and scenarios tabs allowing to directly code the desired interventions in parallel with their respective costs,
- More efficient reporting with a full report directly generated,
- Better design facilitating interactions with the user.
- Addressing the whole Europe with the costs adapted to the local country conditions adapted with the Eurostat country price index.

Hence, new useful data can be added such as the construction date of the building, its rating or protection level in the architectural census and even the visit date and a picture of the whole building.

In addition, the various tabs representing the different stages of the diagnosis have been transferred from the top of the screen to the left of it. This way, reading all the information can be done more naturally, from the left to the right. Also, to be user-friendly, this web-app limits as much as possible the number of clicks or tabs selections needed to enter a parameter or an information.

The user-friendliness of this new application leads to a greater speed of use. Indeed, the web version also helps with the core function of the application, i.e. to provide assistance to the expert making the diagnosis, by improving the global architecture of the application. There is now one tab on the left for the building information inputs, another one underneath to enter all the dimensional coefficients and the two last ones are for creating different renovation scenarios and publishing their results according to the level of information required. Tabs number has been divided by two and the fundamentals data, renovation works and their corresponding costs, can now be assessed together on the same page. Several levels of results can now be chosen, ranging from simple to full reports. Figure 2 below reflects an example of the visual rendering of the evaluation tab:

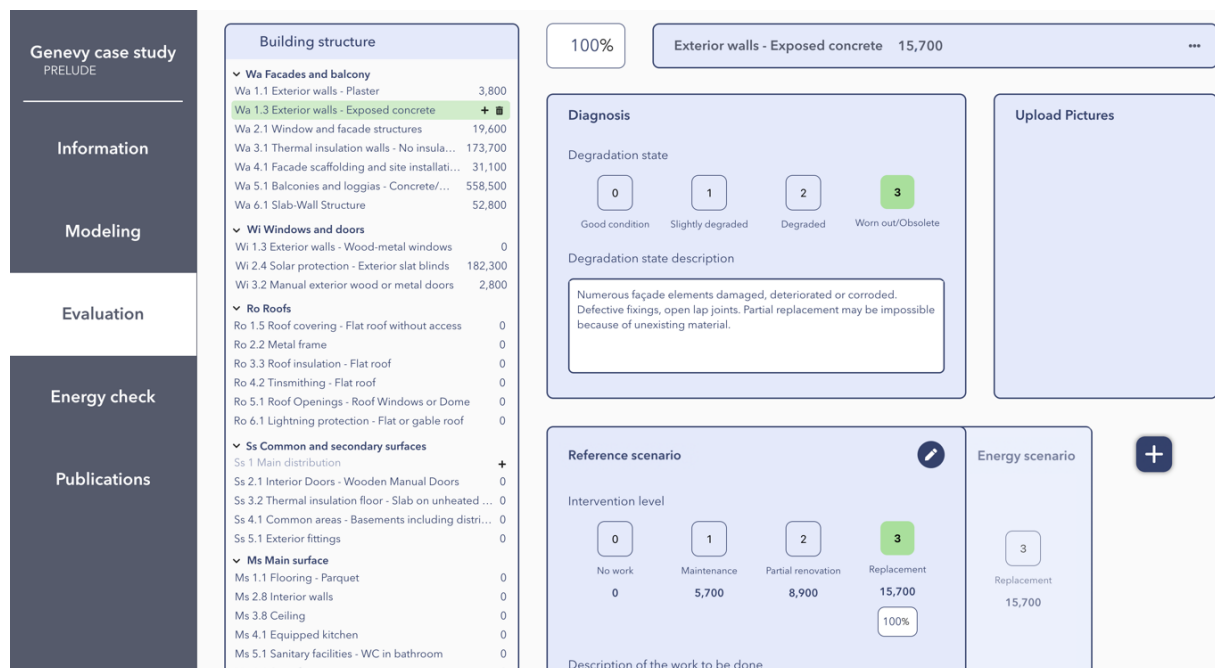


Figure 2: Example of the actual visual rendering of the “Evaluation” tab.

As in the software, some texts can be added to describe in more details the state of the element type and the work to be carried out. Similarly, pictures can also be integrated in the “Evaluation” tab to help the expert and its client understand to which building part the diagnosis is referring to.

The web-application is, for the time being, in French and in English. Translation into other languages could be done later, in the following phases of PRELUDE. Also, the web version of EPIQR is first targeting housing buildings diagnostics. The addition of the remaining building uses present in the software, such as administrative or industrial ones, will be studied afterwards.

To summarize, the EPIQR web-app is based on the existing method but presents a new design and features helping the expert to diagnose the building more easily and quickly and generates results that should be clearer for the clients. It is actually available at the following URL: <https://epistimmo.ch/>. Note that this version will still be in beta until the official release, implying that the backup of the data is for the time being not guaranteed.

3. Updated cost database

The EPIQR method calculate renovation costs, defined as a one-time investment considering both labor and material costs.

Regarding the second selection criteria, e.g. the use of smart technologies in reducing carbon emissions and improving energy savings in building stock, only elements associated with a corresponding and reliable cost were chosen as pertinent. As expected, the number of data collected, each defined by a new type of technology and its corresponding cost, increases the reliability of the financial element. Thus, to fit with the EPIQR data granularity, only significant costs linked to a smart-technology or equipment installed with sufficient frequency or in other words already on the market were considered.

In total and at the moment, 17 smart actions or building technology integrations have been added to the EPIQR database with their corresponding costs and especially in the “Heating” and “Electricity” macro-elements. They are listed as follows:

- 1) Abandonment of fossil fuels: installation of an air-water heat pump
- 2) Abandonment of fossil fuels: creation of a substation and connection to district heating

- 3) Abandonment of fossil fuels: installation of a wood heating system (wood chips or pellets)
- 4) Partial abandonment of fossil fuels with 30% of DHW production produced with a heat pump
- 5) Installation of a heat pump with heat recovery to produce part of the domestic hot water
- 6) Change of circulation pumps or addition of hydro ejectors
- 7) Hydraulic balancing
- 8) Supply and installation of thermostatic valves, purging of the network
- 9) Remove radiators and replace heating elements, fittings and valves. Filling and bleeding.
- 10) Implementation of an energy optimization contract with sensors
- 11) Implementation of an energy optimization contract without sensors
- 12) Installation of energy meters
- 13) Implementation of a technical management of the building
- 14) Installation of presence detectors in the common areas
- 15) Establishment of a group of self-consumption
- 16) Addition of storage elements (battery or inertia wheel)
- 17) Installation of charging stations for electric vehicles

This list is growing as PRELUDE European demo cases are providing more descriptions and installation prices for different smart technology types, most of the costs available in the first version of the web-app come from Swiss projects. Hence, the Swiss cost update factor already in use had to be taken into account and the total cost of each smart technology has been dissected to fit with the EPIQR method structure, i.e. broken down into smaller costs or Building Construction Cost Code (BCC) corresponding to a specific nomenclature including all the construction costs of a project, from its conception to its realization. Every elementary cost corresponding to a specific work is linked to one quantity survey that was measured or counted in a real building, also named the baseline building, and derived from the total expenses for that work. The relation between one specific value measured in the baseline building and its corresponding amount in the diagnosed building depends on dimensional coefficients, that have to be entered in the application by the expert performing the diagnosis. For each building, about ten dimensional coefficients must be inputted (for example: the energy reference surface (ERS) (the sum of all floors area of floors and basements that are included in the thermal envelope and whose use requires heating or air conditioning), the number of dwellings or the windows area, ...etc.

Further work will consist in collecting the remaining costs related to the PRELUDE demo-sites monitoring plans, to first verify the already implemented smart-technology costs in the EPIQR database and then confirm the cost-conversion factors between Swiss and other European country currencies at a certain period.

4. CO₂ emissions integration

To help renovated buildings reach the European Union Climate targets of 2030 and 2050, financial and operation direct CO₂ emissions is not sufficient. Indirect CO₂ emissions linked to each type of work, both those of building fabric, technical installations, but also now with PRELUDE those of new technologies are actually being derived and added to the EPIQR database. New energy technology (electronic control of the building, low current, batteries, inverters) have no negligible CO₂ indirect emissions, especially if we consider their short lifespan and frequent replacement. Similarly to the costs structure, to each individual work EPIQR assigns a CO₂ indirect emission. These data are drawn from Swiss or European databases (KBOB, ecoinvent). The building dimensional and refurbishment work model calculates with the same user inputs additionally to the refurbishment cost the indirect CO₂ emissions. This calculation has absolutely no time cost the EPIQR-WEB user but enables him or her to consider and optimize the total impact of a renovation scenario or renovation roadmap.

PRELUDE case study is used to validate the EPIQR WEB results, comparing the calculated indirect CO₂ emissions with those calculated by other software or databases and preliminary results are promising. As soon as the method is validated, it will be easy to calculate the real impact of new

technologies and replicate this possibility to diagnosed buildings from the very initial stages of the refurbishment project.

Indirect CO₂ emission (typeCO₂) is calculated for all elements types using this formula.

$$typeCO2 = \frac{\sum workCO2}{typeLife} * buildingLife$$

- workCO₂: Indirect CO₂ emission per individual work.
- typeLife: Lifetime per element type.
- buildingLife: Lifetime of building (60 years).

The total indirect CO₂ emission for a building is the sum of all element types indirect CO₂ emissions.

$$buildingCO2 = \sum typeCO2$$

5. Example of diagnosis

The EPIQR method, through its decomposition of the building, guarantees the user to diagnose the whole building without omitting any element. In addition, the presence of images and explanatory texts greatly helps the understanding and uniformity of the data provided.

Genevy case study
PRELUDE

Information

Modeling

Evaluation

Energy check

Publications


Dimensional coefficients

ERS Energy reference surface	<input type="text" value="1000"/>	m ²
Wso Wall surface against the outside	<input type="text" value="152"/>	m ²
Ws Window surface	<input type="text" value="515"/>	m ²
BS Built surface	<input type="text" value="131"/>	m ²
LSS Landscaped surroundings surface	<input type="text" value="516"/>	m ²
FS Floor surface	<input type="text" value="21"/>	m ²
Number of lift shaft modules	<input type="text" value="651"/>	U
HS Habitable surface	<input type="text" value="651"/>	m ²
SS Secondary Surface	<input type="text" value="651"/>	m ²
Main circulation surface	<input type="text" value="651"/>	m ²
Dwelling count	<input type="text" value="651"/>	U
Surface of viewed facades	<input type="text" value="100"/>	m ²

Cost coefficients

Complexity Coefficient: Size of building	<input type="text" value="100"/>	%
Complexity Coefficient: Working conditions	<input type="text" value="100"/>	%
Complexity Coefficient: Access	<input type="text" value="100"/>	%
Building Cost Index	<input type="text" value="143.4"/>	%
Engineering Fees	<input type="text" value="15"/>	%
VAT	<input type="text" value="7.7"/>	%
Miscellaneous and unforeseen	<input type="text" value="15"/>	%

Illustration and definition of the selected coefficient



The sum of all floor areas of floors and basements that are included in the thermal envelope and whose use requires heating or air conditioning.

Comment of the selected coefficient

Place your comment

Figure 3 Example of the modelling tab

For example, for a housing building, the user must enter a list of dimensional coefficients, each of which is accompanied by an image and a text describing precisely what value is expected. The Evaluation tab directly shows the complete structure of the building and encourages the user to question each of the elements. Moreover, each degradation state and necessary works is accompanied by a text helping the user to select the right code and thus to have the correct cost.

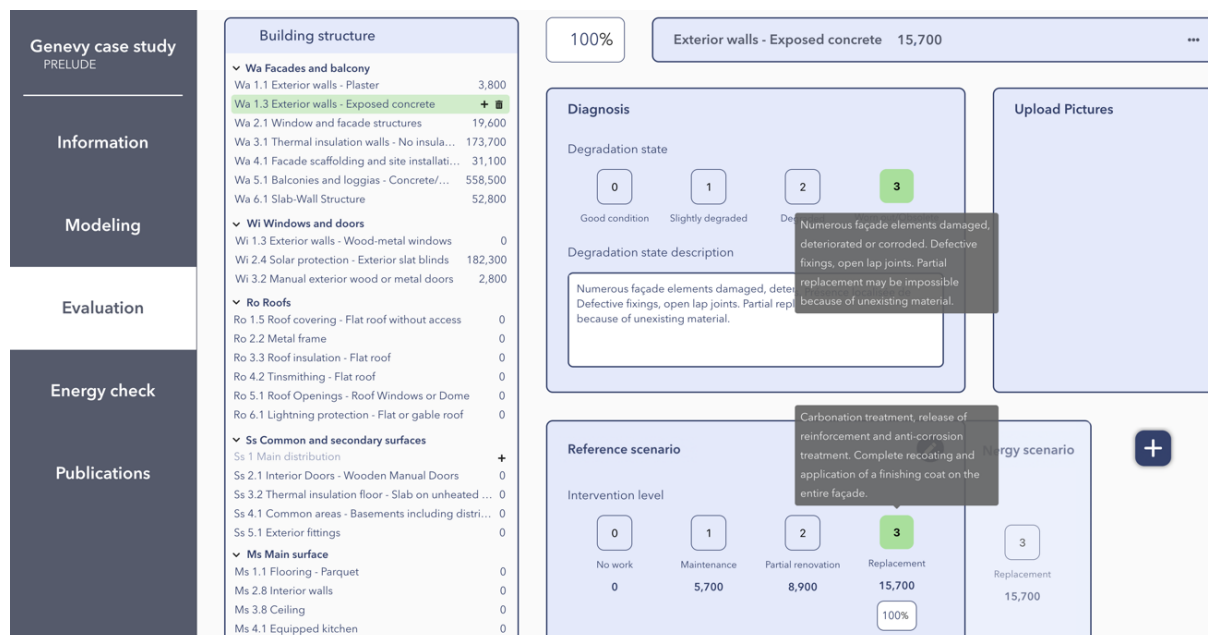


Figure 4 Evaluation tab with the building structure and descriptive texts

Works cost estimation					
EL	Electricity				33'400
	Element	Type	Degradation	Intervention	Cost (excl. tax)
1.1	Emergency lighting	Autonomous power supply	1		-
1.2	Lighting appliance	Lighting fixture	3		7 500
1.2	Electrical panel	Low power distribution	2		25 900

Figure 5: Example of EPIQR output (elements of the “Electricity” group).

6. Conclusion

The EPIQR diagnosis method is addressed to any person or organization involved in the renovation of buildings and helps owners in their decision-making scheme, by comparing different renovation scenarios with their corresponding costs, energy savings and CO2 emissions. The corresponding web-app, whose beta version is now available for residential buildings, was born out of the growing need to have access to IT tools or data from anywhere. Through the modernization of its graphical interface and the implementation of new functionalities, it also allows the expert to diagnose more easily and quickly and to have clearer results for the clients.

In addition to the already existing costs in the EPIQR+ database, namely the ones linked to the diagnosis of architectural (interior and exterior) and technical elements, a non-exhaustive list of expenses needed to make a building smarter have been included in the EPIQR web-app, hence participating in the development of the third renovation strategy set by the European Union through the “Energy Performance of Buildings Directive”. 17 new actions corresponding to the implementation of smart systems were added or updated. They have been selected both for their conformity with the EPIQR method and for their market representation.

Future work will concern in priority the continuity of the development of the EPIQR web-app through, among other things, the diagnosis of other building types as well as the verification of the new costs and CO2 emissions with in particular the data available from the PRELUDE project. EPIQR assessments of test buildings are needed to validate the new interface and its overall costs in different European location.

7. References

- [1] Wikipédia, 2021. *Méthode EPIQR*.
Available at: https://fr.wikipedia.org/wiki/M%C3%A9thode_EPIQR
- [2] Epiqr-Rénovation, s.d. *EPIQR+ Diagnostic et calcul des coûts de rénovation*.
Available at: <https://www.epiqrplus.ch/>
- [3] OFEN, O. f. d. l., s.d. Statistiques de l'énergie solaire, année de référence 2020., s.l.: s.n.
- [4] BKW, 2021. *Les pompes à chaleur: un avantage pour le climat comme pour les propriétaires*.
<https://www.bkw.ch/fr/les-pompes-a-chaleur-un-avantage-pour-le-climat-comme-pour-les-proprietaires>
- [5] TCS, 2020. *Un bon nombre de bornes de recharge en Suisse*. [Online]
<https://www.tcs.ch/fr/tests-conseils/conseils/mobilite-electrique/infrastructure-recharge-suisse.php>
- [6] OFS, O. f. d. l. s., 2022. *Indice des prix de la construction*.
<https://www.bfs.admin.ch/bfs/fr/home/statistiques/prix/prix-construction/indice-prix-construction.html>
- [7] Dumas N., de Kerchove d'Exaerde T, Paule B. Updated EPIQR platform, WP2 : Streamlining data collection Processes, PRELUDE project.



Aalborg Universitet

AALBORG UNIVERSITY
DENMARK

HAMSTER Test Facility – Features and future Potential of a unique bi-climatic Chamber

Vereecken, Evy; Prignon, Martin; Tilmans, Antoine; Mets, Timo De

DOI (link to publication from Publisher):
[10.54337/aau541620389](https://doi.org/10.54337/aau541620389)

[Link to publication from Aalborg University](#)

Citation for published version (APA):
Vereecken, E., Prignon, M., Tilmans, A., & Mets, T. D. (2023). HAMSTER Test Facility – Features and future Potential of a unique bi-climatic Chamber. In H. Johra (Ed.), *NSB 2023 - Book of Technical Papers: 13th Nordic Symposium on Building Physics* (Vol. 13). [253] Department of the Built Environment, Aalborg University. <https://doi.org/10.54337/aau541620389>

HAMSTER Test Facility – Features and future Potential of a unique bi-climatic Chamber

Evy Vereecken, Martin Prignon, Antoine Tilmans, Timo De Mets

Buildwise, Dieudonné Lefèvrestraat 17, 1020 Brussels, Belgium

*Corresponding author – Evy.Vereecken@buildwise.be

Abstract. The HAMSTER project (2016-2022) aimed at designing, building, and validating a bi-climatic chamber. The test facility developed within the project, called the HAMSTER test facility, is a recent versatile bi-climatic chamber that is made to study the dynamic heat, air and moisture performance of building components of realistic size. The hot chamber is furthermore thoughtfully designed to conduct accurate stationary thermal transmittance tests according to the standards. Realistic climatic conditions, like rain, sun, and pressure differences, can be reproduced in the cold chamber so that many different tests can be performed using HAMSTER. After 6 years facing numerous challenges, this new testing facility has been installed at the Buildwise laboratory in Brussels, Belgium.

1. Introduction and background

Buildings are responsible for around 40% of the energy consumption and 36% of the greenhouse gas emissions in Europe [1]. To reach carbon-neutrality by 2050, one of the ambitious goals set out in the European Green Deal, buildings should be constructed or renovated energy efficiently. Additionally, durable building components should be provided. No damage patterns may be induced by improving the energy efficiency. In this respect, the assessment of heat, air and moisture (HAM) transfer in building components is fundamental.

To study the hygrothermal performance of building components, numerical and experimental modeling can be applied. Numerical modeling offers a lot of potential, as it allows the investigation of thousands of varieties in respect to the building component's assembly and its material properties, the boundary conditions, the initial conditions, etc. [2][3]. A major drawback of this numerical approach is however the risk of neglecting important phenomena, resulting in a deviation between numerical output and practice [4]. Hence, experimental studies are indispensable in research on HAM transfer in building components. Experimental work can consist out of field measurements, studying the building components under real boundary conditions. However, a study of well-specified phenomena is often difficult in such field measurements, as e.g. outdoor climatic conditions are difficult or not controllable. Often, this also leads to a long time span needed for the measurements, due to for instance inadequate boundary conditions for the specified test; for instance, a lack of heavy rain loads, winter conditions that are not severe enough for the phenomenon that is studied, etc. To overcome these issues, laboratory measurements can come in handy, as it allows well-specified and controlled boundary conditions. From this perspective, within the HAMSTER project (2016-2022) a unique and versatile bi-climatic chamber, called HAMSTER, has been designed and built [5].

This paper first presents the HAMSTER test facility and its innovative features. Next, a concise overview of the scheduled validation campaign is given, and future research projects using the HAMSTER test facility are described. Ultimately, a conclusion is drawn.

2. The HAMSTER test facility

The bi-climatic chamber, called HAMSTER (acronym for “Heat, Air and Moisture Specialised Test facility for building Elements of Real size”), consists of a hot box, a cold box and a test frame (figure 1a) in which building components (a.o. walls, windows) with real dimensions (up to 3 m high and 3m wide) can be mounted to be analysed. Three standard test frames with a depth of 0,6 m (figure 1b) and two extended test frames with a depth of 1,5 m (figure 1c) are available. By connecting the extended test frames and a standard test frame to each other, an assembled test frame with a depth of 3,6 m can be achieved. This way, also building nodes and roofs can be analysed with the HAMSTER test facility.

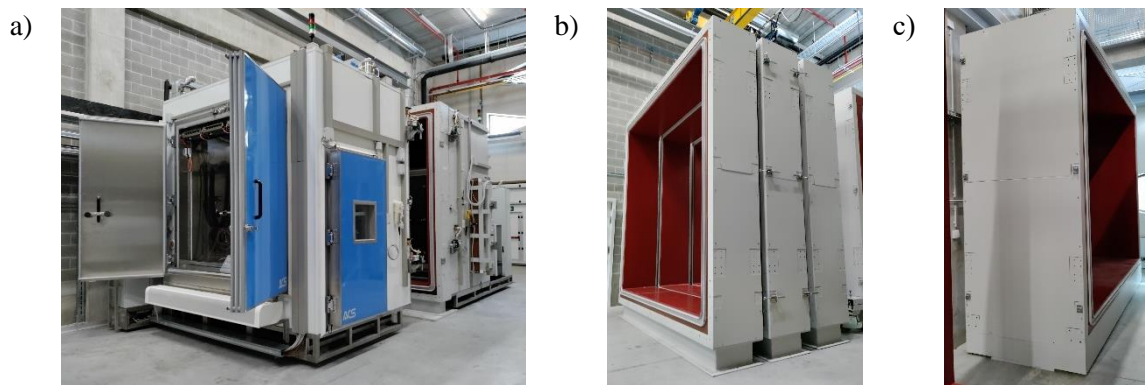


Figure 1. a) HAMSTER test facility, b) standard test frames, c) one of the extended test frames.

The HAMSTER test facility makes U-value measurements possible by use of both the guarded hot box (using the stand-alone metering box, see figure 2a) and the wall-calibrated hot box method, as described in ISO 8990 [6]. The air flow near the test component's surfaces, and thus the heat transfer coefficients, can be regulated by use of fans and by regulating the position of a baffle at both sides of the test component (figure 2b).

To perform hygrothermal studies, dynamic temperature and relative humidity conditions can be imposed in both boxes. In the cold box, infrared lamps enable simulating solar radiation. These infrared lamps are positioned on a tiltable frame (figure 2c), enabling also measurements on (pitched) roofs. The real solar spectrum cannot be replicated with the current test facility. Though, the back wall of the cold box consists of a glazed section, made from high transmittance glass (figure 1a). When desirable, an artificial solar simulator could be purchased at a later stage and placed externally in front of this glazed section. When not using such a solar simulator, the glazed section will be protected by closing the external doors at the back wall of the cold box. To simulate a rain load, rain can be imposed to the test component by use of automatic spray nozzles mounted on a movable beam. Uniform rain distribution over (parts of) the test sample can be imposed. The movable beam can furthermore be provided with, for instance, thermocouples or relative humidity sensors to scan the test component's spatial surface temperature and relative humidity. In hygrothermal studies, also an air pressure difference over the test sample can be imposed to simulate calm to strong wind conditions; though, the intention of the test setup is not to provide extreme conditions or to perform standardized tests on watertightness of building components.

Finally, the airtightness of the test samples can be measured prior to a hot box-cold box experiment. Thereto, an airtightness box (figure 2d) can be connected to the test frame with the test component, and a pressure difference can be imposed.

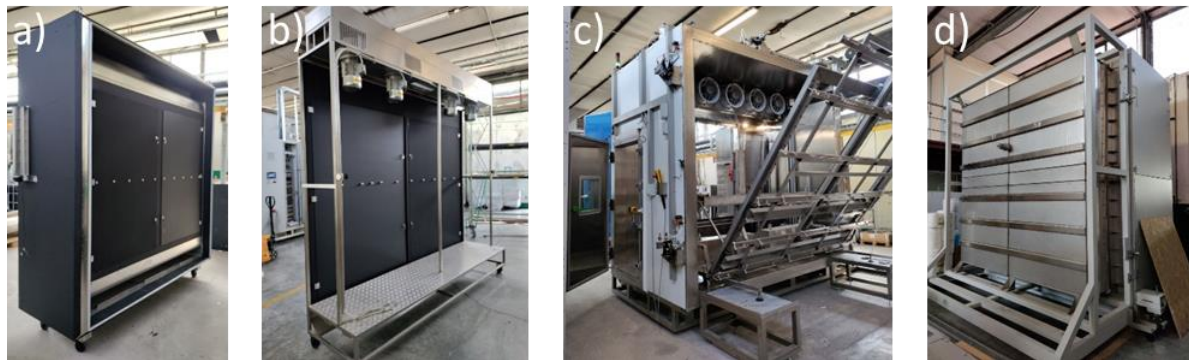


Figure 2. a) metering box, b) baffle, c) tiltable frame for infrared lamps, d) airtightness box.

An overview of the technical specification of the HAMSTER test facility, as requested from the supplier, is given in Figure 3. To achieve a good measurement accuracy, a number of actions have been taken. For instance, the walls of the hot box are provided with an active electrical guard. A thermopile installed across the walls of the hot box measures any temperature difference. By use of heating pads, temperature differences are cancelled, and thus a potential heat flow from the hot box to the laboratory environment is avoided. Furthermore, to restrict air losses induced by the many sensor wires, a flexible sealing solution for cable penetrations is applied.

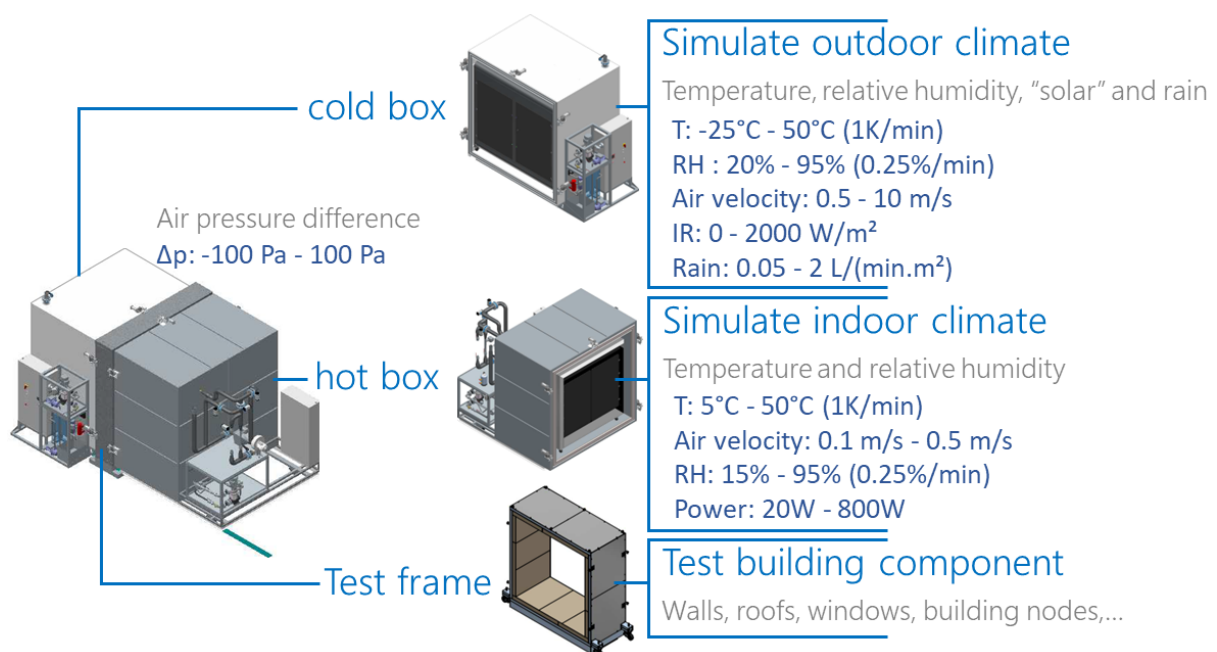


Figure 3. Technical specifications of the HAMSTER test facility, as requested from the supplier.

The HAMSTER test facility can be controlled via a constructor control system. The control system is open, so that an external control system (based on LabView for example) can be used to enable the signal acquisition from the sensors used for the monitoring of the test component and the environment in the bi-climatic chamber. Additionally, the external control system can read the inputs and outputs of the constructor control system and is able to take control of certain control loops.

3. Validation campaign

A validation campaign has currently started in order to check if the requested specifications (Figure 3) are met. In the validation campaign, first the airtightness of the hot box, cold box, test frames and stand-alone metering box has been measured by use of the airtightness box. Other validation tests in this campaign will consist of a.o. a theoretical uncertainty calculation of the power measurements in the hot box and cold box, testing the temperature and humidity ranges and its dynamic performances, analysing the capability of the air conditioning system to providing the specified power, temperature and relative humidity stability, verifying the accessible air speed range and the uniformity of the air speed profile. In the hot box and metering box, also the operation of the thermopile and the electrical guard will be verified. Finally, the operation of the water spraying system will be tested by verifying the variation in the water flow rate, the water temperature stability and the spatial uniformity.

4. Future projects

After the validation and calibration of the HAMSTER test setup, the test setup will be used within several research and development projects. The focus within these projects will be put on energetic challenges, both in the context of constructing new buildings and in the context of renovating our existing building stock, including heritage. Both the performance of innovative and traditional materials and systems will be studied within the projects. Furthermore, the HAMSTER test setup will be used to validate numerical models and other methodologies applied to optimise the design of building components. Two recently initiated projects will be briefly described in what follows.

A first project, called PERCHE, aims to facilitate the renovation process of wooden window frames in pre-war buildings in the Brussels region. The energetic renovation of these window frames is of paramount importance, as it offers a large potential to reduce the building's energy use and to improve the indoor comfort. Though, a possible renovation should reckon the preservation and upgrading of the architectural heritage. Within PERCHE, the HAMSTER test facility will be used to evaluate the thermal performance and the air- and watertightness for different renovation solutions for wooden window frames. A decision tree to choose the most appropriate intervention, taking into account the need for heritage preservation, will be developed.

A second project, OptHyWall, pursues the hygrothermal characterisation of materials and (layers of) building components (e.g. the diffusion resistance of a vapour barrier, the hygrothermal properties of an insulating rendering) as well the initial conditions, and this based on measurements in combination with inverse modelling. The HAMSTER test facility will be used to validate the standardised tools and optimisation techniques developed within the project for real building components. Moreover, within the project, an optimization of the hygrothermal design of building components is pursued.

A thorough scheduling of the different projects will be of huge importance in order to use the bi-climatic chamber in an efficient way and for several projects. Especially for hygrothermal measurements, often several months of testing are required. In this respect, future research will also focus on the definition of well-considered boundary conditions for the experiments, in such a way that the test periods can be shortened.

5. Difficulties

Designing and building a hot box-cold box is a challenging task. To reduce potential pitfalls and difficulties during the design and building process of the HAMSTER test facility, an extensive field study has taken place beforehand. Technical information on the existing hot box-cold box test setups is however often not publicly available. Therefore, several laboratories in possession of a hot box-cold box test facility have been consulted and visited. Though, the plenty and ambitious technical specifications pursued for the HAMSTER test facility still made it not possible to find a supplier familiar with all the necessary technical aspects. Therefore, it was decided to support the future supplier in the design process. For example, numerical simulations were conducted in order to assess the feasibility of the drafted specifications as well as the accuracy achieved for specific tests (e.g. U-

value tests). One specific technical point that required a lot of attention is the realisation of the airtightness of the boxes themselves. Given the many connections and wires and the necessity to be able to impose low air flow rates through the tested elements, a huge effort has been dedicated to reach the needed airtightness level. Apart from the technical challenges, logistical difficulties were encountered. The test facility was built and tested in Italy, after which the test facility had to be demounted to be transported to Brussels. In the Buildwise laboratory a thoughtful positioning was necessary in order to be able to get all the components of the HAMSTER test facility in the laboratory and to make a manipulation of the test frames and the test walls in between different measurements possible.

6. Conclusion

Within the HAMSTER project, a unique and versatile bi-climatic chamber has been designed and built. The test facility offers a full test battery to measure the heat, air and moisture performance of both building components with realistic dimensions and building nodes. Well-considered (controlled) boundary conditions, with inclusion of rain and solar radiation as well as air differences across the test sample, can be imposed. Currently, a validation of the test setup's features is going on. The actual commissioning of the HAMSTER test facility in research and development projects is scheduled for September 2023.

Acknowledgment

The HAMSTER project has been funded by the European Regional Development Fund and Innoviris (Brussels Region, Belgium). These financial supports are gratefully acknowledged.

References

- [1] European Commission 2020 Energy efficiency in buildings.-
https://commission.europa.eu/system/files/2020-03/in_focus_energy_efficiency_in_buildings_en.pdf
- [2] De Mets T, Tilmans A and Loncour X 2017 *Energy Procedia* **132**:753-758.
- [3] Vereecken E, Van Gelder L, Janssen H and Roels S 2018 *Energy Build* **89**:231-244.
- [4] Abuku M, Blocken B and Roels S 2009 *J Wind Eng Ind Aerodyn* **97**:197-207.
- [5] Daems D, Tilmans A, De Mets T and Loncour X 2020 E3 Web of Conferences 172, 19008.
- [6] ISO 8990:1994. Thermal insulation – Determination of steady-state thermal transmission properties – Calibrated guarded hot box.



Aalborg Universitet

AALBORG UNIVERSITY
DENMARK

Study of ventilated low-slope and large span wooden element roofs in the current and future climate

Sekki, Pauli; Saleva, Eero; Laamanen, Pekka

DOI (link to publication from Publisher):
[10.54337/aau541620957](https://doi.org/10.54337/aau541620957)

[Link to publication from Aalborg University](#)

Citation for published version (APA):

Sekki, P., Saleva, E., & Laamanen, P. (2023). Study of ventilated low-slope and large span wooden element roofs in the current and future climate. In H. Johra (Ed.), *NSB 2023 - Book of Technical Papers: 13th Nordic Symposium on Building Physics* (Vol. 13). [275] Department of the Built Environment, Aalborg University. <https://doi.org/10.54337/aau541620957>

Study of ventilated low-slope and large span wooden element roofs in the current and future climate

P Sekki¹, E Saleva¹ and P Laamanen¹

¹Afry Buildings Finland Oy, Espoo, Finland

E-mail: pauli.sekki@afry.fi

Abstract. Finland's building regulations and guidelines rely on ventilation to ensure the hygrothermal performance of structures. For wooden roofs, height of ventilation cavity and area of ventilation openings have been determined depending on roof slope and roof area in guideline. This causes difficulties in practical implementation in low-slope roofs with large span, because the guideline leads to large ventilation openings that can be challenging to be implemented. In practice, roof element suppliers have produced roofs with slightly smaller height of ventilation cavities and areas of ventilation openings. This study examined the hygrothermal behavior of the ventilated wooden roof, where the role of airtightness of vapor barrier and ventilation rate were investigated. The ventilation rates of the simulation model were set based on the results of long-term continuous measurement. First, to ensure the applicability of used model, the mold index calculated from measurements was compared to simulated with the design weather data. Next, hygrothermal behavior was evaluated based on mold index using the design climate data (current and future) for airtight and 'loose' structure with various ventilation rates. Results shows that focusing on airtightness is important. However, the larger ventilation rate has an unfavorable effect on mold index which is emphasized in future climate. Thus, revision of the design guidelines is proposed to restrict the ventilation openings and unnecessarily effective ventilation. In addition, air tightness guidelines should be set more precisely from the perspective of moisture safety.

1. Introduction

Examining the hygrothermal performance of structures with ventilated cavities is a complex problem at the theoretical level. Climate models have been developed to describe temperature, humidity and the radiation factors in building physic design years [1], so that hourly based simulation can be conducted. In practice, the simulation is simplified to a one-dimensional (1D) analysis and utilize a constant ventilation rate, because simulating the ventilation flow in the structure in two- or three-dimensional (2D/3D) is too laborious and the results are uncertain, often to unknown extent. When considering the structure itself, assumptions about airtightness and the possible wetting effect of an air leakage due to the overpressure is required. Thus, varied results are obtained in the sensitivity analysis of the studied structure, and based on the results, it has to be stated that the structure works under certain assumptions, which can be challenging to verify in practice. Furthermore, one has to consider whether the simulation has been able to assess the structure's hygrothermal performance sufficiently.

There has been some interest in studying the hygrothermal performance of ventilated structures in the Nordic countries. Ingebreetsen et al. presented a review of the recent studies of the ventilated roof and façade systems in Nordic climate [2]. The review states that several different factors have a great influence on ventilation ranging from the details of a structure to climatic factors such as temperature

and wind speed. The studies presented suggest recommended theoretical values for air change rate (ACH [1/h]) for the considered situations such as 20 1/h [3] and values applied in simulation for similar structures such as 30 1/h [4]. However, values presented in these studies cannot be directly applied for the evaluation of the ACH of the ventilation gap in studied large span roofs.

Finland's building regulations and guidelines rely on ventilation in the moisture safety of the roof structures. Especially for wooden roofs, the required height of the ventilation cavity and the areas of the ventilation openings have been determined precisely, depending on the roof slope and the roof area. The first guidelines for heat and moisture insulation of structures were given by Association of Civil Engineers RIL in 1948. Later, the primary guidebook - the RIL107 [5] *Guidelines for waterproofing and moisture insulation of buildings* (first edition in 1976) has been updated regularly. In the early stages only simple calculation instructions and principles for achieving a suitable hygrothermal performance were presented. In the edition of RIL107-1989, a guideline table corresponding to the current form was included with slightly different design values. The sources for the values are not presented in RIL107-1989, but Mikko Vahanen, who was the chairman of the committee for RIL107-1989, published the corresponding values in a self-published instruction booklet in 1985 and marked the sources as DIN 4108 and German flat roof guideline (Flachdachrichtlinie). Some minor changes to the original design values were introduced in editions 2000 and 2012. The values in the 2012 edition remain still in the current RIL107-2022. Table 1 shows the design values proposed in RIL107-1981 and RIL107-2022. Although the design values of the guidelines have been imported from Central Europe without a detailed study of its applicability, the guidelines still emphasize the experience-based idea of the importance of ventilation. FRAME [6] report in 2013 shows that a low ventilation rate of a roof (0.5-1 1/h) is advantageous in terms of hygrothermal performance, based on the current and future climate at that time. Nevertheless, the report recommends that ventilation rate should not be limited, because the simulation does not include moisture sources that occur in real structures, such as moisture during construction, air leaks from the interior or rain leaks that require the 'adequate' ventilation.

In terms of the hygrothermal performance of ventilated structures, the airtightness of the vapor barrier has been identified as a significant factor, as Viljanen has summarized [3]. This is taken into account in the Finnish guidelines [5], stating that maximum air infiltration must be less than 4 (q_{50} [$\text{m}^3/(\text{m}^2\text{h})$]) and the recommendation is 1. It can be concluded that the 'normal' q_{50} ranges from 1 to 4.

In Finnish requirements, it is stated that if the structure does not comply with the guidelines, a hygrothermal performance must be demonstrated. However, current requirements do not specify any methods that should be used [7]. The previous guidelines required a statement based on simulation or experimental tests of the hygrothermal performance [8]. In the recent guidelines, it is mentioned that there should be a study carried out by a research institute [5]. Regard to microbes, indications of damage are considered to be exceeding the action level, when the damage is on internal surfaces or in internal structures, or in other premises and structures from which the people inside may be exposed to the released pollutants [9]. However, in Finland there is still debate about what the criteria limits concerning for example the cold attics. Consequently, the criterion for the calculated mold growth index (MGI) allowed in the ventilation cavity of the roof is somewhat unclear.

Table 1. Design guidelines for ventilated roof cavities [5].

Slope		Minimum cavity height [mm]		Inlet opening [‰] from roof area		Outlet opening [‰] from roof area	
1989	2022	1989	2022 ^a	1989	2022	1989	2022
≤ 1:20	≤ 1:40	200	300	5.0	2.5	5.0	2.5
1:20-1:3	1:40-1:10	100	200	2.0	2.5	2.5	2.5
≥ 1:3	≥ 1:10	50	100	2.0	2.0	2.5	2.0

^a Minimum ventilation gap, taking into account thermal insulation deformations and work tolerances. On small roofs or parts of the roof, the ventilation gap can be smaller than the value in the table, if the inlet and outlet openings have a sufficient height difference (at least 500 mm) and the air flow distance in the ventilation gap is short (less than 3 m). Even then, the ventilation gap must be at least 50 mm on steep roofs (≥ 1:20), and at least 100 mm on slope ≤ 1:20.

This study investigates the hygrothermal performance of the low-slope with large span wooden element roof structure in two case buildings, in which the ventilation cavity and openings are clearly below the required values. Role of airtightness of vapor barrier and ventilation rate are studied to evaluate the current design guidelines. The study utilizes the results of experimental measurements and simulation. These experimental results are used to ensure the suitability of the simulation model, and to visually assess the condition of the structures. Finally, the hygrothermal performance is investigated based on the mold index using the current and future design climate data.

2. Material and methods

2.1. Investigated structure and measuring points

Case buildings were built 3-4 years ago. Schematic drawings of the roof plan, the section and the eaves details of the investigated buildings are presented in figure 1. Slope of the roof in both cases (a) and (b) is 1:40. Buildings are located in (a) Southern and (b) Southeastern Finland respectively. Ventilation is assumed from lower to upper eaves due to temperature difference [5]. Prevailing wind direction is south in both cases, however the prevailing wind direction (W) is in case (a) towards the main facade with upper eaves and in case (b) towards lower eaves.

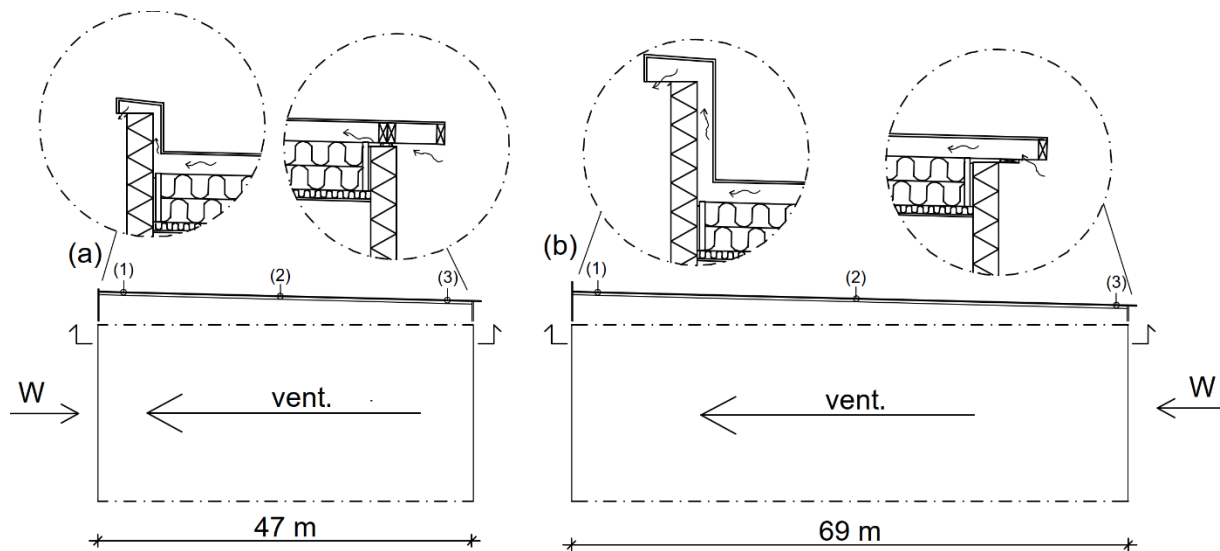


Figure 1. Schematic plan drawings of the investigated roofs (case a and b) and the sections showing measuring points (MP) 1-3. Vent. represents the assumed ventilation direction based on the slope.

According to guidelines, the minimum ventilation cavity height is 300 mm and inlet/outlet opening area 2.5 ‰ from roof area. In both cases, the guided values are not achieved. The cavity height of the structure is only 120 mm for both cases. In case (a) roof area is around 2735 m² and ventilation gap at lower and upper eaves 18 mm and 48 mm thus openings at lower and upper eaves are 0.4 ‰ and 1.0 ‰ from roof area (gap length ~ 60 m). Limited ventilation gap at lower eaves is due the fire regulations; Securo FB 36 mm fire break has been utilized. Conventional fiberglass insect nets (# 2 mm) on other eaves are used. In case (b) roof area is around 19222 m² and ventilation gap at lower and upper eaves 120 mm and 100 mm thus openings at lower and upper eaves are 1.7 ‰ and 1.5 ‰ from roof area (gap length ~ 280 m). Eaves are at height around (a) 6 to 7 and (b) 7 to 10 meters.

2.2. Experimental measurements

Measurements for T and RH was conducted using Vaisala's HUMIGAP HMP110 probes and Delta Ohm HD4V3TS2 Active Hotwire air speed transmitter (range 0.1...5.00 m/s). Devices were combined with

Mira's wireless DLS system. Instruments were installed into the ventilation cavity through the side of the beam of the adjacent cavity as presented in figure 2.

Outdoor T and RH were measured near the lower eaves of the case buildings. Also, the open weather data (T, RH and wind (w), later Ext. referring to external source of data) from weather station near the case buildings from [10] was utilized in the analysis. A visual inspection was performed during the installation of the measuring devices, and no indication of moisture damage was found.



Figure 2. Installation of the measuring devices and overview of the air cavity.

2.3. Simulation model

WUFI PRO 6 was applied for simulation, in which the heat and moisture transport processes are described by the coupled differential equations (1) and (2) [11].

$$\frac{\partial H}{\partial T} \frac{\partial T}{\partial t} = \frac{\partial}{\partial x} \left(\lambda \frac{\partial T}{\partial x} \right) + h_v \frac{\partial}{\partial x} \left(\frac{\delta}{\mu} \frac{\partial p}{\partial x} \right) \quad (1)$$

$$\rho_w \frac{\partial u}{\partial \phi} \frac{\partial \phi}{\partial t} = \frac{\partial}{\partial x} \left(\rho_w D_w \frac{\partial u}{\partial \phi} \frac{\partial \phi}{\partial t} \right) + \frac{\partial}{\partial x} \left(\frac{\delta}{\mu} \frac{\partial p}{\partial x} \right) \quad (2)$$

where H is enthalpy of moist building material [J/m^3], T temperature [K], λ thermal conductivity [W/mK], h_v evaporation enthalpy of water [J/kg], δ water vapor diffusion coefficient in air [$\text{kg}/(\text{msPa})$], μ vapor diffusion resistance factor of dry material [-], ρ_w density of water [kg/m^3], C_p specific heat [J/kgK], u water content [m^3/m^3], ϕ relative humidity [-], D_w liquid transport coefficient [m^2/s] and p water vapor partial pressure [Pa].

Structure layers and materials used for the simulation of the case buildings are shown in table 2, in which the properties of utilized materials are also listed. Material values are obtained from the WUFI database, except bituminous felt.

Table 2. Material layers and hygrothermal properties.

Layer	Material	Thickness [mm]	λ [W/(mK)]	ρ [kg/m ³]	C_p [J/kg]	μ [-]	DWS/DWW ^a [m ² /s]
1	Bituminous felt	2x3	0.23	1100	1000	50000	0
3	OSB3 board	18	0.105	595	1400	165	3e-10/3e-11
4	Ventilation cavity	120	0.723	1.3	1000	0.11	0
5	Mineral wool	330	0.037	30	840	1	0
6	Vapour barrier PE	0.2 ^b	2.3	130	2300	40000	0
7	Mineral wool	48	0.037	30	840	1	0
8	Gypsum board	13	0.2	850	850	8.3	4.5e-6/1e-6

^a DWS = D_w for suction and DWW = D_w for redistribution which are depended on the water content

^b 1 mm in model

Design climate data for heat and moisture simulation in current (Jokioinen 2011) and future (Jokioinen RCP85-2080) climate [12] is applied as exterior boundary condition. Interior boundary conditions are set to 21 °C and relative humidity varies according to the humidity and temperature (T_e) of the outdoor air, so that the moisture excess Δv is 5 g/m³ when $T_e \leq 5$ °C and 2 g/m³ when $T_e \geq 15$ °C (intermediate values are interpolated). The heat transfer coefficient inside and outside of the structure were 0.125 and 0.0588 [m²·K/W], respectively. In addition, the mode “Explicit Radiation Balance” was applied and pre-selected values for “Roofing, bituminous felt” was utilized. Ventilation cavity is modelled using Air Layer 120 mm; without additional moisture capacity from WUFI material database. Additional 1 mm thick layers are used in cavity boundaries using Air Layer 120 mm; with additional moisture capacity as a buffer material (no ventilation). Ventilation is modelled as a WUFI feature called “Air change source” [11], in which a long-term continuous measurements were used to assess the range of ventilation rates. The effect of air leakage was taken into account by utilizing moisture source term “Air Infiltration model IBP” in WUFI with stack height of 8 m and overpressure of 10 Pa for whole insulation layer (5). The sealing solutions for the joints of studied element roofs are highly developed. Thus, q_{50} of 1 or less are usually achieved in the buildings with considered roof element type. To ensure the applicability of the used model, the MGI calculated from measurements was compared to simulated with the design weather data. Also, the boundary conditions were compared based on the MGI. The mold growth index was estimated applying the Finnish mold growth model [13]. The analysis is based on MGI comparison because MGI combines T and RH into single comparable numerical value. Parameter for mold sensitivity class MSC1 (sensitive) was applied to ventilation cavity which corresponds to OSB in WUFI Mould Index VTT [14].

Differences between the current and the future climate was studied in the three years period for airtight (q_{50} of 1) and 'loose' (q_{50} of 4) structure with various ventilation rates from theoretical minimum 0.5 to 25.

3. Results and discussion

3.1. Experimental

The average results and estimated ACH of measuring period is presented in table 3. The velocity in case (a) is partially below the measurement range of the device, which slightly reduces reliability especially in MP 2. Flow measurement from all three points would also have been desired. However, the results show the effect of prevailing wind direction indicating increase in absolute humidity [g/m³] (AH) in windward side. The ACH of case (b) is more effective and thus a greater effect on the temperature is observed at the lower eaves, while in case (a) the temperature of the ventilation gap is more uniform.

Table 3. Average results from measuring points.

Case: MP	v [m/s]	ACH ^{a, b} [1/h]	T [°C]	RH [%RH]	AH [g/m ³]
a: 1	0.153	7.9-11.9	13.9	62	7.09
a: 2	0.08	4.1-6.2	14.3	54	6.44
a: 3	-	-	13.7	53	6.25
b: 1	0.43	14.6-21.9	13.7	63.6	6.95
b: 2	0.45	15.3-22.9	13.2	61.8	6.72
b: 3	-	-	11.4	68.5	7.13

^a ACH = v [m/h]*ventilation cavity cross section area/ventilation cavity volume

^b Measured v is concerned to be v_{max} . Depending on the flow intensity the average v_{avg} is somewhat lower. Lower limit is set based on fully developed laminar flow between two parallel plates $v_{avg} = 2/3 * v_{max}$

Numerous factors from measurement data can be observed that affect the hygrothermal performance of the roof. As an example of the effect, the wind direction in the summertime is presented in figure 3. Arrow (1) shows the effect of the wind on temperature during sunny day; T decreases on the windward side. In case (a) the arrow (2) shows that the AH at MP3 follows exterior AH when the wind is towards to upper eaves, and at the same time the AH in MP1 is at lower level. This indicates that the part of the ACH in windward side can be assumed to be the ‘pumping’ effect of uneven air flow on eave, which,

however, does not generate flow through the ventilation cavity. When the wind is towards to lower eave the AH in MP3 is at the same level or only slightly above MP1 and MP2, however below the exterior AH as shown with arrow (3). This demonstrates that the ACH is minimal, but the ventilation air flow passes through the cavity from lower to upper eave. Similar findings were discovered in case (b). However, the differences in AH between measuring points were found to be minor comparing to case (a).

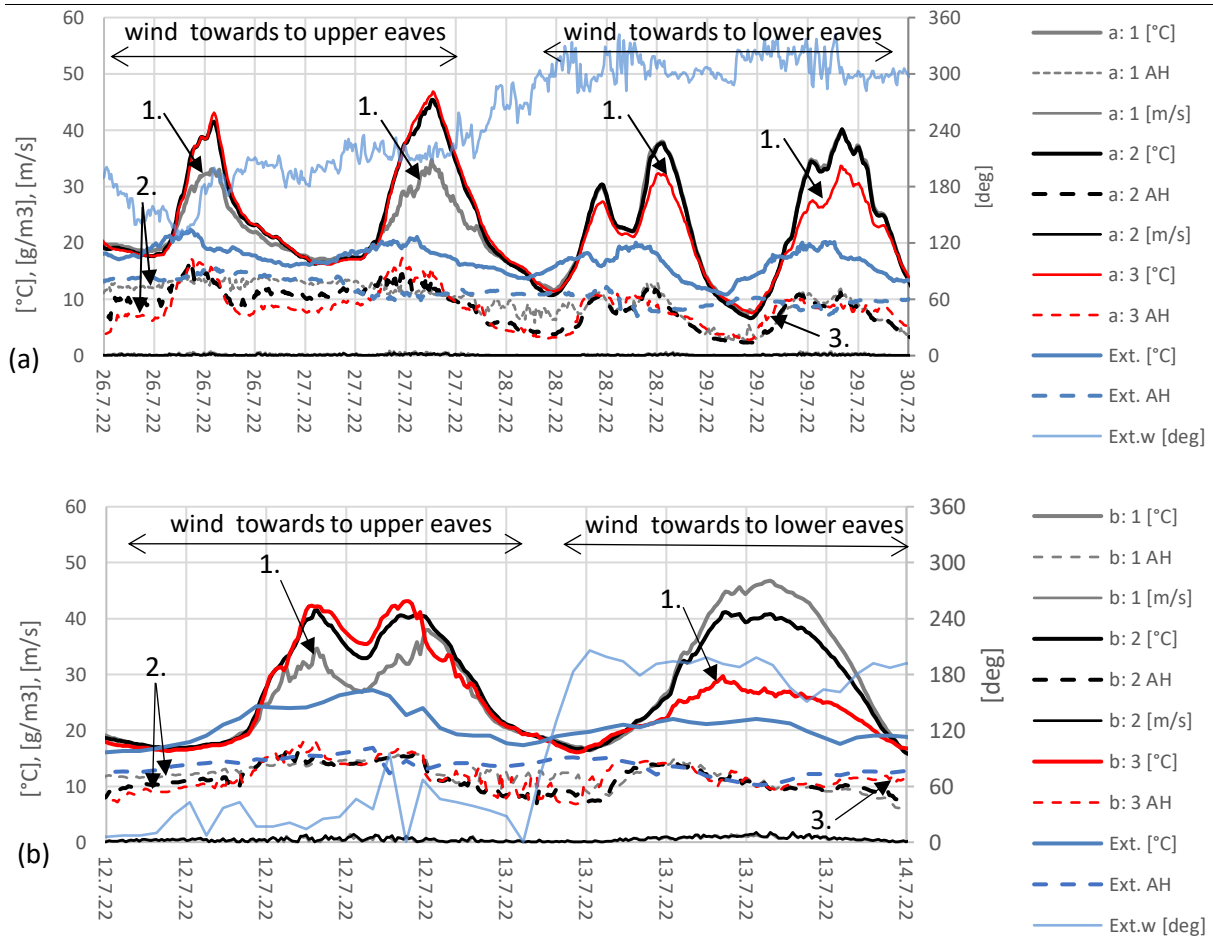


Figure 3. Results in case (a) and (b). a:1, a:2, a:3 and b:1, b:2, b:3 is referring to measurement points in the setup shown in figure 1. Ext. refers the data from weather station.

In addition, an interest finding from the results that is in relation to temperature variation was observed. Results shows the increasing effect of the daytime temperature rise on the air velocity. Moreover, the AH of the air in the ventilation cavity increases significantly due to temperature rise. On the other hand, the AH decreases below the outdoor air AH at night when the temperature decreases. These observed changes in AH clearly originate from the temperature dependence of the sorption of building materials; Increasing T in material causes moisture release into the ventilation cavity and, correspondingly, the cold material absorbs moisture. Considering the hygrothermal analysis, WUFI model does not take into account the temperature dependence of the sorption of materials. However, the temperature dependency of sorption of wooden materials is widely studied [15] and there are presented simulation models to investigate temperature dependence of sorption in structural level e.g. [16]. Therefore, taking temperature dependence into consideration in the simulations would be an interest for further studies.

3.2. Computational analyse

The applicability of used model is assessed in figure 4. Comparison of the MGI between continuous measurements and model are shown in figure 4 (a). In case (a), the measured ventilation rates correspond to the values ACH 5 and 10 and the MGI values for MP a:1 and a:2 correspond to the results of the model respectively. Regarding point a:3, the ventilation rate is unknown. Since the potentials causing the ventilation air flow the temperature difference and the wind are affecting to opposite directions, the ventilation is assumed to be ‘pumping’ and highly dependent on the wind. In this case the effect of the wind increases the ACH at the upper eave and decreases at the lower eave. Based on the measurements and assumption of the ventilation behavior, it can be estimated that the ACH is slightly lower in MP a:3 than in MP a:1 and a:2. Referring to this assumption, lowest MGI in MP a:3 is consistent. Case b represents almost an ideal implementation of the building and the ventilated roof, such that the temperature difference and the wind are affecting to same direction. Therefore, the ventilation rate is higher and consistent between MP b:1 and b:2. The measured ventilation rates of case b correspond to the value ACH 20. Air velocity was not measured in the windward eave in MP b:3, but ACH is assumed being at least same as in MP b:1 and b:2. The AH difference in measuring points is minor. However, the ventilation causes decrease in temperature near the lower eave and therefore causes higher MGI in MP b:3. Figure 4 (b) presents the comparison of the boundary conditions which shows that the measured conditions are slightly less challenging than the design climate.

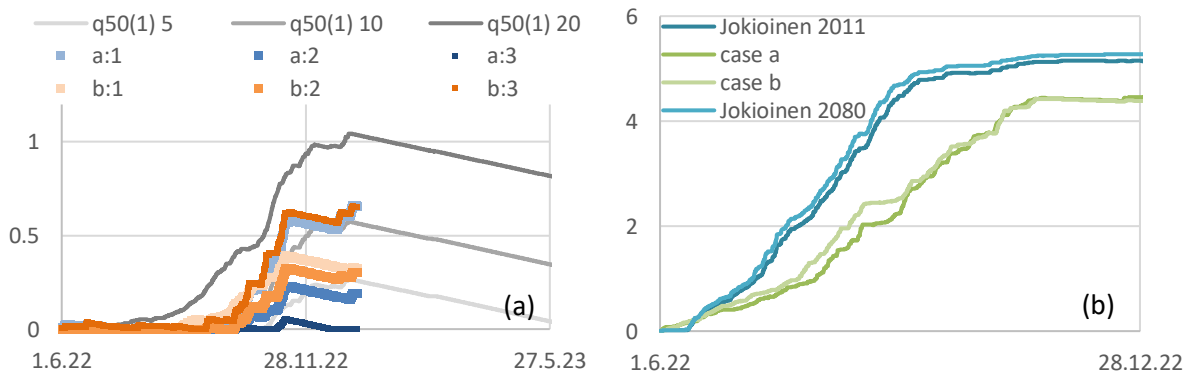


Figure 4. (a) MGI in ventilation cavity based on experimental (points, referring to figure 1) and based on simulation (lines) in which q50 refers to q_{50} and number in brackets to the rate and second number to ventilation rate [1/h]. (b) Calculated MGI based on design climate / weather data (exterior air).

It can be concluded that in case (b) when the structure is well and consistent ventilated the result of the model is slightly more critical than the experimental results. On the other hand, in the case (a) with lower ACH, especially near the eaves on the windward side, the situation can be more critical in practice. Nevertheless, the MGI results corresponds in magnitude to visual observation that no mold was detected in the inspection, as $MGI < 3$ indicates mold growth visible only under a microscope [13]. Thus, the simulation model with design climate boundary conditions gives a promising estimate of the hygrothermal performance of the structure.

In the analysis of hygrothermal performance of the structure in current and future climate, the effect of airtightness and ventilation rate was studied. Results in the current climate condition are shown in figure 5, which indicates that higher ventilation rate and more ‘loose’ case produce increase in the MGI. The preferred situation is obtained with $q_{50} = 4$ if ACH is 5 and with $q_{50} = 1$ if ACH ranges from 0.5 to 10.

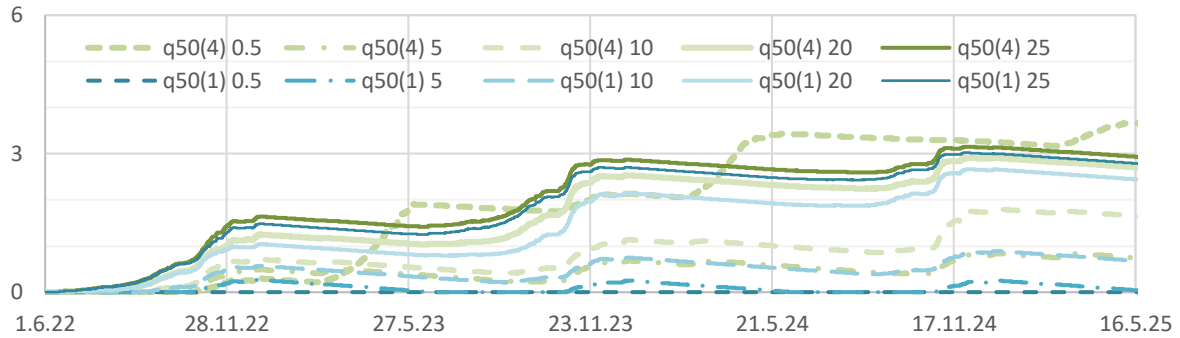


Figure 5. MGI with different q_{50} (1 and 4) and ventilation rates (0.5 to 25).

Figure 6 shows the results in the future climate condition. The results are more radical and show that, according to the utilized scenario, the structure must be airtight, and no significant ventilation should be allowed. The optimal solution would be an airtight structure with $q_{50} \leq 1$ and a very limited theoretical ACH of 0.5 1/h.

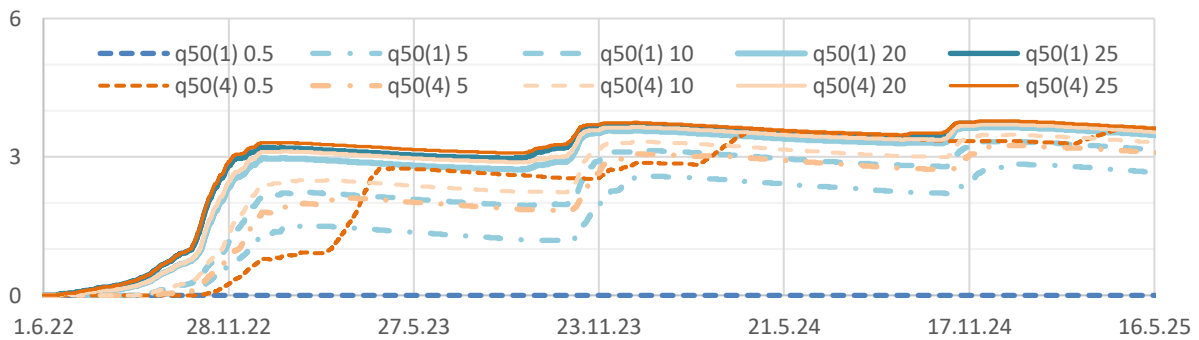


Figure 6. MGI in future climate. MGI with different q_{50} (1 and 4) and ventilation rates (0.5 to 25).

Examining the MGI is a straightforward method to evaluate hygrothermal performance of structures. However, acceptable limit of the MGI is still uncertain in the long-term analysis. Thus, setting the criterion for MGI as low as < 1 that [6] suggests may be too critical for ventilated roof cavities, when the fact that the cavity is connected to the outside air but outside of the air barrier is taken into account. MGI results using the design climate data was in the range of 0.5-3, when corresponding values of the investigated cases were utilized ($q_{50} = 1$ and ACH = 5-20). In our opinion, the MGI criterion that should be aimed for in design could be $MGI < 3$, so that the results at the end of the period is no longer increasing. However, this puts the recommendation of conducting hygrothermal behavior by using the future climate conditions [1] in a difficult question, because our results for the MGI in future climate were mainly around 3-4 and still rising ($q_{50} = 1$ and ACH = 0.5 as an exception). This finding suggest that only very minor ACH is acceptable in future climate.

Measurements show that the ventilation rate in the cavity might vary especially if openings are restricted. Thus, the effect of different ACH can be studied as a computational sensitivity analysis if measured values are not available. However, estimating the magnitude of the ACH can be difficult, thus measurements are recommended, though measuring the ACH can be challenging for several roof types. In these cases, the field investigations including T/RH measurements might be more reliable for ensuring hygrothermal performance, compared to a computational analysis.

With the examined roof type, sufficient ventilation was achieved in terms of hygrothermal performance, even though the ventilation openings were significantly smaller than in the guidelines. The MGI results also indicates that ventilation gap could be beneficial to constrict on the windward side.

4. Conclusions

The hygrothermal performance of the low-slope with large span wooden element roof structure were studied. The current design guidelines for airtightness and ventilation were evaluated based on experimental and computational study.

The Finnish design guidelines for roof ventilation have so far mostly emphasized the need for vigorous ventilation, regardless of the fact that the roof absorbs moisture from ventilation air in certain seasons. The results of the computational study show that the higher ventilation rate has an unfavorable effect on the mold index which is emphasized in future climate, and focusing on airtightness is important for ensuring the hygrothermal performance. Thus, revision of the design guidelines is proposed to rather restrict the ventilation openings and unnecessarily effective ventilation. In addition, air tightness required in the design guidelines should be set more precisely considering the moisture safety.

The results show that the examined roof elements can be built with significantly smaller ventilation gaps and ventilation cavity height than those required in guidelines, however, what are the more adequate design values of the ventilation gaps and cavities are worth further study. Experimental results show that the practical challenge is the site-specific microclimate differences, which are affected by the prevailing wind directions, as well as the shape and size of the ventilation gaps. Thus, it is necessary to conduct further field studies for assisting the revision of guidelines, in which the effect of these parameters on actual ventilation rate should be examined, in addition to the temperature and relative humidity in air cavity.

Acknowledgement

The experimental arrangements and the measurement data have been implemented with funding from Lapwall Oy. The author would like to thank Iina Maso and Yishu Niu for language editing and proofreading.

References

- [1] Laukkarinen A et. al. 2022 *Climatic design conditions for the heat and moisture behaviour of building envelope structures and summer-time cooling need of buildings – Final report of the RAMI project [in Finnish]* Tampere University Civil Engineering Research report 3
- [2] Ingebreten A B Andenæs E and Kvande T 2022 Microclimate of Air Cavities in Ventilated Roof and Façade Systems in Nordic Climates *Bldg* **12(5)** 683
- [3] Viljanen K, Lu X and Puttonen J 2021 Hygrothermal performance of highly insulated external walls subjected to indoor air exfiltration *J. Build. Phys.* **45(1)** 67-110
- [4] Mundt-Petersen S and Harderup L-E 2015 Predicting hygrothermal performance in cold roofs using a 1D transient heat and moisture calculation tool *Build Environ* **90** 215-231
- [5] RIL107 Editions 1976-2022 *Guidelines for water and moisture insulation of buildings* [in Finnish] Association of Civil Engineers RIL Finland
- [6] Vinha J et. al. 2013 *Effects of climate change and increasing of thermal insulation on moisture performance of envelope assemblies and energy consumption of buildings (FRAME)* Tampere University of Technology Research report 159
- [7] *Government Decree on the moisture-technical functionality of buildings 782/2017* [in Finnish] www.finlex.fi
- [8] *C2 RakMK 1998 Moisture, regulations and guidelines* www.finlex.fi
- [9] *RT 103528 Moisture and microbial damage to the building. General* [in Finnish] Rakennustietosäätiö RTS sr 2023
- [10] Finnish meteorological institute <https://www.ilmatieteenlaitos.fi/havaintojen-lataus#!/>
- [11] WUFI Pro 6.5 online help
- [12] Tampere University Building Physics Research Group <https://research.tuni.fi/rakennusfysiikka/kosteusanalysointimenetelma/rakennusfysikaaliset-mitoitusvuodet-2022/>
- [13] Tampere University Building Physics Research Group <https://research.tuni.fi/rakennusfysiikka/suomalainen-homemalli/>

- [14] WUFI applications <https://wufi.de/en/2017/03/31/wufi-mould-index-vtt/>
- [15] Zelinka SL, Glass S V and Thybring E E 2020 Evaluation of previous measurements of water vapor sorption in wood at multiple temperatures *Wood Sci Technol* **54** 769–786 <https://doi.org/10.1007/s00226-020-01195-0>
- [16] Colinart T, Glouannec P, Bendouma M and Chauvelon P 2017 Temperature dependence of sorption isotherm of hygroscopic building materials. Part 2: Influence on hygrothermal behavior of hemp concrete *Energy Build.* **151(1)** 42-51



Aalborg Universitet

AALBORG UNIVERSITY
DENMARK

Modelling hygrothermal performance of wood assemblies exposed to fungi growth

Roy, Camille ; Derome, Dominique; Frenette, Caroline

DOI (link to publication from Publisher):
[10.54337/aau541621854](https://doi.org/10.54337/aau541621854)

[Link to publication from Aalborg University](#)

Citation for published version (APA):
Roy, C., Derome, D., & Frenette, C. (2023). Modelling hygrothermal performance of wood assemblies exposed to fungi growth. In H. Johra (Ed.), *NSB 2023 - Book of Technical Papers: 13th Nordic Symposium on Building Physics* (Vol. 13). [277] Department of the Built Environment, Aalborg University.
<https://doi.org/10.54337/aau541621854>

Modelling hygrothermal performance of wood assemblies exposed to fungi growth

Camille Roy¹, Dominique Derome¹, Caroline Frenette²

¹University of Sherbrooke, Civil and Building Engineering Department, Sherbrooke, QC J1K 2R1, Canada

²Cecobois, Quebec City, QC G1V 4P1, Canada

camille.roy6@usherbrooke.ca

dominique.derome@usherbrooke.ca

caroline.frenette@cecobois.com

Abstract. This research project aims to document the spread of the biodegradation in wood-frame buildings and, more specifically, to investigate the aggravating impact of the presence of the rotting fungus *Serpula lacrymans* in wood-based materials on the hygrothermal performance of wood-framed wall and floor assemblies. The proposed methodology is to calibrate a hygrothermal model of wood contaminated by varying stages of *S. lacrymans*. The *S. lacrymans* has a particular ability compared to other fungi in that it can move its water source to seek nutrients. Hyphen cords have been seen on brick and concrete elements, as a bypass mean to reach wood. Thus, this fungus is modelled with two means: modified hygrothermal properties and addition of parallel paths for moisture transfer in the assemblies. To develop these, characterizing healthy and contaminated wood is necessary to be used as input in the models. The simulations are performed for residential building envelope assemblies under current and future climatic conditions.

1. Introduction

Some wood-destroying fungi are increasingly present in Canada, and particularly in Quebec, and this increase seems to coincide with climate change. This is the case for the *Serpula lacrymans* fungus, known to be a type of dry rot. Reports of wood-framed assemblies exposed to this fungus growth are increasing.

Upon the discovery that a building is contaminated by *S. lacrymans*, two interventions can be done, either decontamination or demolition and both solutions are necessarily expensive. It is therefore relevant to deepen the knowledge on the spread of the fungus to help identify the extent of the problem adequately in each situation and, by the same token, limit the financial and technical impacts for owners. Thus, hygrothermal simulations are used to assess the situation and offer owners a better basis for deciding whether to demolish or renovate. Avoiding demolition by carrying out decontamination would allow owners to reduce the expenses related to the loss of their residence and reduce the trauma associated with it [1]. Moreover, avoiding demolition would contribute, in certain cases, to the conservation of architectural heritage.

Some research on the development of *S. lacrymans* in buildings has been conducted in Europe. This information can hardly be applied to Quebec, since the wood species, building systems and construction techniques, and climatic conditions are different from those of Europe [2]. Studies that simulate the

growth of fungi in wooden structures will generally do so from clear wood and from regarding better designed new constructions [3], [4]. This research project differs since it is aimed at existing buildings, and the simulations aim to ascertain different degrees of wood contamination.

The goal of this project is to develop an understanding of the behaviour and spread of *S. lacrymans* in wood-framed building assemblies in Quebec, Canada, to assess what damage the fungus will cause under different environmental conditions. Since *S. lacrymans* has been known to be found in crawlspaces [5], different scenarios of insulation, ventilation and water sources are simulated. The characterization of hygrothermal properties and structural resistance of wood samples affected to different degrees by *S. lacrymans* in Quebec's historical and future climatic contexts will undoubtedly contribute to increasing the local scientific knowledge on this subject. Figure 1 shows images of contaminated conditions.

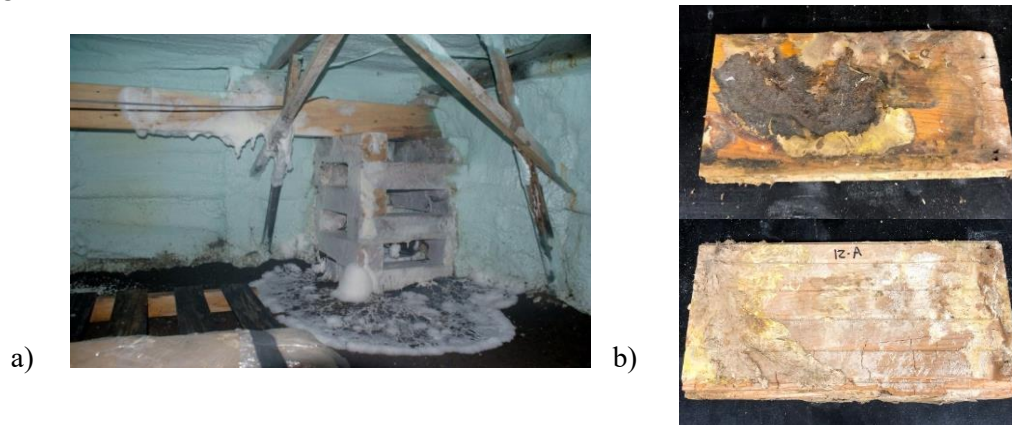


Figure 1. Contaminated conditions: a) contamination after energy retrofit intervention b) contaminated floor samples.

2. Methodology

2.1 Characterization of materials

Samples of contaminated wood, collected directly from affected residences spread over the Quebec territory, are experimentally characterized. The properties of the characterized wood are then used as input in the simulations. The wood species studied are pine, spruce, and fir. The three wood species are the most common in residential construction in Quebec [6].

Measurements on the samples include density, porosity, water vapor permeability, water vapor sorption, capillary water absorption, and water content at capillary saturation. These properties are needed to simulate the fungus-affected materials directly in the investigation software. The water transport capabilities of the fungus will be integrated into the model, which requires the development of a new approach. Amongst characterization, dry density of the samples is determined by the ratio of their dry mass to their dry volume.

Pore volume is equal to the total volume of a sample from which the matrix volume is subtracted. The matrix volume is determined by the quotient of the dry mass of a sample over the density of the wood cell walls. The value of matrix density used in this study is 1533 kg/m^3 [7].

The water vapor permeability of the samples is measured experimentally using permeability cell (wet cup/dry cup), here aluminum container of 100 mm x 100 mm cross section, water, desiccant or saline solutions to control relative humidity in the cell. The cell is covered with a slice of wood. The perimeter of the sample is sealed with bee wax to allow moisture to flow only in one direction. The cell is exposed to an environment with a different relative humidity than the one inside. The change in mass of the cell over time gives a flux for a permeable material considering its area and thickness as installed on the cell.

Water vapor sorption isotherm is acquired through a series of seven desiccators, with water, desiccant, or saline solutions to control relative humidity and using the mass for samples at

equilibrium with environments of varying relative humidities. Capillary water uptake coefficient, A_{cap} , is measured by imbibition. All three grain directions are tested for all samples. The water content at capillary saturation, w_{cap} , is obtained when the mass values have stopped increasing drastically and the plot they form as a function of time flattens.

A particular behaviour of the *S. lacrymans* compared to other fungi is its ability to transfer water from its source to dry areas to seek nutrients. Hyphen cords have been seen on brick and concrete elements, as a bypass means to reach wood. Thus, this fungus is modelled with two means: modified hygrothermal properties, as described above, and with the addition of parallel paths for moisture transfer in the assemblies. Work on this latter aspect is on-going.

In addition, with the aim of obtaining damage indicators, mechanical strength tests are also performed to obtain comparative data on the structural capacity of wood at different levels of contamination. Bending tests are conducted on clear wood samples to obtain a bending modulus.

This work is ongoing. To date, five houses have provided wood samples and another six are under material procurement. Most characterisation is underway. An overview of all acquired results will be presented at the conference.

2.2 Assemblies

The simulations are performed for residential wood-framed building envelope assemblies. Wall assemblies are selected based on observations of the documented contamination cases, using construction methods characteristics of the 1945-1975 period. The typical assembly consists of a low concrete foundation wall or crawl space, supporting a wood-framed wall. The wall has a brick cladding and a gypsum interior and is insulated with mineral wool and tar kraft paper that serves as a vapour barrier. The wood floor considered in this project is constituted of joists, plywood floor sheathing, subfloor planks and vinyl flooring. A visual representation of this assembly is shown in Figure 2. The bottom of this shallow crawlspace is often drenched earth, sometimes covered with a thin concrete slab on grade. Four crawlspace conditions are simulated: flooded crawlspace, water leak, ventilated and unventilated crawlspace.

Four scenarios of crawlspace insulation are considered. The first scenario considers no insulation, the second scenario considers an insulated foundation wall, the third considers insulation under the floor plywood sheathing between joists, and the fourth is an all-insulated crawlspace, which considers an insulated foundation wall and insulation under the floor. The three types of insulation used for crawlspace are expanded polystyrene, mineral wool, and sprayed urethane. Assemblies and materials are shown in Table 1.

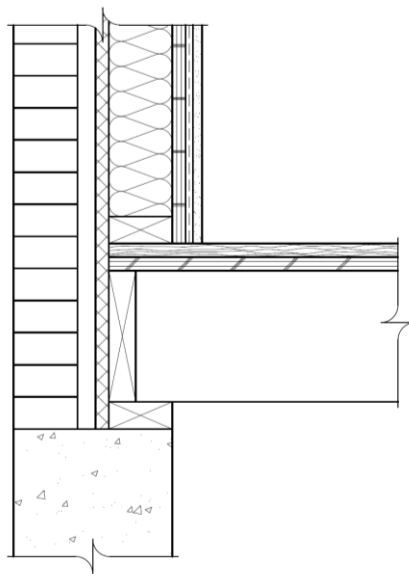


Figure 2. Assembly detail

Table 1. Composition of the assemblies modelled

Wall Assemblies	Layers
Wall	Gypsum board / Wooden laths / Tar Kraft paper / Mineral wool / Wood studs / Wall sheathing / Air gap / Brick cladding
Foundation wall	Concrete
Floor	Subfloor planks / Plywood sheathing / Wood joists
Variants	No insulation / Insulated floor / Insulated foundation wall / Insulated floor and foundation wall

2.3 Simulation

2.3.1 Simulation Set-Up. The hygrothermal simulations of the building envelope assemblies use the Delphin software. Delphin is a software that simulates coupled heat, moisture, and matter transport in porous building materials, and can be used to evaluate hygrothermal problems, such as condensation, mould growth risks and wood decay damage [8].

2.3.2 Outdoor Climate. The climates of eight different cities in the province of Quebec are used in the simulations. These cities were chosen according to the available climate data and to cover the targeted territory. Current conditions are modelled with a reference year based on the past 30 years of hourly weather data [9]. The parameters used to choose the reference year are temperature, relative humidity, and precipitations. The Intergovernmental Panel for Climate Change (IPCC) has studied climatic change with several possible future emissions scenarios. As a result of the IPCC sixth Assessment Report (AR6) [10], five scenarios, based on how quickly greenhouse gas emissions are lowered, are stated. The calculations for the scenarios also consider socioeconomic changes such as population, urban density, wealth, land use and education. A pessimistic and an optimistic scenario, based on the IPCC recommendations, are used to model future climatic conditions. The most optimistic scenario is the SSP1-1.9 where global CO₂ emissions are down to net zero around 2050 to hit 1.5°C above preindustrial temperatures and decrease to 1.4°C by 2100. The pessimistic scenario is the SSP5-8.5 where current emissions levels double by 2050 and by 2100, the average global temperature is 4.4°C higher [10].

2.3.3 Indoor and crawlspace conditions. In addition to outdoor climatic conditions, indoor climate loads must be considered. ASHRAE 160 [11] provides tables of temperature and relative humidity for the indoor climate as a function of the outdoor temperature. Since the literature specific to indoor climatic conditions in a crawlspace in Quebec is scarce, research has been extended to Northern Europe. The work of Vanhoutteghem et al. [12] shows that the changes of temperature in Denmark takes the form of a sinusoidal function with a positive peak in summer and a negative peak in winter. Another approach based on equations is used by Laukkanen and Vinha for southern Finland [13]. This approach is also a sine function that considers the annual average outdoor temperature, the temperature amplitude of a year and time. Using climate data from the cities targeted by this study in Quebec, a sine function, similar to those described for Denmark and Finland, can be plotted to define the indoor climate of the crawlspaces. As mentioned above, four crawl spaces conditions are simulated: flooded crawlspace, water leak, ventilated and unventilated crawlspace.

2.3.4 Development of a new simulation approach. As mentioned, *S. lacrymans* modifies the properties of the wood it degrades and transfers liquid water from the water source through the wood-based components. Current methods for estimating wood damage caused by decay are developed for generic types of rot. To take into account the particular behaviour of *S. lacrymans*, the simulations will be run with step changes where the physical properties of the wood will be changed gradually to tend towards

the properties measured experimentally. Additionally, to simulate the water pumped by the fungus, a layer of waterlogged porous material that represents *S. lacrymans* will be added during the step changes, according to the growth rate of the fungus, as well as point water sources.

2.4 Analysis

The post-processing of hygrothermal simulation results allows to evaluate the behaviour of the simulated elements. Thus, hygrothermal data can be used to evaluate the development of mould and decay in wood elements.

The model used to calculate the estimated wood damage caused by decay is the VTT model [14]. In order to predict the development of decay in wood, the progression of decay is evaluated by the loss of mass in the wooden components. The VTT model uses two processes. The first process is the activation process where an α parameter is defined as a function of relative air humidity (RH in %), air temperature (T in °C) and time (t in hour). The α parameter is dimensionless and varies between 0 and 1 where 1 is the initiation of mass loss. The α parameter varies with climate conditions and is calculated from the following equations (1, 2):

$$\alpha(t) = \int_0^t d\alpha = \sum_0^t (\Delta\alpha), \text{ where}$$

$$\Delta\alpha = \frac{\Delta t}{t_{crit}(RH, T)}, \quad \text{where } T > 0^\circ\text{C and } RH > 95\%$$

$$\Delta\alpha = -\frac{\Delta t}{17520} \text{ otherwise}$$

$$t_{crit}(RH, T) = \left[\frac{2,3T + 0,035RH - 0,024T \times RH}{-42,9 + 0,14T + 0,45RH} \right] \times 30 \times 24 \text{ [hour]} \quad (1)$$

The second process used for the calculation is mass loss (ML in %). When the α parameter has reached 1, mass loss begins. Unlike the activation process, the mass loss is irreversible and therefore, never decreases. It can be estimated as follows:

$$ML(t') = \int_{t \text{ at } \alpha=1}^{t'} \frac{ML(RH, T)}{dt} dt = \sum_{t \text{ at } \alpha=1}^{t'} \left(\frac{ML(RH, T)}{dt} \times \Delta t \right)$$

$$\frac{ML(RH, T)}{dt} = -5,96 \times 10^{-2} + 1,96 \times 10^{-4}T + 6,25 \times 10^{-4}RH \text{ [%/hour]} \quad (2)$$

Although this model was developed to estimate wood degradation in European wood species, it is applicable to estimate wood degradation in Quebec as an indicator [14]. The results of the mass loss calculation of the VTT method can be used indirectly to predict the loss of mechanical strength of the wood structural components over time. The VTT rot model is used as a basic approach for the growth and deterioration induced by rot fungi. When data becomes available, the growth pattern will be adjusted to fit *S. lacrymans*.

3. Results

The main output observed with this research is the mass loss occurring in structural elements of the assemblies simulated. As the mass loss is a function of temperature and relative humidity of the materials, a first simulation exercise is presented here looking at the order of magnitude of these two parameters. Table 2 presents the healthy and the contaminated wood properties used for the simulation. The values are an average of the properties measured on contaminated pine wood samples. As the specific heat (c_p) and conductivity (λ) are not characterized experimentally yet in this project, they stay the same in the simulation.

Table 2. Healthy and contaminated wood properties modelled

Base parameter	Healthy value	Contaminated value	Unit
ρ	554.3	339.4	kg/m ³
c_p	2775	2775	J/kgK
λ	0.208	0.208	W/mK
μ	4.54	3.00	-
W_{sat}	653.2	401.2	kg/m ³
W_{80}	72.0	44.2	kg/m ³
A_{cap}	0.02	0.04	kg/m ² s ^{1/2}
K_{leff}	7.4e-10	3.4e-09	s

Figure 3 shows the temperature variations over one year in the upper left corner of the pine joist over a non-insulated, non-ventilated crawlspace for historical climate. The temperature follows the same tendency for both healthy and contaminated wood. The average temperature of healthy wood stands at 11.01°C over a year and at 10.88°C for contaminated wood over the same period.

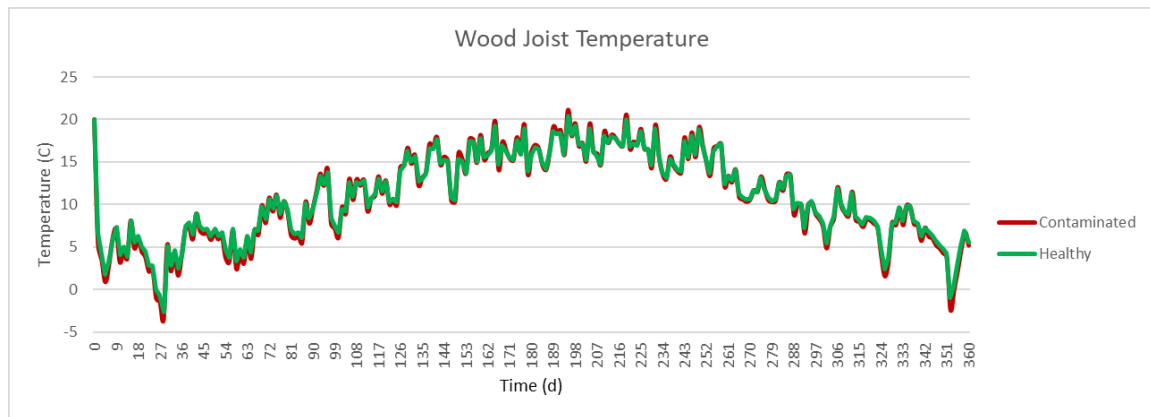


Figure 3. Temperature variation in pine joist for healthy and contaminated wood

Figure 4 presents the relative humidity at the same point in the joist. The contaminated wood seems to be more sensible to the environmental variations throughout the simulation. The healthy wood, however, has a higher and more stable relative humidity over the year.

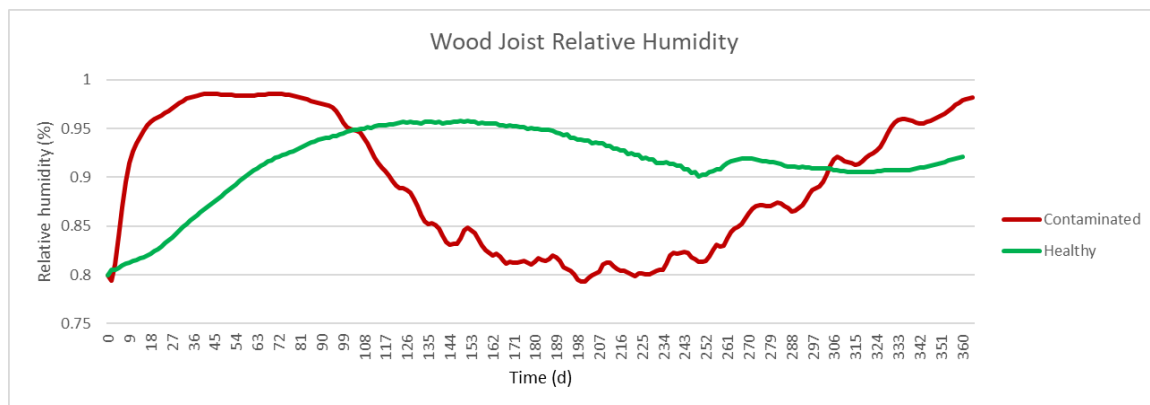


Figure 4. Relative humidity variation in pine joist for healthy and contaminated wood

4. Discussion and preliminary conclusion

This project aims to quantify how the hygrothermal behaviour of wooden structural components is affected by the spread of *S. lacrymans* in different climatic and environmental conditions. The preliminary results show that, although the temperature of the wooden material is not really affected by the change of hygric properties, the material has a different behaviour regarding relative humidity. On-going work includes more parametric simulation studies and completion of the property characterization campaign, which results will be updated in the conference presentation.

When it comes to severe cases of biodegradation, as seen in presence of *S. lacrymans*, this study aims at providing basic knowledge for more effective management of the problem.

References

- [1] Maltais D, Cherblanc J, and Malenfant A 2021 “La contamination de sa demeure par la mэрule pleureuse : vécu des propriétaires occupants et conséquences sur leur vie personnelle, conjugale, familiale, sociale et professionnelle et leur conception de leur chez-soi,” UQAC, Département des sciences humaines et sociales, Chicoutimi
- [2] Schmidt O 2007 “Indoor wood-decay basidiomycetes: damage, causal fungi, physiology, identification and characterization, prevention and control,” *Mycol. Prog.*, vol. **6**, no. 4, pp. 261–279
- [3] Brambilla A and Gasparri E 2021 “Mould Growth Models and Risk Assessment for Emerging Timber Envelopes in Australia: A Comparative Study,” *Buildings*, vol. **11**, no. 6, p. 15
- [4] Brischke C and Meyer-Veltrup L 2016 “Modelling timber decay caused by brown rot fungi,” *Mater. Struct.*, vol. **49**, no. 8, pp. 3281–3291
- [5] VanderGoot J 2017 “Considering Dry Rot: The Co-evolution of Buildings and *Serpula lacrymans*,” *J. Archit. Educ.*, vol. **71**, no. 2, pp. 225–231
- [6] Adpearance Inc. 2020 “SPF Wood Facts, Grades, Uses & Industry Insights | AIFP | PDX, OR,” *American International Forest Products*
- [7] Kollmann F F P and Côté W A 1968 *Principles of wood science and technology*, 1st ed. New York, NY: Springer Berlin
- [8] Bauklimatik-Dresden 2021 “DELPHIN,” <https://bauklimatik-dresden.de/delphin/index.php>
- [9] World Meteorological Organization (WMO) 2017 “WMO Guidelines on the Calculation of Climate Normals,” WMO, Geneva
- [10] IPCC 2022 “Climate Change 2022: Mitigation of Climate Change,” Cambridge University Press, Cambridge, UK and New York, NY, USA
- [11] ASHRAE Standing Standard Project Committee 160 2021 “Criteria for Moisture-Control Design Analysis in Buildings,” ASHRAE, Standard ANSI/ASHRAE Standard 160-2021
- [12] Vanhoutteghem L, Morelli M, and Sørensen L S 2017 “Can crawl space temperature and moisture conditions be calculated with a whole-building hygrothermal simulation tool?,” in *11th Nordic Symposium on Building Physics, NSB2017*, Trondheim, Norway, vol. **132**, pp. 688–693
- [13] Laukkanen A and Vinha J 2017 “Temperature and relative humidity measurements and data analysis of five crawl spaces,” in *11th Nordic Symposium on Building Physics, NSB2017, 11-14 June 2017, Trondheim, Norway* vol. **132**, pp. 711–716
- [14] Viitanen H *et al.* 2010 “Towards modelling of decay risk of wooden materials,” *Eur. J. Wood Wood Prod.*, vol. **68**, no. 3, pp. 303–313



Aalborg Universitet

AALBORG UNIVERSITY
DENMARK

Envelope systems with high solar reflectance by the inclusion of nanoparticles – an overview of the EnReflect Project

M M Ramos, Nuno; Maia, Joana ; Veloso, Rita Carvalho; Souza, Andrea Resende; Dias, Catarina ; Ventura, João

DOI (link to publication from Publisher):
[10.54337/aau541621982](https://doi.org/10.54337/aau541621982)

[Link to publication from Aalborg University](#)

Citation for published version (APA):

M M Ramos, N., Maia, J., Veloso, R. C., Souza, A. R., Dias, C., & Ventura, J. (2023). Envelope systems with high solar reflectance by the inclusion of nanoparticles – an overview of the EnReflect Project. In H. Johra (Ed.), *NSB 2023 - Book of Technical Papers: 13th Nordic Symposium on Building Physics* (Vol. 13). [282] Department of the Built Environment, Aalborg University. <https://doi.org/10.54337/aau541621982>

Envelope systems with high solar reflectance by the inclusion of nanoparticles – an overview of the EnReflect Project

Nuno M. M. Ramos^{1*}, Joana Maia¹, Rita Carvalho Veloso^{1,2}, Andrea Souza¹, Catarina Dias², and João Ventura²

¹ CONSTRUCT-LFC-Departamento de Engenharia Civil, Faculdade de Engenharia, Universidade do Porto, Rua Dr. Roberto Frias, 4200-465 Porto, Portugal

² IFIMUP –Departamento de Física e Astronomia, Faculdade de Ciências, Universidade do Porto, Rua do Campo Alegre s/n, 4169–007 Porto, Portugal

*Corresponding author: nmmr@fe.up.pt

Abstract. High reflectance materials constitute an attractive idea to reduce cooling loads, which is crucial for attaining the Nearly Zero Energy Buildings goal, also presenting the benefit of broadening the range of colours applicable in building facades. The EnReflect project intended to re-design envelope systems by increasing their solar reflectance through nanotechnology. The main idea was to produce novel nanomaterial-based coatings with high near-infrared (NIR) reflectance by tuning their optical properties and testing their compatibility with typical insulation technologies such as ETICS. As such, this project focused on the synthesis of nanoparticles with improved NIR reflectance, the evaluation of the hygrothermal-mechanical behaviour of thermal insulation systems with the application of the improved coating solutions, the characterization of the more relevant material properties and the durability assessment. One of the main achievements was the development of a facile synthesis of a nanocomposite with improved performance in the NIR region that allowed the reflectance improvement of a dark-finishing coating. Also, the incorporation of such nanoparticles had a positive effect on keeping their optical properties after accelerated ageing cycles. The development of numerical simulations allowed the estimation of the maximum surface temperature in Mediterranean climates under different optical parameters. The study of the hygrothermal behaviour of thermal-enhanced façades led to the development of a new durability assessment methodology which contributed to closing a standardization gap.

1. Introduction

The use of thermal insulation materials is an effective way of reducing heat losses in buildings by increasing the thermal transmittance through the building envelope. In addition, new eco-efficient materials and technologies are being developed to mitigate building cooling needs. One of those technologies uses cool materials with high solar reflectance and infrared emittance. The use of such materials, including nanosized cool pigments [1], constitutes an attractive idea to achieve the reduction of cooling loads, a goal that is a condition for attaining the Nearly Zero Energy Buildings goal. Another benefit of this strategy is to broaden the range of colours, overtaking the current white-cool solutions. The idea of the EnReflect project is outlined in Figure 1. The main idea was to fabricate novel nanomaterials with high near-infrared (NIR) reflectance by bandgap engineering to apply to typical envelope systems using a green synthesis approach. The improved performance in the field of Building

Physics was assessed through laboratory tests and advanced simulation. The durability aspects were evaluated through accelerated and natural ageing tests.

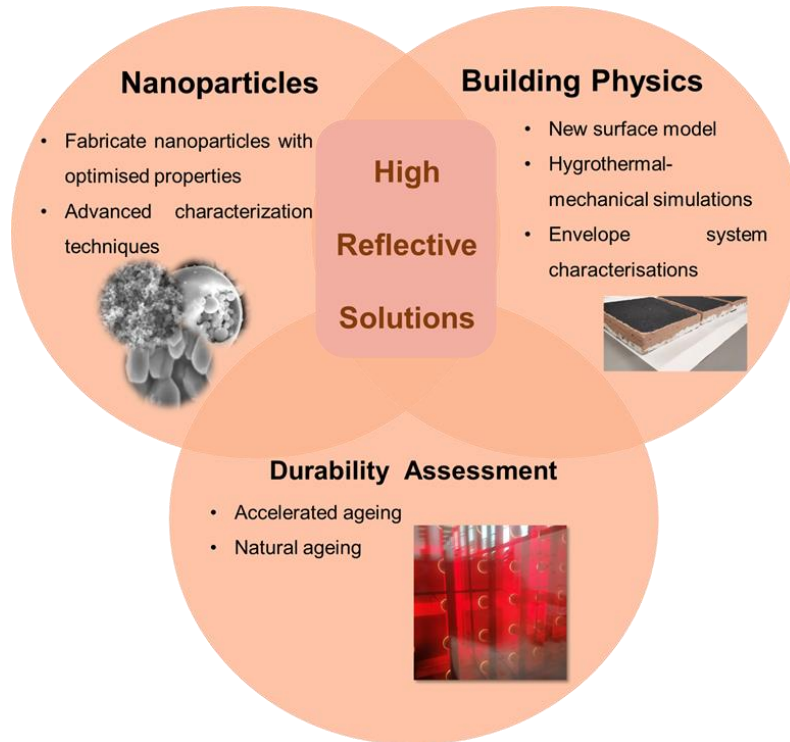


Figure 1. Outline of the EnReflect project.

2. Development and optimization of coatings doped with nanoparticles

This task aimed to develop and optimize the use of nanoparticles in black-coloured high-reflective coatings for envelope applications. Therefore, we fabricated and assessed the optical reflectivity of an extensive range of nanomaterials, including TiO₂ rutile and anatase (25, 40, 800 and 1000 nm), CuO (40 nm), ZnO, Al₂O₃ (13, 300, 1000 nm), black titania (self-doped Ti³⁺ titanium dioxide), black MnFeO₄, Ca₃Mn_{2-x}Ti_xO₇ and CuO@TiO₂ nanocomposites, for different concentrations (1 to 20%). The most promising results were achieved for the TiO₂ rutile and TiO₂/CuO samples. A typical spectral reflectance spectrum for the black colorant doped with 50 nm TiO₂ nanoparticles is shown in Figure 2. From the results, we observe that all the doped samples present a similar performance by partially absorbing visible light, as expected since we are dealing with black coatings. As for the near-infrared region, however, the samples present noteworthy differences. All the specimens show enhanced NIR reflectance when compared to the conventional colorant. The influence of the size and concentration of nanoparticles was also studied. Also, in Figure 2, the reflectance as a function of nanoparticle concentration is displayed, determined according to ASTM E903 [2].

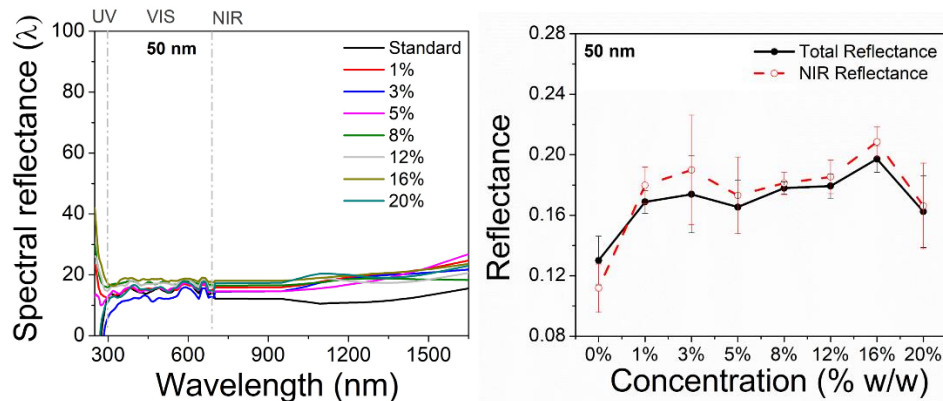


Figure 2. Spectral reflectance behavior for the TiO₂ doped black colorant with 50 nm and corresponding total average and NIR reflectance calculation using ASTM E903

3. Experimental assessment of high reflectance pigments effect

The project analyzed the influence of coatings using different types of high-reflectance pigments applied in ETICS. The experimental assessment of optical properties included: laboratory measurements with a modular spectrophotometer (FLAME-T and FLAME-NIR Ocean Optics) and *in-situ* measurements using a pyranometer (Figure 3). The two methods were compared, evidencing a good correlation, even in the specifically rough surface of ETICS (Figure 4).



Figure 3. Spectrophotometer and pyranometer measurements.

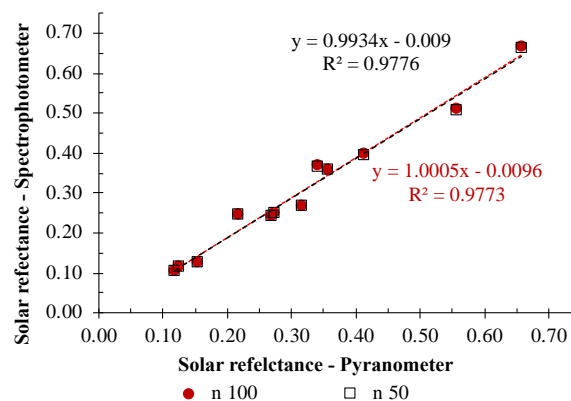


Figure 4. Correlation of the results of spectrophotometer and pyranometer methods.

4. Numerical simulations

The numerical simulations conducted in the project were divided into two parts. First, there was an assessment of the potential benefits of solar reflectance enhancement with nanomaterials. In that sense, the finite-difference time-domain (FDTD) method was implemented using MEEP to obtain an oversight

of the radiative properties of coatings pigmented with TiO₂ nanoparticles. The work [3] established limits for the reflectance dependence on particle size and particle volume fraction. In a second approach, the effect of different solar absorption levels on different wall compositions and climates was simulated using WUFI Pro software, which allowed assessing the impact on surface temperature, condensation potential, and average U-value [4]. Figure 5 and Figure 6 present the maximum exterior surface temperature and accumulate positive exterior condensation potential, respectively, considering different façade orientations (NSEW), two solar absorption coefficients (reflecting the dark and light colour effect) and three distinct climates (Porto – P, Nancy – N and Oslo – O) on the study of thermal rendering systems, using thermal renders (S1, S2 and S3), and external thermal insulation composite systems (ETICS).

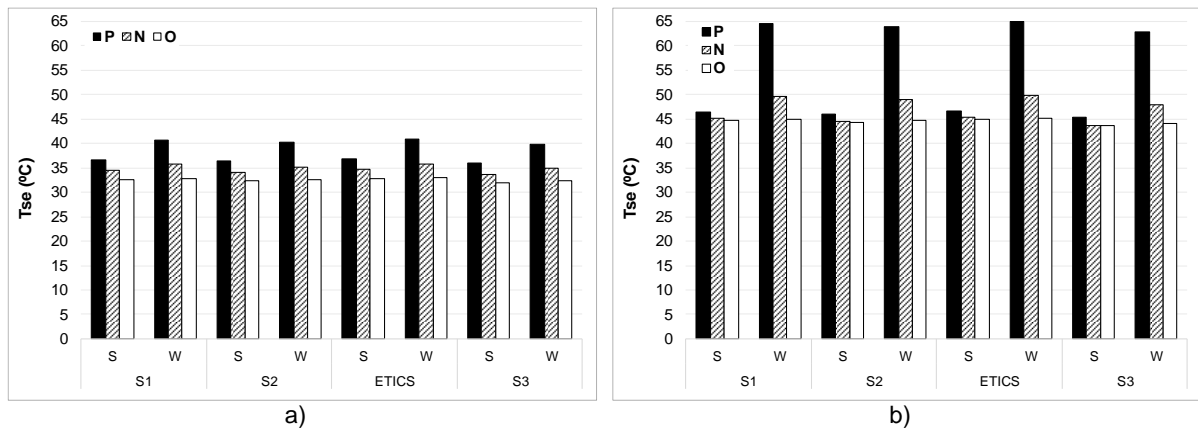


Figure 5. Maximum exterior surface temperature (Tse), considering south and west orientation and solar absorption of: a) 0.27 and b) 0.80.

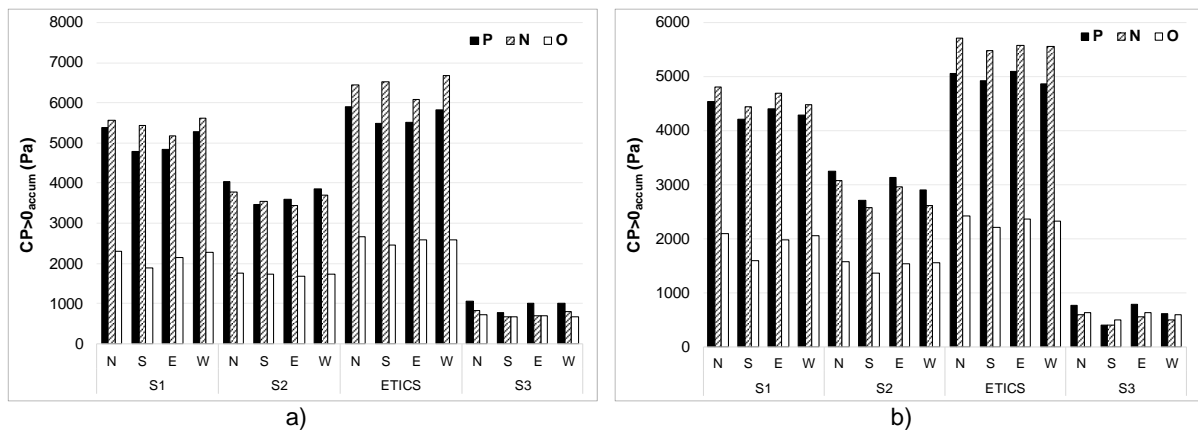


Figure 6. Accumulated positive condensation potential considering the 4 orientations (N, S, E, W) and solar absorption of: a) 0.27 and b) 0.80.

Beyond the properties of thermal insulation systems, the solar absorption coefficient significantly impacts hygrothermal behaviour because it contributes to reducing hygrothermal risk. However, it promotes an increase of thermal stresses, especially in warmer climates with high solar radiation, such as Porto. In contrast, for climates with low solar radiation, a high solar absorption coefficient constitutes a good way to increase hygrothermal performance.

5. Durability assessment

The durability assessment conducted in the project targeted different aspects of the performance of external insulation systems by applying coatings with high-reflectance pigments. The durability of coating formulations when applied in ETICS and thermal rendering systems was tested with laboratory and in-situ experiments. The tests highlighted the impact of incorporating NIR reflective pigments in finishing coatings [5], as they can contribute to the durability of their optical properties by reducing colour change and total reflectance loss (see Figure 7). It was also demonstrated how the peak surface temperatures were reduced, promoting an enhanced service life of the whole system.

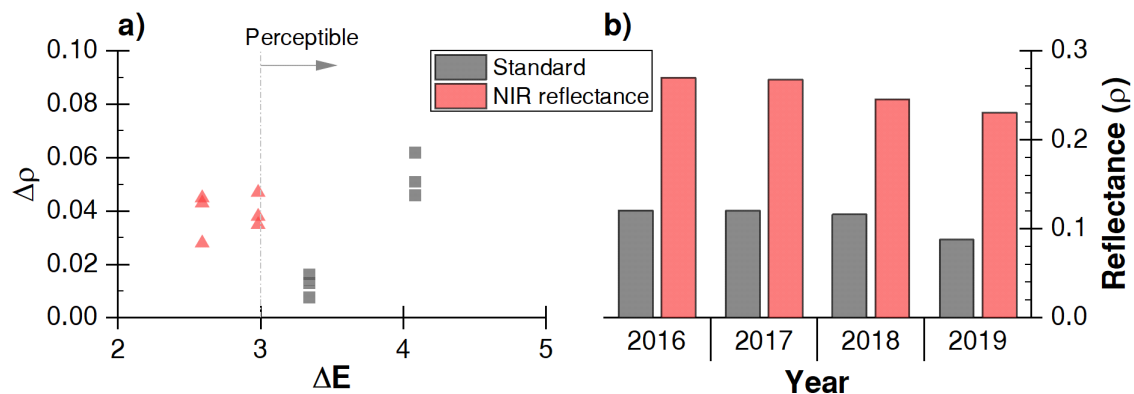


Figure 7. Influence of NIR reflectance pigments on a) colour difference (ΔE) and b) reflectance (ρ)

6. Conclusions

The EnReflect project produced new and relevant data about the fabrication and application of nanoparticles in finishing coatings for façades and their hygrothermal-mechanical behaviour and durability assessment. The work initiated in the project is ongoing as it inspired two PhD projects on the subject that will be completed by 2024.

Acknowledgements

This work was financially supported by: Project PTDC/ECI-CON/28766/2017—POCI-01-0145-FEDER-028766—funded by FEDER funds through COMPETE2020—Programa Operacional Competitividade e Internacionalização (POCI) and by national funds (PIDDAC) through FCT/MCTES and Base Funding—UIDB/04708/2020 of the CONSTRUCT—Instituto de I&D em Estruturas e Construções—funded by national funds through the FCT/MCTES (PIDDAC). R. C. Veloso and A. Souza would like to acknowledge the support of FCT—Fundação para a Ciência e Tecnologia for funding the doctoral grant SFRH/BD/148785/2019 and DFA/BD/8418/2020, respectively.

References

- [1] Veloso R C, Souza A, Maia J, Ramos N M M and Ventura J 2021 *Journal of Materials Science* **56** 19791-839
- [2] ASTM 2020 *Standard Test Method for Solar Absorptance, Reflectance, and Transmittance of Materials Using Integrating Spheres*. (ASTM International)
- [3] Dias C, Veloso R C, Maia J, Ramos N M M and Ventura J 2022 *Energy and Buildings* **271** 112296
- [4] Maia J, Ramos N M M and Veiga R 2018 *Building and Environment* **144** 437-49
- [5] Ramos N M M, Maia J, Souza A R, Almeida R M S F and Silva L 2021 **6** 79



Aalborg Universitet

AALBORG UNIVERSITY
DENMARK

Internal insulation: two condensed guidelines for beginners

Ruisinger, Ulrich; Sonntag, Heike

DOI (link to publication from Publisher):
[10.54337/aau541623517](https://doi.org/10.54337/aau541623517)

[Link to publication from Aalborg University](#)

Citation for published version (APA):
Ruisinger, U., & Sonntag, H. (2023). Internal insulation: two condensed guidelines for beginners. In H. Johra (Ed.), *NSB 2023 - Book of Technical Papers: 13th Nordic Symposium on Building Physics* (Vol. 13). [296] Department of the Built Environment, Aalborg University. <https://doi.org/10.54337/aau541623517>

Internal insulation: two condensed guidelines for beginners

Ruisinger, Ulrich and Sonntag, Heike

Institute for Building Climatology, TU Dresden, Germany

E-mail: ulrich.ruisinger@tu-dresden.de

Abstract. On the way to a reliable and large-scale application of internal insulation, clear and simple guidelines for building practitioners are needed, across all phases of refurbishment planning. Closing this gap was one objective of the “IN2EuroBuild”-project, completed in 2022. As a support in the planning process and for decision-making within the framework of the project, two comprehensive guides for the planning of internal insulation measures were developed. They guide users from the as-is analysis of the building (part one) to the renovation planning of the façade, the selection of suitable insulation systems and the verification and consideration of constructional details (part two). It describes the aspects to be considered during the entire process of planning and implementing an interior insulation measure.

Both parts of the guide are aimed at people who have little or no experience in the field of energy-efficient refurbishment and interior insulation, but who want to be informed and at least have a say. This group of people can include, for example, building owners, investors or public authority employees, but also architects or engineers who have rarely dealt with interior insulation and therefore do not know the various planning bases and dependencies in detail. The reader should be enabled to assess an issue and select a suitable interior insulation system in the numerous, unproblematic cases in which experts do not need to be consulted.

1. Introduction

In the past, there have been several projects and publications that are intended to support the renovation of old buildings by means of interior insulation. However, this has not been able to decisively increase the acceptance of and knowledge about interior insulation among the general public. Previous publications were often aimed at people with the appropriate prior technical knowledge ([1], [2]), as engineers, architects or specialists, or focused on specific sub-areas [3]. Other publications that are too extensive ([1] and [5]) have a deterrent effect, unfocused publications provide too little information [4]. In contrast, there is a lack of concise but nevertheless easily comprehensible information.

It was considered important to keep the size of the publication within reasonable limits in order to achieve greater acceptance by the target audience. That is why it was divided: The first part deals with the building analysis, the second part is about the planning of interior insulation measures. Another advantage is that at the end of each guide there are flowcharts illustrating the step-by-step processing of the required tasks. The boxes in the flowcharts are linked to the corresponding, explanatory sections in the text of the guideline which allows to quickly jump back and forth as needed. This ensures that important topics are not forgotten in the planning process.

2. Guideline 1: Building Analysis

A thorough investigation of the existing building is a necessary condition for a successful refurbishment. Therefore, the first part of the two guides concentrates on the condition analysis and assessment of buildings. In many buildings, unproblematic conditions are found, so that this analysis can be brief.

The explanations start from a simple level of knowledge and they only teach the necessary basics in order to understand and evaluate the general condition of a building. Readers should not be overwhelmed by the complexity or amount of information provided. However, there are also more complex conditions that cannot be assessed easily. In such cases, it is then explicitly recommended to consult experts.

The guideline first conveys the principles of how a building analysis is to be planned in advance. At the beginning, this means gathering and evaluating all possible information about the (construction) history of the building. These are often written sources such as plans, archive documents, expert opinions or invoices, but also oral sources such as users and house-keepers, both current and especially former.

The building assessment focuses on moisture damage, as this is the main cause of damage to buildings. Moreover, these are often easy to assess. Damage that affects the statics, for example, is more difficult to assess and may be even life-threatening, which is why it is not dealt with in these guidelines. Nevertheless, moisture damage can lead to structural damage e.g. in case that load-bearing timber structures are affected.

A two-stage procedure is proposed, in which the structural situation is basically recorded in the first stage. If damage is found, it is documented and provisionally assessed. In the case of damage, a second stage has usually proved useful and is therefore recommended. This involves a more detailed examination of the damage by various measuring methods and, if necessary, with the assistance of experts. These measuring methods are explained with their field of application, advantages and disadvantages.

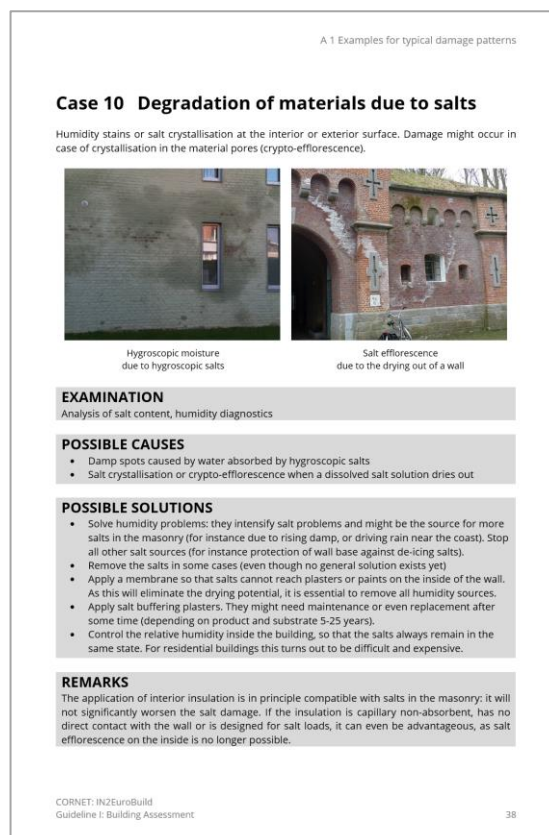


Figure 1. Example of a damage pattern explained in the appendix of the first guide (for better text recognition use the download link in chapter 4)

To provide the necessary basic knowledge, one chapter explains the basic types of possible moisture sources. It is followed by more exact descriptions of their manifold manifestations:

- how do they appear,
- what conditions are necessary (materials, wall constructions),
- what mechanisms lead to the destruction of building fabric?

The analysis part closes with a larger appendix that contains many pictures of damage examples or structural conditions that can favour damage (figure 1). It is necessary to show and explain these as readers might have low knowledge of damage patterns or are insecure. In this way, readers can see how the individual types of damage actually look in practice. Possible causes, reasonable examinations methods and solutions are briefly discussed for each example.

3. Guideline 2: Façade Renovation and Interior Insulation

The aim of the second part of the guideline was to develop clear, simple and reliable design rules for dealing with interior insulation that are applicable to a variety of situations with different wall constructions, different insulation systems and in different climatic regions. Here, all concerns related to the topic of "planning the interior insulation measure" are treated in an all-encompassing manner.

This improves the user's skills and controls in both design and execution; uncertainties associated with interior wall insulation are reduced. Thus, large-scale application of this methodology for building practitioners is enabled. The percentage of yearly renovated buildings as well as the amount of interior insulation used can thus be increased.

This second guide is divided into the following sections

- Façade renovation concept
- Insulation concept and
- Design of structural connection details

Users of the guide are directed step by step through the individual phases by working through all the complexes of topics relevant to them. In doing so, there is no danger that individual circumstances and requirements will be forgotten or insufficiently considered. Planning concepts can thus be created more quickly and easily, and any additional services that may be necessary can be scheduled in at an early stage and included in the cost planning. Simple procedures are described for the design of insulation systems in order to limit the number of cases in which complex numerical simulations are required.

Since the guide itself can seem quite extensive to the user due to its variety of possible scenarios, the supplementary creation of a clear flowchart (figure 2) created a convenient way to get all the necessary information and instructions that apply to the specific building in a very time-saving and clear way, without having to read the entire guide, but also not leaving out any important aspects. By linking the individual steps in the flowchart to the corresponding chapters in the guide, the relevant information and recommendations are always called up when they are needed. Clicking "Back" will take readers back to the flowchart (figure 3).

The flowchart is designed in such a way that there is a simple way for each situation, which is applicable for approx. 70% of all renovation cases. This processing method is marked in green (figure 2). In some cases, more or less extensive examinations or further verification are necessary to assess the construction during planning. In these situations, the user is guided through the yellow or even red paths.

3.1. Façade Renovation Concept

In the façade renovation concept section, general advice is given, e.g. how to deal with moisture loads, dense façade coatings, salt loads or exposed façade elements. Furthermore, drying measures and methods for creating functional sealing systems are described and the connection between interior insulation and driving rain protection as well as the resulting conclusions are explained. Depending on whether the building under consideration is a rendered or exposed brick façade, different necessary and

optional measures and examinations are described in order to obtain a driving rain-proof façade as a basic prerequisite for the application of interior insulation. In the case of rendered façades, this is easy to achieve in most cases. In the case of exposed brick façades, more extensive renovation measures are often required. This ranges from advice on cleaning the façade, crack and joint repair, criteria for material replacement to possible façade coatings and impregnations to ensure protection against driving rain.

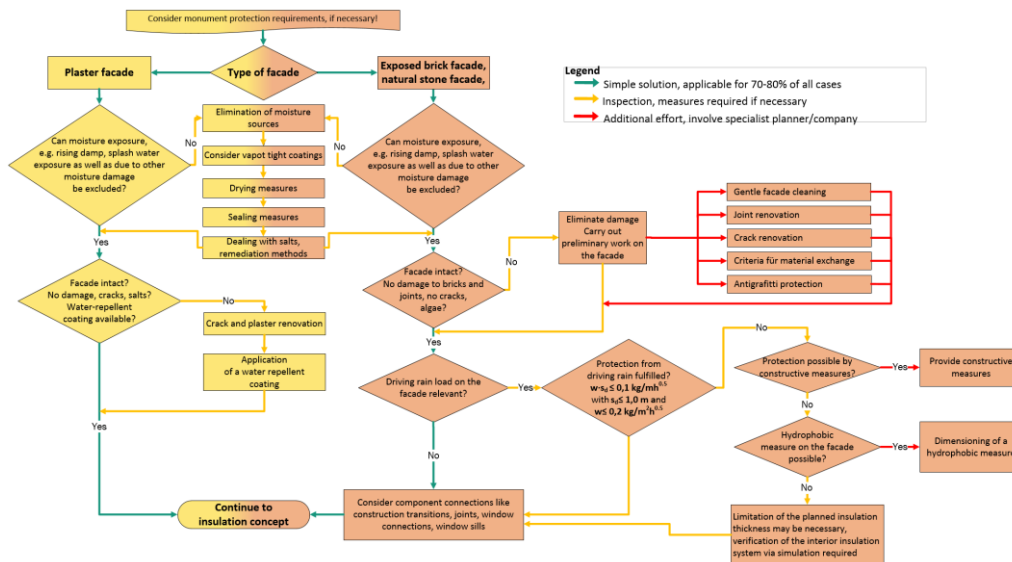


Figure 2. Impression of the flowchart from the façade renovation concept, illustration of the simple solution (green arrows) and the additional measures with higher (yellow and red). To view the flowchart in detail see Figure 3 or use the download link in chapter 4.

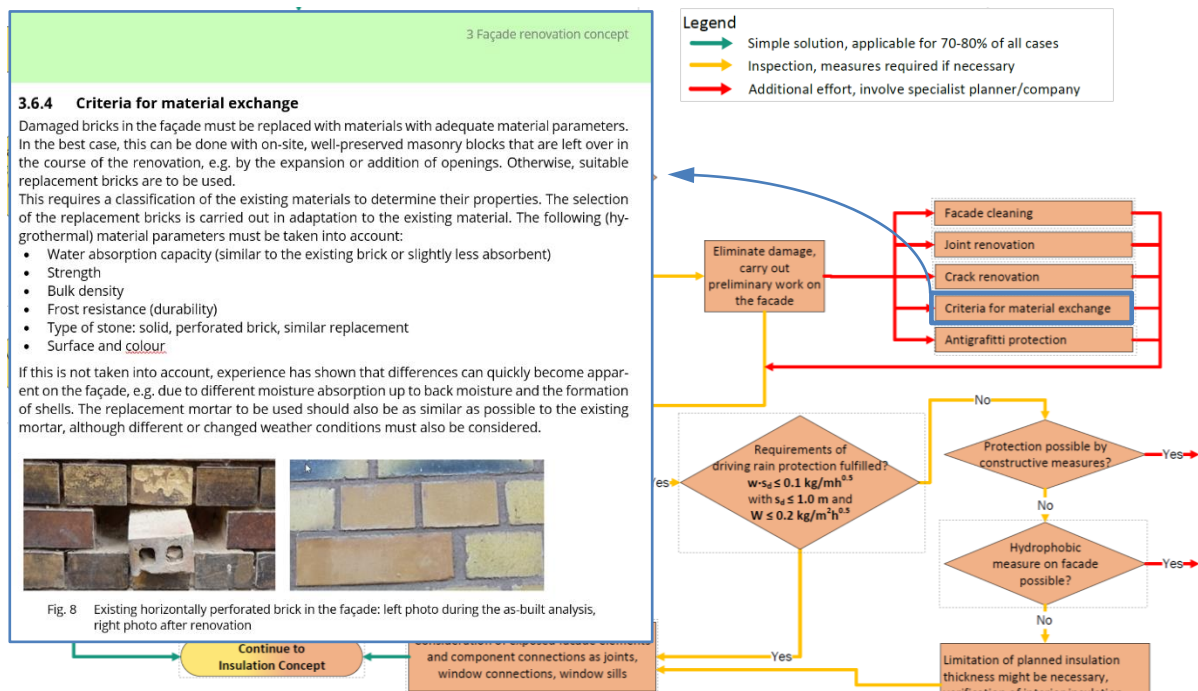


Figure 3. Excerpt from the flowchart for façade renovation; example of the linking to the corresponding chapter in the continuous text (visible limiting values from German WTA guideline 6-5 [6]).

The change from the flowchart to the text of the guideline is illustrated using the example of the criteria for material replacement in brick façades. A link (here outlined in blue in figure 3) opens the corresponding section in the guideline. At the end of the section, another link takes readers back to the flowchart.

The flowcharts are not small in view of the many different questions to be answered. However, almost every step only requires answering one question with "yes" or "no". Nevertheless, it is possible that an issue is not assessed correctly and the wrong path is taken. Therefore, it is always necessary to critically question one's own decisions and, in case of doubt, to consult experts.

3.2. Insulation Concept

In the insulation concept section, users receive assistance in the procedure for creating their insulation design. First of all, they are supported in the selection of possible insulation systems depending on various influencing factors. The systems are classified into different insulation categories (from vapour-permeable and capillary-active to vapour-retarding and vapour-tight systems). In addition, recommendations for the selection for different application scenarios as well as an overview of the most important evaluation criteria for the application of interior insulation are given.

Subsequently, the different levels of proof (proof-free, simplified proof, proof by means of hygrothermal simulation) with the possibilities and limits of applicability are presented and explained for the dimensioning of interior insulation systems.

Within the scope of the project, an additional extended classification for capillary-active, vapour-permeable insulation materials was developed, for which the existing simplified verification procedure is not valid or appropriate. This procedure is described in chapter 4.

For the third stage of the verification, the hygrothermal simulation, the general procedure, the definition of the boundary conditions and other input data, the assignment of the outputs and the selection of the evaluation criteria are described. The proof of suitability is explained using examples of component simulations already carried out.

3.3. Design of constructive connection details

In this section, typical connection details are presented whose execution must be given special consideration in connection with interior insulation measures.

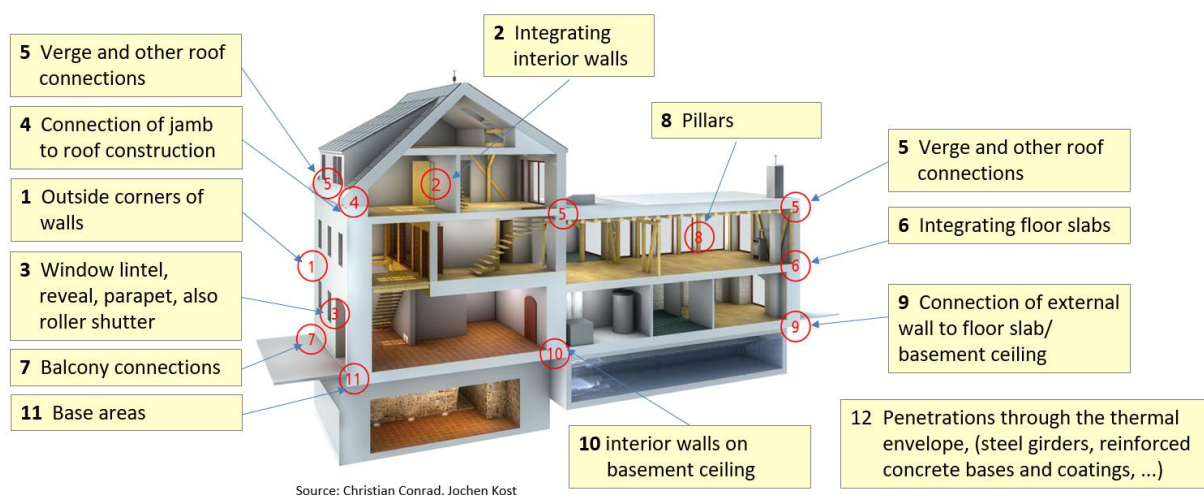


Figure 4. Illustration of common critical connection details in buildings with internal insulation.

In addition, general dimensioning recommendations are given as rough preliminary dimensioning for the most important connection areas, such as window reveals, window sills, connection of solid ceilings

and existing interior walls with identification of suitable materials and flanking measures. Joist ends are treated in a special chapter.

Criteria are described that are relevant for the selection of critical connection details for verification (thermal bridge calculations or hygrothermal component simulations). Possibilities for mitigating these details and alternative solutions are presented and demonstrated by means of detailed calculations.

A catalogue for common detailed solutions for the most important connection areas provide readers with practicable suggestions and specifications for planning and execution.

The guide also contains other frequently requested information, such as on fixing loads to the wall or how to deal with sockets in internally insulated exterior walls.

4. Conclusion

Sustainable refurbishment in connection with the application of interior insulation always requires conscientious step-by-step planning, with an important focus on stock analysis. By working through the described phases of building physics planning and taking into account the specific boundary conditions of the building, it is possible to reduce the potential damage to the building enormously, while at the same time observing deadlines and cost specifications.

The two guides with the linked flowcharts are a good tool to get exactly the information one needs at the moment without having to read the whole guideline or search for a long time. Furthermore, the user is supported in considering all necessary steps without neglecting important investigations. Nevertheless, when using the flow charts, it is recommended to always critically question one's own decisions and to consult an expert as may be necessary.

The guidelines are free of charge and available in different languages, currently German and English (French and Flemish are planned).

The documents can be downloaded from the following link:

<https://tu-dresden.de/bu/architektur/ibk/forschung/projekte/forschungsprojekte-2019/in2eurobuild>

Acknowledgments

The project "IN2EuroBuild - Consistent European guidelines for internal insulation of existing and listed buildings" was funded within the framework of CORNET (no. 247 EBG).

References

- [1] *Renofase* <https://www.renofase.be/> accessed on 14.1.2023
- [2] *Historic buildings and internal insulation* <https://www.ribuild.eu/> accessed on 14.1.2023
- [3] *EnOB-Bewertungsverfahren für Bestandsgebäude mit Holzbalkendecken*, Förderkennzeichen: 0329663O-P, Abschlussbericht, 2016
- [4] Fachverband WDVS e.V.: *Leitfaden Innendämmung 2.0*, available at <https://www.bm-online.de/aktuelles/markt-branche/neuer-leitfaden-innendaemmung/> on 14.1.23
- [5] Fachverband Innendämmung e.V.: *Praxis-Handbuch Innendämmung: Planung - Konstruktion - Details – Beispiele*, Rudolf Müller Verlag, Köln 2016
- [6] WTA guideline 6-5: *Innendämmung nach WTA II - Nachweis von Innendämmsystemen mittels numerischer Berechnungsverfahren*, Fraunhofer IRB Verlag: München, 2014



Aalborg Universitet

AALBORG UNIVERSITY
DENMARK

Quantifying energy-saving measures in office buildings by simulation in 2D cross sections

Witzig, Andreas; Tello, Camilo; Schranz, Franziska; Bruderer, Johannes; Haase, Matthias

DOI (link to publication from Publisher):
[10.54337/aau541623658](https://doi.org/10.54337/aau541623658)

[Link to publication from Aalborg University](#)

Citation for published version (APA):

Witzig, A., Tello, C., Schranz, F., Bruderer, J., & Haase, M. (2023). Quantifying energy-saving measures in office buildings by simulation in 2D cross sections. In H. Johra (Ed.), *NSB 2023 - Book of Technical Papers: 13th Nordic Symposium on Building Physics* (Vol. 13). [317] Department of the Built Environment, Aalborg University. <https://doi.org/10.54337/aau541623658>

Quantifying energy-saving measures in office buildings by simulation in 2D cross sections

Andreas Witzig, Camilo Tello, Franziska Schranz, Johannes Bruderer,
Matthias Haase

Zurich University of Applied Sciences, Switzerland

Abstract. A methodology is presented to analyse the thermal behaviour of buildings with the goal to quantify energy saving measures. The solid structure of the building is modelled with finite elements to fully account for its ability to store energy and to accurately predict heat loss through thermal bridges. Air flow in the rooms is approximated by a lumped element model with three dynamical nodes per room. The dynamic model also contains the control algorithm for the HVAC system and predicts the net primary energy consumption for heating and cooling of the building for any time period. The new simulation scheme has the advantage to avoid U-values and thermal bridge coefficients and instead use well-known physical material parameters. It has the potential to use 2D and 3D geometries with appropriate automatic processing from BIM models. Simulations are validated by comparison to IDA ICE and temperature measurement. This work aims to discuss novel approaches to disseminating building simulation more widely.

1. Introduction

When implementing energy-saving measures it is a challenge to predict its effectiveness and to guarantee indoor comfort. Physics-based dynamical simulation would be a good basis for facility management to make decisions and to optimize HVAC systems. However, proper analysis of the building physics by means of today's software tools is often too elaborate for this aim. Comprehensive modeling of heat storage by the building structure and heat loss through thermal bridges also still requires expert knowledge and is applied only selectively, if at all.

The reason why building simulation is too costly for a widespread application in facility management is that translating the information from building plans into the physical model cannot be done automatically yet. The process includes tasks like identifying walls from complex geometries and estimating heat loss parameters.

A lot of effort has already been put into supporting architectural building design to better integrate building simulation [1] early on with a focus on energy savings [2]. This was reflected in the development of simulation models in the early design phase [3]. The performance of the building design was optimized, and the focus was put on developing design options and their relative differences in performance [4]. To meet the world-wide sustainability goals, the existing building stock needs appropriate transformation of energy systems. The user and operation manager starts to play a major role and thus needs new methods and tools [5]. Computer power intensive finite elements simulation was done focusing on specific building elements like ground slabs [6], or boreholes [7], or fenestration [8]. On the other hand, more and more approaches were published that focus on whole building performance including building fabric, complex fenestration, HVAC systems and controls [9; 10]. Some recent work also highlights the value of simulation models for energy system optimization [11].

There are two megatrends that make a new approach look promising:

1. Building information modeling (BIM) has greatly advanced in the last few years. The digital representation of a building is now ready to contain a variety of parameters and a full 3D model.
2. Computational power has immensely increased since the design of our state-of-the-art tools for building simulation.

Many attempts have been made to integrate energy simulation into the BIM workflow [12; 13]. This work proposes a finite-element discretization for the building structure. It uses a simulation domain that is closer to the BIM representation and relies on physical material parameters. The approach has the potential to reduce the effort for the translation from BIM to the simulation model. It aims at providing detailed information about the thermal-electric interactions in buildings taking the thermal capacity into account. In our current version, we apply 2D numerical simulation of the concrete structure in order to save computational resources. This will prove the concept of getting more insights into the interactions between building fabric and energy flows in buildings. In the long-term vision, 3D simulations will simplify the process at the cost of additional computational power required for the thermal analysis.

In addition to the heat flow in the solid structures, radiation between the walls is properly accounted for resulting in more precise surface temperatures. Air flow in the rooms is approximated by a lumped element model with three dynamical nodes per room. This is in contrast to full 3D fluid dynamics simulations which has both the drawback of extremely high CPU usage as well as a requirement for more knowledge of the occupancy and the user behavior [14].

The dynamic model also contains the control algorithm for the HVAC system and predicts the net primary energy consumption for heating and cooling of the building for any time period. Variants of energy saving measures can be compared and evaluated on a yearly basis with the use of a stochastic model for the outside weather conditions and the user behavior. Besides the physical parameters which are interesting for engineers, the results also contain a cost analysis that is relevant for the owner or manager of the building.

2. Multiphysics model for indoor climate

The building structure consists of solid materials and air volumes. The furniture is neglected in the current model. Also, the water-bearing elements such as heating pipes or the supply and exhaust shafts for ventilation are not represented in detail.

2.1. Basic Physics: Thermal conduction in solids and radiative equilibrium wall-ceiling-floor

Heat transfer and heat storage are calculated with a spatial resolution. For this purpose, the heat flux $\vec{q}(\vec{r}, t)$ and the temperature $\vartheta(\vec{r}, t)$ are modeled as time-dependent field quantities by

$$\rho(\vec{r})c_p(\vec{r}) \cdot \frac{\partial \vartheta(\vec{r}, t)}{\partial t} + \nabla \cdot \vec{q}(\vec{r}, t) = Q_{\text{src}}(\vec{r}, t) \quad (1)$$

$$\vec{q}(\vec{r}, t) = -\lambda(\vec{r}) \nabla \vartheta(\vec{r}, t) \quad (2)$$

The variable $Q_{\text{src}}(\vec{r}, t)$ represents heat sources. Material parameters are listed in Table 1. In the interior spaces, there is also heat exchange via long-wave electromagnetic radiation. Since surface temperatures are in a narrow temperature band, the equation can be linearized. The surface-to-surface radiation model generates a heat source term Q_{rad} in each element j with contributions from the emitted radiosity J_{em} from all neighbouring elements i in the same room.

$$Q_{\text{rad}}(\vec{r}_j, t) = \varepsilon_j A_j \left(\sum_i F_{ij} \cdot A_i \cdot J_{\text{em}}(\vec{r}_i) - e_b(\bar{\vartheta}, t) \right) \quad (3)$$

with surface emissivity ε_j , blackbody hemispherical total emissive power $e_b(\bar{\vartheta})$ and average room temperature $\bar{\vartheta}$, finite element surfaces A_i and view factors F_{ij} [8]. Wavelength dependency of the radiative properties has been set to constant and a hemicube radiation pattern has been chosen.

2.2. Compact model for heat transfer and heat storage in air domains

A lumped thermal system model is applied to non-locally couple the finite element domains [8]. With three dynamical nodes per room, one at the bottom, in the middle, and one at the ceiling, it is possible to account for the air temperature with very few additional degrees of freedom and at the same time provide an accurate temperature distribution at the boundaries of the domains with solid material.

Figure 1 depicts the complete model with 2D finite element solution in the coloured domains and the compact model in the air domains. The compact model is built with the symbols known from electric circuits with parameter values summarized in Table 2.

2.3. Stratification in air domains

Temperature differences in the lower, middle and upper air regions in one room can lead to natural convection. Two thermal power flux terms are introduced, $P_1(t)$ from the lower to the middle and $P_2(t)$ from the middle to the upper node. The stratification process is modelled with a constant power flux in case that warm air is below cold air. For warm air laying on top of cold air, this power is zero since the air layers are stable. Since the physical processes of natural convection are not represented in detail, the stratification model is the most uncertain of all applied models and needs to be calibrated with measurement. However, the advantage of this model is to avoid the discretization of the air domain and to numerically solve the dynamics of air movement.

2.4. Boundary conditions and HVAC system modelling

The temperatures and heat flux densities in the finite element domain are tightly coupled to the temperatures in the lumped element nodes. The heat power fluxes $P_k(t)$ into node k of the compact model is a sum over all elements i from the adjacent finite elements.

$$P_k(t) = \sum_i h_i \cdot (\vartheta_i - \vartheta_k) \cdot A_i$$

where h_i is the heat transfer coefficient listed in Table 2, ϑ_i is the temperature in the finite element, ϑ_k is the temperature in the compact model node k and A_i is the finite element surface area.

Solar irradiation and heat from people or electronic equipment in the rooms are implemented as shown as time dependent heat sources. The time-domain simulation is well-suited to account for their stochastic nature. Power to or from the HVAC system is modeled likewise as a power source or sink in the compact model. In the dynamic simulation, the HVAC control strategy needs also being implemented in order to get realistic temperature curves.

Table 1. Material parameters used in the simulation study.

Material	Mass density $\rho(\vec{r})$ in kg/m ³	Thermal conductivity $\lambda(\vec{r})$ in W/(m · K)	Specific heat capacity $c_p(\vec{r})$ in J/(kg · K)
Concrete	2300	1.15	880
Pavement	1000	1	800
Insulation	200	0.04	1000
Window frames	1380	0.15	900
Quarz glass	2200	0.05	1000
Average for window	1500	0.0264	1000

Table 2. Heat transfer coefficients in $\text{W}/(\text{m}^2 \cdot \text{K})$

h_{ceiling}	4.0
h_{wall}	2.5
h_{floor}	2.0

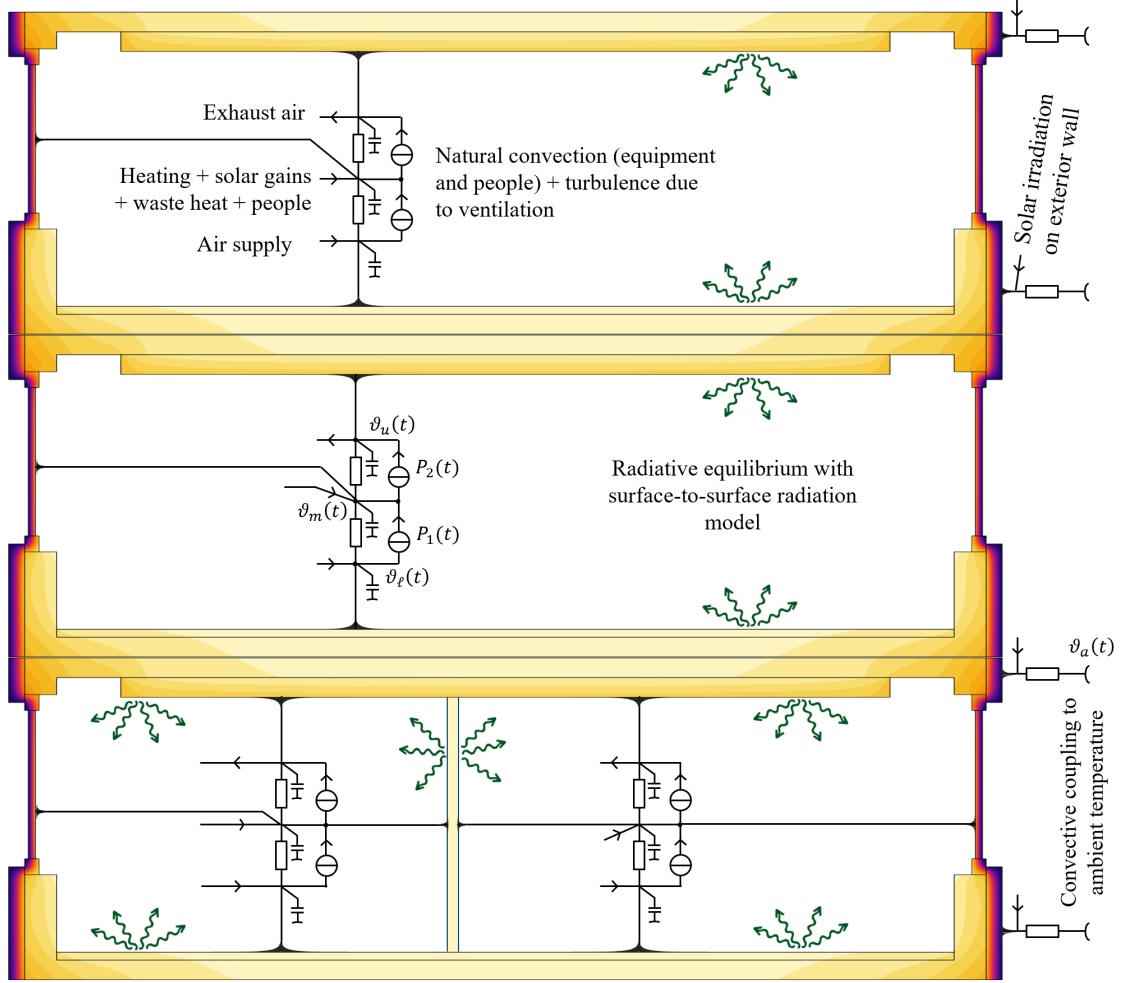


Figure 1. Schematic representation of the simulation model for the case of a building with three floors. Resistors and capacitors represent the heat flux and heat storage in the air domains. Radiative equilibrium is enforced with a surface-to-surface radiation model connecting the boundary elements for each room. A simple model for natural convection is implemented in the power terms $P_1(t)$ and $P_2(t)$. Additional power terms are introduced to represent the HVAC system.

3. Simulation results for various examples

Simulations are done with Comsol Multiphysics [15] on a relatively coarse mesh as shown in Figure 2. The space is 2.4 m high, 5 m wide with windows on each side and has a partition wall separating it into two rooms. Sunshine is only assumed in the right room (heading south). Periodic boundary conditions are imposed at the top and at the bottom of the simulation domain for simplicity

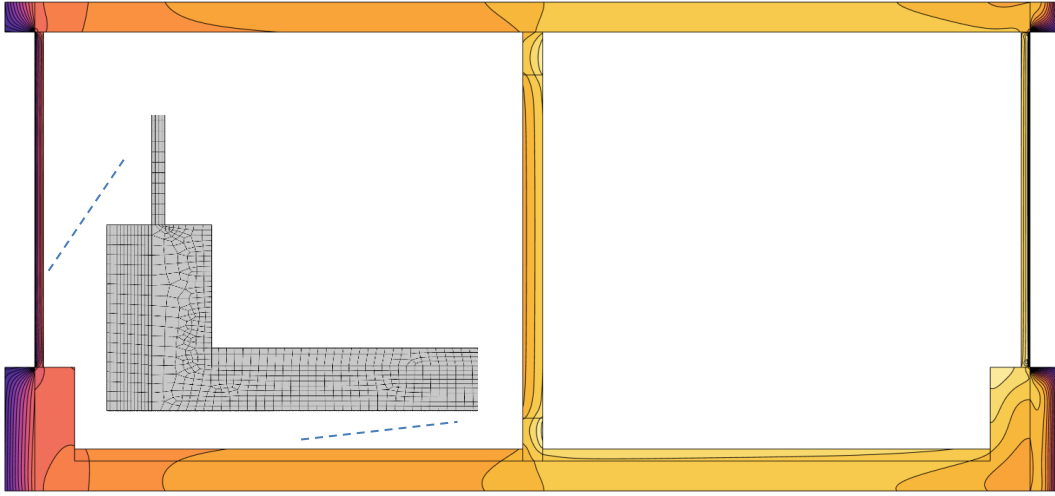


Figure 2. Simulation detail for a structure with two rooms in the evening after a sunny day. Solar irradiation was mainly present in the room heading south (right). Neither of the rooms has the heating turned on. The simulation results show that the room heading north (left) has a lower temperature. Inlet: finite-element mesh.

Simulations first solve for a stationary solution which is the initial condition for the transient study. Solar radiation, outside temperature and thermal loads from people and electronic equipment are an input to the model. Material parameters are summarized in Tables 1 and 2. The coloured areas in Figure 2 shows the temperature profile ranging from yellow (23°C room temperature) to dark blue (ambient temperature $\vartheta_a(t_0) = 4^\circ\text{C}$). The HVAC system has turned off and no automatic sunlight shading is assumed.

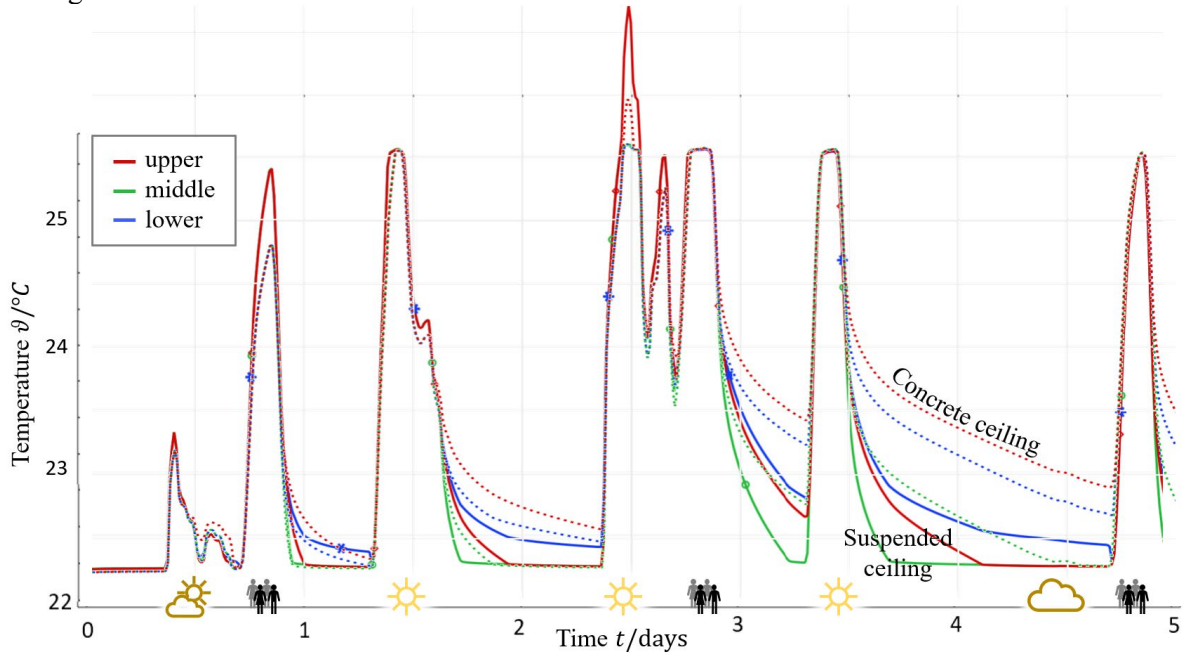


Figure 3. Comparison between different building concepts, one with concrete ceiling (dotted line) and another with suspended ceiling (solid line). Realistic user behaviour and weather data is used as an input. Weather and people symbols are shown to allow an interpretation of the stochastic nature of the input. It is clearly visible that a concrete ceiling significantly balances out thermal loads.

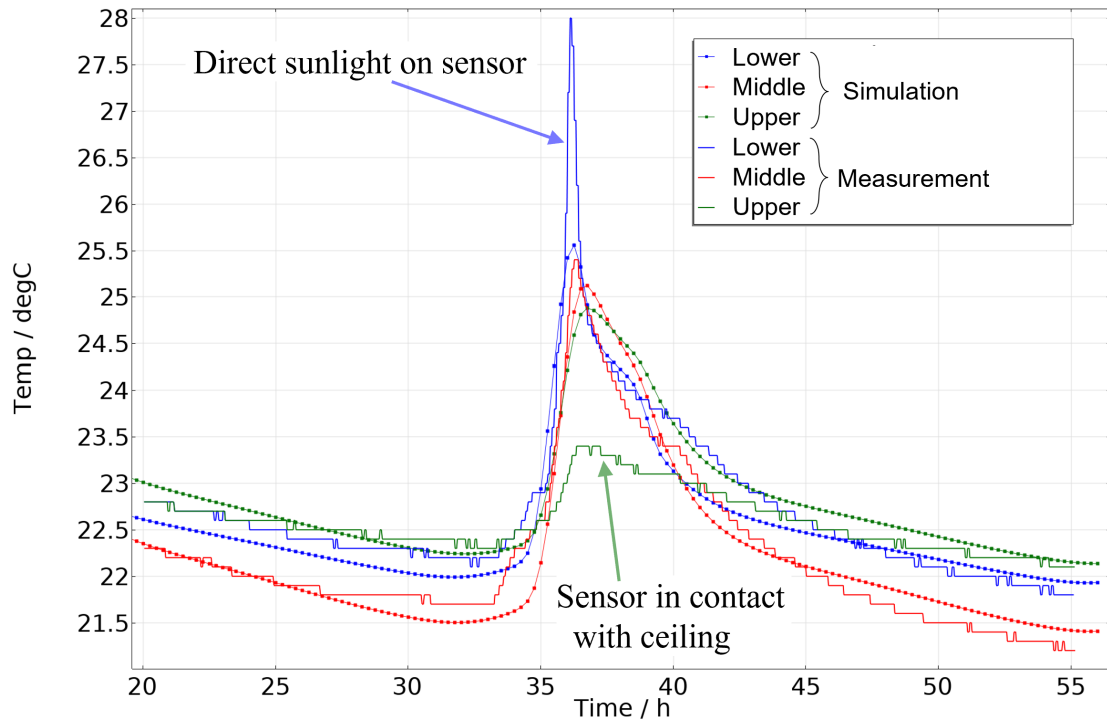


Figure 4. Validation of the lumped thermal system components by comparison of measurement and simulation. The sensor data show significant overshooting in the short time of the day where sunlight is directly shining on the sensor. This effect has not been accounted for in the simulation model.

It is important to see that thermal loss through the building shell is calculated accurately with the full dynamics of the building structure including the thermal storage capability of the building structure. Solar irradiation on the south façade does contribute to the heat balance of the building (although it is minimal in the presented example because the outer layer of the wall is insulating). It is not necessary to introduce U-values as parameters and thermal bridges are naturally solved with adequate precision.

For a second simulation study, a simple HVAC control model has been implemented which heats with a constant power if the room temperature falls below a given lower threshold and cools if it is above an upper limit. Time domain results in Figure 3 for five consecutive days with various amount of sunlight and heating by people. Two different variants of the building structure have been compared, one with suspended ceiling and one with an open concrete ceiling. It is clearly visible that the concrete ceiling has the capability to store energy in the range of one day.

4. Parameter calibration and model validation

The physical parameters used in the thermal conduction and storage in solids are well-known since they are fundamental material parameters. Some of the lumped element components can also be derived from physics, such as the heat transfer between different air layers, or the storage capacity of the air volumes.

Comparison to measurement data has shown that the temperature sensors and in particular their placement bears the largest uncertainty. Figure 4 shows the measurement curve of three sensors compared to the simulation data. It can be seen (no surprise), that direct sunlight on the sensor results in a peak that is not predicted by the numerical model. Furthermore, the sensor for the upper air zone has been directly attached to the concrete ceiling which shaves the temperature peak in comparison to the prediction of the simulation. In order to simplify the model, average materials have been chosen for the window area (see Table 1). This parameter together with the heat transfer coefficient between the middle

air node and the window have been recognized to cause the middle temperature (red curve in Figure 4) to be lower than the bottom and the top air volumes.

When comparing with other simulation tools, the difference from 2D to 3D is the biggest deviation. For validation purposes, in consequence, a 3D simulation domain is used. IDA ICE [16] is chosen as a reference tool. 3D simulations with Comsol currently require 16 GB of main memory and 1h of CPU time for a simulation of two days. A detailed sensitivity analysis of the model parameters and a systematic calibration procedure is in preparation and will be addressed in a separate publication.

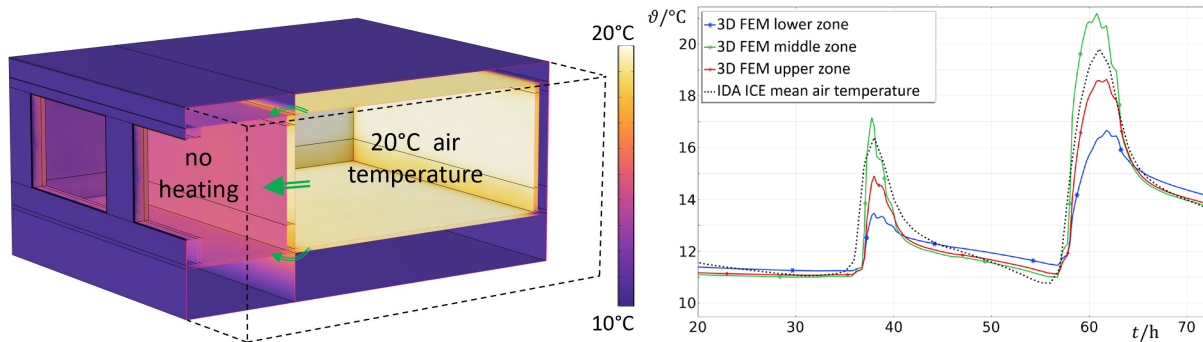


Figure 5. Validation of the 3D FEM simulation model by comparison with an established building simulation. Left: Comsol simulation results, geometry according to ASHRAE Standard 140, Case 960 [17]. Green arrows depict the heat transfer at night. Right: Comparison between 3D FEM and IDA ICE simulation. Very good agreement between the two simulations have been achieved by modifying the heat conductivity of the separation wall in IDA ICE to account for horizontal heat transport in ceiling, floor, and side walls.

5. Conclusion and outlook

An approach to building energy simulation is presented which uses a well-defined set of physical material parameters and a geometric description of the building. The goal is to explore ways to enable facility management to predict energy (and money) saving potential and optimize energy-saving measures. Current advances in building information modeling allow proper geometry processing and complexity reduction. BIM databases will eventually contain all required physical material parameters. Consequently, the building simulation will be substantially simplified.

Secondly, the approach has the ambition to carefully model the concrete structure of the building with its capability of energy storage and with thermal bridges. Some building designs make use of this effect [18; 19] and the construction projects have proven that the concept keeps its promise. It has been shown in Figure 2 that the proposed simulation method supports these innovative designs and could also be applied in the energy management strategy of existing buildings.

Further investigations will explore the setup of 3D simulation structures and the necessary mathematical treatment to speed up transient simulations. On the application side, concrete field tests will be done in equipping buildings with a large number of sensors, collect their data in a digital twin and perform a comprehensive comparison between simulation and measurement. This will help to define use cases in existing buildings for a better management of the building. In addition, this work supports the development of advanced energy management strategies based on passive and active thermal energy storage and electricity grid services.

References

- [1] C. Morbitzer, P. Strachan, J. Webster, B. Spires, D. Cafferty, Integration of building simulation into the design process of an architectural practice, 7th international IBPSA conference, Rio de Janeiro, Brazil, 2001
- [2] P. de Wilde, M. van der Voorden, Computational support for the selection of energy saving building components, 8th international IBPSA conference, Eindhoven, Netherlands, 2003

- [3] Wetter, M. 2011a. "The Future of Building System Modeling and Simulation." In *Building Performance Simulation for Design and Automation*, edited by Jan L. M. Hensen and Roberto Lamberts, 481–504. Oxon: Taylor & Francis.
- [4] David Blum, Javier Arroyo, Sen Huang, Ján Drgoňa, Filip Jorissen, Harald Taxt Walnum, Yan Chen, Kyle Benne, Dragana Vrabie, Michael Wetter, Lieve Helsen. (2021) [Building optimization testing framework \(BOPTTEST\) for simulation-based benchmarking of control strategies in buildings](#). *Journal of Building Performance Simulation* 14:5, pages 586-610.
- [5] Buildings Performance Institute Europe (BPIE) (2016) "Scaling up deep energy renovations. Unleashing the potential through innovation & industrialization", https://www.bpie.eu/wp-content/uploads/2016/11/BPIE_i24c_deepretrofits.pdf
- [6] Neal Kruis & Moncef Krarti (2015) KivaTM: a numerical framework for improving foundation heat transfer calculations, *Journal of Building Performance Simulation*, 8:6, 449-468, DOI: [10.1080/19401493.2014.988753](https://doi.org/10.1080/19401493.2014.988753)
- [7] Julian Formhals, Bastian Welsch, Hoofar Hemmatabady, Daniel O. Schulte, Lukas Seib & Ingo Sass (2022) Co-simulation of district heating systems and borehole heat exchanger arrays using 3D finite element method subsurface models, *Journal of Building Performance Simulation*, 15:3, 362-378, DOI: [10.1080/19401493.2022.2058088](https://doi.org/10.1080/19401493.2022.2058088)
- [8] Goia, F., Haase, M. and Perino, M., Optimizing the configuration of a façade module for office buildings by means of integrated thermal and lighting simulations in a total energy perspective, *Applied Energy* 108 (2013) 515–527, Elsevier
- [9] Haase, M., Andresen, I., and Dokka, TH., The role of advanced integrated facades in the design of sustainable buildings, *Journal of Green Building*, Volume 3 (2), 2009, College Publishing, USA, ISSN 1552-6100
- [10] Haase, M., Marques da Silva, M., and Amato, A., Performance evaluation of a ventilated double-skin façade model, *Energy and Buildings*, 41(2009), pp. 361 – 373, Elsevier, ISSN 0378-7788
- [11] Askeland, M., Georges, L. and Korpås, M., Low-parameter linear model to activate the flexibility of the building thermal mass in energy system optimization, *Smart Energy* 9, Elsevier (2023), DOI: [10.1016/j.segy.2023.100094](https://doi.org/10.1016/j.segy.2023.100094)
- [12] Baydaa Hashim Mohammed, Hasimi Sallehuddin, Nurhizam Safie, Afifuddin Husairi, Nur Azaliah Abu Bakar, Farashazillah Yahya, Ihsan Ali, Shaymaa AbdelGhany Mohamed, Abdul Razzaq Ghumman. (2022) Building Information Modeling and Internet of Things Integration in the Construction Industry: A Scoping Study. *Advances in Civil Engineering* 2022, pages 1-20.
- [13] Luís Sanhudo, João Poças Martins, Nuno M.M. Ramos, Ricardo M.S.F. Almeida, Ana Rocha, Débora Pinto, Eva Barreira, M. Lurdes Simões. (2021) BIM framework for the specification of information requirements in energy-related projects. *Engineering, Construction and Architectural Management* 28:10, pages 3123-3143.
- [14] Tolley, J. and Cook, M., (2017) Predicting the effects of thermal mass in it suites using computational fluid dynamics, proceedings of Building simulation conference Aug 2027, San Francisco, <https://doi.org/10.26868/25222708.2017.321>
- [15] Comsol Multiphysics Reference Manual, <https://www.comsol.com>, Simulations with version 6.1
- [16] Equa Simulation AB, IDA ICE, <https://www.equa.se/en/ida-ice>, Simulations with version 4.8 SP2
- [17] ANSI/ASHRAE Standard 140-2011, Standard Method of Test for the Evaluation of Building Energy Analysis Computer Programs.
- [18] B. Kegel (engineering), S. Aeberhard (report): Energetische Sanierung macht Energieschleuder zum Passivhaus, Energie Experten, Der Blog für mehr Energieeffizienz, <https://www.energie-experten.ch/de/wohnen/detail/energetische-sanierung-macht-energieschleuder-zum-passivhaus.html>, Video by B. Kegel: <https://vimeo.com/405928818>. Winner of the Watt d'Or prize from the Swiss Federal Office of Energy in 2021.
- [19] D. Eberle, F. Aicher (editors), *be 2226, the Temperature of Architecture*, 2019



Aalborg Universitet

AALBORG UNIVERSITY
DENMARK

Studies of hygrothermal processes in a façade by long term high resolution measurements

Björk, Nils Folke

DOI (link to publication from Publisher):
[10.54337/aau541637898](https://doi.org/10.54337/aau541637898)

[Link to publication from Aalborg University](#)

Citation for published version (APA):

Björk, N. F. (2023). Studies of hygrothermal processes in a façade by long term high resolution measurements. In H. Johra (Ed.), *NSB 2023 - Book of Technical Papers: 13th Nordic Symposium on Building Physics* (Vol. 13). [332] Department of the Built Environment, Aalborg University. <https://doi.org/10.54337/aau541637898>

Studies of hygrothermal processes in a façade by long term high resolution measurements

Folke Björk

Professor, Building Technology

¹KTH – Royal Institute of Technology, Dept of Civil and architectural Engineering,
100 44 Stockholm, Sweden

Abstract. Processes for moisture concentration and temperature at different depths in a rather thick wall with mineral wool insulation are studied with a resolution of 1 minute. Damp processes in walls with thick layers of mineral wool differs a lot depending on the weather conditions. Any modelling of heat and moisture in building constructions need to consider this. The fact that the peaks in moisture concentration in some cases come hours before the peak in temperature is something that takes an explanation. It is possible, but not really sure, that this also may have influence on the risk for damage on the structures.

1. Introduction

Undervisningshuset at KTH – Royal Institute of Technology, in Stockholm Sweden is a building, commissioned 2017, is a building intended for teaching, with classrooms and group rooms and lounges of various kinds, but without office premises. The house has a gross area of 2780 m² and is certified to the level “Gold” according to the Swedish environmental certification system “Miljöbyggnad” [1].

With the intention that the building would not only contain teaching but also be an object for teaching and study, it is equipped with a large number of sensors. In total there are 767 sensors in the building and data from these sensors are logged every minute the day around. Among these sensors this building has temperature meters and meters for relative humidity at 6 locations around the building envelope, and at different depths in the walls, which will be described below. This offers a possibility to obtain a detailed view of hygrothermal processes in the building envelope. The directions and the identity numbers of the rooms in which walls the sensors are installed are shown in Figure 1. There are two sets of sensors in the south/west corner, and another two sets of sensors at the north/east corner. In the opposite corners there were one more set of sensors facing south and also one more set of sensors facing north.

Mundt Petersen [2], in his thesis, did measurements in detached single family houses with wood stud constructions. Sensors were placed at different depths of walls and also in the attic. Temperature and RH were recorded every hour. The thesis concludes that in general it is a good agreement between blindly calculated values from WUFI and the measured data.

Goto et al [3] tested wall modules in natural weather and in full scale in the HSB living lab at CTH in Gothenburg. Measurements of temperature and RH were done at four depths in the wall element during 1 year. The wall element was a CLT-structure thermally insulated by PIR. The data were recorded every hour. Conclusion of the study was that the simulation with WUFI give results well in line with the measurements, and that any deviations are explained by how WUFI handles moisture buffering.

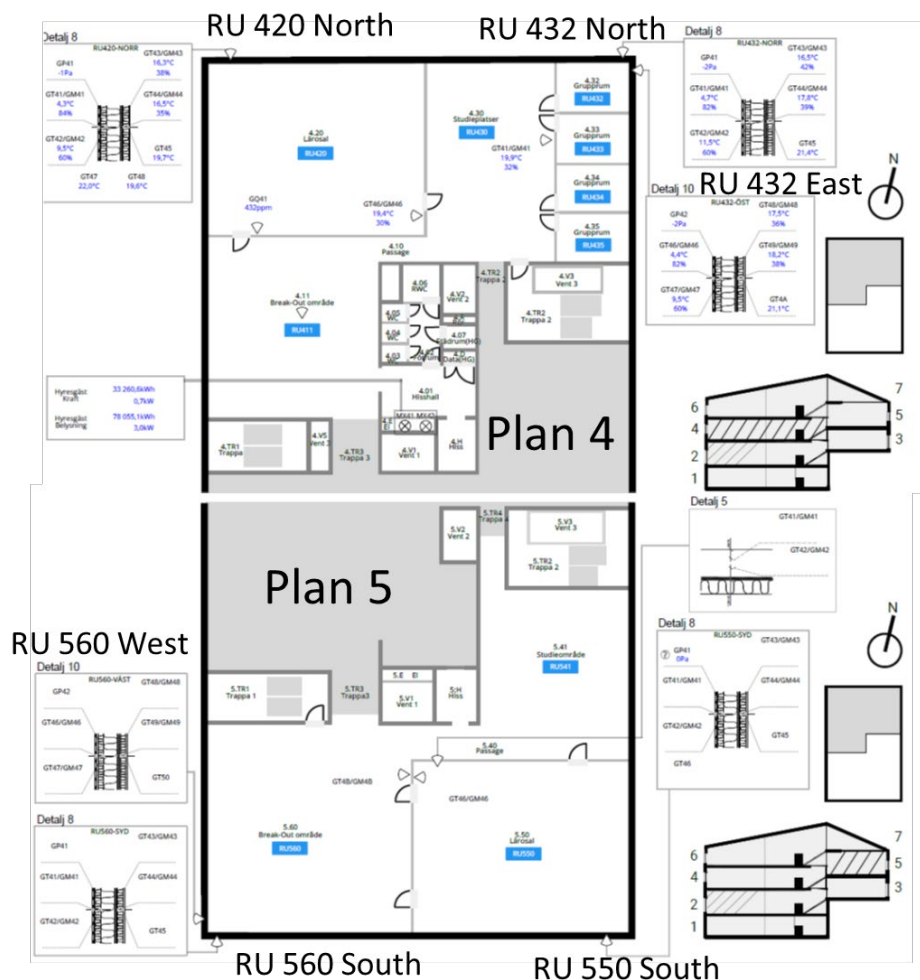
Lindberg et al [4] compared a steady state method for energy consumption with a dynamic method. The effects of thermal inertia in an AAC-wall was noted. Temperature was logged every 10 minutes. In the paper the authors did invite other researchers to proceed doing evaluations using these data.

Kvist Hansen et al [5] studied the effects of moisture accumulation of driving rain. Registration of data for temperature and RH were done every minute and mean values were recorded every hour. They concluded that “the wind-driven rain (WDR) loads have an influence on the moisture conditions in the masonry and behind the applied internal insulation. The direct connection between the measurement of the WDR and the detection of WDR rain events behind the insulation or beam ends was not achieved. A distinct coherence between moisture content and internal and external humidity conditions was however established”.

De Masi et al [6] have data where it seems like the peaks for relative humidity comes before the temperature. This is however not really discussed in the report.

M I Nitzoutzev et al [7] in their study, includes laboratory and full scale experiments for evaluation of thermal insulation solutions for facades also having channels for air transport. One result was that moisture and heat transport occurred in the channels in the thermal insulation in the façade. In this study temperature and RH were measured in the walls.

Mlakar and Shrankar [8] measured temperature and RH at different depths in wall constructions. Data were logged every 3 minute. This study could have given a possibility to study the time scale of the moisture process, but this was not the intention of their work.



2 Aim of the study

It is not the intention to validate any HAM-model by using these data. But data of this kind will be helpful in further development of models. In order to develop the understanding of physical processes observations are needed. So, in this study two observations will be presented. The point of these observations are to bring some more light in what the processes of heat and moisture will be like in thick walls thermally insulated by mineral wool.

Aim of this little study is to show how this quite high frequency in data logging, 1 per minute, offers some opportunities to look at natural processes in a building envelope. Focus will be on two processes.

Process 1: A period of late winter weather typical for the city of Stockholm with cold clear nights and sunny days, with quite big diurnal changes in temperature. This happened February 28, 2021.

Process 2: In late spring in the month of May. Temperatures in night during rainfall are quite low, but raises after the rain when the sun reappears and shines on the facades. This happened May 28 2021.

3. Experimental

3.1 Description of the wall structure

The walls in this building are infill walls with a structure of steel studs. This is illustrated by the drawing in Figure 2. The main structure is 195 mm steel studs placed between the floor slabs, and with mineral wool insulation between them. On the inner side it is a vapour barrier of PE-foil and two layers of gypsum board (12,5 mm thick) on the inside. Next towards the inside are horizontal steel studs 95 mm, with mineral wool in between them. The inner lining are gypsum boards.

Towards the outside it is also 95 mm horizontal steel studs with mineral wool between them. Outside of these studs is a wind stopper made of cellulose fibre reinforced cement board, 9 mm thick, with a sd-value of 0,3 m. Trade mark of this board is Cembrit. The facades are covered with wall tiles that are assembled on wood battens. This façade type is very seldom used in Sweden. The tiles are about 12 mm thick and 30 cm long. They are placed in a way so they overlap in two layers. So the last 15 cm of each tile is exposed to the air and the weather. In total, the wall is a bit more than 400 mm thick, and with 385 mm of thermal insulation.

3.2 How sensors are placed

The sensors for temperature and relative humidity are placed at different depths in the wall as illustrated in Figure 2. The sensor 1 is placed just under the wall slates, fixed to one of the horizontal battens carrying the slates. Sensor 2 is placed between outer layer of thermal insulation and the insulation at the main structure. Sensor 3 is placed on the inner side of the thermal insulation of the main structure, and on the outer side of the vapour barrier. Sensor 4 is on the inner side of the gypsum boards and the vapor barrier.

The sensors are installed with care to avoid disturbances by any heat transport in the steel studs. The sensors are Vaisala “HMP 110 T and RH-sensors”. It is also a weather station on the building that collects data every minute.

In this study we have used data for temperature and calculated moisture concentration out of data for relative humidity. We have also used the dew point meter in the weather station.

4 Results

Data from the weather station, for the two days, with temperature, moisture concentration and also dew point are presented in Figure 3. Moisture concentration is calculated from the data for temperature and relative humidity. Data for February 28 for two places of the building envelope are presented in Figure 4, this is Process 1. Data for May 28 for two places of the building envelope are presented in Figure 5, this is Process 2. There are in many cases peaks in the curves for temperature or moisture concentration. The times for these peaks are presented in Table 1.

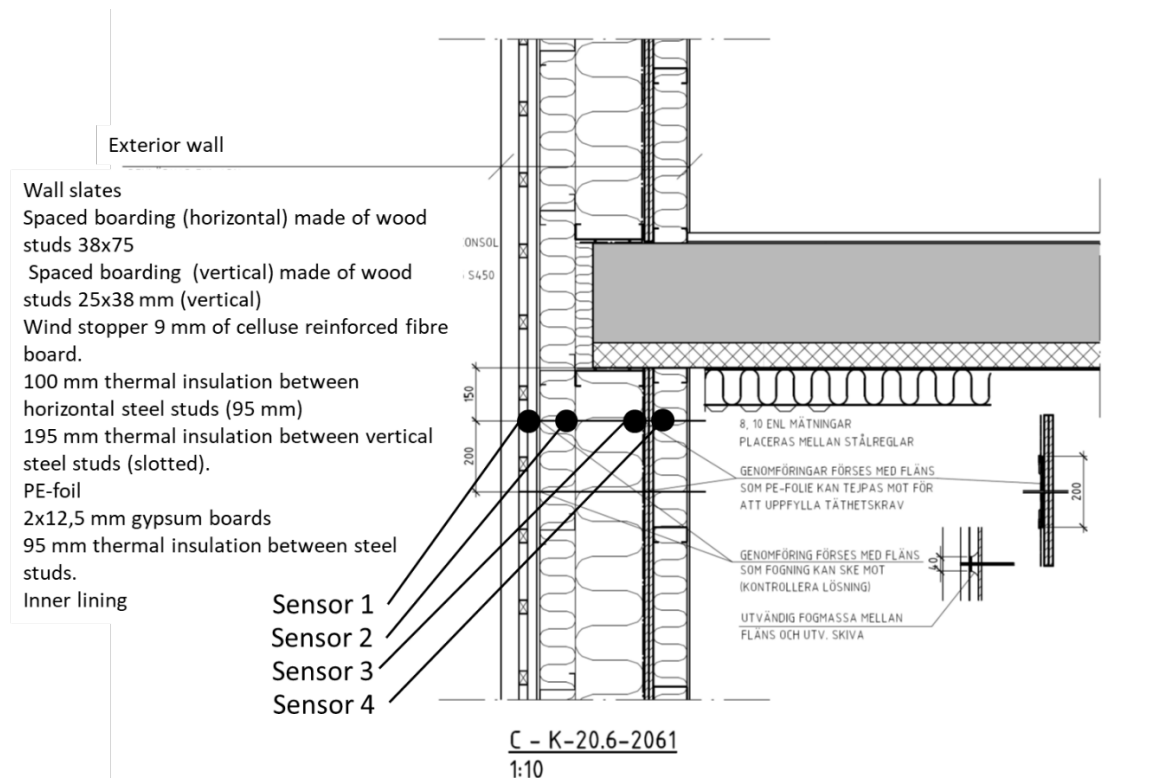


Figure 2. Drawing of a floor to wall connection with the details of the wall construction and a description of where the sensors are installed.

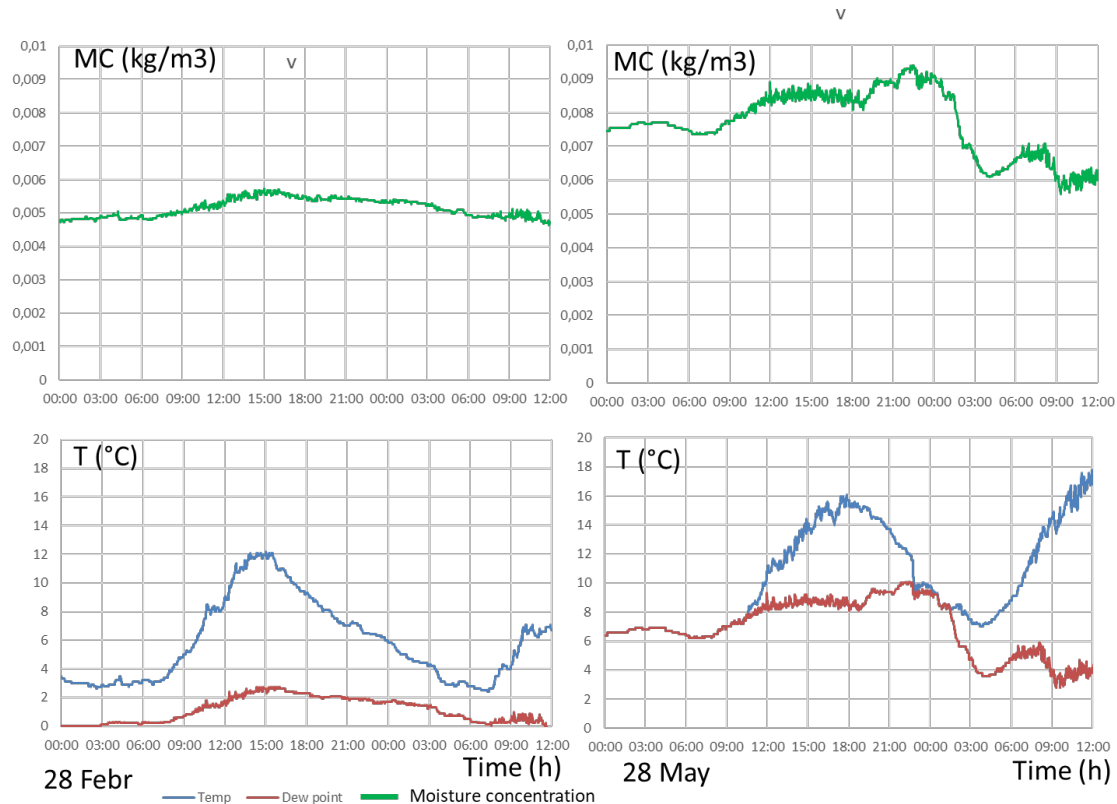


Figure 3. Data from the weather station. February 28 2021 (left) and May 28 2021 (right). Upper charts are for moisture concentration and lower charts for temperature and dew point.

Process 1 means winter weather with clear nights and days. There are rather big diurnal changes in temperature over the day. So, after the night, temperatures behind the facades are quite low. Data from the weather station for February 28, 2021, are presented in the left-hand part in Figure 3. The temperature raises from about 3°C in the night to a peak of about 12°C at about 12 pm. The temperature peak is not very sharp but quite wide. Moisture concentration in the air, calculated from data for temperature and RH are also presented in the diagram. The moisture concentration varies between 0,0048 and 0,0056 kg/m³. The dew point is all the time well below the outdoor temperature.

The temperature process along with the process of moisture concentration in a wall part facing south, RU 560 south, are presented in the left hand part of Figure 4. We can look at the peaks of the curves to understand, or at least notice, what happens.

For the outermost sensor, S1, the peak for moisture concentration comes on hour before the peak in temperature. It is a time delay from S1 to S2. The temperature rise depends on solar radiation and the time delay is because of thermal inertia in the wall construction. The peaks in temperature and moisture concentration for sensor S2 comes here 2 hours after the peaks in S1, and again with the peak in moisture concentration about 1 hour before the peak in temperature. Temperatures in S3 and S4 are to a very small extent influenced by the temperature processes further out in the wall. But the moisture concentration for sensor S3 is as sharp as the peak for sensor S2. It comes about 25 minutes after the peak in S2, and reaches at about the same level of moisture concentration. Moisture concentration at S4 is not influenced of the outdoor process.

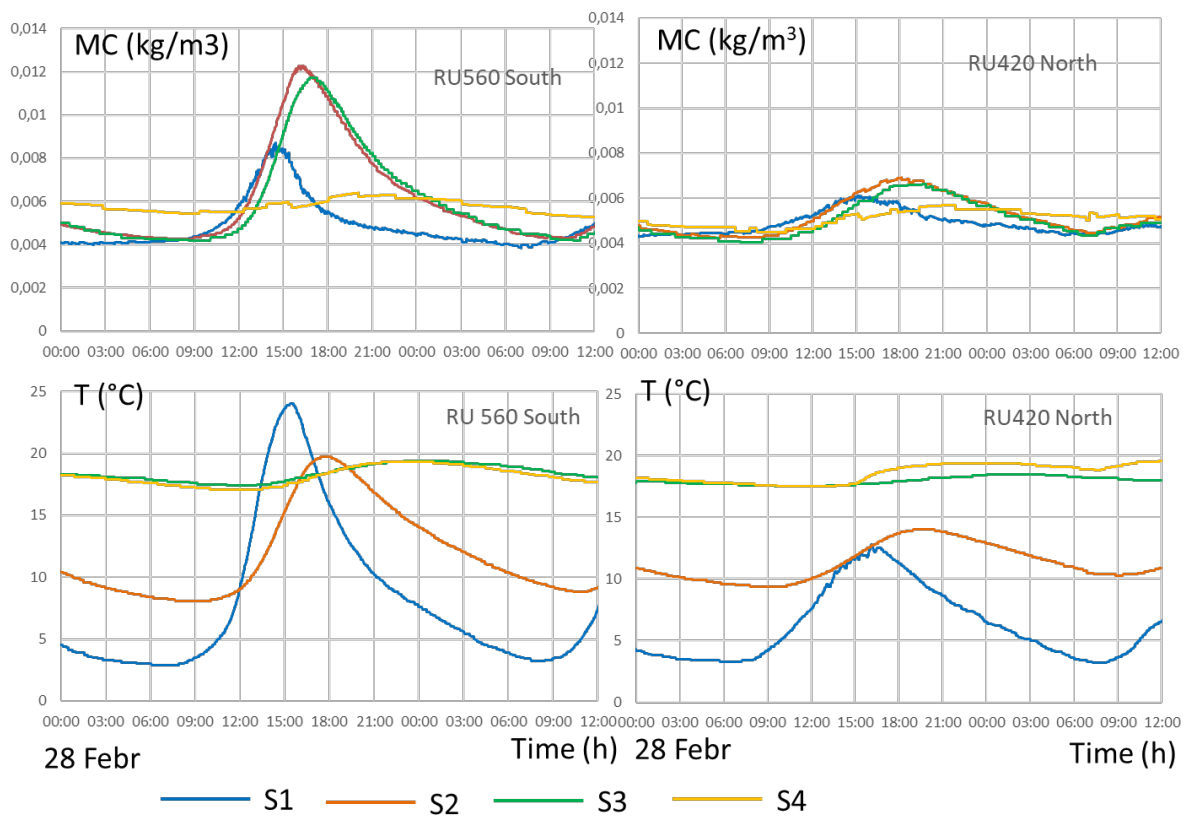


Figure 4. Data for the sensors at R560 south, and R420 North, February 28 2021.

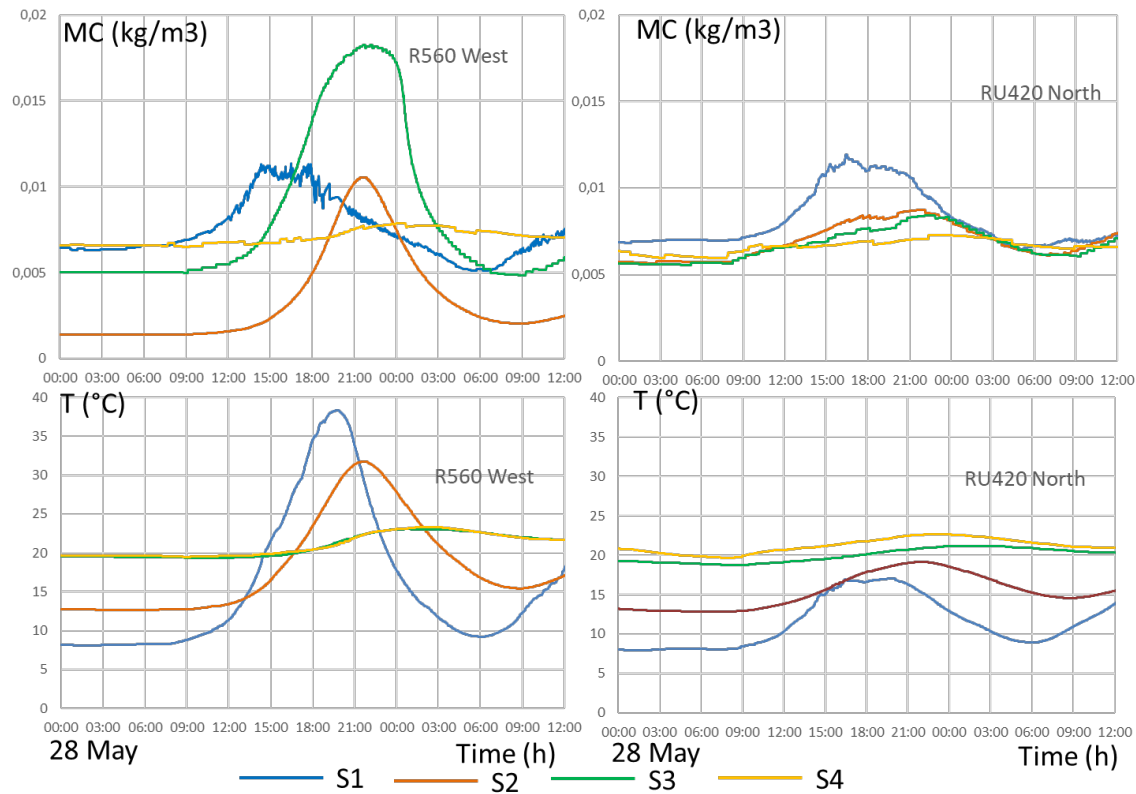


Figure 5. Data for the sensors at RU 560 West and RU 420 North May 28 2021.

Table 1. Times for peaks in temperature and moisture concentration.

Location	Sensor	Peak in T	Peak in MC
Febr 28 2021			
RU 560 south	S1	15:21	14:24
	S2	17:26	16:21
	S3	23:01	16:48
	S4	21:30	19:38
RU 420 north	S1	16:07	14:50
	S2	18:58	18:06
	S3	00:02 (next day)	19:33
	S4	20:53	20:53
May 28 2021			
RU 560 west	S1	19:39	14:22
	S2	21:26	21:26
	S3	No peak	21:37
	S4	No peak	No peak
RU 420 north	S1	16:24	16:24
	S2	21:29	21:29
	S3	No peak	23:35
	S4	No peak	18:14

In the same day, at the point facing north, RU 420 north, right hand part of Figure 4, the temperature in S1 follows quite well the outdoor temperature, although a bit delayed in time. The peak in outdoor temperature, Figure 3 left-hand side, is however quite wide and not very distinct.

The peak in damp, for S1 at RU 420 north, comes about 1 hour before the peak in temperature.

The temperature peak for S2 comes about three hours after the peak in temperature peak in S1, and the peak in moisture concentration also comes about 1 hour before the temperature peak. Also in the north façade temperatures in sensors S3 and S4 are very little influenced by the outdoor temperature. Also here it is a peak in moisture concentration at S3, and this comes 1,5 hours after the peak in moisture concentration at S2.

Process 2 comes after a few days of rainy weather in the month of May, in late spring. Temperatures in night during rainfall is quite low, but raises after the rain when the sun reappears and shines on the facades.

When looking at outdoor temperature and dew point in the right-hand part of Figure 3 it can be seen how they overlap in the night, which is an indication of rain. The temperature starts to raise at about 10 30, so then the rain is over.

Here we look at RU 560 west, which is facing west. Data are presented in the left hand part of Figure 5. The peak in moisture concentration at S1 comes about 5 hours before the peak in temperature. The peak in temperature at S2, comes about 2 hours after the peak in temperature at S1. Temperatures at S3 and S4 are not influenced by the outdoor temperature. However, the moisture concentration has its peaks at the same time as the temperature peak in S2. Moisture concentration at S3 has its peak at a much higher level than the peak at S2.

When we look at the sensors in the wall facing north, right hand part of Figure 5, the temperature process at S1 is very similar to the process in the outdoor air although the temperature is a bit higher at S1 compared to outdoors. The peak in moisture concentration comes about the same time as the peak in temperature.

The peak in temperature at S2 comes about 5 hours after the peak at S1, and the peak for moisture concentration comes at the same moment. Also here temperatures in S3 and S4 are not much influenced by what happens outdoors, but the moisture concentration in sensor 3 has a peak 2 hours after the peak in sensor S2. A possible peak at sensor S4 is also noted although this is isolated by the vapour barrier from the processes in the wall.

Discussion

In the literature measurement data and also the models have usually a resolution of one hour. This is enough in most cases, still we will never be aware of details that might happen in between the recorded data points. So, a report about these processes have a value of itself for improving the basic understanding and to develop new ideas.

The unique thing with this study is that the processes can be followed in detail in quite short time intervals. So it will be possible to conclude whether the level of moisture content in the structures varies and if moistening at different parts of the construction may occur.

These things can be studied by modelling, but here it is possible to follow the processes in an experimental way. The fact that the peaks in moisture concentration in some cases come hours before the peak in temperature is something that takes an explanation.

Conclusions

My reflection about this is that damp processes in walls with thick layers of mineral wool differs a lot depending on the weather processes. Any modelling of heat and moisture in building constructions need to consider this.

It is possible, but not really sure, that this also may have influence on the risk for damage on the structures.

Acknowledgments

I am grateful to KTH-Royal Institute of Technology and to the Facility owner Akademiska hus for their initiative to install and also run the data acquisition system in the building “Undervisningshuset” that makes it a living laboratory.

References

- [1] Medineckiene, M., Zavadskas, E.K., Björk, F., Turskis, Z. (2016), Archives of Civil and Mechanical Engineering 15(1), pp. 11-18
- [2] Mundt Petersen, S. (2013). Comparison of hygrothermal measurements and calculations in a single-family wooden house on the west coast of Sweden. (Rapport TVBH; Vol. 3054). Byggnadsfysik LTH, Lunds Tekniska Högskola. <http://www.byfy.lth.se/publikationer/tvbh-3000/>
- [3] Yutaka Goto, Holger Wallbaum, Johan Olofsson and Ulf Norr, (2020),. Numerical and real-life assessment of the moisture safety of CLT structure with PIR insulation composite under the Swedish climate, Nordic Symposium of Building Physics in the Nordic countries, 2020, <http://doi.org/10.1051/e3sconf/202017210004>
- [4] R. Lindberg, A. Binamu*, M. Teikari, (2004) Five-year data of measured weather, energy consumption, and time-dependent temperature variations within different exterior wall structures. Energy and Buildings 36 (2004) 495–501.
- [5] Qvist Hansen Peter Bjarløv, Ruut Peuhkuri, (2019) The effects of wind-driven rain on the hygrothermal conditions behind wooden beam ends and at the interfaces between internal insulation and existing solid masonry, Energy & Buildings 196 (2019) 255–268
- [6] Rosa Francesca De Masi , Silvia Ruggiero, Giuseppe Peter Vanoli, (2021) Hygro-thermal performance of an opaque ventilated ‘façades with recycled materials during wintertime, Energy & Buildings 245.
- [7] M.I. Nizovtsev , V.N. Letushko , V. Yu. Borodulin , A.N. Sterlyagov, (2020) Experimental studies of the thermo and humidity state of a new building facade insulation system based on panels with ventilated channels, Energy & Buildings 206.
- [8] Jana Mlakar and Janez Strancar, (2013) Temperature and humidity profiles in passive-house building blocks, Building and Environment 60 (2013)



Aalborg Universitet

AALBORG UNIVERSITY
DENMARK

How to predict wind driven rain in a changing climate?

Kubilay, Aytaç; Bourcet, John; Carmeliet, Jan; Derome, Dominique

DOI (link to publication from Publisher):
[10.54337/aau541649835](https://doi.org/10.54337/aau541649835)

[Link to publication from Aalborg University](#)

Citation for published version (APA):
Kubilay, A., Bourcet, J., Carmeliet, J., & Derome, D. (2023). How to predict wind driven rain in a changing climate? In H. Johra (Ed.), *NSB 2023 - Book of Technical Papers: 13th Nordic Symposium on Building Physics* (Vol. 13). [334] Department of the Built Environment, Aalborg University. <https://doi.org/10.54337/aau541649835>

How to predict wind driven rain in a changing climate?

Aytaç Kubilay¹, John Bourcet¹, Jan Carmeliet¹, Dominique Derome^{2*}

¹Chair of Building Physics, Department of Mechanical and Process Engineering, ETH Zürich, 8092 Zürich, Switzerland

²Department of Civil and Building Engineering, Université de Sherbrooke, Sherbrooke Qc J1K 2R1, Canada

Corresponding author: dominique.derome@usherbrooke.ca

Abstract. We are nowadays confronted with changes in moisture-related durability problems arising from climate change. As one example, building facades of historical buildings that before were hardly exposed to frost damage, may in future be exposed to an increase in frost-thaw cycling leading to a higher risk for moisture-related damage. An essential step in hygrothermal and durability analysis is the prediction of wind-driven rain (WDR). A computational fluid dynamics (CFD) Eulerian multiphase model provides WDR catch ratio charts. Building further on this work, methods are developed to predict WDR loads and moisture damage risks.

1. Introduction

Wind driven rain (WDR) is one of the most important loads determining the risk for moisture damage of building envelopes. We are most likely confronted with significant changes in moisture-related durability problems due to climate change. Examples are building facades of historical buildings that before were hardly exposed to frost damage and that may in the future be exposed to an increase in freeze-thaw cycling leading to a high risk for moisture related damage, or displacement of ecosystems making termites and rotting fungi accessing so far winter-protected territories.

An essential step in hygrothermal and durability analysis is the prediction of WDR. WDR may be predicted using semi-empirical or computational methods. The latter approach is based on computational fluid dynamics (CFD), i.e. determination of the wind flow field using RANS (Reynolds-averaged Navier Stokes) for different wind orientations and determination of WDR field using Eulerian multiphase model for different droplet diameter classes and wind directions. The WDR solver developed by the authors using OpenFOAM is open source and available for download [1]. The outputs of solver include WDR distribution on surfaces, wind streamlines and droplet trajectories for different wind speed, wind orientation and droplet diameter.

WDR deposition is modeled using local wind flows, thus care is needed in selecting a computational domain large enough to capture all relevant air movement. We distinguish a WRD study from a local urban climate study, which requires to take into account radiative exchanges and heat and mass transport in porous media in addition to wind flows, and with adequate boundary conditions, as done in e.g. [12, 13]. So WDR studies usually rely on wind flow and direction and rain intensity available from weather files. Future climate scenarios provide guidelines on ranges of probable impacts given different scenarios of greenhouse gas emissions. We acknowledge that climate change predictions may exhibit uncertainties, especially regarding precipitation predictions. Nevertheless, exploring the impact of future scenarios, using our current level of knowledge, may provide stakeholders with points of attention for building design and maintenance.

2. Overview of methodology

In Figure 1, we present a case study discussed in this paper to illustrate the CFD-based prediction of WDR. The building of interest is a complex historical building located in Victoria, BC, Canada: the Empress Hotel, a Canadian Pacific heritage building on the inner harbor of Victoria located on the southeast tip of Vancouver island. First, data must be assembled on the configuration of the building and its neighborhood and on the topography, and wind directions are selected in terms of co-occurrence with rain, based on weather data. Second, a computational domain is built, using more refined computational cells closer to the building, and following guidelines for wind flow development between the domain boundaries and the buildings and for height of the domain respective to blockage ratio (Figure 1a). Third, wind-flow fields are obtained by CFD for different wind directions (Figure 1b, c). Scaling provides the wind velocities for different reference wind velocity.

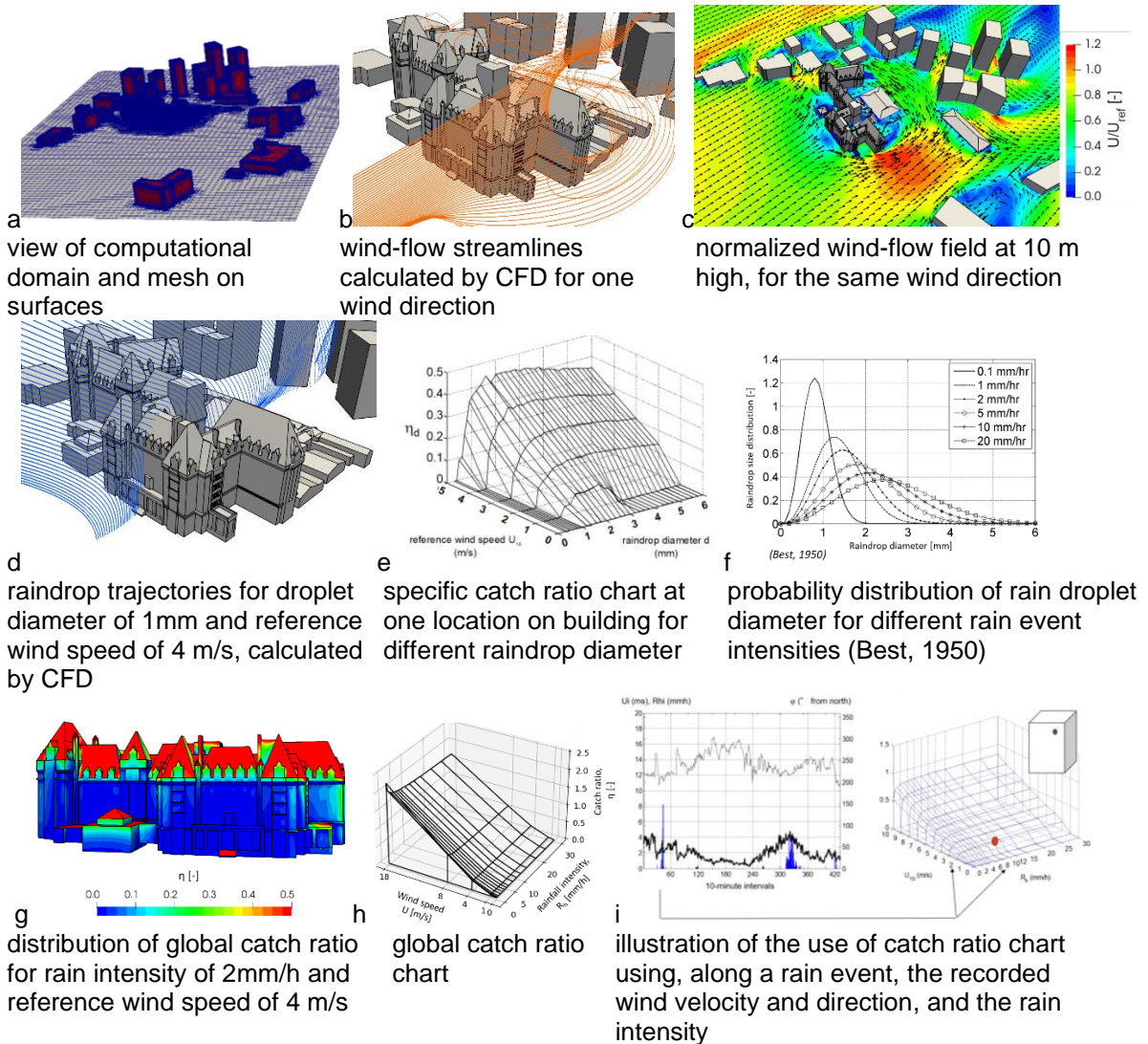


Figure 1. Illustration of the steps of CFD-based WDR method: (a-c) determination of normalized wind flow field; (d-e) determination of specific catch ratio; (f-i) global catch ratio and its use (b,c,d,g from [10] with permission).

Fourth, WDR streamlines are obtained using a Eulerian approach that allows to track the “concentration” of rain at all locations for droplets of a specific diameter (Figure 1d). Intersection of streamlines with solid surface indicates rain deposition, from which specific catch ratios (ratio of rain deposited at any

location compared to rain deposited on the ground far from building interaction) are determined. This calculation is done for 17 sizes of droplets. A specific catch ratio chart can be built showing the catch ratio per droplet size (Figure 1e). Thus, for every location on the building, charts of the specific catch ratio, giving the ratio between WDR as a function of droplet diameter and wind speed is obtained. Sixth, as rain events of different intensities present different probability distributions for droplet sizes (Figure 1f, as measured e.g. Best [2]), the determination of global catch ratio requires aggregating specific catch ratio along rain intensity distribution. Combining specific charts with information of the droplet size distribution for different rain intensities, global catch ratio can be represented for every location of the building façade for a reference rain intensity and reference wind speed for different wind directions (Figure 1g, h). Using this information, the WDR load on facades can be predicted for the period of interest (Figure 1i). An overview of this method, as developed and extensively validated by the authors can be found in [9], and full description in [3-8].

The drawback of this method is its computational cost. Therefore, methods have to be developed that allow predicting accurately WDR load and moisture damage risk at low computational cost. In this paper we present two methods. The first is simplifying analysis by reducing the sampling sets. The second is simplifying determination of moisture risk by using a climatic index accounting for wetting versus drying potential.

3. Determination of impact of climate change on wind driven rain load during long time periods

In a first method, we use a statistical method, i.e. Latin Hypercube Sampling (LHS) that allows to select a small set of correlated WDR data. Using statistical sampling from cumulative distribution functions (CDFs) of correlated 10-year data for wind direction, wind speed and rainfall intensity, samples are generated based on the frequency of occurrence which represent long term WDR conditions. It is found that 200 samples generated by LHS show the same WDR load as compared to wetting over a period of 3 years. For more details on the method, we refer to [10]. Advantage of the method is that the WDR load on complex buildings for long periods can be determined with much less computational effort, which allows to study the influence of climate change on WDR. The method is applied to the Empress hotel, Victoria, BC, Canada and the difference in global catch ratio obtained with full meteorological conditions versus LHS is shown in Figure 2.

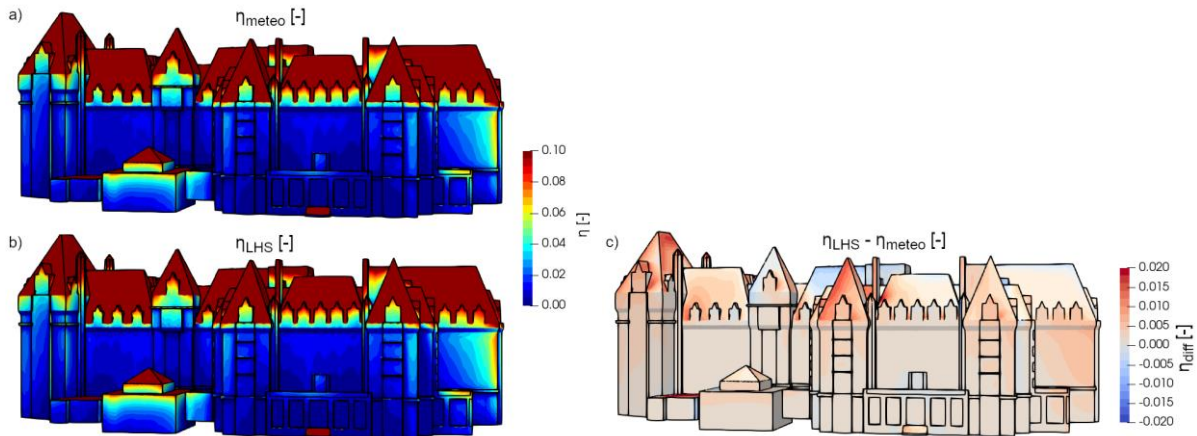


Figure 2. Global catch ratio distribution over the western façade of the building using a) 3 years of measured meteorological conditions and (b) LHS with a sampling size of 200. (c) Difference between a) and b). (From [10] with permission).

Climate change will have an impact on the Victoria Region: winter, fall, and spring will become more wet and summers will become more dry. We found that parts of facade that are currently exposed to a higher amount of WDR show also the highest increase in future WDR load. Further, keeping wind conditions constant, the change in future WDR load is mostly due to increase in rainfall (up to 25%) and the change in wetting distribution is minimal, while the largest impact is expected in future when wind

velocity changes. We show the applicability of this method to quickly and accurately predict the WDR load and identify locations that show high risk for various wind-rain scenarios with respect to the climate change.

4. Durability assessment of complex historical building using dynamic climate index

In a second method, a WDR study on the Canadian parliament serves as basis for an assessment of long-term time-varying wetting load due to WDR and potential evaporation, using several years of meteorological data (Figures 3 and 4). A cumulative assessment can provide a fast method to identify critical locations and periods for moisture damage. More information is available in [11].

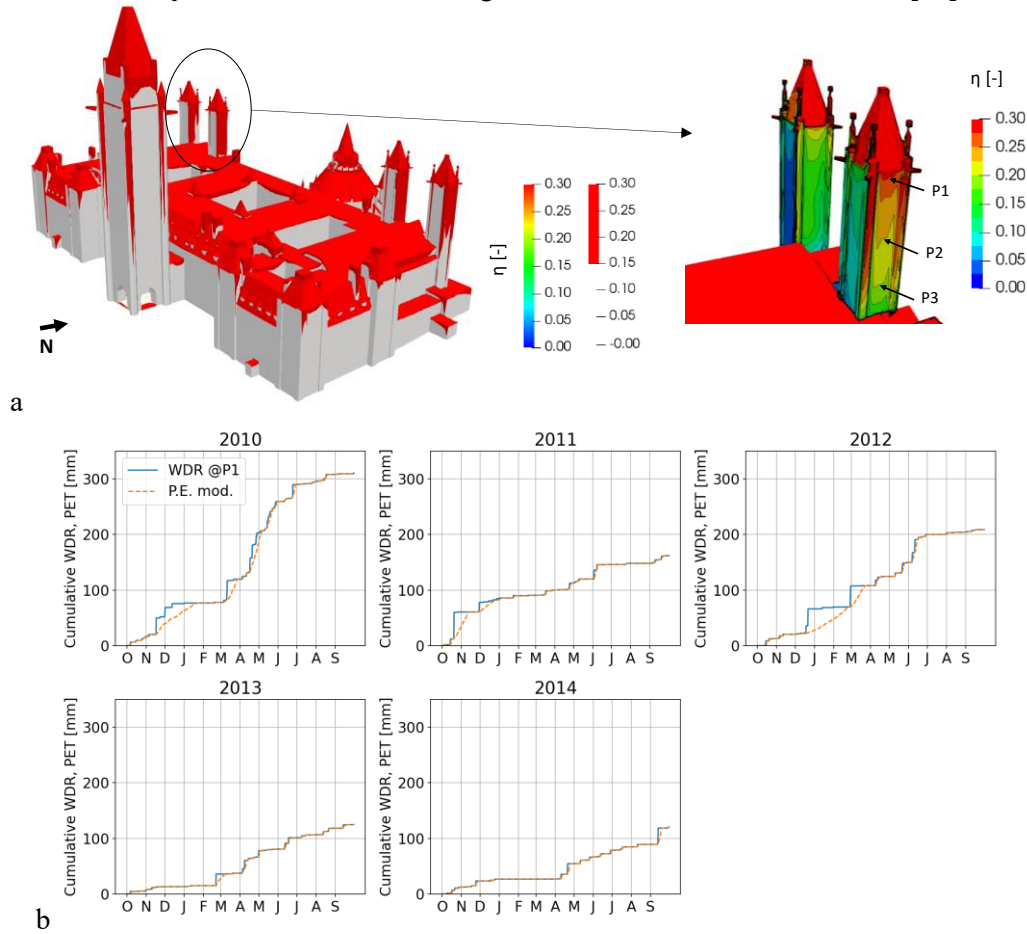


Figure 3. Wind-driven rain deposition on the Parliament Building, Ottawa: a) distribution of long term (10 years) catch ratio larger than 0.15, shown in red, and close-up of redistribution on two western small towers, showing a catch ratio is 0.3 for part of masonry; b) cumulative WDR deposited and evaporation potential at the said location, compared over 5 years. Critical periods show WDR above PET (from [11] with permission).

The new durability assessment method proposed is based on a dynamic climatic index. The Climatic Index is defined as the ratio between the annual wetting load and annual drying potential. The potential evaporation is determined based on the Penman equation, which only depends on climate conditions but depends per orientation. It is independent of the location on the building facade, and the storage and transport of heat and moisture within the building envelope. The advantage of this method is that it is not dependent on material properties, allowing for the evaluation of the building prior to material selections or without knowledge of material hygrothermal properties.

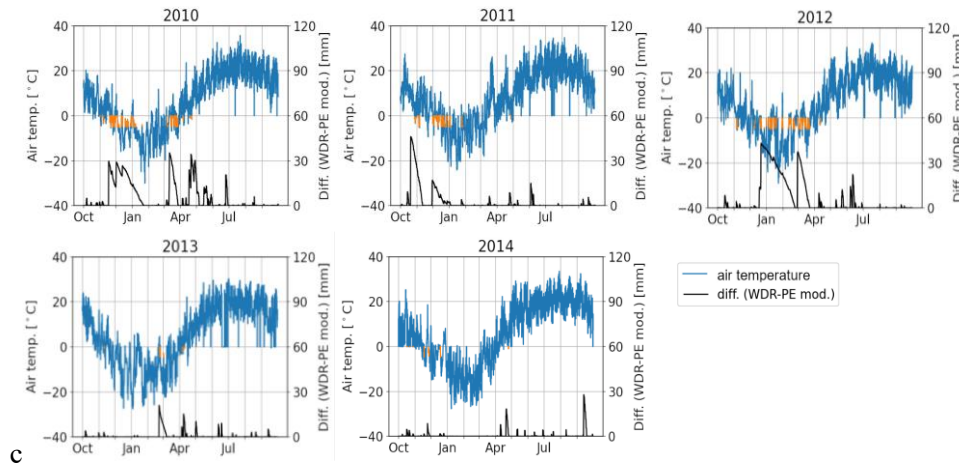


Figure 4. Wind-driven rain deposition on the Parliament Building, Ottawa: Plots of critical periods and air temperature, with co-occurrence with freezing temperature (-5 to 0°C) highlighted in orange. (from [11] with permission).

5. Conclusions

Wind driven rain (WDR) is a major source of moisture on the building envelope. As more and more extreme rain events expected due to climate change, moisture-related damage risks in buildings could increase in the future, reinforcing the need for accurate spatial and temporal distribution of WDR in the built environment. We propose here two methods to further the use of WDR information in interpretation and prediction of such risks.

We also would like to mention that WDR can be considered in solutions to building durability and urban comfort, not necessarily only as a source of problems in building durability. Further work including understanding the role of rain as a moisture source in mitigation of urban heat island effects, which are exacerbated during heat waves, should be considered. For example, this WDR approach has been embedded in a suite of models for local urban modelling [12, 13].

References

- [1] Website for downloads and tutorials: <https://carmeliet.ethz.ch/research/downloads/wind-driven-rain.html>
- [2] Best AC. (1950). The size distribution of raindrops, *Q. J. R. Meteorol. Soc.*, 76:16-36.
- [3] Kubilay A, Derome D, Carmeliet J. (2017). Analysis of time-resolved wind-driven rain on an array of low-rise cubic buildings using large eddy simulation and an Eulerian multiphase model, *Building and Environment*, 114: 68-81.
- [4] Kubilay A, Carmeliet J, Derome D. (2017). Computational fluid dynamics simulations of wind-driven rain on a mid-rise residential building with various types of facade details, *J. Building Performance Simulation*, 10:125-143.
- [5] Kubilay A, Derome D, Blocken B, Carmeliet J. (2015). Numerical modeling of turbulent dispersion for wind-driven rain on building facades, *Environmental Fluid Mechanics*, 15: 109-133.
- [6] Kubilay A, Derome D, Blocken B, Carmeliet J. (2015). Wind-driven rain on two parallel wide buildings: field measurements and CFD simulations, *J. Wind Engin. and Industrial Aerodynamics*, 146:11-28.
- [7] Kubilay A, Derome, Blocken B, Carmeliet J. (2014). High-resolution field measurements of wind-driven rain on an array of low-rise cubic building, *Building and Environment*, 78: 1–13.
- [8] Kubilay A, Derome D, Blocken B, Carmeliet J. (2014). Numerical simulations of wind-driven rain on an array of low-rise cubic buildings and validation by field measurements, *Building and Environment*, 81:283-295.

- [9] Derome D, Kubilay A, Defraeye T, Blocken B, Carmeliet J. (2017). Ten questions concerning modeling of wind-driven rain in the built environment, Building and Environment, 114: 495–506.
- [10] J Bourcet, A Kubilay, D Derome, J Carmeliet. (2023). Representative meteorological data for long-term wind-driven rain obtained from Latin Hypercube Sampling–Application to impact analysis of climate change, Building and Environment 228, 109875.
- [11] Kubilay A, Bourcet J, Gravel J, Zhou X, Moore TV, Lacasse MA, Carmeliet J, Derome D. (2021). Combined use of wind-driven rain load and potential evaporation to evaluate moisture damage risk: case study on the Parliament Buildings in Ottawa, Canada, Buildings, 11:476.
- [12] Kubilay A, Allegrini J, Strebel D, Zhao Y, Derome D, Carmeliet. (2020). Advancement in urban climate modelling at local scale: urban heat island mitigation and building cooling demand, Atmosphere, 11:1313.
- [13] Kubilay A, Derome D, Carmeliet J. (2018). Coupling of physical phenomena in urban microclimate: A model integrating air flow, wind-driven rain, radiation and transport in building materials, Urban Climate, 24:398-418.



Aalborg Universitet

AALBORG UNIVERSITY
DENMARK

Influence of Energy-saving Renovation Plan on the Hygrothermal Distribution Inside Kyo-machiya Soil Walls Considering their Moisture Buffering Effect

Liu, Pei; Iba, Chiemi

DOI (link to publication from Publisher):
[10.54337/aau541650556](https://doi.org/10.54337/aau541650556)

[Link to publication from Aalborg University](#)

Citation for published version (APA):

Liu, P., & Iba, C. (2023). Influence of Energy-saving Renovation Plan on the Hygrothermal Distribution Inside Kyo-machiya Soil Walls Considering their Moisture Buffering Effect. In H. Johra (Ed.), *NSB 2023 - Book of Technical Papers: 13th Nordic Symposium on Building Physics* (Vol. 13). [341] Department of the Built Environment, Aalborg University. <https://doi.org/10.54337/aau541650556>

Influence of Energy-saving Renovation Plan on the Hygrothermal Distribution Inside Kyo-machiya Soil Walls Considering their Moisture Buffering Effect

P Liu* and C Iba

Department of Architecture and Architectural Engineering, Graduate School of Engineering, Kyoto University, Kyoto 615-8540, Japan

*Corresponding author: be.liupei@archi.kyoto-u.ac.jp

Abstract. Kyo-machiya are traditional townhouses in Kyoto that represent an important aspect of cultural heritage preservation. Because of the poor thermal insulation performance, they require energy-saving renovations. However, their unique soil walls possess a moisture-buffering effect that can be strongly influenced by the applied renovation plan and are expected to remain functional even after renovation. Conventional renovation methods apply an inside vapor barrier to the interior insulation to prevent condensation between the insulation and wall; however, applying this barrier may hinder the buffering effect and deteriorate the unique interior appearance of the soil wall. Therefore, we conducted a case study on the hygrothermal environment of a typical Kyo-machiya structure in winter when the moisture generated by indoor activities was adsorbed by soil walls. We used the finite difference method to divide the various renovated envelope systems into thin layers and calculated the temperature and humidity distributions. Based on these results, we propose the use of exterior insulation for renovations, owing to its excellent thermal performance. However, if the space between the adjacent buildings is insufficient, interior insulation can be applied without a vapor barrier.

1. Research background

Kyo-machiya (Figure 1) are traditional townhouses in Kyoto that represent a significant part of Kyoto-style streets. They are not only used as residential homes but also as a part of the regional cultural heritage. The preservation of Kyoto City streets as prominent tourist destinations relies on the maintenance of their integrity, with Kyo-machiya serving as the primary architectural features (Figure 2). However, ensuring the longevity of these structures for future generations presents a challenge, given the deterioration they have endured over the past seven decades [1].

With the westernization trend in Japan, vernacular houses, including Kyo-machiya, were renovated, and rooms were combined or remodeled to increase floor area [2]. As originally constructed, houses in relatively warm areas in Japan, including Kyo-machiya, provide a high natural air change rate and were designed to reduce indoor temperatures during summer. Hosham et al. clarified that indoor temperature can be 2 °C lower than the corresponding outdoor temperature in summer [3]. However, their extensive air leakage owing to their unique structure, as well as their poor thermal insulation resulting from their traditional appearance and materials, can lead to discomfort and high heating energy consumption during winter [4], as shown in a study conducted by Ooka in the Hokuriku district, confirming cold and discomfort in winter [5]. Therefore, a unique and appropriate energy-saving renovation technique must be developed. A study conducted by Iba discussed the hygrothermal environment in a newly constructed Kyo-machiya, in which the condensation risk related to the thermal insulation retrofit was emphasized

as the next step [6]. Although a study conducted by Yokobayashi examined the buffering effect of soil walls, they were not evaluated at a building scale [7]. In this study, we evaluated Kyo-machiya using numerical modeling to clarify the impact of different renovation plans on the thermal and buffering performances of its unique soil walls.

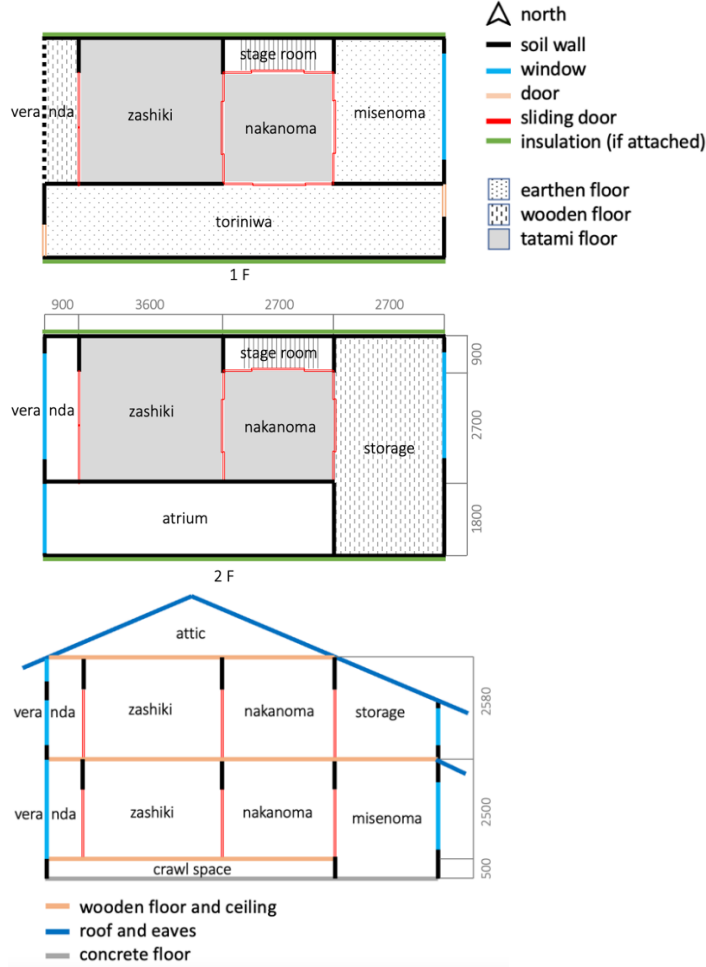


Figure 1. Layout of a model of a Kyo-machiya (unit: mm).



Figure 2. Example of Kyoto-style streets.

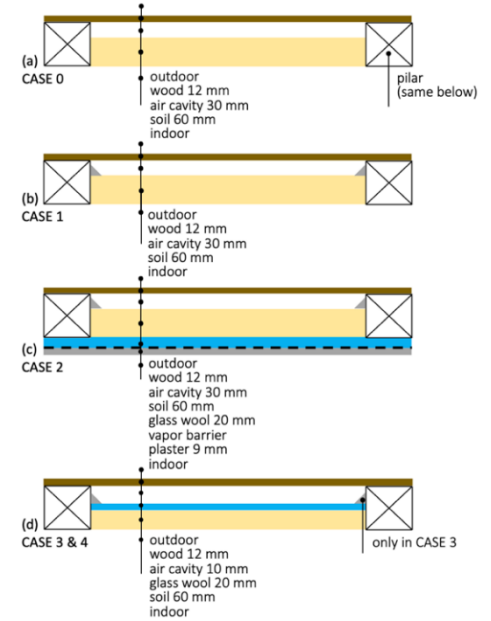


Figure 3. Renovation cases.

2. Methodology

2.1. Basic equations

The model employed for the case studies was constructed in the Julia Programming Language using the forward difference method to express the governing equations for heat and moisture transfer through the building envelope as follows [8,9]:

$$(c\rho + c_w\rho_w\psi)\frac{\partial T}{\partial t} = \frac{\partial}{\partial x}\left\{\lambda\frac{\partial T}{\partial x} + r\left(\lambda'_{\mu g}\frac{\partial \mu}{\partial x} + \lambda'_{Tg}\frac{\partial T}{\partial x}\right)\right\} \quad (1)$$

$$\rho_w\psi\frac{\partial \psi}{\partial t} = \frac{\partial}{\partial x}\left(\lambda'_{\mu g}\frac{\partial \mu}{\partial x} + \lambda'_{Tg}\frac{\partial T}{\partial x}\right) \quad (2)$$

where c , ρ , and λ refer to the material's specific heat, $\text{J}\cdot(\text{kg}\cdot\text{K})^{-1}$, density, $\text{kg}\cdot\text{m}^{-3}$, and thermal conductivity, $\text{W}\cdot(\text{m}\cdot\text{K})^{-1}$, respectively; ψ refers to the moisture content of the material, $\text{m}^3\cdot\text{m}^{-3}$; μ refers to chemical potential of free water, $\text{J}\cdot\text{kg}^{-1}$; $\lambda'_{\mu g}$ and λ'_{Tg} respectively represent the moisture conductivities determined by the chemical potential difference, $\text{kg}\cdot(\text{s}\cdot\text{m}\cdot(\text{J}\cdot\text{kg}^{-1}))^{-1}$, and temperature difference, $\text{kg}\cdot(\text{s}\cdot\text{m}\cdot\text{K})^{-1}$; and the subscripts w and g refer to water and vapor, respectively. This model was used to conduct one-dimensional heat and moisture transfer simulations in the direction of wall

component thickness. The heat and moisture fluxes on the envelope surfaces were calculated using the Robin boundary conditions.

A multizone airflow network model was developed to estimate the airflow through the gaps between rooms and air leakage from window sashes. The mass flow rate through horizontal gaps can be expressed as [8]

$$G = \rho_{air} q (\Delta p)^{\frac{1}{n}} \quad (3)$$

and that through the vertical gaps as

$$G = \frac{\rho_{air} q}{h_{top} - h_{btm}} \int_{h_{btm}}^{h_{top}} (\Delta p)^{\frac{1}{n}} dh \quad (4)$$

where G refers to the mass flow rate of air, $\text{kg} \cdot \text{s}^{-1}$; q is the unit airflow rate, $\text{m}^3 \cdot \text{s}^{-1} \cdot \text{Pa}^{-1/n}$, depending on the gap area (which depends on the width and length) and the air leakage characteristic value n .

2.2. Calculation conditions and different renovation patterns

Intermittent heating was assumed to be provided only to the nakanoma and zashiki on the first floor (Figure 1). The calculation was performed from October to January using the December and January results as outputs. Standard Expanded AMeDAS Weather Data based on the years 2011–2020 (provided by the Meteorological Data System Co., Ltd.) were used as outdoor boundary conditions. The heating temperature and schedule were set based on a field survey conducted from 2015 to 2019 in a real Kyo-machiya, whose layout and envelope composition were similar to those of the model used in this study [10]. The preferred heating temperature was set as 20 °C, the heating time for the nakanoma (working space) was set to 6:00–9:00 during weekdays with no heating on weekends, and the heating time for the zashiki (bedroom) was set to 17:00–22:00 during weekdays and 6:00–22:00 during weekends. Nakanoma and zashiki were equipped with 1000 and 1500 W heaters, respectively. The initial temperature and humidity conditions of all envelope materials were set as 7 °C and 80%, respectively.

Table 1. Material properties.

Material	Thickness (mm)	Density ($\text{kg} \cdot \text{m}^{-3}$)	Specific heat ($\text{J} \cdot (\text{kg} \cdot \text{K})^{-1}$)	Vapor permeability ($\text{kg} \cdot (\text{m} \cdot \text{s} \cdot \text{Pa})^{-1}$)	Thermal conductivity ($\text{W} \cdot (\text{m} \cdot \text{K})^{-1}$)	Comment
Soil wall	60	1300	880	1.38×10^{-11}	0.5	First level floor and exterior layer of north and south soil walls
Wood	15	400	1300	1.10×10^{-12}	0.10	
Plywood	12	550	1300	1.11×10^{-13}	0.15	Second level floor and roof-base
Glass	3	/	/	0	0.78	Only resistance was considered
Fusuma	20	/	/	3.07×10^{-12}	0.068	Wood frame covered with paper; Only resistance was considered
Tatami	55	230	2300	2.00×10^{-12}	0.11	Only used in the nakanoma and zashiki
Ground (earth)	/	1900	1400	/	1.0	Floor of the misenoma and toriniwa
Concrete	150	2200	840	2.98×10^{-12}	1.6	
Roof tile	16	2000	760	/	0.96	A waterproof layer is provided under the tile
Glass wool	20	/	/	1.70×10^{-10}	0.032	Only resistance was considered

The material properties assumed for the Kyo-machiya construction and renovation are listed in Table 1, and the five renovation cases evaluated in this study are described in Figure 3 and Table 2. Case 0 refers to the baseline model used to express poor thermal performance, Cases 1 and 4 were used to evaluate the importance of enhancing airtightness, and Cases 2 and 3 were used to evaluate the influence of different insulation locations on the hygrothermal distribution in the soil wall. In all cases, partial insulation was only applied to the north and south exterior walls, and no insulation was provided on the roof or floor. This represents the most feasible renovation scenario, considering the unique structure of Kyo-machiya.

Table 2. Evaluated cases.

Case name	Insulation condition	Airflow rate
Case 0 (baseline)	None	100%
Case 1	None	10%
Case 2	Interior insulation after vapor barrier	10%
Case 3	Exterior insulation	10%
Case 4	Exterior insulation	100%

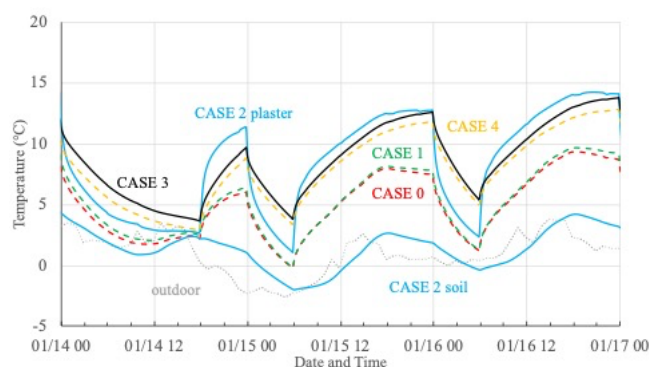


Figure 4. Surface temperature on the northern soil wall of the zashiki.

3. Results

3.1. Interior surface temperature

Figure 4 shows the surface temperature changes in the northern soil wall of zashiki for each case during the coldest period (1/14–1/16). In Case 2, the temperature is shown for the surface between the insulation and soil wall and for the interior surface of the plaster layer; in all other cases, it is shown for the surface in contact with the indoor air. The temperature in Case 4 was similar to that in Case 3, although the former exhibited a lower peak value and a slightly slower rate of increase over time. Cases 0 and 1 exhibited similar trends; the difference between the two cases indicated that the enhanced airtightness slightly increased the peak temperature and its rate of increase. Case 2 exhibited the lowest soil wall temperature, and its change trend closely followed the outdoor air temperature. However, the corresponding interior temperature (plaster surface) exhibited the highest peak value and fastest rate of increase, although it also exhibited the fastest rate of decrease. The Case 3 results indicated that use of exterior insulation could keep the entire wall warm, whereas the Case 2 results indicated that the use of interior insulation left the wall at extremely low temperatures that even dropped below 0 °C. Thus, even if no condensation occurs on the interior surface of the soil wall (according to the results presented in Section 3.2), penetrated rainwater can freeze and damage its exterior surface.

3.2. Interior surface relative humidity

Figure 5 shows the change in surface relative humidity on the northern soil wall of the zashiki for each case. Similar to the surface temperatures in Figure 4, Case 2 shows the relative humidity of the surface between the insulation and soil wall, and of the interior surface of the plaster layer; in all other cases, it is shown for the surface in contact with indoor air. In all the cases, the relative humidity remained below 80%, indicating that no condensation occurred. For the Case 2 soil wall surface, the relative humidity remained constant because the soil wall was isolated by a vapor barrier.

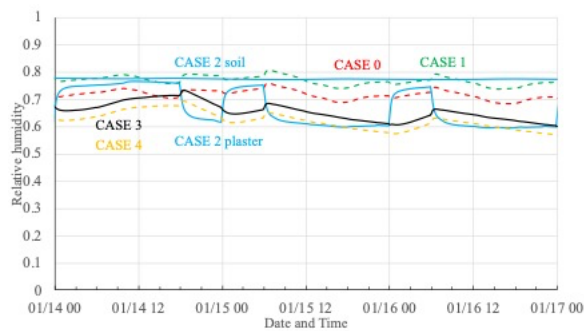


Figure 5. Relative humidity on the northern soil wall of the zashiki.

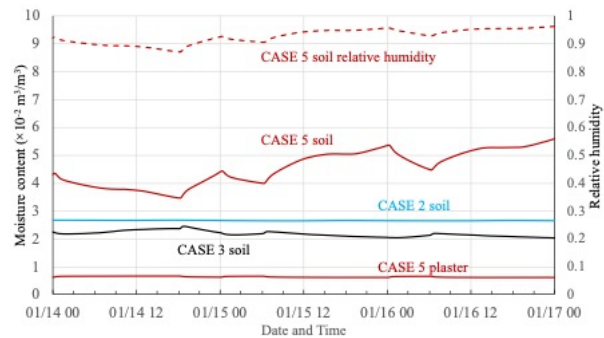


Figure 6. Moisture content and relative humidity on the northern soil wall of the zashiki with and without the vapor barrier.

4. Discussion

As Figure 5 indicates, the use of a vapor barrier would prevent the soil wall from adsorbing and releasing moisture; therefore, we evaluated an additional case, Case 5, in which the vapor barrier used in Case 2 was removed. Figure 6 shows the resulting moisture content and relative humidity on the northern soil wall of zashiki. The figure demonstrates that without a vapor barrier, the moisture content on the interior surface of the soil wall changed dramatically, indicating that the soil adsorbed and released moisture. However, when the relative humidity was lower than 100%, no condensation occurred.

5. Conclusions

The Kyo-machiya renovation plan significantly influenced the soil buffering effect. The following conclusions can be drawn based on the results of the simulations conducted in this study:

1. Insulation must be combined with enhanced airtightness to improve renovation effectiveness.
2. Partial insulation is inadequate for reaching the target temperature.
3. Exterior insulation is the preferred option; however, when not feasible, interior insulation can be effective. In both cases, a vapor barrier was unnecessary because of the ability of the soil wall to adsorb moisture. Considering the difficulty of applying a vapor barrier, this could provide useful information in practice.

However, as no humidifier was considered in these simulations, the full risk of condensation without a vapor barrier remains to be evaluated. In addition, although the relative humidity of the soil wall remained below 100% after the vapor barrier was removed, condensation still may occur between the wall and wooden beams. Therefore, a two-dimensional calculation should be conducted in future research to confirm moisture dispersion on the soil wall surface.

References

- [1] Kyoto as a city of History. Available online: <https://www.city.kyoto.lg.jp/sogo/page/0000305428.html> (accessed on 30 December 2022)
- [2] Matsubara S and Matsubara N 1991 *Energy Build.* **16** 851-60
- [3] Hosham A and Kubota T 2019 *Buildings* **9** 22
- [4] Iba C, Kaihara N and Honma Y 2019 *Journal of the Housing Research Foundation* **45** 35-46 (in Japanese)
- [5] Ooka R, 2002 *Build. Environ.* **37** 319-29
- [6] Iba C and Hokoi S 2022 *Energies* **15** 1913
- [7] Yokobayashi S and Sato M 2015 *Energy Procedia* **78** 2814-19
- [8] Ishikawa K, Iba C, Ogura D, Hokoi S and Yokoyama M 2021 *Energies* **14** 3309
- [9] Nakajima M, Hokoi S, Ogura D and Iba C 2020 *Build. Environ.* **169** 106575
- [10] Ko Y 2016 *Evaluation of Preference, Thermal Comfort and Environment Control Behavior of Residents in Kyo-machiya* (Master's Thesis: Kyoto University, in Japanese)



Aalborg Universitet

AALBORG UNIVERSITY
DENMARK

The impact of the solar absorption coefficient of roof and wall surfaces on energy use and peak demand

Salonvaara, Mikael ; Desjarlais, André

DOI (link to publication from Publisher):
[10.54337/aau541650886](https://doi.org/10.54337/aau541650886)

[Link to publication from Aalborg University](#)

Citation for published version (APA):

Salonvaara, M., & Desjarlais, A. (2023). The impact of the solar absorption coefficient of roof and wall surfaces on energy use and peak demand. In H. Johra (Ed.), *NSB 2023 - Book of Technical Papers: 13th Nordic Symposium on Building Physics* (Vol. 13). [350] Department of the Built Environment, Aalborg University. <https://doi.org/10.54337/aau541650886>

The impact of the solar absorption coefficient of roof and wall surfaces on energy use and peak demand

Mikael Salonvaara¹ and André Desjarlais¹

¹Building Envelope Materials Research, Oak Ridge National Laboratory, Oak Ridge, TN 37830, USA

Abstract. Climate change, electrification to decarbonize the building sector, and the rise of renewable energy sources have made reducing the peak demand even more important than solely reducing the overall energy use. Solar radiation can have a significant impact on the energy use of buildings. However, previous studies on solar absorption in building envelopes have focused on cool roofs. Less effort has been made to evaluate the impact of solar radiation on heat loss and gain on walls. This paper summarizes a preliminary study to estimate the magnitude of the benefit low solar absorptance surfaces have on reducing peak demand and focuses on simulating a residential building with two types of U.S. code-compliant wall structures, a standard lightweight wall assembly, and a thermally massive mass timber wall, to evaluate the impact of the solar absorption coefficient of the surfaces on the heating and cooling energy use and peak demand. This effort aimed to identify whether a more comprehensive study should be undertaken to develop further the calculation tools previously developed for estimating the energy benefits for roofing systems in the U.S. by adding a similar tool for wall assemblies. Reducing the solar absorption coefficient from 0.9 to 0.3 resulted in up to 46% lower cooling demand and a 70% increase in heating demand depending on the climate. Peak demand reductions for heating and cooling energy were similar to the reduction in heating or cooling energy use. However, the annual energy use changed up to only 12% as lowering the solar absorption coefficient reduces cooling demand but increases heating demand. Whether the total impact overall is harmful or beneficial depends on the climate and type of structure. Additionally, a cool roof calculator was used to estimate the impact of solar radiation on roofs. The learning from this study is that the exterior color and the solar absorption coefficient should be chosen based on the climate to positively impact the energy use profile and peak demand.

1. Background

A sharp peak in electrical demand can be observed in almost every building during the busiest hours of the day. Although a share of this peak may be attributed to equipment used in the building, a significant portion is caused by increased demand for air conditioning in the late afternoon/early evening. The peak in demand requires additional power plant capacity; causes more demand than supply in the power grid, requires the utility to purchase power at typically higher rates to satisfy the demand; and may result in increased air pollution. Most importantly for the building owner or tenants, unnecessary peak demand may result in monthly charges many times higher than base electrical rates. One of the best approaches to shrink peak demand is to reduce the heat load on a building, especially the solar load that drives the need for air conditioning. Few passive heat reduction strategies can match the energy-saving potential of modern reflective roofing technology. Unfortunately, the energy impacts of solar-reflective walls are less well documented. To help building owners and designers become more cognizant of peak electrical

demand's energy and economic impact, this research quantifies the reductions in peak demand, greenhouse gas emissions, and economic costs associated with cool roof and wall technologies. This information is especially important since few articles to date on building energy savings have adequately addressed peak demand issues. When deciding on the paint color of walls, little consideration is usually placed on how it impacts energy use and peak demand. White brick and black walls have become a fashion statement in recent years. For white and black paint, the solar absorption coefficient can range between 0.3 and 0.9.

2. Impact of solar absorption on walls and building energy use

The whole-building simulation model EnergyPlus™ v22 [5] was used to evaluate the impact of wall solar absorption on the DOE prototype building [6]. The DOE prototype building, following the IECC 2021 energy code [7], used in the simulations is a two-story, single-family building on a slab. A heat pump provides heating and cooling. The conditioned window-to-wall ratio is 15%. The conditioned area is 220 m² (2,377 ft²),

The simulations included two different U.S. code-compliant wall types: a lightweight wall and a solid mass timber wall. The schematics of the walls and the layer thicknesses are shown in Figure 1. The lightweight base wall is a 2x4 wood framed wall (38 mm x 89 mm) with insulation having an R-value of 2.29 m²K/W and 400 mm on-center framing. Table 1 lists the continuous insulation values and mass timber thickness used in the simulations that meet U.S. code requirements for these three climate zones. The three climates used in the simulations are the hot-humid Houston, TX; mild Los Angeles, CA; and cold Golden, CO.

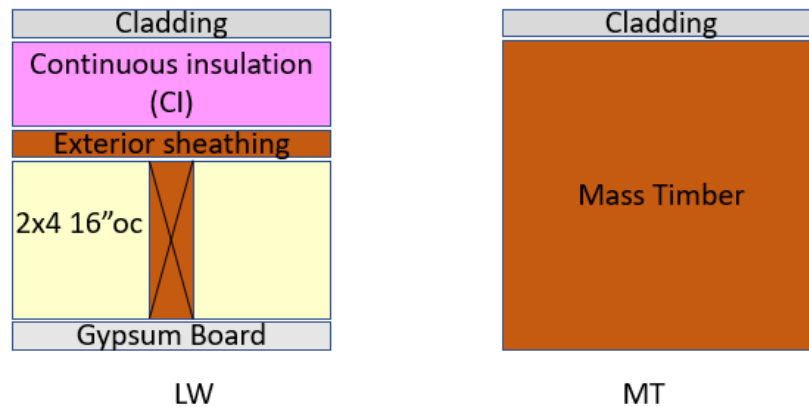


Figure 1. The lightweight (LW) and the mass timber (MT) walls used in the annual simulations.

Table 1. Climate zone, location, and layer descriptions for the lightweight and mass timber walls used in simulations.

Climate zone, city, state	Lightweight wall continuous insulation R-value (m ² K/W) and whole wall U-value (W/m ² K)	Mass timber wall thickness and U-value (W/m ² K)
2A, Houston, TX	No continuous insulation, U-0.47	152 mm mass wood, 0.69
3B, Los Angeles, CA	25 mm extruded polystyrene R-0.88, U-0.35	175 mm mass wood, 0.55
5B, Golden, CO	51 mm extruded polystyrene R-1.76, U-0.27	240 mm mass wood, 0.46

2.1. Impact of wall solar absorption on annual heating and cooling energy use

Table 2 shows the annual heating and cooling energy uses of the lightweight (LW) and mass timber (MT) buildings with different solar absorption coefficients on walls relative to the absorption coefficient of 0.7. The largest impact is in the mild climate of Los Angeles, CA, where the heating and cooling

energy use can almost double or cut in half depending on the choice of exterior color of the walls. However, we can also see that the impact on the total energy use is much less due to the opposite impacts of solar absorption on heating and cooling.

Table 2. Annual energy uses relative to building with wall solar absorption coefficient of 0.7. LW=lightweight wall building, MT=mass timber wall building, MT(LW)=mass timber wall building with the same wall U-value as in the lightweight wall.

Energy use	City, state	Wall	Solar absorption coefficient			
			0.3	0.5	0.7	0.9
Heating	Houston, TX	LW	108%	104%	100%	97%
		MT	117%	108%	100%	93%
		MT(LW)	113%	106%	100%	94%
	Los Angeles, CA	LW	115%	107%	100%	94%
		MT	143%	120%	100%	84%
	Golden, CO	LW	107%	103%	100%	97%
Cooling	Houston, TX	MT	111%	105%	100%	95%
		LW	89%	95%	100%	105%
		MT	87%	93%	100%	107%
	Los Angeles, CA	MT(LW)	90%	95%	100%	105%
		LW	74%	87%	100%	114%
	Golden, CO	MT	65%	82%	100%	120%
Total, including fan energy	Houston, TX	LW	87%	94%	100%	106%
		MT	82%	91%	100%	109%
		MT(LW)	96%	98%	100%	102%
	Los Angeles, CA	MT	97%	99%	100%	102%
		LW	92%	96%	100%	105%
	Golden, CO	MT	102%	100%	100%	103%
	Golden, CO	LW	104%	102%	100%	99%
		MT	107%	103%	100%	97%

The impact of the solar absorption coefficient is stronger in the building with mass walls. Table 3 shows the relative performance of the building with mass timber walls as compared to the lightweight wall building. For example, when the solar absorption coefficient is 0.9 on walls, the mass timber building consumes about 18% less heating or cooling energy than the lightweight wall building in Los Angeles, CA. However, when the solar absorption coefficient changes to 0.3, heating energy use is 14% more, and cooling energy use is 31% less in the mass timber building than in the lightweight wall building. The same impact of thermal mass can be seen in Houston, TX: A building with mass walls having the same U-value as in the lightweight building (MT(LW) in Table 2). The lightweight wall building in Houston, TX, was converted into the thermally massive one with the same U-value. The building with thermally massive walls experienced lower annual heating and cooling energy use than the building with lightweight walls. The wall solar absorptance had the same relative change in cooling in both buildings but a higher relative impact on heating in the mass wall building.

Table 3. Relative annual energy performance of the mass timber wall building to the lightweight wall building (annual energy use in the mass timber building/annual energy use in the lightweight building).

Energy use	City, State	Solar absorption coefficient			
		0.3	0.5	0.7	0.9
Heating	Houston, TX	107%	103%	99%	96%
	Los Angeles, CA	114%	103%	91%	82%
	Golden, CO	122%	120%	117%	115%
Cooling	Houston, TX	99%	100%	101%	102%
	Los Angeles, CA	69%	73%	77%	82%
	Golden, CO	82%	85%	88%	90%
Total, including fan energy	Houston, TX	102%	101%	100%	100%
	Los Angeles, CA	94%	89%	85%	83%
	Golden, CO	116%	114%	112%	110%

2.2. Impact of wall solar absorption on cooling peak demand

The absorption of solar energy on walls significantly impacts the buildings' peak cooling demand. The largest relative impact in this study was in Los Angeles, CA, which has mild heating and cooling demand. Figure 2 shows the impact of the solar absorption coefficient on the peak cooling demand in the lightweight and mass timber buildings in the three climates. The effect of solar is slightly higher in the mass timber building. Los Angeles, CA, experiences the strongest impact of solar in the relative performance, followed by Houston, TX, and then Golden, CO.

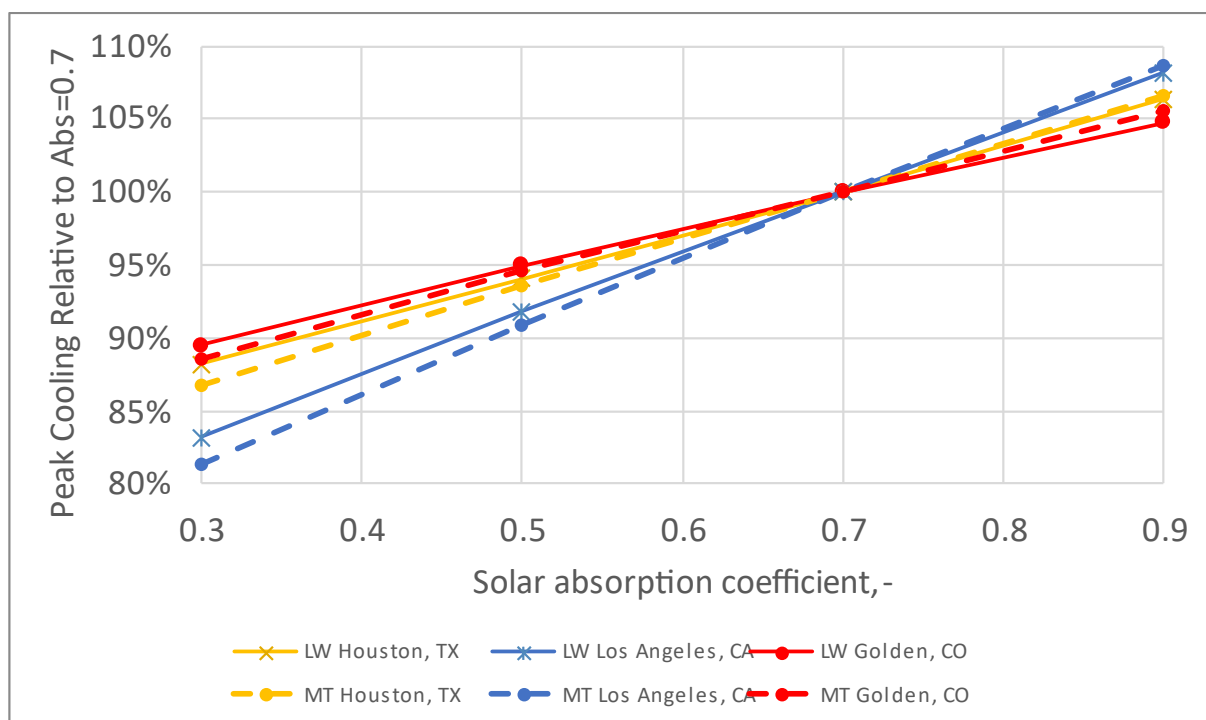


Figure 2. Impact of solar absorption coefficient on cooling power as a function of solar absorption coefficient in three climates and buildings with either lightweight or mass timber wall assemblies. Comparison is relative to the solar absorption coefficient of 0.7.

3. Impact of solar radiation on roofs

To better understand the benefits of low-slope cool roofs in reducing peak energy demand, researchers at Oak Ridge National Laboratory performed a cursory examination of the seasonal variation in peak electric demand for a variety of different climates across North America using a web-based interactive tool dubbed the “DOE Cool Roof Calculator” [1,2] which was developed and validated using models [3] and field data [4]. We evaluated the energy benefit of a cool roof applied to an 1860 m² (20,000 ft²) roof with IECC 2021-compliant insulation levels [7]. Energy costs [8,9] and equipment efficiencies (air conditioning COP of 2.5 and furnace efficiency of 85 percent) were typical for 2021, and we assumed a peak demand charge of \$25/kW. We modeled the energy and cost differences between roof surfaces having a solar reflectance of 0.05 and 0.60 with a thermal emittance of 0.90. Their findings suggest that even though usage savings may be higher in hot climates than in cooler climates, almost all climates exhibit a seasonal variation in the peaks for roof-related air conditioning demand. A summary of their findings is shown in Table 4.

Table 4. The annual energy cost savings in eight climate zones and cities in the U.S. when solar reflectance is changed from 0.05 to 0.60.

Climate Zone	City	R-value		Annual Savings, US\$		
		m ² K/ W	hr ft ² F/Btu	Usage	Demand	Total
1	Miami, FL	4.4	25	\$1,060	\$860	\$1,920
2	Houston, TX	4.4	25	\$400	\$820	\$1,220
3	Atlanta, GA	4.4	25	\$380	\$840	\$1,220
4	Baltimore, MD	5.3	30	\$120	\$680	\$800
5	Chicago, IL	5.3	30	-\$140	\$680	\$540
6	Minneapolis, MN	5.3	30	-\$100	\$680	\$580
7	Fargo, ND	6.2	35	-\$200	\$580	\$380
8	Fairbanks, AK	6.2	35	-\$1,320	\$500	-\$820

As illustrated in Table 4, the total value of usage plus demand energy savings offered by the cool roof is sizable, averaging more than \$800 annually in many climate zones for a typical commercial building. Consequently, cool surfaces may offer a significant opportunity for net energy cost savings even at the highest levels of insulation mandated by the latest building codes. Moreover, the savings value of cool surfaces is further reinforced because modern cool surfaces frequently cost no more than darker non-cool surfaces. As a result, all the savings identified in the analysis tend to drop to the bottom line without additional cost encumbrances.

One of the most striking results from this analysis is that the estimated cost savings due to peak energy demand reduction provide a substantial majority of the net heating and cooling energy cost savings throughout all climate zones studied. In fact, peak demand savings account for over 40% of total cost savings in the warmest climate zones and up to 100% in the coldest climate zones. In addition, while energy use cost savings vary widely by climate zone (falling to negative values in the coldest climates), peak demand cost savings tend to be more significant and consistent throughout all climate zones. Similarly, in a field study, Parker et al. [10] found 10% savings in cooling energy use, while peak demand was reduced by 35% when increasing the solar reflectance of a commercial roof from 0.23 to 0.68. Consequently, the analysis suggests that any projection of cool roof cost savings that neglects to include peak demand reduction has little chance of providing an accurate estimate.

4. Conclusions

The authors investigated a limited set of assemblies and climates for this paper. The simulations for walls and roofs with a range of solar absorption coefficients show a significant impact of solar radiation on the roofs and the walls on the heating and cooling energy use and peak demand. In addition to the immediate economics of peak demand, other savings associated with peak demand need to be considered. Because additional electrical generating capacity is required to meet peak demand levels, this will likely lead to increased air pollution and environmental impacts due to the need to construct new generating facilities and the less-than-efficient operation of existing facilities. Peak power demand is also strongly associated with the overall heating of large cities and urban areas, commonly referred to as the urban heat island effect (UHIE). Increased warming of urban areas may lead to increased production and accumulation of ground-level ozone, which may lead to increased health risks and a growing number of “Ozone Action Days” in cities and towns. Finally, increasing peak electricity demand may increase the potential for “brownouts,” especially during unusually hot weather events. Using cool surfaces to prevent these impacts can contribute to environmental justice efforts since pollution from peak power plants, the UHI effect, and brownouts and blackouts disproportionately affect lower-income areas and communities of color.

Acknowledgments

This manuscript has been authored in part by UT-Battelle, LLC, under contract DE-AC05-00OR22725 with the U.S. Department of Energy (DOE). The publisher acknowledges the U.S. government license to provide public access under the DOE Public Access Plan (<http://energy.gov/downloads/doe-public-access-plan>).

References

- [1] Petrie, T.W., J.A. Atchley, P.W. Childs, and A.O. Desjarlais. 2001. Effect of solar radiation control on energy costs— A radiation control fact sheet for low-slope roofs. *Proceedings on CD, Performance of the Exterior Envelopes of Whole Buildings VIII: Integration of Building Envelopes* Atlanta, Ga.: American Society of Heating, Refrigerating and Air-Conditioning Engineers, Inc.
- [2] Petrie, T. W., Wilkes, K. E., & Desjarlais, A. O. (2004). “Effects of Solar Radiation Control on Electricity Demand Charges – An Addition to the DOE Cool Roof Calculator.” *Proceedings of the Performance of the Exterior Envelope of Whole Buildings IX International Conference*, December 5-10, 2004.
- [3] Wilkes, K.E. 1989. Model for roof thermal performance. Report ORNL/CON-274. Oak Ridge, Tenn.: Oak Ridge National Laboratory.
- [4] Wilkes, K.E., T.W. Petrie, J.A. Atchley, and P.W. Childs. 2000. Roof heating and cooling loads in various climates for the range of solar reflectances and infrared emittances observed for weathered coatings. *Proceedings 2000 ACEEE Summer Study on Energy Efficiency in Buildings*, pp. 3.361-3.372 Washington, D.C.: American Council for an Energy Efficient Economy.
- [5] U.S. Department of Energy (2022). “EnergyPlus Energy Simulation Software.” Washington, D.C. www.energyplus.net.
- [6] U.S. Department of Energy (2021). “Prototype Building Models. Residential.” Washington, D.C.: <https://www.energycodes.gov/prototype-building-models>
- [7] International Energy Conservation Code (IECC (2021). <https://codes.iccsafe.org/content/IECC2021P1>.
- [8] U.S. Energy Information Administration (2022). *State Electricity Profiles*. www.eia.gov.
- [9] U.S. Energy Information Administration (2022). *Natural gas prices*. www.eia.gov.
- [10] Parker, D., Sherwin, J., Sonne, J., Barkaszi, S., "Demonstration of Cooling Savings of Light Colored Roof Surfacing in Florida Commercial Buildings: Our Savior's School," Lawrence Berkeley Laboratories, Florida Power and Light Company, Florida Energy Office, June, 1996. <http://www.fsec.ucf.edu/en/publications/html/fsec-cr-904-96/>.



Aalborg Universitet

AALBORG UNIVERSITY
DENMARK

Laboratory tests on decay of natural fibre insulation materials suggest a more differentiated evaluation and higher RH thresholds

Tanaka, Eri; Schwerd, Regina; Hofbauer, Wolfgang; Zirkelbach, Daniel

DOI (link to publication from Publisher):
[10.54337/aau541651346](https://doi.org/10.54337/aau541651346)

[Link to publication from Aalborg University](#)

Citation for published version (APA):

Tanaka, E., Schwerd, R., Hofbauer, W., & Zirkelbach, D. (2023). Laboratory tests on decay of natural fibre insulation materials suggest a more differentiated evaluation and higher RH thresholds. In H. Johra (Ed.), *NSB 2023 - Book of Technical Papers: 13th Nordic Symposium on Building Physics* (Vol. 13). [370] Department of the Built Environment, Aalborg University. <https://doi.org/10.54337/aau541651346>

Laboratory tests on decay of natural fibre insulation materials suggest a more differentiated evaluation and higher RH thresholds

E Tanaka¹, R Schwerd¹, N Krueger¹, W Hofbauer¹, D Zirkelbach¹

¹Fraunhofer-Institute for Building Physics, Fraunhoferstr. 10, 83626 Valley, Germany

daniel.zirkelbach@ibp.fraunhofer.de

Abstract. To reduce CO₂ emissions and save grey energy, natural materials like wood and wooden materials are becoming more and more important. However, these products are particularly sensitive to moisture, as they can be attacked by mould or decay fungi. In contrast to mould growth, which typically is associated with visual impairment and health problems, the growth of decay fungi may result in structural defects which clearly must be excluded. Up to now it is mostly assumed that wooden materials are more sensitive to such attack than solid wood. Therefore, different wood fibre insulation materials were inoculated with decay fungi and exposed to different climates to determine the requirements for the decay process and to compare them with the requirements of decay by the same fungi of solid wood. The results prove that some natural fibre materials are equally or even more resistant to decay fungi than solid wood, while others are less. The resistant products can therefore be assessed like solid wood – for which already temperature dependent thresholds and in part also transient decay prediction models are available. Maybe even specific higher moisture levels can be acceptable. However, the results also suggest a differentiated view on natural fibre insulations, as they have a very different susceptibility to wood decay. Uniform and significantly lower limits than for solid wood are not justified.

1. Introduction

While building materials made from renewable raw materials have many advantages for reasons of sustainability and carbon footprint, and are therefore increasingly favoured, their widespread use is often hindered by uncertainty regarding moisture sensitivity and decay, which often result in not precisely known application limits.

Under European outdoor climate, the occurring combinations of relative humidity (RH) and temperature may allow for microbial growths like algae or mould over significant periods of the year. At least on materials, exposed to the outdoor climate directly on the exterior surface or behind a vented or ventilated facade or roof cover, mould growth cannot be completely excluded, it can only be limited to an uncritical level. Absolute limit values for RH, independent on the temperature, are pretty unrealistic and hardly helpful. A more accurate transient approach for such a definition of the uncritical level was presented in [1] based on the mould growth prediction models described in [2] and [3]. Also ASHRAE standard 160 does not limit the acceptable mould growth level to zero, which is rather unrealistic, but generally to a mould index (MI) value of 3 according to [3][4][5]. Especially at low temperatures and high humidity levels as well as in parts of the construction without air gaps, decay fungi can pose a higher risk than mould growth. This can be derived from the limit curves for wood rot, which are below the ones for

mould growth in the temperature range below approximately 3 °C [2][5] but also from practical experience, where obvious mould growth conditions according to the available models but no mould growth were observed [6]. In difference to mould, the growth of rot fungi often does not become visible directly and is normally only observed or detected by damages or mass loss. That means, in analogy to the mould evaluation that a starting growth of the rot fungi in the materials is accepted, while mass loss generally has to be avoided. Thus, the mass loss would be comparable to MI 3 which serves as critical limit for mould growth. According to the WTA guidelines for wooden constructions and interior insulations [8][9] it is common practice, to verify the inner part of the constructions (especially inside the airtightness layer) concerning mould growth, but not the interface between interior insulation and wall or the exterior parts of wooden constructions. The mould risk is avoided or limited to an uncritical level by a largely airtight and gap-free construction method. However, if wood or wooden materials are present at these positions, the decay risk must be analysed.

Up to now, limit values specified in standards and guidelines for such materials have been generally quite low, which considerably restricts their range of application. Manufacturers, however, claim to have good experience beyond the previously permissible areas of application. For solid wood, many investigations on durability and moisture respectively decay fungi resistance have already been performed. Also moisture and temperature dependent limit curves [9][10][11][12] as well as transient evaluation models are either already available [13][14][15] or will be available in near future [16]. Such transient models allow for a more sophisticated evaluation depending on coinciding heat and moisture conditions and their duration. For this reason, laboratory investigations were carried out on wood fibre insulation materials [13] to compare the moisture and decay fungi resistivity of wood fibre interior insulation materials to the one of solid wood at different critical temperature and humidity conditions (preliminary results after 20 weeks of incubation were published in [17]). The gained results are a first step into the direction of a more accurate transient evaluation of the hygrothermal conditions occurring in wooden and other natural fibre materials concerning infestation by wood decay fungi.

2. Setup of the decay investigations in the laboratory

For the lab tests, four typical wood fibre materials, which are used as interior insulation according to the specifications of the manufacturers, are compared to pine sapwood, which can be considered one of the most sensitive solid woods. The materials represent typical categories like rigid insulation boards or flexible mats, different levels of hydrophobization as well as dry and wet production process. Test specimens of 50 mm x 50 mm are used with a thickness of 40 mm for the fibre insulation and 10 mm for the solid pine sapwood samples. The products are described in **Table 1** as far as the information was made available by the manufacturers. Pictures of the specimens are provided in **Figure 1** and **Figure 2**.

Table 1: Wood fibre insulation materials for interior insulation used for the lab tests.

Material Index	Short description	Product information
A	Dry insulation board 0.5 %	dry production process, density 110 kg/m ³ with hydrophobic agent: 0.5 % by mass
B	Dry insulation board 0.8 %	dry production process, density 150 kg/m ³ with hydrophobic agent: 0.8 % by mass
C	Flexible fibre mat	dry production process, density 60 kg/m ³ with flame retarding agent / no hydrophobic agent
D	Wet insulation board	wet production process, density 160 kg/m ³ no hydrophobic agent

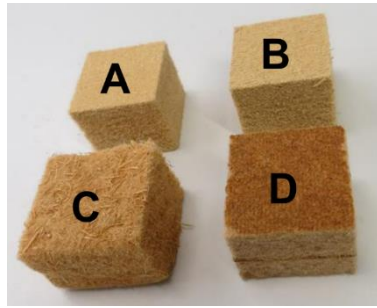


Figure 1: The four investigated wood fibre insulation materials



Figure 2: The reference material solid pine sapwood

As test fungi three different decay fungi are used, which are either commonly used for decay tests in the standards or are under suspicion to have a high affinity for wood fibre materials: *Coniophora puteana* (DSM 3085), *Trametes versicolor* (DSM 3086) and *Schizophyllum commune* (HOKI F 00315, proprietary isolate). In addition, *Serpula lacrymans* (CBS 235.33) was used in the investigations. *S. lacrymans* is responsible for many severe damages in building practice. The inoculation with the test fungi is performed by overgrown (untreated) pinewood dowels to avoid transfer of nutrients together with the mycelium (**Figure 3** and **Figure 4**).

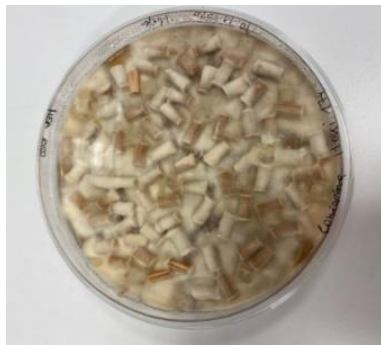


Figure 3: Overgrown wooden dowels with test fungi *Coniophora puteana*



Figure 4: Transfer of the dowels into the test specimen for inoculation

Each specimen is equipped with four dowels, each for one of the four fungi. While the growth of the different species on and around the dowels can be observed separately, the mass loss can be only measured as one single value for all species. Despite this disadvantage, an inoculation with four dowels was chosen to reduce the number of specimens to a feasible level of 180 in 6 incubation units. The inoculated test specimens (pre-conditioned to constant weight at the target climate) are placed in sterilized and airtight incubation units and exposed to constant high RH values of 95, 97 and 100 % RH at 25 °C - conditions just below respectively in a favourable range for decay fungi growth, proven in previous studies like [10]. The whole test setup for the inoculation period of about 340 days is shown in **Figure 5**.

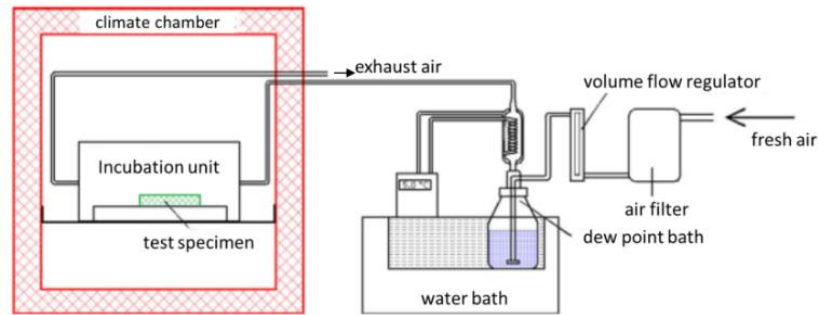


Figure 5: Test setup for the incubation period in the lab with climate chamber, incubation unit and supply of preconditioned and filtered air, first used in [18], [19].

3. Evaluation of the test results

Start and progress of the decay fungi growth was observed by different methods: visual observation by the naked eye and by the means of a stereo magnifying glass, qualitative description of the recognizable biological processes by a biological index, quantification of the mycelium cover of the surface, spread of the mycelium inside the opened specimens and determination of the mass loss of the specimens.

3.1 Visual observation

At the beginning the decay fungi mycelium was growing mainly on the dowels itself and only small differences could be observed between the different specimens: After 23 weeks (**Figure 6**) the tendency of strongest superficial growth on the pine samples was already recognizable, followed by the “wet” board D and the two “dry” boards B and A. The flexible fibre mat C shows no growth at all – also the initial mycelium growth only on the dowel had disappeared. This observation was more and more increased until the end of the investigation period after 48 weeks (**Figure 7**).

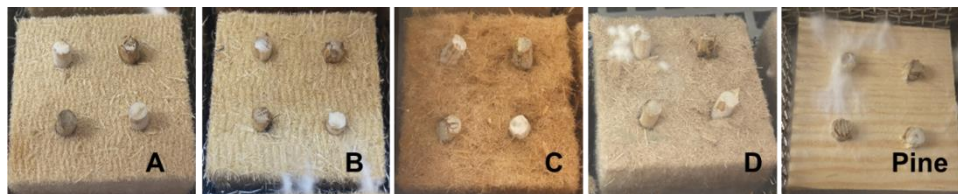


Figure 6: Visual observation after 23 weeks: Strongest decay mycelium growth on pine, followed by the “wet” board D and the “dry” boards B and A. C shows no growth at all – also the initial mycelium growth only on the dowel has disappeared.

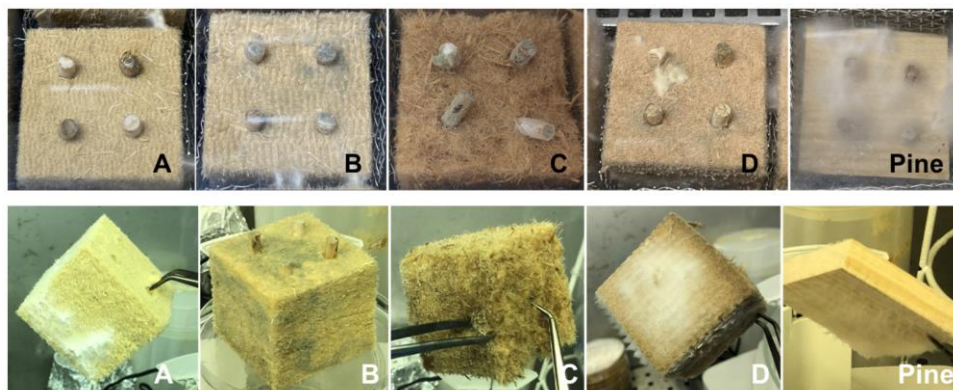


Figure 7: Visual observation after 48 weeks: View from the top (top) and from the bottom or side (bottom). Strongest growth of decay fungi mycelium on the pine specimen, but present also on all other specimens.

Unfortunately, and despite all precautions, mould growth could not be avoided in all cases. While it was initially feared that the mould would completely displace the rot, the results show that, even in case of mould appearance in the incubation unit, the white decay fungi mycelium was only temporarily reduced, but still present on the sides or bottom surfaces at the end of the test period.

3.2 Index evaluation

A second evaluation describes the visible biological processes in a scale, which is described in **Table 2**. The scale is clearly non-linear and more qualitative than quantitative. However, levels 0 to 2 mean either no growth or growth mainly on the dowel, but not on the specimen itself. As mainly the specimen is of interest and only small influence from the material type on the growth on the dowels is assumed, primarily levels above 2.5 or 3 are of relevance.

Table 2: Index of observed biological processes

Level	Description
0	No Growth visible
1	Little growth on the dowel
2	Strong growth on the dowel
2.5	Growth also on the material around the dowel
2.8	Growth also visible on other dowels
3	Expansion of the growth over the whole specimen
3.5	Expansion of the growth over the whole specimen, white hyphens visible also in distance from the dowels
3.6	Expansion of the growth over the whole specimen, white hyphens visible also in distance from the dowels but stronger than at 3.5
3.8	Expansion of the growth over the whole specimen, white hyphens visible also in distance from the dowels but stronger than at 3.6

The results of this second evaluation are shown in **Figure 8** for the first 133 days. As expected, with higher RH levels the microbial growth is accelerated. In the box with only 95 % RH most materials remain below 2.5 and only the dry board B just reaches 3.0. At 97 % RH, the pine wood samples show the most critical results above a level of 3 which is exceeded after 70 days. The wet board values increase slightly later and lower, the other boards do not exceed the value of 3.0. In the box with 100 % RH all materials except the flexible mat exceed 3.0 after about 40 days. Wet board and solid wood behave very similar and reach values of 3.5, the two dry boards remain slightly lower. However, due to the non-linear scale and a certain dominance of the values up to 3.0, which are of little relevance for the assessment of the fibre materials themselves, this evaluation alone does not allow a clear differentiation between some materials.

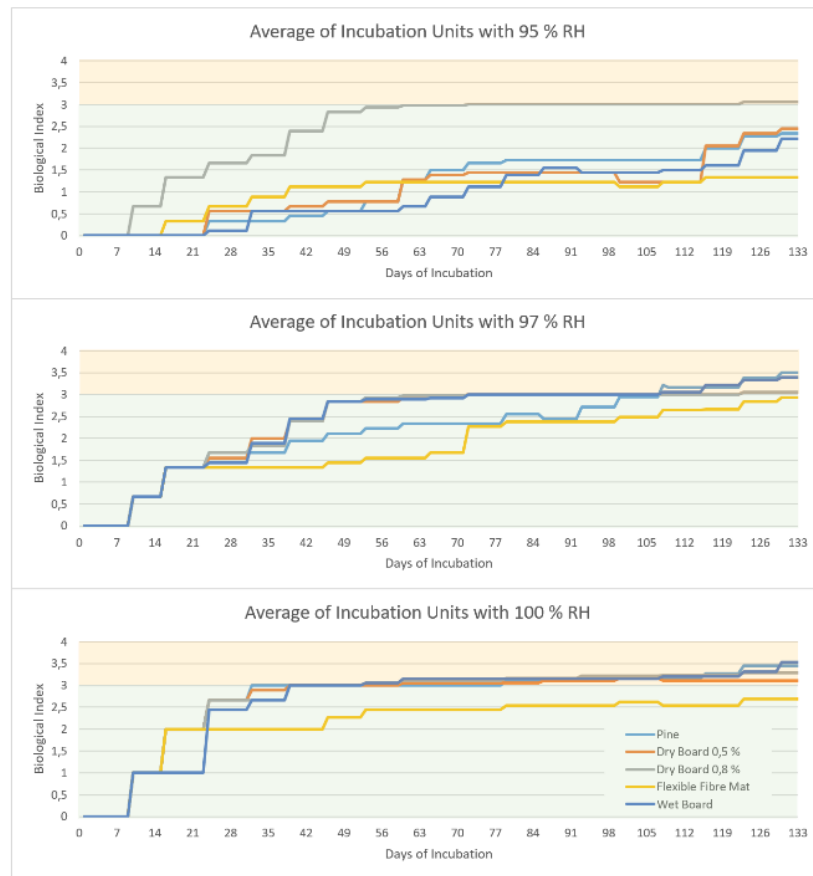


Figure 8: Index acc. to **Table 2** during the first 133 days: Different growths speed on the dowels of the test materials and the reference specimens at the three RH levels. Only pine and the wet board reach values up to 3.5 in that period.

Therefore, an additional indicator was introduced: the cover ratio of the mycelium on the visible specimen surface in percent on average of the same type of material. The estimation of the cover ratio was obtained by means of a grid which was applied schematically on the surface of the specimen. The given values are average values ($n = \max. 9$, as the number of specimens was reduced by sampling for mass loss evaluation throughout the duration of the test). The results are presented in **Figure 9** (bottom) after 200 days of incubation in addition to the previous evaluation. The scale value difference between the solid wood and the wet fibre board is with 3.8 to 3.6 only very small. If additionally, the surface cover ratio is considered, the difference becomes much clearer with about 23 % in case of the solid pine wood to only 9 % in case of the wet fibre board. The two dry boards A and B only show a surface cover ratio below 4 % and the flexible fibre mat still no growth at all. Thus, the surface cover for the solid wood is a factor of 2.5 higher compared to the wet board, 5 times higher than dry board B and 10 times higher than dry board A.

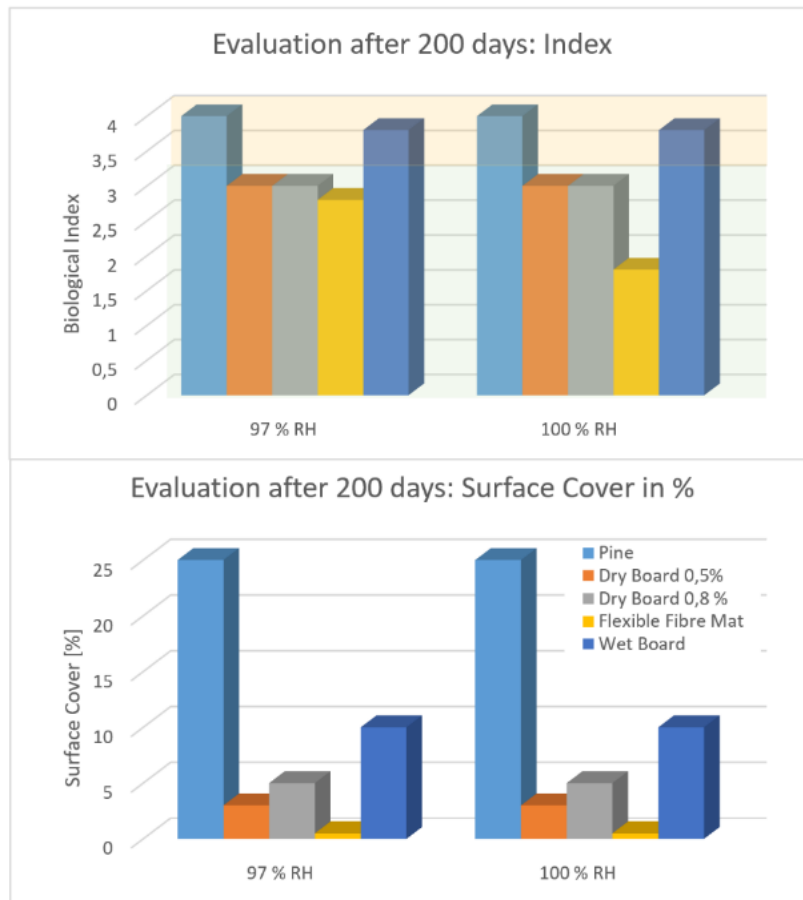


Figure 9: Index acc. to **Table 2** after 200 days (top) and coverage of the specimen surface with decay mycelium in percent (bottom) in the boxes with initially 97 % RH (left) and 100 % RH (right).

3.3 Mass loss evaluation

The third evaluation is based on the measurement of mass loss over time, which was performed after 20, 26, 35 and 48 weeks on three specimens in each case. The resulting average values are presented in **Figure 10**. For decay tests in the laboratory, normally only mass losses more than 5 % are to be regarded as unambiguous. This limit is indicated as dashed red line in the figure for orientation. In case of the flexible fibre mat, the results are not reliable due to excessive fibre loss of the specimens that became unstable with increasing humidity. As this result is in contradiction with the observations of the first two evaluations, where no microbial growth at all was observed on this material, the indicated mass loss seems not to be caused by material degradation. The results of material C are therefore greyed out.

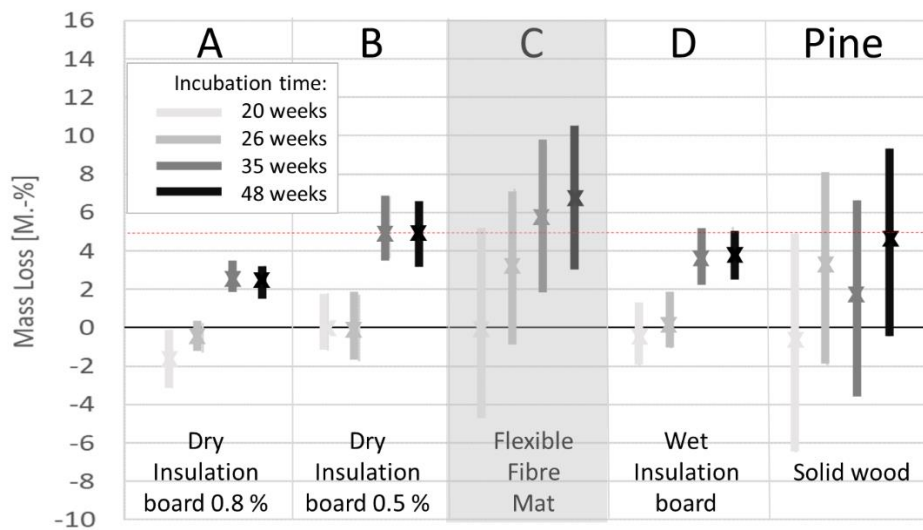


Figure 10: Evaluation of mass loss after 20, 26, 35 and 48 weeks

For the other materials, as expected, an increasing mass loss over time can be observed. Considering all four measurements the mass loss of the pine samples is higher than the mass loss of the three evaluable fibre materials A, B and D. Material B has slightly higher losses when only the third and fourth measurements are considered. However, some loss of fibers cannot be completely ruled out for the other materials either. Therefore, the ranking concerning the mass loss is as following: highest losses for the pine specimens, similar but slightly lower values for the dry board B, followed by the wet board D and lowest losses for the dry board A.

4. Discussion of the lab test results

The measured mass loss was smaller than expected, especially when compared to former investigations like [13] or [15], which showed under similar favorable conditions (temperature > 20 °C and high humidity near 100 % RH) sometimes more than 20 % mass loss after only 4 months. In the first weeks of the test period, presumably slightly lower humidity conditions than planned prevailed in the incubation units. This may have slowed down and delayed the decay process to a certain extent. Certainly, the occurring mold growth may have had a retarding effect on the wood rot processes. To check whether the rot fungi have been affected by drought or mold, the vitality of the fungi on the dowels (taken from the specimens after 48 weeks). was verified by growing them again on nutrient medium in petri dishes at the end of the test procedure in the lab. After only four days the mycelium of the decay fungi became visible again in all four petri dishes, although cross contaminations cannot entirely be excluded. However, this confirms that the decay fungi were still alive and active, even if no strong degradation could be observed. In addition, current results from another ongoing research project [20] with the same incubation method also show similar low mass loss values.

Additionally, other effects can influence the mass loss level. One point is the relation between fungi mycelium and specimen size, which may play an important role: the more fungi mass is added, the higher will be the initial mass loss of the specimen. In the mentioned previous investigations [5][15], the transferred mycelium was clearly bigger in relation to the specimen compared to the current investigation and presumably also included parts of the nutrient from the petri dishes, while now hardly any nutrients were transferred as only infested dowels were used. Therefore, the applied test method has the advantage that likely more realistic start conditions for the infestation are used.

It must therefore be assumed that every different test setup may also lead to different mass losses. The hygrothermal conditions without any mass loss (safe area) as well as the initiation period should not, in contrast, be affected by the test method. As in normal constructions in practice only spores but no

mycelia are present, all lab tests can be assumed to be on the safe side concerning the duration until the start of material degradation. However, after the start, the degradation could also proceed faster in practice, as far as the decay fungi can spread over a wider area of the material's surface, while in the lab no additional spores are available and the starting point is limited to the dowel.

In summary it can be stated that the results of the performed investigations showed significant growth of decay fungi mycelium and mass loss of the specimens. All fungi were still alive at the end of the tests and the question, whether the examined wood fibre materials or the solid wood specimens are more resistant against decay fungi could be clearly answered - even if quantitative statements are only possible to a limited extent due to the partly unclear boundary conditions.

5. Conclusions and outlook

The four involved wood fibre materials show a rather good decay resistivity at high moisture levels and have proven to be more resistant against decay fungi than solid pine sapwood. Therefore, the same or even higher limit values or limit curves can be used for the evaluation of these materials like for solid wood. Such limits are currently available as limit curve depending on RH and temperature in WTA guideline 6-8 [9] but also as transient decay prediction model according to [10] and they are topic of current research in ongoing projects [16].

However, the presented proceeding is only valid for particularly moisture resistant wooden or natural fibre materials. In a follow-up project [20] currently further natural fibre materials are investigated, and preliminary results show that other wood fiber materials can also be clearly less resistant than solid wood. That means that the resistivity needs to be verified individually for every product. For this purpose, a preferably simple and quick laboratory test will be beneficial.

For the tests performed here, still four decay fungi were used. But the results here seem to indicate, that at least *Serpula lacrymans* and probably also *Trametes versicolor* are only of little relevance in the performed test and for the investigated materials, while *Coniophora puteana* and *Schizophyllum commune* seem to be the more critical fungi for that purpose. The results seem to proof that the materials show an analogous sensitivity at different temperatures and humidities. That would suggest that a single test under rather extreme boundaries, like the one, proposed in EN 113[21], could be sufficient for the classification "equal or more resistant than solid wood". However, this assumption needs to be verified using a much broader data base than the one available from this project. Furthermore, separate classes for different sensitivities will be required, adequately representing both lower and obviously higher resistance of different wood and natural fibre materials by individual limit value curves. Such classifications could simplify and improve the evaluation of the decay risk of constructions with materials made of natural fibre materials. On this basis, it can then also be better examined whether mould or decay is the relevant damage mechanism in each case.

Acknowledgement

The CORNET/IGF project 247 EBG In2EuroBuild was supported by the the Ministry of Economic Affairs and Climate Action on the basis of a decision by the German Bundestag via the AiF within the scope of the funding program of the Industrielle Gemeinschaftsforschung (IGF).

6. References

- [1] Viitanen H, Krus M, Ojanen T, Eitner V, Zirkelbach, D 2015 *Mold risk classification based on comparative evaluation of two established growth models*. (Energy Procedia 78 (2015), pp. 1425-1430 <http://dx.doi.org/10.1016/j.egypro.2015.11.165>
- [2] Sedlbauer K 2001 Prediction of mould fungus formation on the surface of and inside building components Stuttgart: Dissertation University Stuttgart
- [3] Viitanen H, Ritschkoff A 1991 *Mould growth in pine and spruce sapwood in relation to air humidity and temperature*. Uppsala: Swedish University of Agriculture Sciences, Department of Forest Products, 1991

- [4] ASHRAE Standard 160 2016 *Criteria for Moisture-Control Design Analysis in Buildings*. (Atlanta: American Society of Heating, Refrigerating, and Air-Conditioning Engineers)
- [5] Viitanen H et al. 1996 *The critical conditions causing mould and decay problems in buildings* Helsinki User-oriented and cost effective management, maintenance and modernization of building facilities, CIBW70 '96 Symposium ed. Aikivuori H and Aikivuori A Association of Finnish Civil Engineers RIL, 1996, pp. 435–438.
- [6] Nusser B, Teibinger M, Bednar T 2010 *Messtechnische Analyse flachgeneigter hölzerner Dachkonstruktionen mit Sparrenvollämmung Teil 1: Nicht belüftete Nacktdächer mit Folienabdichtung*. Bauphysik 32 (2010), Heft 3. S. 132-142
- [7] WTA-Merkblatt 6-4 2016 *Innendämmung nach WTA I: Planungsleitfaden* (Wissenschaftlich technische Arbeitsgemeinschaft Denkmalpflege und Bauwerkserhaltung) WTA Publications
- [8] WTA-Merkblatt 6-5 2014 *Innendämmung nach WTA II: Nachweis von Innendämmsystemen mittels numerischer Berechnungsverfahren* (Wissenschaftlich technische Arbeitsgemeinschaft Denkmalpflege und Bauwerkserhaltung) WTA Publications
- [9] WTA-Merkblatt 6-8 2016 *Feuchtetechnische Bewertung von Holzbauteilen - Vereinfachte Nachweise und Simulation*. (Wissenschaftlich technische Arbeitsgemeinschaft Denkmalpflege und Bauwerkserhaltung) WTA Publications
- [10] Viitanen H, Vinha J et al. 2010 *Moisture and Biodeterioration Risk of Building Materials and Structures*. Journal of Building Physics 33 3, p 201-224.
- [11] Kehl D, Plagge R and Grunewald J 2012 *Wann geht Holz kaputt? Nachweisteknische Beurteilung von Holz zerstörenden Pilzen*. 23. (Heringsdorf/Usedom: Hanseatische Sanierungstage) Beuth Verlag, Berlin, p 61-73.
- [12] Brischke C 2007 *Untersuchungen abbaubestimmender Faktoren zur Vorhersage der Gebrauchsdauer feuchtebeanspruchter Holzbauteile*. (Hamburg: Dissertation Universität Hamburg)
- [13] Zirkelbach D, Ruisinger U et al 2021 *Einheitlicher europäischer Leitfaden für die Innendämmung von Bestandsbauten und Baudenkmalern* (Project Report)
https://www.tihd-dresden.de/fileadmin/user_upload/pdf/Traegerverein/Projekte/IGF247EBG_IN2EuroBuild_Publikation.pdf
- [14] Saito H, Fukuda K and Sawachi T. 2012 *Integration model of hygrothermal analysis with decay process for durability assessment of building envelopes*. Build. Simul. 5, p 315-324.
- [15] Viitanen H, Toratti T et al. 2010 *Towards modelling of decay risk of wooden materials* European Journal of Wood and Wood Products 68 3, p 303–313.
- [16] Ongoing Research Project PTJ 2022 *Energieoptimiertes Bauen: NaVe - Nachweisverfahren für Schadensmechanismen bei der hygrothermischen Simulation* (FKZ: 03ET1649B)
- [17] Zirkelbach D and Tanaka E 2021 *Evaluation of decay resistance of wood fibre insulation based on hygrothermal simulation and comparative laboratory tests*. (London: Proceedings 1st International Conference on Moisture in Buildings ICMB21)
- [18] Hofbauer W, Breuer K, Krueger N and Sedlbauer K 2005 *Toxic mould versus façade-jungle – a comparison of undesirable biological growth on indoor surfaces and outer building coatings*. Proceedings of the 10th International Conference on Indoor Air Quality and Climate. Volume II(2). Indoor Air 2005 September 4-9 2005, Beijing, China: 2450-2454.
- [19] Hofbauer W, Krueger, N, Renzl A, Mayer F, Sedlbauer K and Breuer K 2014 *Towards a better understanding of wood decay*. 13th International Conference on Indoor Air Quality and Climate 2014. Vol.3: Proceedings of Indoor Air 2014: 59-63.
- [20] Ongoing Research Project AIF CORNET ThermNat 2022 *Building components with sustainable materials: focus (hygro-)thermal conditions* (IGF-Vorhaben-Nr. 271EN)
- [21] EN 113 1996 *Wood preservatives – Method of test for determining the protective effectiveness against wood destroying basidiomycetes – Determination of the toxic values*.



Aalborg Universitet

AALBORG UNIVERSITY
DENMARK

Use of Thermography for Quantitative Building Envelope Thermal Performance Analysis

Mukhopadhyaya, Phalguni; Mahmoodzadeh, Milad; Gretka, Voytek; Lee, Ivan

DOI (link to publication from Publisher):
[10.54337/aau541985169](https://doi.org/10.54337/aau541985169)

[Link to publication from Aalborg University](#)

Citation for published version (APA):

Mukhopadhyaya, P., Mahmoodzadeh, M., Gretka, V., & Lee, I. (2023). Use of Thermography for Quantitative Building Envelope Thermal Performance Analysis. In H. Johra (Ed.), *NSB 2023 - Book of Technical Papers: 13th Nordic Symposium on Building Physics* (Vol. 13). [383] Department of the Built Environment, Aalborg University. <https://doi.org/10.54337/aau541985169>

Use of Thermography for Quantitative Building Envelope Thermal Performance Analysis

P Mukhopadhyaya¹, M Mahmoodzadeh², V Gretka³, Ivan Lee⁴

¹ Department of Civil Engineering, University of Victoria, 3800 Finnerty Road, Victoria, BC, V8P 5C2, Canada

² Department of Building Specialty Services, Morrison Hershfield Ltd., Victoria, BC V8W 1C6, Canada

³ Department of Building Specialty Services, Morrison Hershfield Corp, Atlanta, GA, 30346, USA

⁴ Department of Building Specialty Services, Morrison Hershfield Ltd., Vancouver, BC V5C 6S7, Canada
phalguni@uvic.ca

Extended Abstract

The thermal transmittance characteristic of the exterior building envelope is a critical consideration in reducing space heating/cooling loads and carbon footprints of residential and commercial built environments. Hence, the importance of the method for determining the thermal transmittance characteristics of building envelopes cannot be over-emphasized.

Traditional approaches to estimating thermal transmittance in building energy simulations are based on nominal values provided by building material databases. Thermal transmittance values are calculated based on the reciprocal of the sum of each layer's thermal resistance in the wall assembly. This approach assumes one-dimensional heat flow and ignores lateral heat flux through thermal bridges. However, these assumptions are rarely true, and highly conductive building components such as metals create lateral heat flows to other components in three dimensions that are not accounted for in basic parallel flow assumptions.

The advent and availability of computer simulation tools have enabled better estimation of thermal bridging effects and thus overall thermal transmittance characteristics of building envelopes. Based on computer simulation results, ASHRAE 90.1 and Building Envelope Thermal Bridging Guide (BETB) provides information and guidelines for estimating the thermal transmittance values of wall assemblies incorporating the effects of thermal bridges. However, though simulation results are useful and insightful they do not reflect the actual thermal performance of existing building envelopes due to the construction variability or degradation of materials or components. In this context, in-situ thermal measurement tools (e.g., heat flux sensor (HFS), infrared thermography (IRT), etc.) are considered potential options for the actual thermal performance of exterior building envelopes.

In-situ thermal performance assessment of exterior building envelopes using HFSs is an invasive and lengthy process (test duration is 72+ hours). However, thermal performance assessment of exterior building envelopes using infrared thermography is a rapid process which generates a spatial 2D distribution of temperatures that incorporate effects of thermal bridges, natural convection inside the building, construction deficiencies and non-homogeneity of construction materials. Quite naturally, a thermogram generated by an infrared camera is a better representation of the actual thermal performance of exterior building envelope performance compared to the point source HFS measurements.

Since most of the existing buildings in North America and Europe were constructed prior to the establishment of energy policies, quantifying the thermal performance of exterior building envelopes is a critical step in identifying retrofit opportunities in existing buildings. Hence, researchers at the University of Victoria (UVic) have established a research program to study the use of external infrared thermography to quantify the thermal performance of exterior building envelopes for energy audits of buildings.

The overarching objectives of the research program at UVic with the use of infrared thermography are:

1. Evaluating Patterns of Building Envelope Air Leakage.
2. Determination of thermal transmission characteristics of exterior building envelopes.
3. Quantitative thermal performance assessment of exterior building envelopes.
4. Thermal performance assessment of exterior building envelopes with Unmanned Aerial Vehicles (UAVs).

This technical presentation aims to demonstrate the reliable use of infrared thermography (IRT) to estimate the thermal performance of opaque parts of building envelopes. Both qualitative and quantitative approaches are reviewed, and tests were conducted on a conditioned at-scale structure comprised of four wood-framed wall assemblies commonly used in Canada. From the critical analyses of these test results, a novel relative quantitative infrared index (IRI) has been developed as a tool to facilitate effective and rapid evaluation of the thermal performance of building envelopes. It has been demonstrated that wall thermal performance rankings based on IRI are consistent with their actual thermal transmittance values. This consistency was observed on multiple occasions with different boundary conditions. However, these observations need further validations from different type of constructions and climatic conditions.



Aalborg Universitet

AALBORG UNIVERSITY
DENMARK

The co-operation between the University and the Industry association in the application of building physics results to practice

Kauppinen, Timo; Hienonen, Markku; Fedorik, Filip

DOI (link to publication from Publisher):
[10.54337/aau541651956](https://doi.org/10.54337/aau541651956)

[Link to publication from Aalborg University](#)

Citation for published version (APA):

Kauppinen, T., Hienonen, M., & Fedorik, F. (2023). The co-operation between the University and the Industry association in the application of building physics results to practice. In H. Johra (Ed.), *NSB 2023 - Book of Technical Papers: 13th Nordic Symposium on Building Physics* (Vol. 13). [396] Department of the Built Environment, Aalborg University. <https://doi.org/10.54337/aau541651956>

The co-operation between the University and the Industry association in the application of building physics results to practice

Timo Kauppinen¹, Markku Hienonen², Filip Fedorik³

¹Arctic Construction Cluster Finland, Finland;tkk@mutsal.fi, ²The Finnish Society of Building Inspectors, Finland; ³Oulu University, Oulu, Finland.

Abstract

Indoor air questions in Finland have been constantly featured in the media. There are indoor quality deficiencies, not only in existing as well as in new buildings. The problems of indoor conditions can be divided into those caused by design, implementation and use. At the civil engineering department, University of Oulu, you can now specialize in building health. This is a new orientation option, which can be studied at the University of Oulu only. Arctic Construction Cluster Finland was established to restart the once-abolished civil engineering department. The cluster represents all branches of construction, and supports the civil Engineering department. The team for healthy buildings at the Arctic Cluster cooperates with the university's good indoor air and building health team. This is a position paper, where we introduce the operational priorities of the building cluster and the healthy buildings team, cooperation with the indoor air and building health group at Oulu University and the trends which will affect and change the building branch. There are still shortcomings in solutions to indoor conditions problems, which are caused by several factors. Education and training must be developed. Knowledge in hygrothermal performance of buildings is essential to improve it into interdisciplinary and comprehensive approach. Civil engineers must recognize factors that affect building health. Health care staff then investigate the consequences. Different actors should be brought together better than at present.

1. Introduction

Indoor air issues in Finnish homes and workplaces have been constantly featured in the media. The issues have been discussed concerning existing as well as new buildings. The risks related to indoor conditions can be divided into those caused by design, implementation, and use. The costs resulting from the indoor environmental defects, e.g., bad indoor air quality (IAQ) and other factors, resulting in high costs due to reduced work productivity, absenteeism and repair. However, the IAQ is internationally considered relatively good in Finland. In Finland, various actors, such as municipalities and cities, have developed solutions to the problems of indoor conditions. The situation is improving. In the future, with the different players in the construction industry and the university's closer cooperation, the performance and IAQ of the buildings can be improved. Modelling of buildings and, on the other hand, the development of building automation systems and monitoring, in particular, is key to develop building design, implementation and use. However, the current operational model needs time to reach results that benefit everyone. The development of the construction industry is currently affected

by several different trends, the most significant of which in the long term is climate change [1], [2] and its effect on buildings and housing in general. The increase in temperature is especially aimed at the northern parts of the northern hemisphere, (Figure 1) [3].

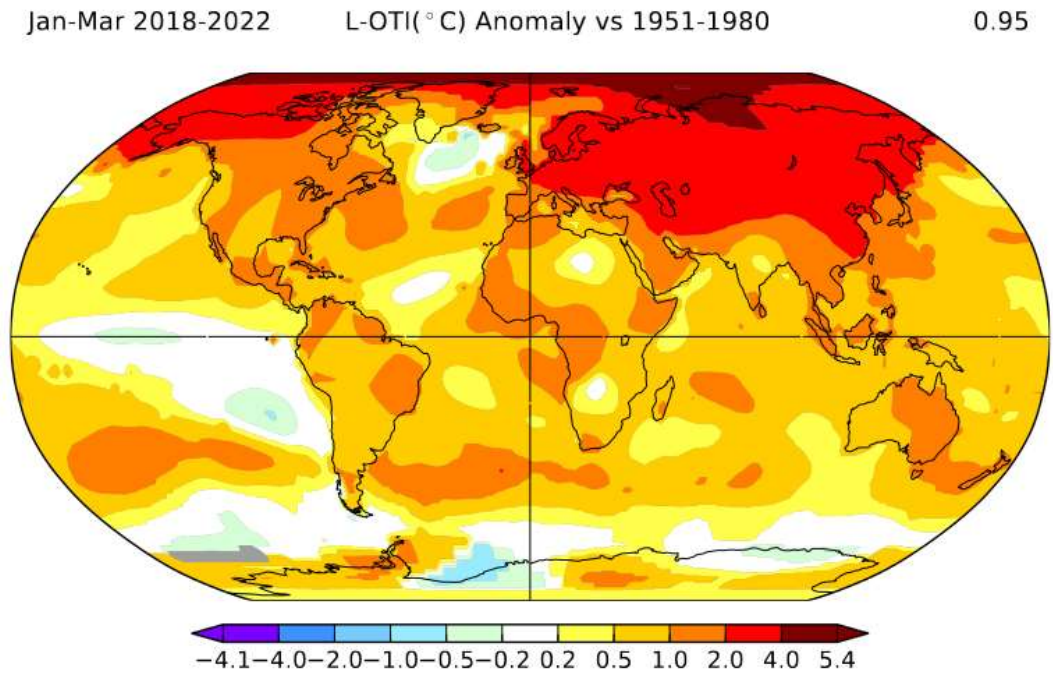


Figure 1. Global warming. Source: NASA National Aeronautics and Space Administration, Goddard Institute for Space Studies. The changes of temperatures, January-March.

Climate change causes an increase in temperature, which may lead in summer times to indoor temperature level that can cause health issues of occupants in service and residential buildings. Then, instead of traditional long cold periods in winter, there may be a temperature fluctuation causing periodic freezing-thawing periods. The amount of rain and wind may increase, in which case wind-driven rains will load the structures more than at present. Increased humidity causes flooding, and on the coasts, rising sea water level poses a danger to buildings near the coast [1].

The Building Supervision Office of the city of Oulu (BSO) has participated in research projects [4], where as one part the effect of weather conditions different from the current one, such as wind-driven rain and heavy wind, on the structures in use was evaluated computationally. The result was that some of the existing structures do not perform well enough. In this case, the risk of moisture damage increases.

The trend in real estate management is "knowledge-based management", business intelligence based on data in use. This is possible, created by digitalization. The building performance, indoor conditions and energy efficiency can be monitored in real time. This requires proper instrumentation and metering, results processing and reporting, that could be compared to industrial production and quality control. The final product of the building is planned, healthy and good IA . Ensuring the performance of the building from the project planning to the operation phase can be implemented on a monitoring basis, but generally accepted procedures still need to be developed.

With digitalization, building modeling is a commonly used tool (BIM). A digital twin can be created from the building, and various solutions can be tested with it. Planning tools have developed rapidly, but there are still bottlenecks in coordinating different data models, that we have to do manually. The

requirements and needs of building users are also changing. In the future, the built environment and buildings will be required to have resilience, the ability to maintain operational capability in changing conditions, and the readiness to face disruptions and crises and recover from them.

The factors presented above will also affect the educational requirements of the construction and real estate sector. If we want the building to perform "as designed", the importance of managing building physics is increasing in order to ensure the health of building users and the performance of structures and systems.

2. New specialization: Good Indoor Air and Building Health

In response to the new challenges, new building health specialization was established at the Civil Engineering Research Unit at the University of Oulu, Finland and it is possibly the only one worldwide so far [5]. A building health expert must understand the requirements for good indoor air, physical conditions and related health effects, as well as legislation and regulations related to built environment. The student gets the skills to work as an expert, research and planning tasks related to indoor environment quality, and moisture management. The courses of the new building health study program are implemented across faculty boundaries.

The background for starting the training is the need highlighted by Arctic Construction Cluster Finland to promote building health and indoor air expertise and healthy building in the region and in the country, and to produce experts in the field for the service of business and public organizations. The new training is based on constantly developing research knowledge, with the applications of which it is possible to improve the level of building health and indoor air expertise to an even higher level. Recent research objectives in the field have been, e.g., proactive facility management based on continuous monitoring of the indoor environment and conditions, the effects of improving the energy efficiency of buildings on indoor environmental quality, occupant health and wellbeing. The results opened up interesting development directions (Figure 2).

Main research areas:

- Indoor environmental quality (IEQ)
- Building physics
- Dampness and mold associated with IEQ

Main application areas:

- Continuous monitoring
- School buildings, IEQ, health and learning outcomes
- Assessment of dampness and mold in buildings
- Effects of improved energy efficiency of buildings on IEQ, occupants' health and wellbeing
- Developing new methods to assess and model IEQ in relation to building occupants' health and wellbeing

A new environmental laboratory is also being planned together with Oulu University of Applied Sciences.

3. Measures in the construction sector: Arctic Construction Cluster Finland

3.1. Arctic Construction Cluster Finland

The cluster unites Northern Finland's construction industry companies, educational institutions and authorities to work for the best of the construction industry and regional development. At the moment, almost 100 experts are involved in Cluster's activities, mainly company and community members, but

also individual members. They are divided to work by industry in six divisions and in one cross-cutting industrial team, healthy buildings [6].

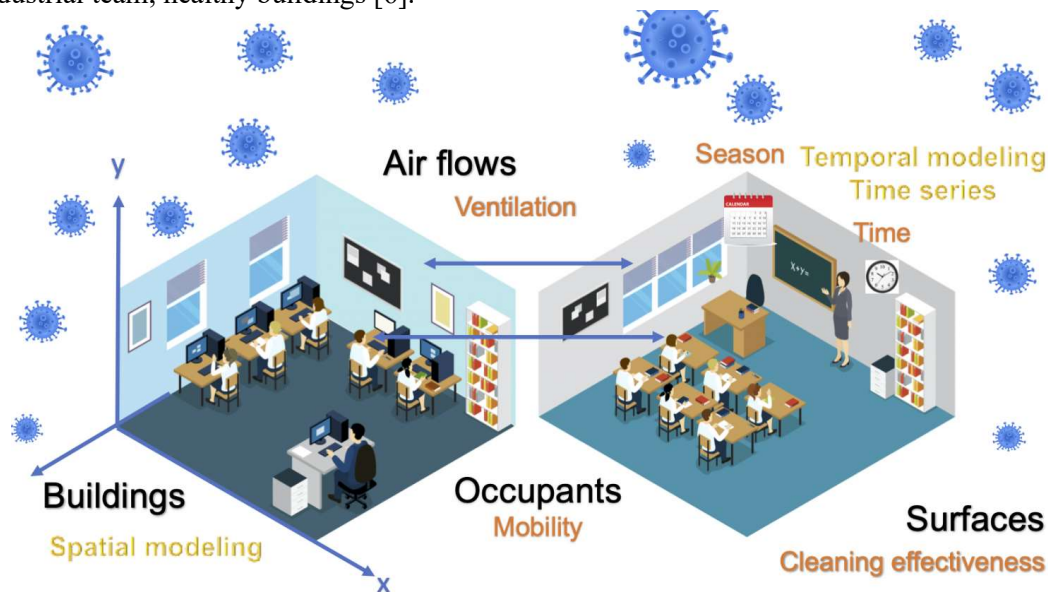


Figure by U. Haverinen-Shaughnessy & Hannele Heikkilä-Tuomaala

Figure 2. Research towards healthy, productive and sustainable indoor environments. (www oulu.fi/en/university/faculties-and-units/faculty-technology/civil-engineering-research-unit)

The university chain includes the University of Oulu as well as the universities of applied sciences in the region and Oulu region's vocational school. The activities are coordinated by a board formed by the division heads. The cluster is a platform for industries and members to meet, an active cooperation network with agreed goals, rules of the game and organized mutual communication, which the parties can utilize in a planned manner. In the cluster, industrial branches highlight productive or necessary training, research or investigation needs in the field, for which the training chain or divisions seek solutions also with the resources supported by the cluster. Through cooperation, border fences are opened within the construction industry and efforts are also made to streamline control processes.

3.2. Main goals in general

One of the core missions of Arctic Construction Cluster Finland is to increase collaboration across borders both for business as well as education. The main goals are: 1. Youth - attractiveness of the building sector, how to get young people to all levels of education and how to get labor force, 2. Circular economy (incl. taxonomy) 3. House of the future including subthemes such as Dry Construction Chain, Indoor Environment, Energy Efficiency and Management, Architecture, Cultural Issues.

3.2.1. Healthy Buildings-team.

Healthy Buildings-team of Arctic Construction Cluster brings companies' perspectives and problems to the university's attention, and at the same time can disseminate the latest research results for the use of companies and different communities. The current focus of the healthy buildings-team is commissioning the performance of buildings, which also covers indoor conditions and health of buildings.

4. Trends: Climate change

4.1. *Increasing temperatures and changing conditions*

Global climate change causes challenges in buildings in Finland [7]. The climate in Finland has warmed about two degrees during the last hundred years. According to forecast, Finland's climate will warm especially in winter. The wind-driven rain load received by structures exposed to the weather, such as facades, balconies and roofs, will may cause a significant need for repairs in the existing building stock. The durability of old structures is often defective. Structural details such as joints and junctions should operate properly. Freezing-thawing-phenomena will load structures more than continuing cold period in the winter. With increasing moisture content increases risk of moisture and microbial damages, that are one of the health threats caused by the climate change. Repairing moisture damages in the existing building stock has been estimated already approximately 10 years ago to be 30 billion euros [7], [8]. Majority of Finland's building stock is 30–60 years old. These buildings are designed according to the regulations and practices of the time. Part of these buildings has already been renovated; some buildings are approaching the next renovation cycle the other buildings are waiting the renovation. So called repair dept is almost continuous in some building groups.

The calculated and observed temperatures of service buildings and apartments are already high in the current climate. The insulation level is improved and the air tightness is better. Sun protection solutions alone are not enough to keep room temperatures at a sufficiently low level during the warm season. Active cooling is also needed, especially during heat waves. Increased balcony glazing has also caused increase indoor temperatures. Air heat pumps are more general in one-family houses and apartments mainly for cooling, but also for heating. Cooling should be especially aimed at buildings where elderly people live, like service homes. They have the greatest health risks. Without further actions high temperatures will increase significantly in Finland and cause health problems for elderly people as the population is aging.

4.2. *Increasing moisture and wind*

Stormwaters, heavy rains and melting snow can cause flooding of waterways - mainly in rivers and lakes [7]. Flooding of surface waters can also be caused by high water levels in lake areas as a result of consecutive wet periods, ice damming at the time of ice run, clogging of flow openings and channels, and ice damming of subcooled water, i.e. ice flood. The effects of climate change on waterway floods depend on the causes of the floods and the location of the waterways. Floods can be divided into three different types of floods: stormwater, waterway and seawater floods. Flood types depend on how they are generated, in which case the effects of climate change vary by flood type. The essential thing is that there are lot of buildings in risky areas even the construction in such areas is regulated. Every year there are red flood damages by the rivers as well as in urban areas.

5. Trends digitali ation, modelling and knowledge-based management

The value of data-managed built assets in Finland is EUR 500 billion, traffic EUR 55 billion and infrastructure approx. EUR 42 billion. It has been estimated that data loss is a brake on productivity growth in the real estate and construction industry: 50% of data is lost when at the same time we want significant productivity growth. The benefits of digitization in the construction sector have also been evaluated: Increase in productivity 12-20% with the help of digitization. This means better and more construction per year worth 2–3 billion euros. Estimated benefits over the life cycle – design are: Benefits in design costs 8%, in planning time 30%, and benefits during the life cycle – construction: Construction costs 3%, lead time 10% [9]. A significant problem is the integration of data and data models of the built environment [10]. Data does not flow over interfaces, if no interfaces are defined. For this reason, construction documentation must be developed, for example by defining generally

acceptable and required criteria. A well-documented construction ensures the quality of operation. At least the minimum criteria for documentation had to be defined. The same also applies to measurements and data processing during the use stage of the building [11], [12]. From the management perspective of data-driven service innovation, one question is: How the data created in the building construction phase can be utilized in the use phase? Combined with the costs of mold and moisture repairs, the repair debt, and the savings potential obtained through digitalization, we talk about very large sums.

. Summary

Changing conditions set challenges and demands on construction, while new tools and procedures are in use. These must be prepared and adopted for both, practice and teaching. The importance of building physics will be particularly emphasized. Its teaching may have previously been left behind or its skills are not up to the current requirements. When evaluating the performance of buildings, a holistic view is important. The building performance is the sum of several factors, and these factors are also dependent on each other. The importance of building services and HVAC-technology increases. Renovation to the existing building stock will be essential, and in some cases must have to consider demolishing an old building. The recent trends of building stock should be integrated for better performing buildings, in the aim to have safe and healthy cost-optimized spaces.

References

- [1] IPCC, 2022: Climate Change 2022: Impacts, Adaptation, and Vulnerability. Contribution of Working Group II to the Sixth Assessment Report of the Intergovernmental Panel on Climate Change [H.-O. Pörtner et al., (eds.)]. Cambridge University Press. Cambridge University Press, Cambridge, UK and New York, NY, USA, 3056 pp., doi:10.1017/9781009325844.
- [2] Energy Performance of Buildings Directive (EPBD), a part of “Fit of 55”-package.
- [3] <https://data.giss.nasa.gov/gistemp/maps/>
- [4] RESCA OULU / Tulevaisuuden talot ja uusiutuva energia - Uusiutuvan energian pilottialue. (RESCA Oulu/The houses of the future and renewable energy). www.rescaoulu.fi, www.tulevaisuudentalot.fi, BSO Oulu. <https://www.ouka.fi/oulu/rakennusvalvonta> (in Finnish)
- [5] <https://www.oulu.fi/en/university/faculties-and-units/faculty-technology/civil-engineering-research-unit>
- [6] <https://www.rakennuskluusteri.fi/about>
- [7] Jukka Lahdensivu et al.: Moisture damage and high temperatures in buildings in changing climate – RAIL. Publications of the Government's analysis, assessment and research activities 2023:2 (in Finnish). ISBN PDF 978-952-383-278-7. <http://urn.fi/URN:ISBN:978-952-383-278-7>
- [8] Reijula, K et al. (2012). Rakennusten kosteus- ja homeongelmat. Eduskunnan tarkastusvaliokunnan julkaisu 1/2012. (Damp and Mould problems of Buildings, publications of Parliament of Finland, Audit Committee). ISBN 978-951-53-3454-1 (nid.), ISBN 978-951-53-3455-8
- [9] Markku Hedman, RTS, et al.; presentations at RYTV-Edelläkijät (RYTV-pioneers). Webinar organized by buildingSmart Finland 3.10.2022. <https://drive.buildingsmart.fi/>
- [10] Inka Lappalainen et al.: Future housing. Innovative service solutions and networks enabled by data economy. VTT Technology 391. May 2021. ISBN 978-951-38-8751-3, ISSN 2242-122 (online). VTT Technical Research Centre of Finland.
- [11] Kauppinen, T, Hienonen, M. Monitoring Based Commissioning (MBCx) in Energy and Facility Management. BauSIM2016, September 14-16, 2016, Technische Universität Dresden, Germany. pp. 260-266 in Conference Proceedings of Central European Symposium on Building Physics CESBP 2016 / BauSIM, ISBN (E-Book): 978-3-8167-9798-2, Fraunhofer IRB Verlag, Stuttgart
- [12] IEA Annex 47. Commissioning overview. A Report of Cost-Effective Commissioning of Existing and Low Energy Buildings. Chloe Legris et al (editors). Nov. 2010. <http://www.ieaannex47.org>



Aalborg Universitet

AALBORG UNIVERSITY
DENMARK

Water uptake measurement for thermal renovations – comparison between non-destructive method, the Karsten tube, and automatic laboratory measurements

Meißner, Frank; Sonntag, Heike; Morandell-Meißner, Anita

DOI (link to publication from Publisher):
[10.54337/aau541652209](https://doi.org/10.54337/aau541652209)

[Link to publication from Aalborg University](#)

Citation for published version (APA):

Meißner, F., Sonntag, H., & Morandell-Meißner, A. (2023). Water uptake measurement for thermal renovations – comparison between non-destructive method, the Karsten tube, and automatic laboratory measurements. In H. Johra (Ed.), *NSB 2023 - Book of Technical Papers: 13th Nordic Symposium on Building Physics* (Vol. 13). [407] Department of the Built Environment, Aalborg University. <https://doi.org/10.54337/aau541652209>

Water uptake measurement for thermal renovations – comparison between non-destructive method, the Karsten tube, and automatic laboratory measurements

Frank Meißner¹, Heike Sonntag², Anita Morandell-Meißner²

¹GWT TUD GmbH, Freiburger Str. 33, 01067 Dresden

²Technische Universität Dresden, 01062 Dresden

frank.meissner@tu-dresden.de, heike.Sonntag@tu-dresden.de,
Anita.Morandell_Meissner@tu-dresden.de

Abstract. The energy-efficient renovation of existing buildings requires precise knowledge of the wall structure. When using interior insulation systems, the driving rain resistance of the façade is also decisive for the function of the entire wall structure. When using interior insulation on exposed brick facades, the verification can often only be done with the help of a hygrothermal simulation. In practice, a non-destructive method, the Karsten tube or various modifications, is used to assess this essential characteristic value quickly. However, the measured values obtained from this method do not agree with the laboratory-measured values determined on a test specimen taken from the laboratory. This article presents measurements on bricks from several refurbishment projects to determine the cause. They were carried out both in the installed state with the in-situ method and subsequently after brick removal on the same materials under laboratory conditions to bring about comparability concerning the material. This article presents the automatic detection of water uptake of porous materials compared to the in-situ measurement with the Karsten tube. It evaluates the measurement results of both measurement methods.

1. Introduction

If an existing building is to be renovated for energy efficiency and the exterior facade appearance is to be preserved, it is often necessary to use interior insulation. In this case, it cannot be ruled out that condensation will form inside the wall construction under cold external conditions. It is, therefore, important to ensure that moisture is transported away, back to the outside or inside, to avoid moisture accumulation in the construction. Additional moisture from the outside must be prevented in any case; because humidity above the critical for the material can cause damage. The drying of moisture from the outside is more difficult due to an additional inner insulation layer. This moisture must be transported away by capillary-active interior insulation in the summer months. The driving rain protection of the facade is of decisive importance for reliable drying because the drying potential of the exterior wall is reduced by the interior insulation.

In order to assess the existing driving rain protection of an existing facade, various measurement methods exist, which are realized non-destructively or by taking test specimens. The property to be examined here is the water uptake coefficient w of the exterior surface according to [1]. A substance with the base A is immersed in water. The substance is weighed at certain time intervals and the mass of the absorbed water m is obtained as a function of the time t . This results in the water absorption coefficient:

$$W_w = m/A * \sqrt{t} \text{ in } [\text{kg/m}^2 * \text{h}^{0,5}]$$

It indicates how much water is absorbed per unit of time. It is required for the hygrothermal simulation of the wall system and is used to calculate the liquid water transport.

An inexpensive but inaccurate method, such as the Karsten tube, the Pleyers tube, or the Franke plate, is usually used for an initial rough in-situ inventory. For accurate investigations of the W_w -value, a laboratory measurement via sampling is necessary. The results of the in-situ and laboratory measurements only rarely agree. Numerous refurbishment research projects have shown that the W_w -value measured with the Karsten tube was considerably lower than the measured values of the laboratory measurement for brick-faced facades. A higher W_w -value, as is often the case with plastered exterior facades, according to [2], could not be measured for brick facades. In addition, this article deals exclusively with the recording of the W_w -value of the masonry brick since the brick joints are usually assessed and renovated separately during the renovation process. For hygrothermal characterization of building materials, a wide variety of parameters are required, which enable the use of complex simulation tools such as DELPHIN or WUFI. An important parameter is the water uptake coefficient, which can be determined in various ways using non-destructive or destructive measuring methods [3]. For an exact determination of the W_w -value, an automatic water uptake measurement is carried out in the laboratory, in-situ measurements on existing objects are carried out using the Karsten tube.

2. Investigated masonry and test procedure

The measurements described here were carried out on a single-shell masonry structure taken in one piece, which was transported in dry condition to the Laboratory. It comprised a four-row masonry composite.

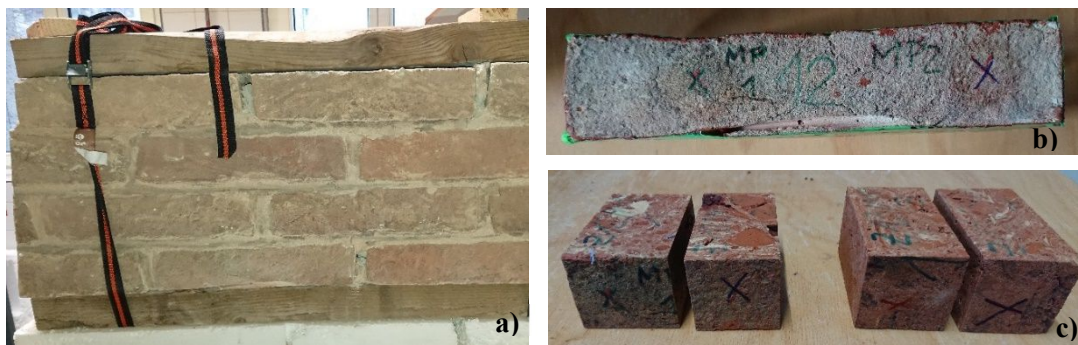


Figure 1. Masonry structure (a), brick from masonry structure (b), specimen for automatic measurement (c)

The W_w -value of this masonry bond was measured at a total of 5 measuring points using the Karsten tube. The Karsten tube or pipe method is a testing device that allows to test the water penetration in facades (non-destructive method). It consists in a glass tube with water and a seal as a connection to the facade (see figure 2 b). The penetrating water can be read at regular intervals [4].

Afterward, this masonry was divided into individual bricks, and the W_w -value was again determined with the Karsten tube at four identical measuring points, as in the first test step, in order to detect the

possible influence of the masonry bond on the measurement. In addition, the surface was mechanically cleaned at half of the individual points in this step. Afterward, parts of the bricks with individual measuring points were separated from the single bricks and cut to form test specimens with a base area similar to the previous measurements for the automatic laboratory measurements. The test specimens were dried and prepared for the following measurement process: The lateral surfaces of these test specimens were sealed vapor-tight. The specimens were preconditioned for seven days in a desiccator with a humidity of 32.8% r.h. (According to the standard, the measurement is to be carried out on preconditioned specimens [1]). The W_w -value was measured on the original surface of all specimens, which had now been cleaned.

3. Measurement methods used

In the first and second test steps, the Karsten tubes were tightly applied to the masonry bond and the individual brick, respectively, with a plastic sealing material and filled with water. The location of the individual measuring points is shown in Fig. 2. The amount of water flowing into the brick was recorded at specific time intervals - mostly 30 s, later 60 s - for approx. one hour and then converted into the corresponding W_w -value via the free suction area of the test tube. The sealing material usually reduces this test area, which was converted into the measurement result via the reduced cross-section.

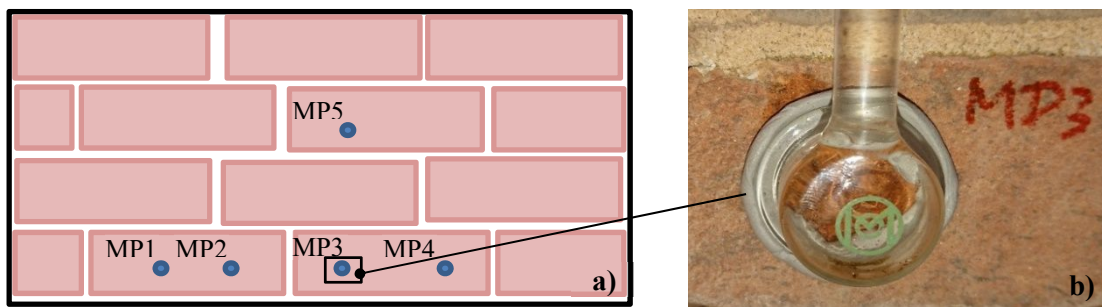


Figure 2. Position of the measuring points (a), measuring point 3 with Karsten tube (b)

In the third test step, the prepared and preconditioned test specimens were placed in a measuring apparatus that automatically measures the water uptake via a scale with a connected data logger. For this purpose, the specimen is clamped in a specimen holder, and a water vessel is coupled via a mechanical lifting system to start the experiment. The measurement interval can be set variably from a minimum of 3 s. The data is then stored together with the data logger. The measured data are then calculated together with the specimen geometry and the dry mass to form the water uptake coefficient. In contrast to the otherwise standard manual measurement, according to [1], the measurement process can thus be recorded continuously and over a long time without interrupting the water uptake by the measurement-related sample removal.

The measurements with the Karsten tube in the first and second experimental steps determined very different and strongly scattering results. The evaluation of the individual measurements was carried out via the calculation tool according to [5], which uses the model according to Smettem et al. [6]. The reduction of the measurement area due to the sealing material was taken into account in Table 1 via the values in brackets (MW). In the automatic measurements, a good agreement of the water uptake coefficients was measured for the specimens used, which came from two single bricks. The individual results are shown in table 1.

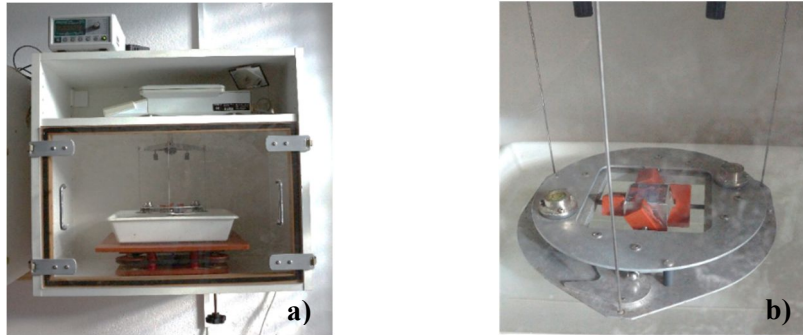


Figure 3. Automatic measuring apparatus water uptake (a), sample acquisition laboratory measurements (b)

Table 1. Measured W_w -values at the individual measuring points in the renovation project 1

	Test step 1 Wall bond Karsten tube	Test step 2 single brick Karsten tube	Test step 3 Automatic measurement
MP 1	12,55 kg/m ² h ^{0.5} (15,30 kg/m ² h ^{0.5})	22,53 kg/m ² h ^{0.5} (26,23 kg/m ² h ^{0.5})	29,38 kg/m ² h ^{0.5}
	Surface uncleaned	Surface mech. cleaned	Surface mech. cleaned
MP 2	11,49 kg/m ² h ^{0.5} (13,47 kg/m ² h ^{0.5})	12,70 kg/m ² h ^{0.5} (15,00 kg/m ² h ^{0.5})	29,13 kg/m ² h ^{0.5}
	Surface uncleaned	Surface uncleaned	Surface mech. cleaned
MP 3	4,10 kg/m ² h ^{0.5} (4,97 kg/m ² h ^{0.5})	5,06 kg/m ² h ^{0.5} (6,25 kg/m ² h ^{0.5})	29,02 kg/m ² h ^{0.5}
	Surface uncleaned	Surface uncleaned	Surface mech. cleaned
MP 4	5,97 kg/m ² h ^{0.5} (6,59 kg/m ² h ^{0.5})	(a) Surface mech. cleaned	29,98 kg/m ² h ^{0.5}
	Surface uncleaned		Surface mech. cleaned
MP 5	12,21 kg/m ² h ^{0.5} (14,28 kg/m ² h ^{0.5})		
	Surface uncleaned	(b)	(b)

(value) – Measured value as a result of the reduction in the measuring area due to the seal of the Karsten tube

(a) – missing values; invalid measurement due to Karsten tube contact difficulty with surface

(b) – no measurement at this measurement point

The time course of the water uptake is shown in the two diagrams below based on measuring point 1 and measuring point 2. The good agreement of the water uptake measurement during automatic recording can be seen in figure 6. The manual measurements with the Karsten tube took about 1 hour, the automatic laboratory measurements about 2-3 hours. Therefore, only the first section is shown to compare these measurements.

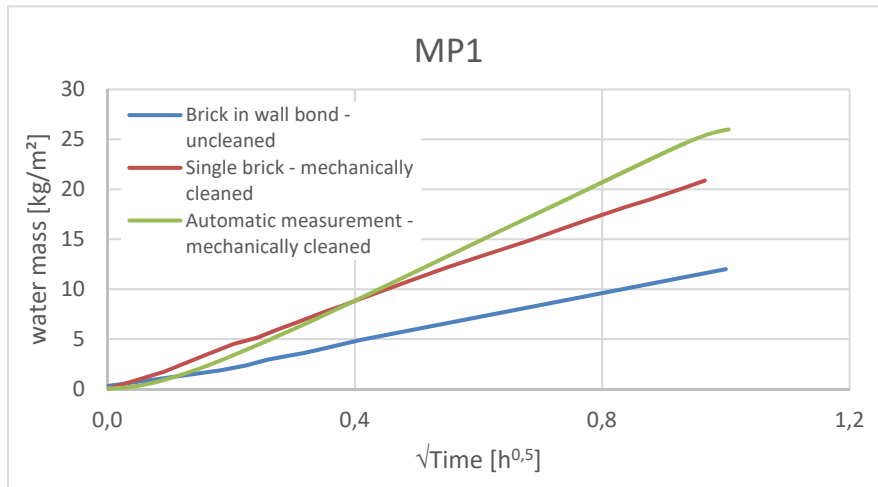


Figure 4. Water uptake MP1 - without consideration of the sealing material

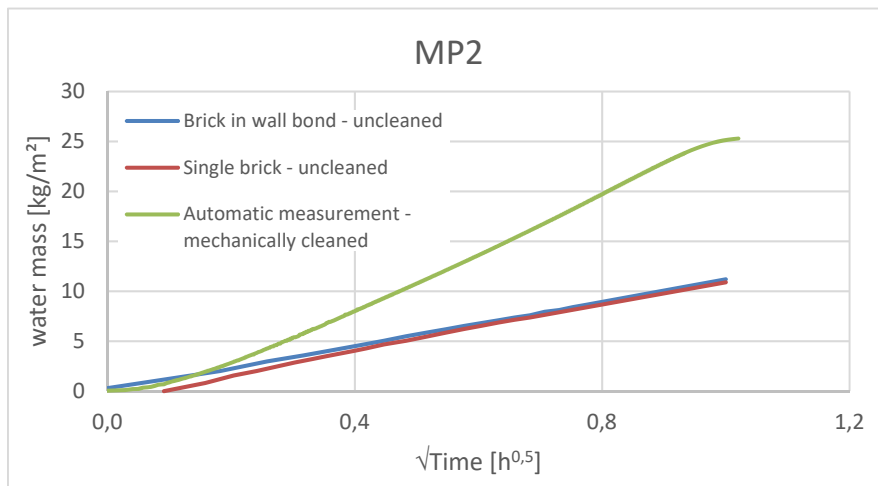


Figure 5. Water uptake MP2 - without consideration of the sealing material

As can be seen clearly in figure 4 and 5, loosening the wall bond and measuring the W_w -value on the individual brick does not yet produce any significant change in the result. The situation is different with preparatory cleaning. If it is omitted, large deviations occur since wetting of the surface to be measured is impeded or restricted, and water uptake is thus delayed. These effects can be limited by mechanical cleaning, e.g., with a textile brush. It has to be ensured that the outer layer of the existing material (e.g., the firing skin of the brick) is not destroyed.

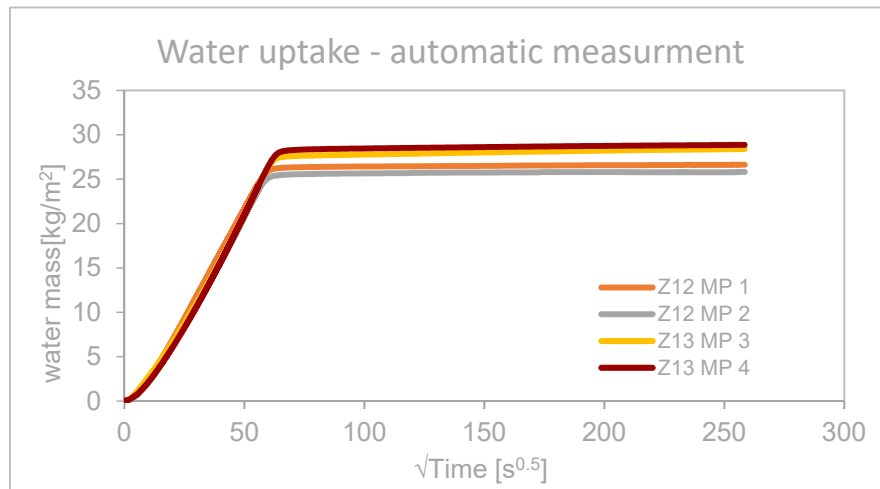


Figure 6. Water uptake curves of the automatic measurements

4. Measurements on existing facades

To further deepen the above results, several measurements were also carried out on two other brick-faced existing facades, with the Karsten tubes and automatic water uptake tests, and compared with each other. In these projects, the measured water uptake was to be used to investigate the functionality of the interior insulation to be applied in order to improve the driving rain impermeability of the exterior wall in the next step, if necessary, and to prevent excessive moisture penetration of the exterior facade after renovation. This value is necessary to determine whether procedures on the existing facade are needed. According to WTA standard 3.17 the recommended value for water absorption is $0.2 \text{ kg} / \text{m}^2 \text{ h}^{0.5}$. [7] If this value is exceeded, renovation measures (e.g. hydrophobic treatment) on the facade are necessary. In the following table the results obtained are shown.

Table 2. Measured values at the individual measuring points in the renovation project 2

	Existing facade 1	Existing facade 2
Number of measuring points Karsten tube	3MP/3 single brick	6MP/6 single brick
Averaged W_w -value [$\text{kg}/\text{m}^2\text{h}^{0.5}$]	7,97	1,99
minimum W_w -value [$\text{kg}/\text{m}^2\text{h}^{0.5}$]	5,41	1,16
maximum W_w -value [$\text{kg}/\text{m}^2\text{h}^{0.5}$]	9,78	3,83
Number of measuring points Automatic measurement	10 sample/ 2 single brick	8 sample/ 4 single brick
Averaged W_w -value [$\text{kg}/\text{m}^2\text{h}^{0.5}$]	7,02	2,41
minimum W_w -value [$\text{kg}/\text{m}^2\text{h}^{0.5}$]	5,97	1,83
maximum W_w -value [$\text{kg}/\text{m}^2\text{h}^{0.5}$]	8,08	3,09

The measurements taken here on the facades of the two projects investigated show that the in situ and laboratory measurements show relatively good agreement at smaller W_w -values. The still-existing deviations may indicate the different initial conditions of the existing facade since its moisture condition cannot be preset as precisely as in the automatic laboratory measurements, where the specimens are dried and preconditioned.

5. Summary

In the evaluation of the measurements presented here, it becomes clear that the driving rain tightness of an existing brick-covered facade can certainly be estimated roughly with an in-situ measurement method, such as the Karsten tube if the values determined in the process are not too high ($W_w < 10 \text{ kg/m}^2 \text{ h}^{0.5}$) and the measured values do not scatter too much. When evaluating these measurement results, careful selection of the measurement points is essential to avoid misinterpretation. In addition, this preliminary measurement can be used to decide at which points to take material samples for the subsequent laboratory measurement.

In the case of high W_w -values and strong scattering of the individual values, the measuring points should be analyzed in more detail. If necessary, further individual measurements should be carried out. The surface of the measuring points should also be cleaned mechanically. The protection from driving rain of the facade is of decisive importance for reliable drying because the drying potential of the exterior wall is reduced by the interior insulation. For the assessment of the driving rain resistance of an existing facade and the dimensioning of a driving rain protection measure, the exact measurement of the W_w -value with the good agreement of the individual values is only possible by taking individual test specimens from the existing construction. An in-situ method can then be used again to check the success of a renovation measure.

References

- [1] DIN EN 15148, 2003 Beuth Verlag, *Bestimmung des Wasseraufnahmekoeffizienten bei teilweisen Eintauchen*
- [2] Haindl, Schöner et. al, 2016 IBP, *Bauen im Bestand, Was ist bei Karsten & Co zu beachten*
- [3] Plagge, R., Scheffler, G., Grunewald, J. 2005 Ernst & Sohn, Bauphysik 27, Heft 6. *Automatische Messung des Wasseraufnahmekoeffizienten und des kapillaren Wassergehaltes von porösen Baustoffen.*
- [4] Karsten, R., 1960, Straßenbau, Chemie und Technik Verlagsgesellschaft mbH. *Bauchemie für Schule und Baupraxis.*
- [5] Stelzmann, M., 2020 Fraunhofer, *Entwicklung und Validierung eines Verfahrens zur Untersuchung des Schlagregenschutzes von Fassaden denkmalgeschützter Bestandsgebäude*
- [6] Smettem et. al, 1994 WaterResourcesResearch,30(11):2925–2929, *Three-dimensional analysis of infiltration from the discinfiltrometer: 1. A capillar-basedtheory*
- [7] WTA Merkblatt 3-17-10. 2010. IRB Verlag. *Hydrophobierte Imprägnierung von mineralischen Baustoffen.*



Aalborg Universitet

AALBORG UNIVERSITY
DENMARK

ASSESSING THE RELATIVE IMPORTANCE OF MUCOSAL EXPOSURE AND INHALATION EXPOSURE TO AIRBORNE PARTICLES

Duan, Mengjie; Liu, Li; Da, Guillaume; Wang, Yi; Géhin, Evelyne

DOI (link to publication from Publisher):
[10.54337/aau541653952](https://doi.org/10.54337/aau541653952)

[Link to publication from Aalborg University](#)

Citation for published version (APA):

Duan, M., Liu, L., Da, G., Wang, Y., & Géhin, E. (2023). ASSESSING THE RELATIVE IMPORTANCE OF MUCOSAL EXPOSURE AND INHALATION EXPOSURE TO AIRBORNE PARTICLES. In H. Johra (Ed.), *NSB 2023 - Book of Technical Papers: 13th Nordic Symposium on Building Physics* (Vol. 13). [10001] Department of the Built Environment, Aalborg University. <https://doi.org/10.54337/aau541653952>

ASSESSING THE RELATIVE IMPORTANCE OF MUCOSAL EXPOSURE AND INHALATION EXPOSURE TO AIRBORNE PARTICLES

Mengjie Duan^a, Li Liu^{a,*}, Guillaume Da^b, Yi Wang^{c,d}, Evelyne Géhin^b

^a School of Architecture, Tsinghua University, PR China

^b Université Paris-Est, CERTES (EA 3481), UPEC, F-94010, Créteil, France

^c State Key laboratory of Green Building in Western China, Xi'an University of Architecture and Technology (XAUAT), PR China

^d School of Building Services Science and Engineering, XAUAT, PR China

*Corresponding email: liuli_archi@tsinghua.edu.cn

ABSTRACT

Particles deposited on mucosa or penetrating into lower airway are two exposure routes. Quantifying administered dose of these two routes gives us idea for future advanced individual protection. Here, we report an in-vitro method to assess the administered doses of eyes, lips, and lower airway. A CT-scanning and 3D-printing based human replica is developed, and exposed in front of the 0.6-5 μ m monodispersed fluorescent particles. At small size particles (<2.5 μ m), the administered dose intensity of penetrating into lower airway inhalation ($\sim 59.41 \times 10^{-2}$ g/g, 0.6 μ m) is higher than that of eyes and lips ($\sim 5.97 \times 10^{-2}$ g/g, 0.6 μ m). Conversely, the administered dose intensity of lower airway inhalation ($\sim 9.39 \times 10^{-2}$ g/g) becomes higher than that of eyes and lips ($\sim 6.24 \times 10^{-2}$ g/g) at 5.0 μ m particles. This work provides us an effective and economical way to assess exposure risks of particulate contaminants.

Keywords: Human replica; Micro-sized particles; Monodisperse; Fluorescence; Experiment

1 INTRODUCTION

Exposure to micron-sized particles cause serious adverse health issues, which receive numerous attentions. Generally, there are two exposure routes for particles. One is mucosal deposition (e.g. eyes and lips), the other is penetrating into lower airway. Scientists have done a lot of researches about the relationship between these two particulate exposure routes and health effects. Epidemiological studies report the particulate-caused diseases based on inference of associations between exposure and response variables (Weis, et al. 2005). Animal models or *in vitro* cells have long proved the toxicology of particle dose and associated adverse health effects, i.e. dose-response effect (Lock, et al. 2018). However, lacking of quantitative dose contributes to the greatest uncertainties to such studies. Individual protection strategies for indoor particulate contaminants need more accurate dosage assessment. Exploring human replica remains one of the big challenges until now. Previous studies that employed anatomically correct model mainly focus on thermal comfort or inhalation exposure (Lizal, et al. 2012). Empirical work based on partial or full body replicas are hardly reported.

Here, we propose a new method to quantify the administered dose on facial mucosa and penetrating into lower airway. Individual human replica is developed with geometrical details' face and airway based on CT-scanning and 3D-printing. Relative importance of mucosal exposure and lower airway exposure to 0.6-5.0 μ m monodispersed particles are finally achieved.

2 METHODOLOGY

Real human geometric data is obtained from computed tomography scan of a healthy Chinese male. The in-vitro human replica is developed by 3D-printing. It includes face, oropharynx, trachea, the first 5-generation bronchi and the lung void. Through connecting with a pump, it inhales steadily with 11 ± 1 L/min flow rate by mouth.

The replica exposed to 0.6-5 μ m monodispersed fluorescent particles generated by VOAG 3450[®] (TSI, U.S.A.). The size distribution is monitored by APS 3321[®] (TSI, U.S.A.). Administered doses on eyes

and lips are measured by cumulative deposition mass. The dose of lower airway is calculated by particles penetrating from the first 5-generation bronchi into lung void. SKC BioSampler[®] was used for collecting the suspended fluorescent particles in the lung void, while preset foils were used to sample the particles deposited on the surface of the lung void and face mucosa. Administered dose is calculated by fluorescent intensity-mass curves normalized by Fluoro Max-4[®] (HORIBA, Japan).

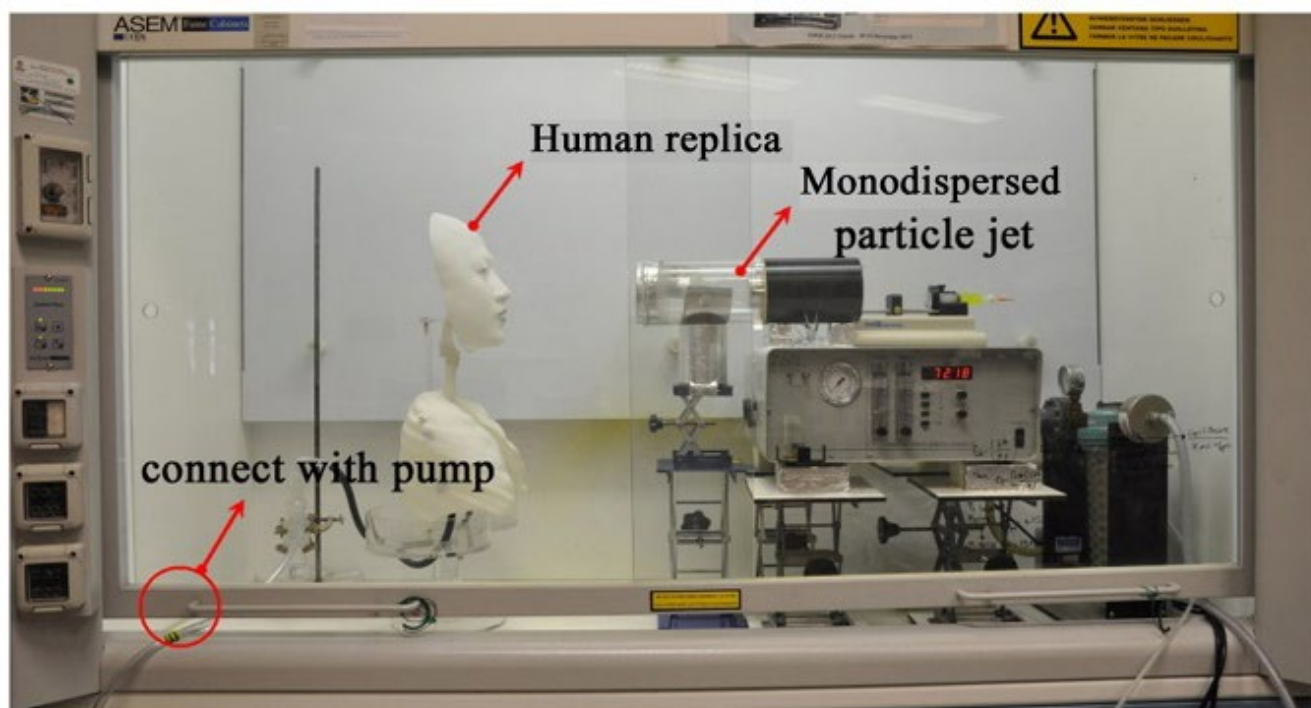


Fig. 1 Experimental set-up

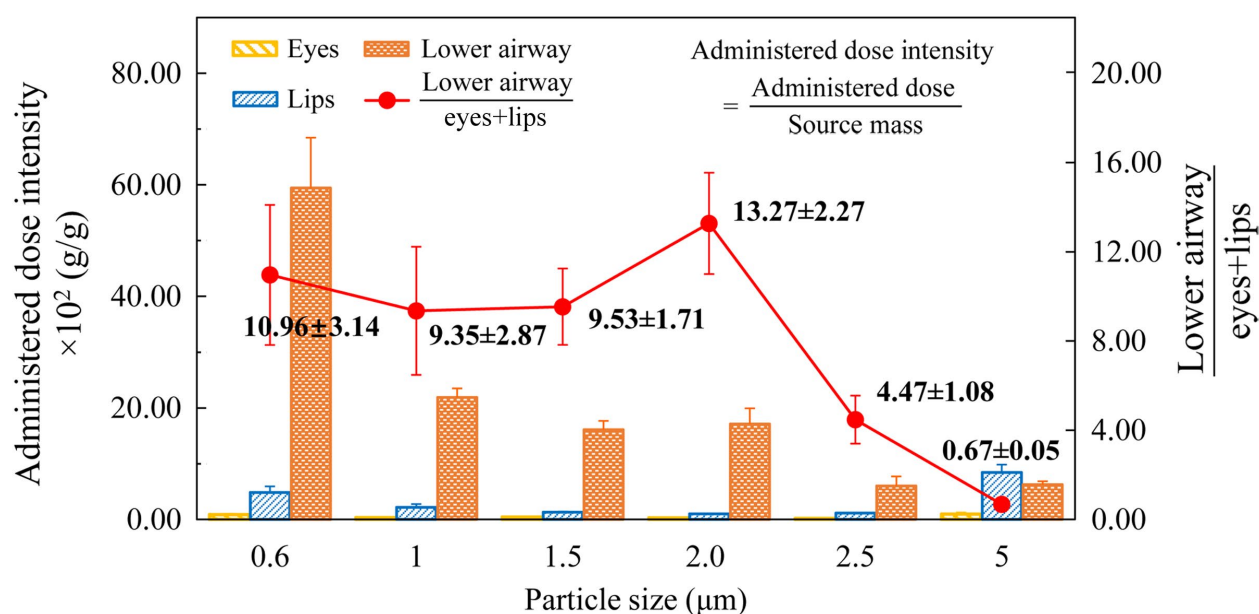


Fig. 2 Administered dose intensity of mucosal deposition and lower airway inhalation

3 RESULTS & DISCUSSION

As shown in Figure 2, the administered dose intensity of mucosa (eyes and lips) range from $(5.69 \pm 1.27) \times 10^{-2}$ – $(1.29 \pm 0.10) \times 10^{-2}$ g/g when the particle size is small (0.6–2.0 μm). Almost 10 times larger than that of lower airway. With particle size increasing, this ratio significantly drops. Especially for 5.0 μm particles, the administered dose intensity of mucosa is $(9.39 \pm 1.27) \times 10^{-2}$ g/g, which is even lower than that of lower airway. Furthermore, lips contribute over 90% of mucosal deposition. The results demonstrate that lower airway exposure becomes dominated in short-distance exposure when the particle size is small (less than 2.5 μm). But for large-size particles (>5.0 μm), facial mucosa, especially the lips, takes more risk than lower airway. Our results also reveal that the cutoff size, 5.0 μm , which differs the coarse and fine aerosols, might be inaccurate at least for assessing exposure risks for individuals.

4 CONCLUSIONS

In this work, we develop a human replica for accessing administered dose on facial mucosa and lower airway. The results based on our experimental bench imply that lower airway exposure is dominated for particle size less than 2.5 μm . But mucosal exposure plays an important role for 5.0 μm particles. Although the human replica still has unneglectable differences with real-life-conditions, the existing workbench inspires a new method to conveniently access administered dose in-vitro.

ACKNOWLEDGEMENTS

This work was supported by the National Key Research and Development Program of China (Grant No. 2017YFC0702700), the National Natural Science Foundation of China (Grant No. 51778520) and 2017 Sino-French Cai Yuan Pei program ([2017]6242).

REFERENCES

- Lizal, Frantisek, et al. (2012) Development of a realistic human airway model. *J. Engineering in Medicine* 226:197-207.
- Lock, Jaclyn Y, et al. (2018) Mucus models to evaluate the diffusion of drugs and particles. *Adv. Drug Deliver. Rev.* 2018: 34-49.
- Weis, Brenda K, et al. (2005) Personalized Exposure Assessment: Promising Approaches for Human Environmental Health Research. *Environ. Health Persp.* 113:840-848.



Aalborg Universitet

AALBORG UNIVERSITY
DENMARK

Assessing the impact of ventilation on the potential airborne infection risk in hospital lung function room

Fu, Yuqi; Liu, Shuo; Chen, Weijie; Ruan, Guohui ; Liu, Li

DOI (link to publication from Publisher):
[10.54337/aau541663876](https://doi.org/10.54337/aau541663876)

[Link to publication from Aalborg University](#)

Citation for published version (APA):
Fu, Y., Liu, S., Chen, W., Ruan, G., & Liu, L. (2023). Assessing the impact of ventilation on the potential airborne infection risk in hospital lung function room. In H. Johra (Ed.), *NSB 2023 - Book of Technical Papers: 13th Nordic Symposium on Building Physics* (Vol. 13). [10002] Department of the Built Environment, Aalborg University. <https://doi.org/10.54337/aau541663876>

Assessing the impact of ventilation on the potential airborne infection risk in hospital lung function room

Yuqi Fu^{1,2}, Shuo Liu^{3,4}, Weijie Chen⁵, Guohui Ruan⁵, Li Liu^{1,2,*}

¹ Department of Building Science, Tsinghua University, Beijing, China

² Laboratory of Eco-Planning & Green Building, Ministry of Education, Tsinghua University, Beijing, China

³ State Key Laboratory of Green Building in Western China, Xi'an University of Architecture and Technology, Xi'an, China

⁴ School of Building Services Science and Engineering, Xi'an University of Architecture and Technology, Xi'an, China

⁵ GIRFA Sci & Tech Co.,Ltd, Guangdong, China

*Corresponding email: liuli_archi@tsinghua.edu.cn

SUMMARY

Controlling the spread of respiratory infectious diseases in healthcare settings is important to avoid nosocomial infection. We utilized computational fluid dynamics (CFD) simulation, real-time carbon dioxide (CO₂) monitoring, microorganism culturing, and microorganism sequencing to quantitatively assess the exposure risk of healthcare workers to infectious respiratory particles (IRPs) in one lung function room under two ventilation configurations. The original ventilation system supplied 2 air changes per hour (ACH) for fresh air and 2 ACH for recirculated air, while the retrofitted ventilation system supplied 6 ACH of fresh air. Indoor CO₂ concentration and microorganism concentration decreased after the retrofit. The ventilation modification significantly improved the discharge efficiency for 5 µm IRPs and 50 µm IRPs. The intake fraction of 5 µm aerosols and 50 µm aerosols for HCW decreased by 0.005% and 0.006%, respectively. This study also reviewed the effectiveness of the above methods when evaluating building retrofit.

KEYWORDS: Nosocomial infection, building retrofit, airborne microorganisms, CFD simulation, carbon dioxide monitoring

1 INTRODUCTION

The COVID-19 pandemic has posed considerable threats and challenges to global health services, especially in the medical environment. As an important component of respiratory departments, HCWs in the lung function room also bear a high risk of inhaling infectious respiratory particles (IRPs) exhaled by patients during lung function test (LFT). Routine LFTs, such as spirometry, need patients to take off the mask, communicate with HCWs, and repeatedly perform forced exhalation, which usually results in coughing and sputum emission (Hull et al. 2020). Currently, the influence of ventilation on exposure risk of HCWs to IRPs in the lung function room is not quantitatively assessed.

2 MATERIALS/METHODS

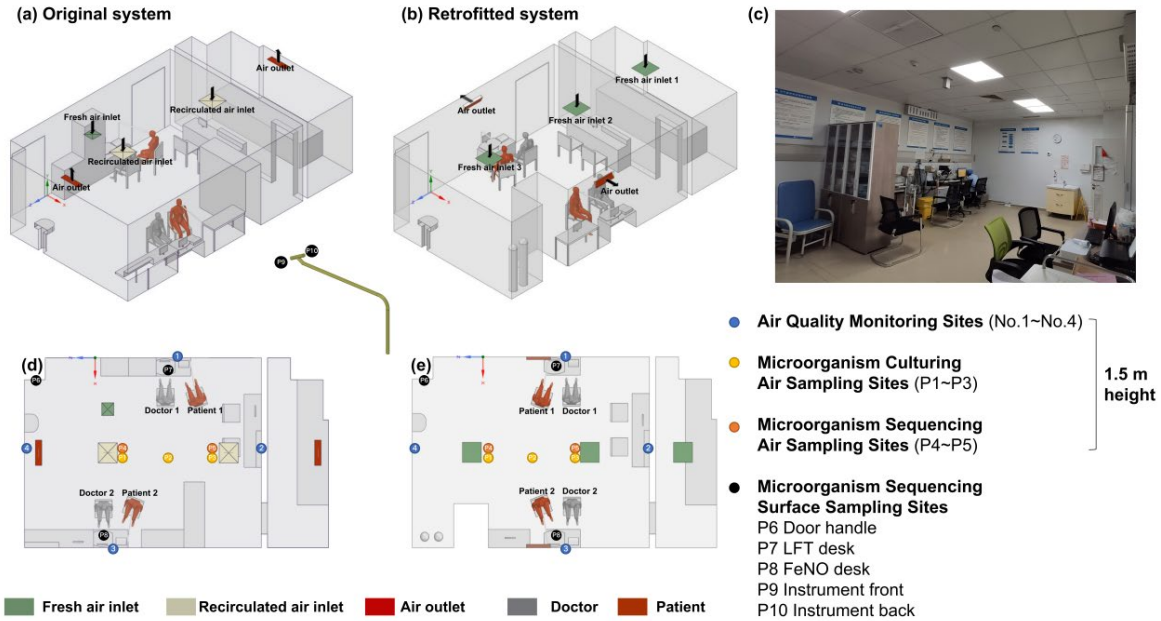


Figure 1. Lung function room model with (a) original ventilation system and (b) retrofitted ventilation system for CFD simulation, and with labeled sampling points under (d) original system and (e) retrofitted system

The selected lung function room in the hospital was a general rectangular-shaped room without any window. The dimensions of the testing room were 6.9 m (L) x 5.2 m (W) x 2.6 m (H) with a capacity of 2 treatment positions (1 HCW and 1 patient for every position), and the dimensions of the collocation room were 5.2 m (L) x 1.9 m (W) x 2.6 m (H). The original ventilation system included 1 small fresh air inlet (2 ACH), 2 recirculated air inlets (2 ACH), and 2 air outlets. The retrofitted ventilation system included 3 fresh air inlets (6 ACH) and 2 air outlets located above the working desks at treatment positions. Detailed descriptions are graphed in **Figure 1**.

3 RESULTS

When the fresh air change rate increased from 2 h⁻¹ to 6 h⁻¹ and stop using recirculated air, the intake fraction of 5 μm and 50 μm particles for doctor 1 increased by 0.077% and 0.022%, respectively. When the fresh air change rate increased from 2 h⁻¹ to 6 h⁻¹ and stop using recirculating air, the intake fraction of 5 μm and 50 μm particles for doctor 2 decreased by 0.005% and 0.006%, respectively

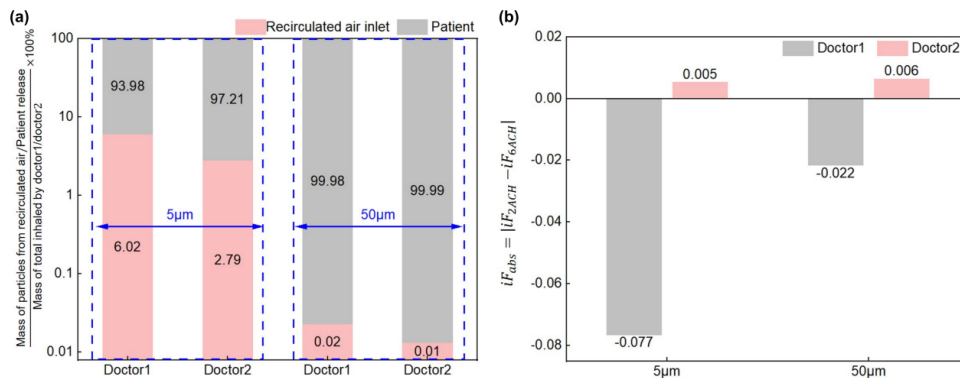


Figure 2. Size-resolved intake fraction of healthcare workers

The carbon dioxide concentration (all $p < 0.01$) were inversely correlated with the amount of fresh air. Ventilation variation was found in indoor microorganism concentration. The indoor bacteria level under 6 ACH (mean: 118±40 CFU/m³, 49-191 CFU/m³) was significantly ($p < 0.05$) lower (72.04% decrease) than that under 4 ACH (mean: 422±312 CFU/m³, 120-1187 CFU/m³). The indoor fungi level under 6 ACH

(mean: 29 ± 30 CFU/m³, 0-99 CFU/m³) was significantly ($p < 0.01$) lower (62.34% decrease) than that under 4 ACH (mean: 77 ± 24 CFU/m³, 35-99 CFU/m³). The concentration of airborne bacteria that can reach the small airways and even the alveoli was reduced by 68.15% and the concentration of airborne fungi was reduced by 70.37% (Guo et al. 2021). The diversity of aerosols was affected by the ventilation systems. Intra-group comparison of the surface fungi showed a higher chao1 index ($p < 0.001$) and Shannon index ($p < 0.05$) under 4 ACH than 6 ACH. Airborne bacteria ($p < 0.01$) and fungi ($p < 0.05$) showed a higher Shannon index under 6 ACH than 4 ACH but revealed no statistically significant difference in the chao1 index ($p > 0.05$). Surface bacteria revealed no statistically significant difference in the chao1 index ($p > 0.05$) and the Shannon index ($p > 0.05$) under different ventilation systems.

4 CONCLUSIONS

Taken together, this is a study that quantitative and qualitatively assessed the exposure risk of HCWs in the lung function room and reviewed the evaluation techniques. The results of the study showed that the diversity of microorganisms was influenced by the ventilation system, specifically, the amount of fresh air. Architectural retrofit should not only take the ventilation system (air change rate) into account but also consider the filtration system and position of air vents and personnel. Meanwhile, adequate air and surface disinfection accompanied by limited patient flow would better reduce the risk of nosocomial infection and cross-infection. As each of CFD simulation, real-time carbon dioxide monitoring, microbial culturing, and microbial sequencing has limitations, techniques that can directly trace IRPs should be considered.

5 REFERENCES

- Qian, H., Li, Y., Seto, W., Ching, P., Ching, W., & Sun, H. (2010). Natural ventilation for reducing airborne infection in hospitals. *Building and Environment*, 45(3), 559–565.
- Zhao, Y. H., Qu, H., Wang, Y., Wang, R., Zhao, Y., Huang, M. X., Li, B., & Zhu, W. M. (2022). Detection of microorganisms in hospital air before and during the SARS-CoV-2 pandemic. *European review for medical and pharmacological sciences*, 26(3), 1020–1027.
https://doi.org/10.26355/eurrev_202202_28011



Aalborg Universitet

AALBORG UNIVERSITY
DENMARK

Airborne transmission of disease in stratified flow

Nielsen, Peter V.; Zhang, Chen; Liu, Li

DOI (link to publication from Publisher):
[10.54337/aau541985833](https://doi.org/10.54337/aau541985833)

[Link to publication from Aalborg University](#)

Citation for published version (APA):
Nielsen, P. V., Zhang, C., & Liu, L. (2023). Airborne transmission of disease in stratified flow. In H. Johra (Ed.), *NSB 2023 - Book of Technical Papers: 13th Nordic Symposium on Building Physics* [10003] Department of the Built Environment, Aalborg University. <https://doi.org/10.54337/aau541985833>

Airborne transmission of disease in stratified flow

Peter V. Nielsen, Aalborg University, Denmark

Chen Zhang, Aalborg University, Denmark

Li Liu, Tsinghua University, China

Introduction

Airborne transmissions take place as a transport of virus or bacteria via the aerosol flow in rooms. The transmission can be part of the exhalation flow from the source of infection, it can move in the thermal flow from a warm or a cold source, be transported in the ventilation flow or other air movement in the room, and it can be spread by the turbulent diffusion in the room. The distribution of aerosols tends to be evenly distributed if the flow in the room is fully mixed.

Things will be different if the room air is stratified. A vertical temperature distribution may create stratified layers with either lower or higher concentrations of exhalation from the infected person (source person). Consequently, it could be interesting to use this effect to create a system with a low cross-infection risk between people in the room, [1] [2]. This possibility will be discussed in the following. Another effect in a system with vertically upward increasing temperature is the prospect of obtaining a cooling effect in the room with low location of the supply opening and high location of the return opening. This is the basic principle in displacement ventilation.

Stratified flow can also occur in other air distribution systems if they are highly loaded, as in rooms with a mixing ventilation system. In the following when we write “MV”, we assume a fully mixed air distribution and by “DV” we assume stratified air distribution.

Exhalation and inhalation of aerosols

The airborne transmission of diseases in a stratified flow will occur via virus-laden aerosols (droplet nuclei) through human respiratory activities. Therefore, it is necessary to simulate the human exhalation and inhalation process in fine details. “Aerosol dynamic” measurements have hence been performed with breathing thermal manikins, which have the face geometry as described in Table 1, [3] [4] [5] [6].

Table 1. Definition of nose and mouth.

Nose:

Two symmetrical jets. 30° between the jets
Jets 60° inclined toward the chest
50 mm² each nostril opening (diameter 8 mm)

Mouth:

100 mm² with semi-ellipsoidal shape
Horizontal discharge of exhaled air

The details of the face geometry are important as boundary conditions in experiments and in Computational Fluid Dynamics (CFD) predictions. Other important boundary conditions are the activity level of the person (heat release and thermal boundary layer), breathing frequency and volume flow rate. Movement of the face

(direction of exhalation), height of person, movement of the person might also be important for a detailed description in an aerosol dynamic experiment. The airborne transmission of aerosols will increase when we investigate speaking, shouting, singing, and coughing. The parameters in Table 1 change. The mouth area and exhalation direction vary in speaking, singing, and coughing [7]. The number of droplets and aerosols increase [8].

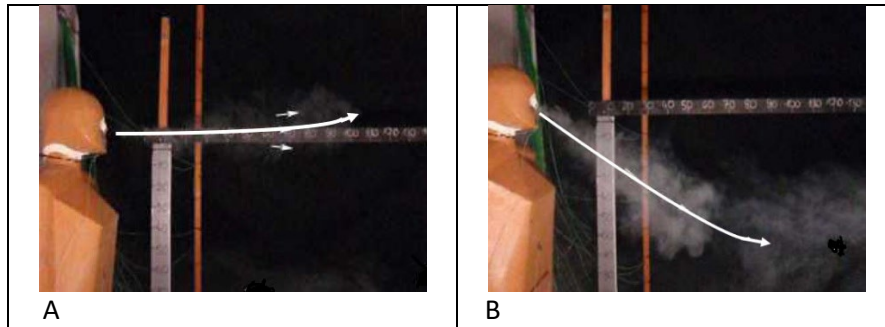


Figure 1. Exhalation 2.5 seconds after start of a sequence in a room with DV. A) Exhalation through mouth. B) Exhalation through nose [9].

Figure 1 shows the flow in the microenvironment around a manikin in surroundings with a vertical temperature gradient of 2.0 K/m. Figure 1A shows that the exhalation from the mouth forms an initial horizontal jet, and the flow is locked up by the temperature gradient just above the mouth in this case. The exhalation through the nose is different from the mouth flow, cf. Figure 1B. It starts with a downward jet and turns into a horizontal flow at some distance because it is also "locking up" in the vertical temperature gradient. The final flow has very different horizontal locations in the two cases. The initial exhalation temperature is 34° in both cases, but the exhalation jet mixes with the surrounding air and reduces the temperature to a local value in some distance.

The inhalation of a person also depends on several parameters. The air is inhaled from the thermal boundary layer around the body if the person does not move or turn around. Inhaling from the boundary layer means that a person will get his/her inhaled air from a lower level in the room than from the head height [1]. This is a positive effect if there is a concentration gradient in the room since the concentration at the bottom of the occupied zone can be low in displacement ventilation. The effect of the body boundary layer will disappear when the person is moving forward with more than 0.2 m/s [3].

Microenvironment, $x < 1.5$ m

The microenvironment around a person is the area where the air movement and the contaminant distribution processes are both influenced by the person and by the surrounding air conditioning system. The microenvironment can include two persons if they are standing in short distance $x < 1.5$ m.

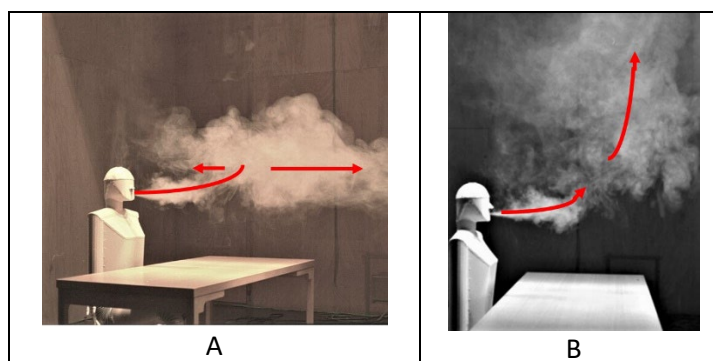


Figure 2. Exhalation flow from the mouth inside and outside the microenvironment. A) Stratified flow with a temperature gradient at head height of 0.5 K/m. B) Exhalation flow in a similar case with fully mixed flow without any temperature gradient, 0.0 K/m.

The vertical temperature distribution does influence the flow in the microenvironment. Figure 2A shows the exhalation flow from the mouth in the case of DV with a gradient of 0.5 K/m. The flow is an instantaneous jet close to the mouth, and it moves upward, at some distance, and spreads horizontally at head height due to the lock-up effect in the case of Figure 2A. The situation is typical for DV, because a gradient of 0.5 to 1.0 is within the comfortable conditions and a certain gradient is required to obtain an efficient energy solution.

Figure 2B shows the situation in the case of fully mixed flow, MV, in the room. The exhalation from the mouth is first an instantaneous jet mixed with the surrounding air, but in principle it will move continuously up to the ceiling area due to the temperature difference. Although the exhalation flow will rise in both cases, it will be possible to stand closer to a person in the MV case without being influenced by the exhalation flow of the opposite person. This effect is documented in many measurements of cross- infection risks between two persons at short distance inside the common microenvironment, (< 1.5 m) [3] [4] [5] [6].

Let us look at a situation where the cross-infection risk between two persons is expressed as the inhalation of tracer gas (aerosols) from one person to the other. Figure 3 shows the exposure of a target person expressed as normalized exposure $c_{exp}/c_R (= \epsilon)$, where c_{exp} is the exposure of inhaled tracer gas standing opposite to a source manikin and c_R is the concentration in return opening (fully mixed value). Although traces gas cannot be directly used as a measure for the health risk assessment, it can give an indication of this risk.

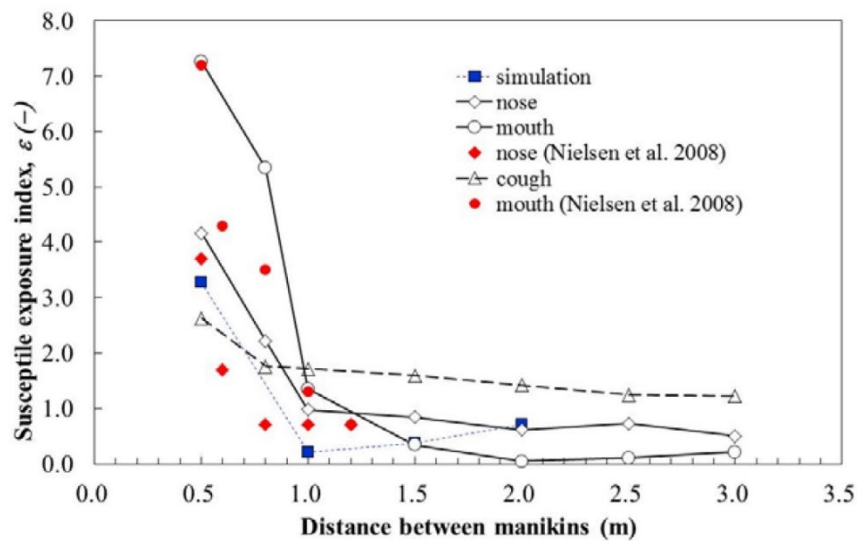


Figure 3. Exposure of target manikin versus distance between the two manikins of same height in a room with displacement ventilation. Results are shown for both breathing through the mouth, through the nose, for coughing, and for CFD predictions [5].

It is obvious that there is a large increase in the cross-infection risk when the two persons are standing close to each other (in a common microenvironment, $x < 1.5$ m). This is both the case for breathing through the mouth and through the nose. It is also seen from [10] that the increase in this exposure is expected to be low in the case of MV, in agreement with the two situations shown in Figure 2. The effect is due to the influence of the temperature gradient on the exhalation flow, which is different for different ventilation systems. The

normalized exposure, c_{exp}/c_R , at the distance 0.35 m is, for example, around 7.0 for displacement ventilation, 4.3 for vertical ventilation, 1.8 for diffuse ceiling ventilation, and only 1.5 for mixing ventilation, [6]. Thermal stratification has an unfortunate effect on exposure in the microenvironment, and fully mixed (MV) conditions with a normalized exposure up to 1.5 (at 1.35 m) are to be preferred. It should be noted that it can be difficult to obtain MV conditions at certain load conditions and at some certain geometries in the system.

Macro-environment, $x > 1.5$ m

Figure 3 also shows the conditions in the macro-environment of a displacement ventilated room ($x > 1.5$ m). The exposure is below the fully mixed value, and it is different for breathing through the nose (0.7) than for breathing through the mouth (0.2). The values are preferable values in a ventilated room, and they are achieved because people's inhalation is from the lower part of the room via the personal thermal boundary layer. The concentration of exhaled aerosols is often low in this lower part of a room with displacement ventilation. The results show that detailed boundary conditions for the breathing function of the source manikin must be essential in stratified flow.

What will challenge this overall low cross-infection risk between people in the room in case of DV? Let us look at the parameters discussed earlier. Results in Figure 3 are for people of same height and without moving. Walking and movement of the face could increase infection risk [3]. Blocking the target manikin's boundary layer by a table may increase infection risk. Breathing through the nose instead of the mouth could increase infection risk. The activity level of the person (heat release and thermal boundary layer), breathing frequency, and volume flow rate will have an influence. Mouth area and exhalation direction vary in speaking, singing, and coughing [7] and could modify the lock-up height.

The position of the human exhalation layer depends on several variables as the size and location of the vertical temperature gradient in the room. In addition, this gradient is dependent on the heat load and temperature level in the room, on vertical and horizontal location of heat loads etc. Different situations obtained with a seated and a standing person (distance 4 m) in a room with different heat loads and flow rates, have normalized exposures from 0.6 to 1.75, [11].

Fully mixed flow will be an alternative safe solution, but it requires a higher flow rate of outdoor air [12]. The system should be well-designed without creating any stratification at high heat load.

Conclusion

The use of the stratification effect made it possible to create a reduced cross-infection risk for long range airborne transmission in some situations, but we need research in system layout to find solutions which will give a safe environment in all practical situations. A solution must be followed up with some necessary restrictions/information of use, if necessary. Another possibility is to use mixing ventilation and accept a higher flow rate of outdoor air.

It is also a question whether or not it is acceptable to select a solution with the stratified flow, which shows high exposure at the close distance between people (< 1.5 m); if it can be solved with mixing ventilation where the cross-infection risk is lower at close distance, although a higher flow rate to the room is required to obtain an overall acceptable infection risk.

References

- [1] Brohus H, Nielsen PV. Personal Exposure in Displacement Ventilated Rooms. *Indoor Air*. 1996;6(3):157-167. doi: 10.1111/j.1600-0668.1996.t01-1-00003.x
- [2] Kosonen R, (ed.), Melikov AK, Mundt E, Mustakallio P, Nielsen PV. Displacement Ventilation. Forssa: REHVA: Federation of European Heating and Air-conditioning Associations, 2017. (REHVA Guidebook; Nr. 23).
- [3] Bjørn E, Nielsen, PV, 'Dispersal of Exhaled Air and Personal Exposure in Displacement Ventilated Rooms', *Indoor Air Online*, 2002, bind 12, nr. 3, s. 147-164. <https://doi.org/10.1034/j.1600-0668.2002.08126.x>
- [4] Nielsen PV, Winther FV, Buus, M, Thilageswaran, M, Contaminant Flow in the Microenvironment Between People Under Different Ventilation Conditions, *ASHRAE Transactions*, nr. Part 2, 2008, s. 632-640.
- [5] Liu L, Li Y, Nielsen PV, Wei J, Jensen RL. Short-range airborne transmission of expiratory droplets between two people. *Indoor Air Online*. 2017;27(2):452-462. Epub 2017. doi: 10.1111/ina.12314
- [6] Nielsen PV, Xu C, Multiple airflow patterns in human microenvironment and the influence on short-distance airborne cross-infection – A review, *Indoor and Built Environment*, 2021. <http://dx.doi.org/10.1177/1420326X211048539>
- [7] Abkarian M, Mendez S, Xue N, Yang F, Stone HA, Speech can produce jet-like transport relevant to asymptomatic spreading of virus, *Proceedings of the National Academy of Sciences of the United States of America*, 25 Sep 2020, 117(41):25237-25245, DOI: 10.1073/pnas.2012156117
- [8] Pan S, Xu C, Yu CWF, Liu L, Characterization and size distribution of initial droplet concentration discharged from human breathing and speaking, *Indoor and Built Environment*, 2022, Vol. 0(0) 1–14 DOI:10.1177/1420326X221110975
- [9] Nielsen PV, Jensen RL, Litewnicki M, Zajas JJ, Experiments on the Microenvironment and Breathing of a Person in Isothermal and Stratified Surroundings. i *Healthy Buildings 2009: 9th International Conference & Exhibition*, September 13-17, 2009, Syracuse, NY USA. The International Conference & Exhibition of Healthy Buildings, Syracuse, NY, USA, 13/09/2009.
- [10] Nielsen PV, Winther FV, Buus M, Thilageswaran M, 2008, Contaminant Flow in the Microenvironment between People under Different Ventilation Conditions, *ASHRAE Trans.*, pp. 632–640.
- [11] Bjørn E, Nielsen PV. Passive Smoking in a Displacement Ventilated Room. Aalborg: Dept. of Building Technology and Structural Engineering, 1997. 6 s. (Indoor Environmental Technology; Nr. 69, Bind R9714).
- [12] Li, Y, Nielsen, PV & Sandberg, M 2011, 'Displacement Ventilation in Hospital Environments', *ASHRAE Journal*, bind 53, nr. 6, s. 86-88.



Aalborg Universitet

AALBORG UNIVERSITY
DENMARK

Exploring the Role of Ambient Temperature in Exhaled Jet Related to Cross Infection between Individuals by CFD

Qian, Hua; Ma, Jianchao; Nielsen, Peter V.

DOI (link to publication from Publisher):
[10.54337/aau541987560](https://doi.org/10.54337/aau541987560)

[Link to publication from Aalborg University](#)

Citation for published version (APA):
Qian, H., Ma, J., & Nielsen, P. V. (2023). Exploring the Role of Ambient Temperature in Exhaled Jet Related to Cross Infection between Individuals by CFD. In H. Johra (Ed.), *NSB 2023 - Book of Technical Papers: 13th Nordic Symposium on Building Physics* [10004] Department of the Built Environment, Aalborg University. <https://doi.org/10.54337/aau541987560>

Exploring the Role of Ambient Temperature in Exhaled Jet Related to Cross Infection between Individuals by CFD

Hua Qian¹, Jianchao Ma¹, Peter Nielsen²

¹ School of Energy and Environment, Southeast University, Nanjing, China

² Department of the Built Environment, Aalborg University, Aalborg, Denmark

Abstract

The ubiquity of respiratory infectious diseases amongst human populations is well-recognized, yet the exact mechanisms and pathways of their transmission continue to be a subject of ongoing research. Numerous recent studies have begun to reveal that the dynamics of exhaled flow, including parameters such as airflow patterns, temperature variations, and temperature gradients, among others, have a substantial correlation with the propagation of respiratory ailments.

In this research paper, our primary objective was to delve into the influence of ambient temperature on the exhaled jet flows exchanged between two individuals. To accomplish this, we utilized Computational Fluid Dynamics (CFD), in conjunction with transient simulation methodologies to conduct the study. Grid-independent was checked. Results were verified by experiments in the literature.

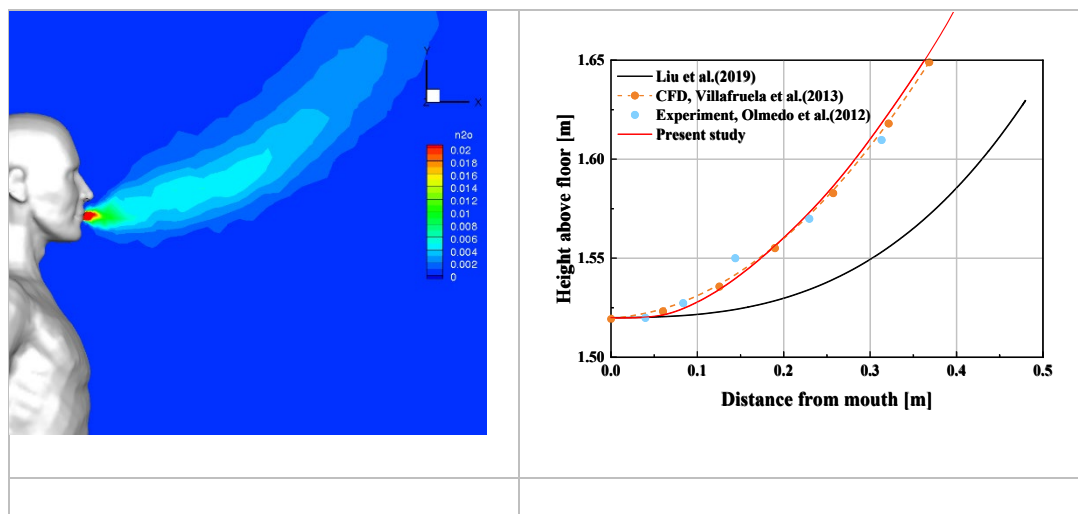


Figure 1 Simulation results and comparison with experimental data in the literature

We constructed a simulated scenario representing the exchange of exhaled jet flow between two individuals situated in diverse temperature conditions. The computational results gleaned from this scenario were then juxtaposed with data obtained from controlled experimental conditions.

The transient simulation data revealed intriguing patterns. It was observed that exhaled jet flows exhibited a greater propensity to ascend in environments with lower temperatures, whereas the flow trajectory tended to remain comparatively horizontal in higher temperature conditions.

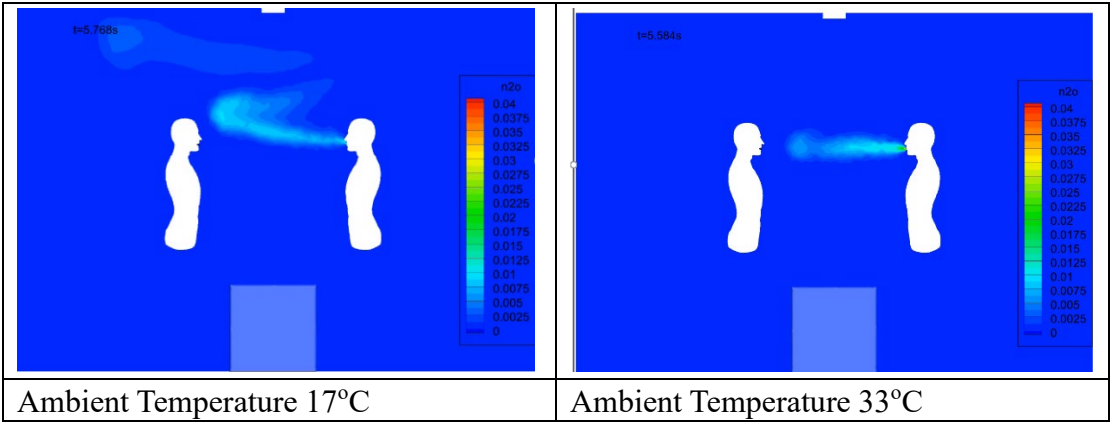


Figure 2 Transient simulation results at different ambient temperature

These observations emphasize the critical role that environmental temperature plays in shaping the pattern of exhaled jet flow between individuals. Hence, it is of paramount importance to take into consideration the ambient temperature when conceptualizing the design of indoor spaces to effectively mitigate the risk of cross-infection. Our study accentuates the imperative of incorporating environmental considerations into the design of strategies aimed at preventing the transmission of respiratory diseases. This research underscores the potential benefits of a multidisciplinary approach, combining insights from physics, engineering, and epidemiology, in enhancing our understanding of disease transmission and in the development of effective countermeasures.



Aalborg Universitet

AALBORG UNIVERSITY
DENMARK

Experimental evaluation of PCM embedded radiant chilled ceiling for efficient space cooling

Mousavi, Seyedmostafa; Rismanchi, Behzad; Brey, Stefan; Aye, Lu

Published in:

NSB 2023 - Book of Technical Papers: 13th Nordic Symposium on Building Physics

DOI (link to publication from Publisher):

[10.54337/aau609928685](https://doi.org/10.54337/aau609928685)

Creative Commons License

CC BY 4.0

Publication date:

2023

Document Version

Publisher's PDF, also known as Version of record

[Link to publication from Aalborg University](#)

Citation for published version (APA):

Mousavi, S., Rismanchi, B., Brey, S., & Aye, L. (2023). Experimental evaluation of PCM embedded radiant chilled ceiling for efficient space cooling. In H. Johra (Ed.), *NSB 2023 - Book of Technical Papers: 13th Nordic Symposium on Building Physics* (Vol. 13). Article 333 Department of the Built Environment, Aalborg University. <https://doi.org/10.54337/aau609928685>

General rights

Copyright and moral rights for the publications made accessible in the public portal are retained by the authors and/or other copyright owners and it is a condition of accessing publications that users recognise and abide by the legal requirements associated with these rights.

- Users may download and print one copy of any publication from the public portal for the purpose of private study or research.
- You may not further distribute the material or use it for any profit-making activity or commercial gain
- You may freely distribute the URL identifying the publication in the public portal -

Take down policy

If you believe that this document breaches copyright please contact us at vbn@aub.aau.dk providing details, and we will remove access to the work immediately and investigate your claim.

Experimental evaluation of PCM embedded radiant chilled ceiling for efficient space cooling

Seyedmostafa Mousavi^{1,*}, Behzad Rismanchi¹, Stefan Brey² and Lu Aye¹

¹ Renewable Energy and Energy Efficiency Group, Department of Infrastructure Engineering, The University of Melbourne, VIC 3010, Australia

² Invaus Pty Ltd., Melbourne, VIC 3000, Australia

* Corresponding author: sm.mousavi@unimelb.edu.au

Abstract. Because of climate change, together with rapid urbanisation and continuous population growth, the global demand for space cooling is increasing dramatically. Under a business-as-usual trajectory, there will be a more than threefold rise in the number of in-use air conditioners worldwide by 2050. A radical shift to innovative space cooling technologies is therefore essential, ones that can sustainably meet the growing requirements. Phase change material embedded radiant chilled ceiling, called PCM-RCC, offers an emerging alternative for more sustainable space cooling provision. This system provides a range of benefits to end-users, in terms of efficiency and indoor environmental quality, together with demand-side flexibility. PCM-RCC, however, is still under development, and further research is needed to realise its full capabilities. The present work experimentally analyses the thermal-energy performance of a PCM-RCC system using a full-scale test cabin equipped with PCM ceiling panels. Here, the transient thermal behaviour of the panels besides the cooling energy delivered in charging-discharging cycles are examined. Additionally, the indoor thermal comfort and peak energy demand reduction enabled by the present PCM-RCC are discussed. Based on the results, typically 4–5 hours of chilled water circulation overnight could sufficiently be able to fully recharge the panels in the morning. Over 80% of the occupancy time was found within Class B thermal comfort defined in ISO 7730. About 70% of the system's daily electricity usage time was during off-peak hours. The significance of implementing optimal predictive operating schedules was also highlighted to fully utilise PCM-RCC's potentials.

1. Introduction

Since 1990, the energy consumed for space cooling has tripled, significantly impacting the electricity infrastructures. In 2021, the demand for space cooling experienced the largest annual increase among all building end-uses, accounting for around 16% of the global final energy consumption in the building sector (~2000 TWh) [1]. This is mainly driven by the growing global demand for air conditioners (ACs) as a result of continuous climate change and population growth [2]. The number of in-use ACs worldwide jumped from 1.6 billion units in 2020 to 2.2 billion in 2021 [1,3]. On a business-as-usual trajectory, this number is expected to more than triple by 2050 [4].

The data signifies how vital it is for the building and construction sector to firmly adopt not only effective policies but also more advanced, energy-efficient space cooling technologies [5]. Over the past several years, academia and industry have searched for potential technologies to enhance the cooling efficiency of AC units. One such technology involves the use of phase change material (PCM) embedded radiant chilled ceiling (RCC), herein called PCM-RCC. In this system, the PCM acts as a

thermal battery and is charged overnight via the chilled water flowing through the ceiling panels (freezing cycle). It is then discharged during the daytime by absorbing the interior sensible heat (melting cycle). Thanks to the radiant cooling and thermal energy storage mechanisms, PCM-RCC offers end-users a variety of advantages in terms of efficiency and indoor environmental quality (IEQ), together with demand-side flexibility. Lower energy consumption, better space utilisation, improved thermal comfort, quiet operation, enhanced IEQ with limited recirculation of pathogens, as well as peak load shifting are the benefits of the PCM-RCC technology, compared to classic AC systems [2].

Notwithstanding broad interest in PCM-RCC applications among the scientific and industry communities, the technology has not yet transitioned to its ‘limited availability’ stage. Several studies investigated PCM-RCC’s cooling potentials (for example, see [6-9]); however, concerns about how this technology should be designed and operated in real-life scenarios need to be credibly addressed.

This study carries out a field study on a full-scale test cabin equipped with a new PCM-RCC system to explore the capabilities of the system and potential challenges that it might encounter in real-world settings. Here, the transient thermal behaviour of PCM ceiling panels plus the cooling energy delivered in charging-discharging phases are evaluated. Then, the level of interior thermal comfort as well as the peak electricity demand reduction provided by the present PCM-RCC are discussed.

2. Research method

2.1. Experimental setup

2.1.1. Test cabin. The current experiments were carried out on a full-scale test cabin equipped with a PCM-RCC system (Figure 1), located at the University of Melbourne. This test cabin, which is of a conditioned volume of 96.7 m³, is fully exposed to real-world climatic conditions. R4.3 and R4.8 sandwich panels were utilised for the cabin structure. Advanced floor-to-ceiling glazing with interstitial Venetian blinds and a vision area of 13.5 m² was also used to create a seamless connection to the natural surroundings, as is common in today’s modern architectural design. More details of the cabin structure (e.g., layers thickness, conductivity, capacity, and density) can also be found in [10].

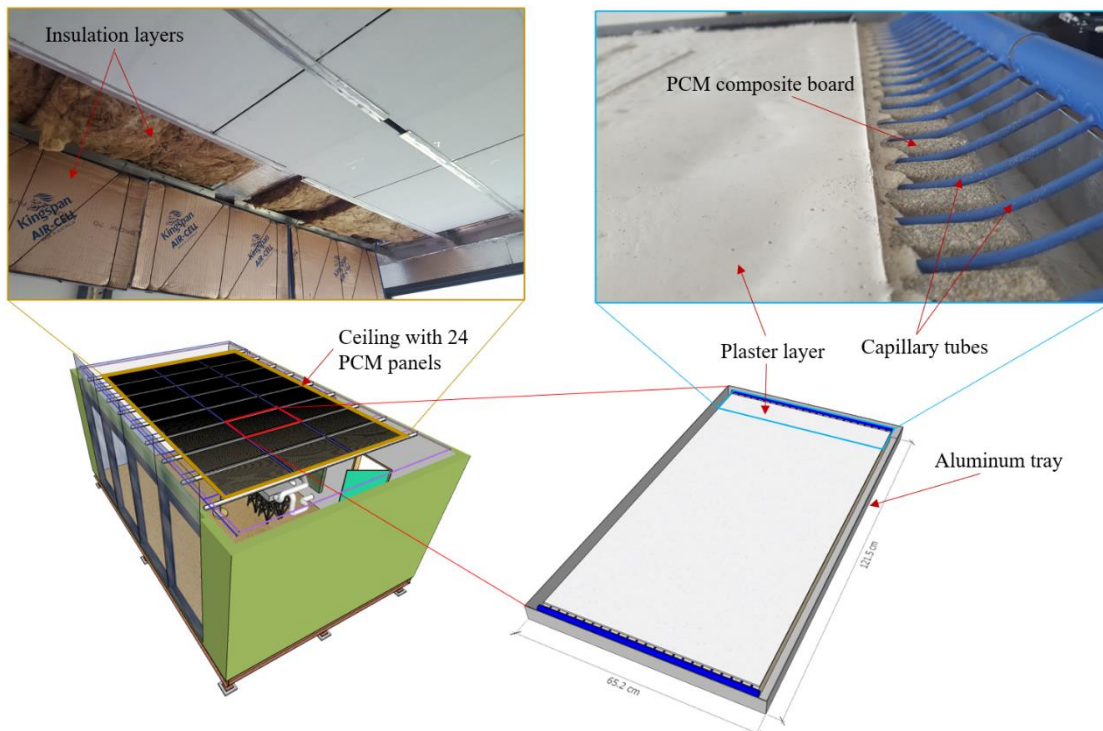


Figure 1. PCM ceiling panels used for the proposed PCM-RCC system.

2.1.2. Shape-stabilised PCM composite boards. As seen in Figure 1, organic-based shape-stabilised PCM boards placed in a 1.5 mm-thick aluminium tray were used for the present PCM-RCC system. These PCM boards with dimensions of 121.5 cm (L) \times 65.2 cm (W) \times 2.5 cm (D) have a phase change range of 15.6–19.6°C, a density of 765 kg/m³, and a latent heat capacity of 900 kJ/m². Thermal conductivities of the PCM board in solid and liquid phases were also measured using a C-Therm conductivity analyser, and the values were found to be 1.02 and 0.68 W/m.K (with $\pm 5\%$ uncertainty), respectively.

Approximately 60% of the cabin's ceiling area was covered by 24 PCM panels installed in eight parallel rows. For the current panel design, as shown in Figure 1, capillary tube mats were used for chilled water circulation during PCM recharge cycle. These thin capillary tubes are flexible and easy-to-assemble by plastic welding [2,8]. Based on lessons learnt in the authors' previous study [3], a 3-mm-thick plaster layer was applied on top of PCM boards to improve the thermal contact between the capillary tubes and the PCM. Panels were also covered with additional insulation layers to decrease energy losses caused by heat transfers to the roof. Additionally, the panel surfaces were painted using high-emissivity paint to increase the ceiling emissivity rate.

2.1.3. Chilled water supply and distribution system. The hydronic distribution unit, as well as the arrangements of PCM ceiling panels, is shown in Figure 2. Each row, consisting of three PCM ceiling panels in series, is independently connected to the chilled water supply and return lines. Chilled water, provided by an air-source heat pump, is pumped and circulated within the ceiling panels to extract heat from PCM until the controlling setpoints of the recharge schedule are met. The supply and return lines, plus all fittings, were properly insulated to avoid heat losses from the surroundings. The operation of equipment (circulating pumps, heat pump, fans, heater) was remotely controlled via a programmable logic controller. In this configuration, the panels and the cabin air temperature can be easily monitored, and different control strategies can be implemented remotely.

2.1.4. Dedicated outdoor air system (DOAS). A dedicated outdoor air system (DOAS) supplies cooled, dehumidified outdoor air to the indoor space, principally to handle the internal latent loads. DOAS units are often used in conjunction with a parallel cooling system. Radiant ceiling panels are the optimum choice as a parallel system to be coupled with a DOAS unit [11]. Here, a DOAS system was installed in the cabin to deliver fresh air and supplementary cooling, when needed. With this parallel cooling system design, the potential for indoor air quality problems can be further minimised.

2.1.5. Data acquisition and monitoring. Multiple sensors and internet-of-things (IoT) devices were installed in the cabin to read and collect essential variables for the present PCM-RCC performance evaluation. These variables are classified into five main categories as presented in Table 1.

Table 1. Categories of measured variables in this study

Measurement category	Measured variable
PCM ceiling panel	(1) PCM panel temperature, (2) Panel heat flux
Indoor climate	(1) Room and wall surface temperatures, (2) CO ₂ level, (3) Relative humidity (RH), (4) Light level, (5) Occupancy
Hydronic unit	(1) Water flow rate, (2) Supply and return water temperatures
Power consumption	(1) Power usage, (2) Voltage, (3) Current
Weather station	(1) Ambient temperature, (2) Global and reflected solar radiation, (3) Outdoor RH, (4) Rainfall, (5) Wind speed and direction

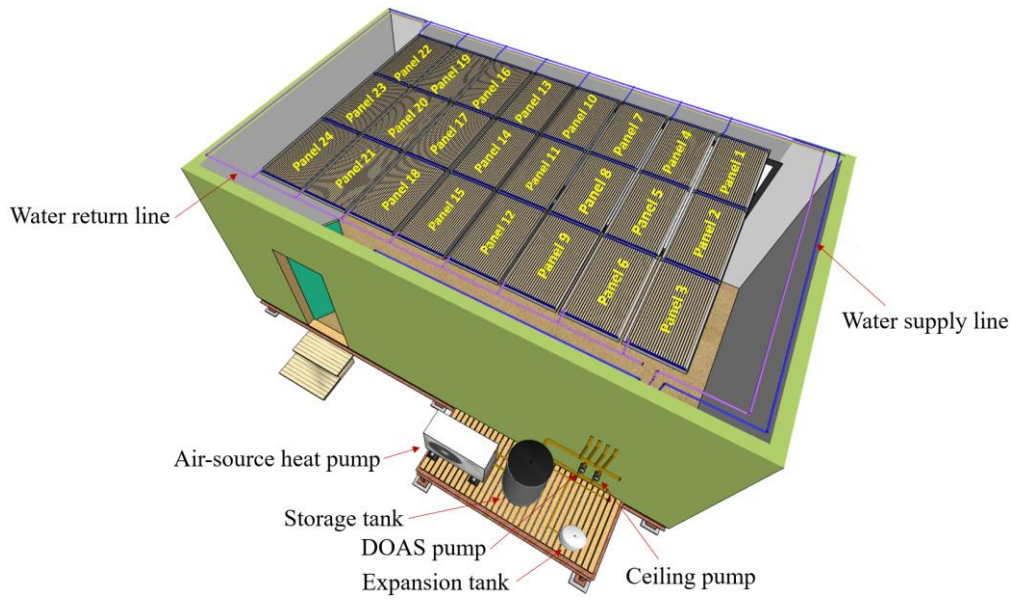


Figure 2. PCM-RCC hydronic system and the arrangements of PCM panels in the test cabin.

2.2. Operational schedule

The PCM-RCC operating schedule, shown in Table 2, was planned based on the current ceiling layout and PCM panel design, findings of the authors' previous field testing, as well as recommendations given in the IEQ-related standards/guidelines.

Table 2. PCM-RCC operating schedules for the experiments.

Component	Controller logic
Ceiling pump	Un-occupied period ¹
	Run the pump for 4 hours overnight (03:00 am – 07:00 am) ²
	Occupancy period
	Run the pump during DOAS fan operation if PCM panels are mostly liquid ($T_{PCM, middle\ layer} > 18.5^{\circ}C$) AND $T_{indoor} > 24^{\circ}C$ ³ .
DOAS unit	Un-occupied period
	Run DOAS (fan only) from 10:00 pm – 07:00 am if $T_{indoor} > 22^{\circ}C$ AND $T_{outdoor} < T_{indoor}$. AND
	Run DOAS (fan + secondary pump) from 12:00 am – 03:00 am if $T_{indoor} > 22^{\circ}C$ ⁴ .
	Occupancy period
	Run DOAS fan based on 0.5-hr ON/1-hr OFF schedule ⁵ . AND
	Run DOAS secondary pump during fan operation ⁶ if $T_{outdoor} > 26^{\circ}C$ AND $T_{indoor} > 24^{\circ}C$ ³ .
Heat pump	Un-occupied period
	Run the heat pump when the ceiling pump or DOAS secondary pump is activated, to supply chilled water with a setpoint of 10°C.
	Occupancy period
	Run the heat pump if the ceiling pump or DOAS secondary pump is activated.
Heater	Run the heater in early morning (06:30 am – 08:30 am) ⁷ if $T_{indoor} < 20^{\circ}C$ ³ .

¹ 9:00 am – 7:00 pm was referred to as occupancy time. Outside of this period was considered as un-occupancy time.

² According to the preliminary assessments of PCM-RCC operation in different weather condition, maximum of 4-5 hours was required to fully recharge PCM panels.

³ Indoor temperature limits were defined based on ISO7730 standard.

⁴ DOAS operation overnight effectively prevents cabin overheating and regulates indoor relative humidity.

⁵ With averagely 90 L/s of airflow rate, DOAS fan operation with 0.5-hr-ON/1-hr-OFF schedule provides minimum fresh air for occupants during the occupancy time.

⁶ Secondary DOAS pump operation aimed to provide supplementary cooling during occupancy time, if required.

⁷ This schedule was set up to manage the possible issue of overcooling in early mornings after the recharge cycle.

3. Results and discussions

3.1. Charging-discharging performance of PCM ceiling panels

Figure 3 shows the measured indoor (globe) temperature, PCM ceiling temperatures, and ceiling heat flux (HF) during system operation in three consecutive summer days. Figure 4 displays the hourly estimated partial enthalpy in both melting and freezing paths plus the liquid fraction of PCMs in the ceiling panels. As observed, the active recharge cycle on the first day started with the initial ceiling temperature and PCM liquid fraction of approximately 18.5°C and 71%, respectively. After 4 hours of chilled water circulation with an average water flow rate of 470 L/hr, the PCM panels were sufficiently recharged. Positive HF values during the daytime confirm that the PCM ceiling panels steadily absorbed heat from the cabin interior as the PCM phase was changing (solid → mushy → liquid). Furthermore, the DOAS unit and ceiling pump were intermittently operated to provide supplementary cooling and maintain the desired comfort condition. This supplementary cooling also added a residual cooling capacity to the PCM, extending the active time of the panels in late afternoon. For the first day, the ceiling panels remained active until 07:30 pm. A sharp increase in panel temperatures was then observed, indicating that the PCMs had almost fully melted.

As the data shows, the second day started with cabin and ceiling temperatures of around 22°C and a PCM liquid fraction of 100% (fully liquid). In accordance with the defined operating schedule, the DOAS was activated before the ceiling pump operation overnight to ventilate and cool the cabin using cool night-time ambient air. The estimated values of partial enthalpy and liquid fraction for PCM panels in the early morning demonstrate that they were almost fully recharged. The cooling storage capacity of the PCM ceiling almost covered the entire occupancy time, thanks to the extra cooling periodically provided by the DOAS and ceiling operations. The same initial state of temperatures and PCM liquid fraction was also observed for the third day. However, since the ambient temperature on this day dropped significantly in the afternoon, no supplementary cooling was required after 02:00 pm, and the PCM ceiling's storage capacity, despite being exhausted around 04:00 pm, was sufficient to maintain an acceptable level of thermal comfort.

Focusing on the PCM ceiling recharge period overnight, it was obtained that the efficiency of the recharge cycle followed a gradual decline during the next hot days. It was uncertain whether fully-recharged PCM panels could be achieved with the same active recharge schedule since the PCMs were completely melted, and heat accumulated in indoor space after consecutive hot days. The HF patterns also confirm that the first 1 – 2 hours of the active recharge period dealt with removing indoor sensible

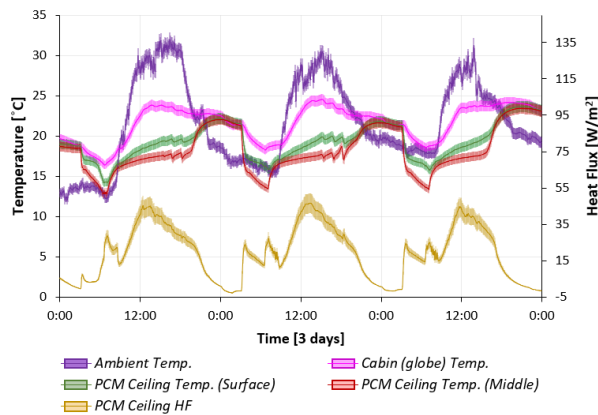


Figure 3. Measured cabin (globe) and PCM ceiling temperatures plus PCM ceiling heat flux.

(note: The experimental uncertainty, shown with the measured data, is estimated with a 95% confidence interval.)

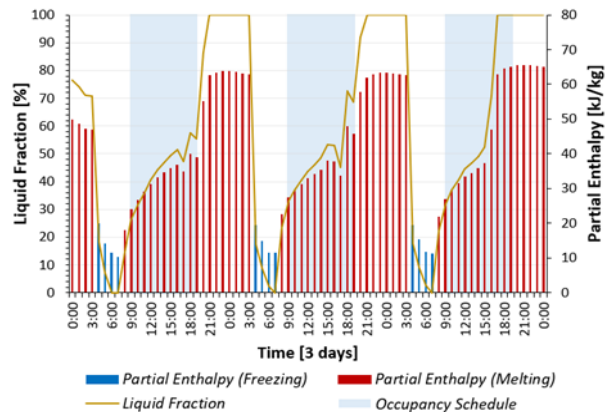


Figure 4. Partial enthalpy and liquid fraction of PCM ceiling panels.

heat, thus slowing the freezing rate of the PCM. Although the current operating schedule aimed to respond to the transient thermal behaviour of indoor space and PCM ceiling panels, a more dynamic, optimal predictive schedule with precise weather forecasting is still required to carefully control uncertainties in the system's performance.

3.2. Ceiling cooling energy

Using the heat transfer balance method at the radiant ceiling surface, the heat flux between the indoor space and PCM ceiling panels can be formulated as follows:

$$\dot{Q}_{abs,ceiling}'' = \dot{Q}_s'' + \dot{Q}_{ir}'' + \dot{Q}_c'' + \sum \dot{Q}_r'' \quad (1)$$

where the subscripts s , ir , c , and r denote, respectively, transmitted solar radiation absorbed by the radiant ceiling surface, radiative flux with internal heat sources, convective heat flux with the interior environment, and radiative heat flux with other indoor surfaces. Besides, the heat extracted from PCM ceiling panels by chilled water during the recharge period is equal to:

$$\dot{Q}_{ext,water}'' = \frac{\dot{m}_w C_{p,w} (T_{rw} - T_{sw})}{A_{panels}} \quad (2)$$

Here, \dot{m}_w is the water flow rate [kg/s], $C_{p,w}$ is the specific heat capacity of water [4182 J/kg.K], A_{panels} is the PCM ceiling area [m²], and T_{rw} and T_{sw} are the return and supply water temperatures [°C], respectively.

During the three-day experiment, the average total heat transfer coefficient from the PCM ceiling panels to the indoor space was calculated to be 8.48 ± 0.97 W/(m².K), taking into account both radiative and convective heat transfer paths. This value is consistent with the relevant standards, e.g., REHVA, EN1264-5, and EN15377-1. Meanwhile, comparing the total daily energy absorbed by PCM ceiling panels from the indoor space with the total heat extracted from the panels by chilled water during the active recharge period reveals almost equal values of cooling energy absorbed and extracted (Figure 5). The small difference observed on the first day could be due to the residual cooling capacity existed initially in the PCM panels with the liquid fraction of 71%, resulting in less heat being extracted during the chilled water circulation time. The differences in the extracted-absorbed values for the second and third days might also be due to the accumulated indoor heat being removed directly by the hydronic system. As mentioned in Section 3.1, the first 1 – 2 hours of the active recharge overnight dealt with removing indoor sensible heat before extracting heat from the PCM panels.

3.3. Thermal comfort assessment

Low quality and deteriorated indoor thermal comfort conditions lead to individual dissatisfaction and negatively influence their well-being, performance, and productivity [2]. This highlights that thermal comfort must be cautiously monitored, such that any issues can be urgently addressed. Heating, ventilation, and air-conditioning (HVAC) systems are the key elements in delivering desired indoor thermal comfort; thus, an inappropriate design and implementation of these systems raise the occurrence probability of thermal comfort issues during daily building operations.

The predicted mean vote (PMV) is a well-known, commonly-used index in thermal comfort assessments [12]. As listed in Table 3, ISO 7730 and EN 16798-1 specify different categories for indoor thermal comfort depending on PMV levels. Here, the PMV method was used to evaluate the thermal comfort conditions provided by the present PCM-RCC system. PMV values were determined using a developed program, and the results were validated by comparison with those obtained from the CBE thermal comfort tool [13]. The measured data for air temperature, globe temperature, and indoor relative humidity were used for PMV calculations. The metabolic rate of 1.2 met (for reading, typing, and filing activities) and the minimum air velocity of 0.05 m/s (due to the limited air movement in radiant cooling systems [3]) were assumed. Also, a clothing factor of 0.65 clo was considered for the summer season based on the analyses of the RP-884 database for HVAC buildings.

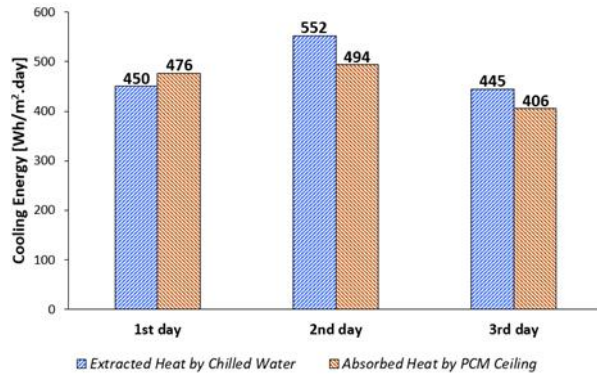


Figure 5. Total energy absorbed by PCM ceiling panels from indoor environment and energy extracted from the ceiling during chilled water circulation periods.

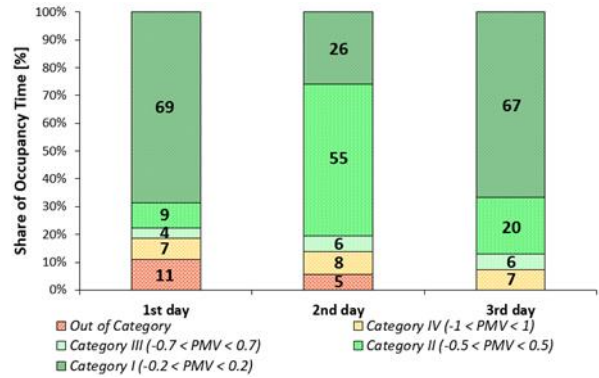


Figure 6. PMV-based thermal comfort level during occupancy hours in each day.

Table 3. Classification of thermal comfort conditions specified by ISO 7730 and EN 16798.

Category		PMV
ISO 7730	EN 16798-1	
A	I	$-0.2 < PMV < 0.2$
B	II	$-0.5 < PMV < 0.5$
C	III	$-0.7 < PMV < 0.7$
-	IV	$-1.0 < PMV < 1.0$

Assuming an occupancy time of 9:00 am – 07:00 pm, the results reveal that the PCM-RCC system is capable of maintaining an acceptable level of indoor thermal comfort. The “Out of Comfort Category” and/or “Category IV”, indicated in Figure 6, was mostly due to overcooling in the mornings caused by the active recharge. To address this issue, which was already predicted by the authors, a small electric air heater was installed and operated in the early mornings following the defined operating schedule (see Table 2). However, its heating capacity was not adequate as expected. In addition, temperature measurements were taken at heights of 0.1 m (for a person’s ankle), 1.1 m (for a seated person’s head), and 1.7 m (for a standing person’s head) to confirm that the vertical temperature difference was always less than 2°C, as the ISO 7730 standard specifies within “Class A”.

3.4. Total electricity usage

Considering the Time of Use (ToU) tariff in Victoria, Australia, the daily time is typically divided into off-peak (22:00–7:00), shoulder (7:00–15:00 & 21:00–22:00), and peak (15:00–21:00) periods. Figure 7 shows the electricity usage of PCM-RCC components during different Victoria’s ToU periods. The most electricity consumed belongs to the off-peak time with 58.5% of daily usage on the first day, 59.1% on the second day, and 80.2% on the third day. This confirms the capability of PCM-RCC systems in shifting a major part of peak cooling load to off-peak hours.

One limitation of this study was the absence of a similar second test cabin equipped with only radiant ceiling panels, without PCM. Such a setup would have allowed us to compare the energy usage of both RCC and PCM-RCC systems across different ToU periods. However, a preliminary analysis using a validated simulation model revealed that removing PCM from the radiant ceiling panels would increase the system’s operating time by 45-50% during the day. This additional load is mostly observed during shoulder hours (~65%) and the rest during peak time.

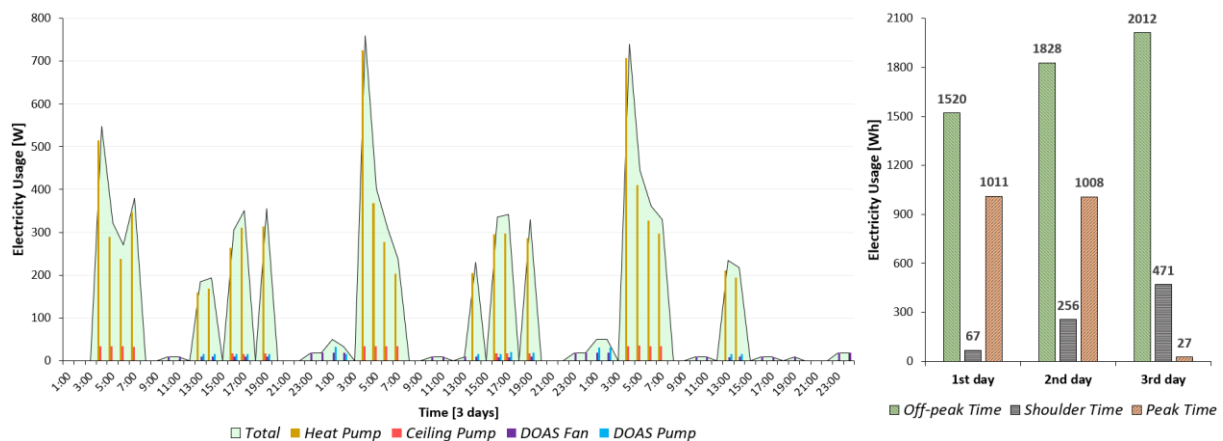


Figure 7. Measured electricity usage of PCM-RCC components in different Victoria's ToU periods.

4. Conclusions

This work introduced a new PCM-RCC technology developed for space cooling and discussed whether the design is functioning as expected. Using a full-scale experimental setup, the transient thermal behaviour of the proposed PCM-RCC in addition to the indoor thermal comfort and peak electricity demand reduction provided were examined. Overall, the system demonstrated satisfactory performance in terms of space cooling provision during the daytime, load shifting from peak to off-peak time, as well as providing thermal comfort. The findings and concluding remarks are:

- Applying a thin plaster layer to the top surface of PCM panels sufficiently resolved the issue of low thermal contact between the PCM composite board and water capillary tubes. Typically, 4–5 hours of chilled water circulation overnight could fully recharge the PCM panels.
- The average total heat transfer coefficient from the PCM ceiling surface to the interior space was estimated to be $8.48 \pm 0.97 \text{ W/(m}^2 \cdot \text{K)}$. This meets the requirements of the relevant standards.
- Over 80% of the whole occupancy time (09:00 am – 07:00 pm) was found within ± 0.5 for PMV. The cabin overcooling in the early morning following the active recharge cycle was shown to be the cause of the thermal discomfort. Despite considering a heating provision, the capacity of the electric air heater was not adequate as expected.
- About 70% of the daily electricity usage time of the PCM-RCC system was during the off-peak hours as in Victoria's ToU.
- The operating schedule presented here responds to the transient thermal behaviour of the indoor environment and the PCM ceiling panels. The results nevertheless highlight the importance of a more dynamic, optimal predictive schedule that considers real-time weather forecasting. Modelling and simulations are crucial in identifying the optimum operating strategy of the PCM-RCC system.

References

- [1] IEA 2022 *Space Cooling* (International Energy Agency: Paris, France)
- [2] Mousavi S, Rismanchi B, Brey S and Aye L 2021 *Renewable Sustainable Energy Rev.* **151** 111601
- [3] Mousavi S, Rismanchi B, Brey S and Aye L 2022 *Energy Rep.* **8** pp 54–61
- [4] Zhou Y, Zheng S and Zhang G 2020 *Build. Environ.* **174** 106786
- [5] IEA 2017 *Insights Brief: Space Cooling* (International Energy Agency: Paris, France)
- [6] Skovajsa J, Drabek P, Sehnalek S and Zalesak M 2022 *Appl. Therm. Eng.* **205** 118011.
- [7] Bogatu D -I, Kazanci O B and Olesen B W 2021 *Energy Build.* **243** 110981
- [8] Jobli M, Yao R, Luo Z, Shahrestani M, Li N and Liu H 2019 *Appl. Therm. Eng.* **148** pp 466–77
- [9] Weinläder H, Klinker F and Yasin M 2017 *Energy Build.* **156** pp 70–77
- [10] Mousavi S, Rismanchi B, Brey S and Aye L 2023 *Build. Simul.* **16**
- [11] Conroy C L and Mumma S A 2001 *ASHRAE Trans.* **107** pp 578–85
- [12] Cheung T, Schiavon S, Parkinson T, Li P and Brager G 2019 *Build. Environ.* **153** pp 205–217
- [13] Tartarini F, Schiavon S, Cheung T and Hoyt T 2020 *SoftwareX* **12** 100563

NSB 2023

Book of Technical Papers: 13th Nordic Symposium on Building Physics

The 13th Nordic Symposium on Building Physics (NSB 2023) took place at Aalborg University in the city of Aalborg, Denmark, from the 12th to the 14th of June, 2023. This conference was organised by the Department of the Built Environment of Aalborg University, with the help of fellow researchers from Aarhus University, the University of Southern Denmark and the Technical University of Denmark.

NSB is a renowned international conference series in Building Physics, held every three years since 1987. Although organised in Nordic countries, the conference is in English and is not limited to cold climates. It has grown to attract participants worldwide, to the point that more than half of the participants have been from other countries.

This symposium is intended to be a forum for scientists, practitioners, PhD students and other building professionals to share new research results, demonstrate innovative and sustainable building technologies, and discuss current and future challenges and solutions within building physics, heat, air and moisture transfer in buildings, and on aspects of moisture problems in the built environment, energy performance and indoor environmental quality. The NSB 2023 central theme is "Building physics as a key player for the sustainable built environment". The conference focus is primarily on the following aspects that all require a thorough understanding of building physics.

This Book of Technical Papers gathers the 37 peer-reviewed Technical Papers presented at NSB 2023.